DOCTOR OF PHILOSOPHY

Rate Effects in Fine Grained Soils

Quinn, Turlough

Award date:
2013

DOCTOR OF PHILOSOPHY

Rate Effects in Fine Grained Soils

Turlough Quinn

2013

University of Dundee

College of Art, Science & Engineering
School of Engineering, Physics and Mathematics
Department of Civil Engineering

Rate effects in fine grained soils

Turlough Quinn

A dissertation submitted for the
degree of Doctor of Philosophy
to the University of Dundee
August 2013

Declaration

This is to certify that, the candidate is the author of the thesis; that, unless otherwise stated, all references cited have been consulted by the candidate; that the work of which the thesis is a record has been done by the candidate and that it has not been previously accepted for a higher degree.

Turlough Quinn (candidate), Dundee, 30th August 2013

Dr. Michael Brown (supervisor), Dundee, 30th August 2013

Acknowledgements

This work is funded by an EPSRC grant.

My first acknowledgement goes to my project supervisor Dr Michael Brown. I extend my thanks to Michael for his support and assistance throughout the project. He has made himself available for advice and willing to offer assistance at all times throughout the course of the project.

I would like to thank Keith Lauder who helped settle me into postgraduate research in the geotechnical research group at the University of Dundee. I would like to thank the members of the geotechnical research group at the University of Dundee, all of whom have offered advice and assistance throughout the course of the project.

I would like to thank the technical staff within the Department of Civil Engineering at the University of Dundee whom has manufactured modified and repaired equipment through the project. In particular I would like to thank William “Mark” Truswell whom has always provided support and advice, and medical assistance when needed. I would also like to thank John Anderson, Mike McKernie, Alec Anderson, and Willie Henderson for their help in the workshop.

I would like to thank my friends whom have supported and encouraged me throughout the project, in particular Craig and Rachel Baxter, David Dunne, Seamus Considine and Eugene Mahony, all of whom I am very grateful to for their friendship.

Finally I would like to thanks my family, Brian, Marian, Bridgitta and Edel for their support throughout the project. In particular my thanks go to my parents, Brian and Marian, whom have provided essential support and encouragement, without which the completion of this project would not have been possible.

Abstract

The strain rate dependent behaviour of fine grained soils is an important aspect of geotechnical engineering. During dynamic or rapid events such as earthquakes and rapid pile testing, a fine grained soil will display significantly different behaviour than may be observed over the long life span of a structure. There is currently little understanding of the factors which influence the behaviour of fine grained soils during dynamic events (extremely high strain rates), making their response difficult to predict.

This research investigates the behaviour of fine grained soils subjected to a wide range of constant strain rates in monotonic triaxial compression testing. Each test is conducted under drained conditions to observe the behaviour of soils as they transition from a drained response at lower strain rates, through to an undrained or viscous response at higher strain rate tests. Where the response of soils is drained or partially drained, higher strain rate tests measure a decrease in strength. The point of transition from partially drained to undrained behaviour corresponds to the lowest strain rate dependent strength. Further tests at higher strain rates measure consistently greater strength.

The strain rate dependence of three fine grained soils is investigated, enabling a comparison of strain rate effects with soil index properties. The influence of initial state on the strain rate dependence of these Kaolin based model soils is also evaluated. The drained to partially drained response of the soils to strain rate increase is controlled by the coefficient of consolidation. Tests at high strain rates show the undrained or viscous strain rate effect on strength is related to liquidity index.

Local strain instrumentation allowed comparison of strain rate effects on small strain stiffness. At higher strain rate the soils display increasingly linear behaviour. At non-linear elastic strains, liquidity index appears to control the magnitude of the strain rate effects on stiffness.

Keywords; Strain rate effect. High strain rate triaxial testing. Fine grained soils. Liquidity index. Linear elastic threshold strain. Volumetric threshold strain. Strain rate coefficient.

Table of Contents

List of Figures

Chapter 2; Literature Review

Chapter 3; Methodology

Chapter 4; Results and Discussion of Shearing Behaviour

Chapter 5; Rate Effects at Large Strains (>1%)

Chapter 6; Rate Effects at Small Strains (<1%)

List of Tables

Chapter 2; Literature Review

Chapter 3; Methodology

Chapter 4; Results and Discussion of Shearing Behaviour

Chapter 5; Rate Effects at Large Strains (>1%)

Chapter 6; Rate Effects at Small Strains (<1%)

Notation

A	activity
A	coefficient Equation (3-11)
CF	clay Fraction
C_C	primary compression index
C_α	coefficient of secondary consolidation
C_r	reload-unload compression index
c_v	coefficient of consolidation
e	void ratio
E_0	1-dimensional stiffness
G	shear modulus
G_0	initial shear modulus, measured with axial bender elements
G_{max}	initial shear modulus measured with local strain gauge.
G_S	specific gravity of soil particles
I_P	plasticity index
I_L	liquidity index
I_V	viscosity index, C_α/C_C
k	permeability
m_v	coefficient of compressibility
m	exponential strain rate parameter (undrained)
n	coefficient (Equation 3-11)
m_G	increase in shear modulus per $\log_{10}$ increase in strain rate
m_α	$C_\alpha/(C_c-C_r)$
$m_{\alpha 2}$	C_α/C_c
MI	metastability Index
M	critical state line
N	location of critical state line in compression plane
P	rate exponent (linear elastic threshold)
p'_0	initial mean effective stress (at end of consolidation)
p'_e	equivalent mean effective stress on normal consolidation line
p'	mean effective stress
p	total stress
p_r	reference pressure, 1kPa

q	deviatoric stress
q_{ref}	deviatoric stress at reference strain rate
S_U	shear Strength
S_t	sensitivity
t	time
u	pore pressure
v	specific volume
V	normalised velocity
V_t	value of normalised velocity at transition
V_2	modified normalised velocity
w	water content
w_P	plastic limit
w_L	liquid limit
$\alpha(\varepsilon_s)$	strain rate coefficient (on small strain stiffness)
β	strain rate parameter in hyperbolic model
γ	shear strain
Γ	location of critical state line in compression plane
δ	increment
ε_A	axial strain
ε_R	radial strain
ε_s	shear strain
ε_V	volumetric strain
ε_F	strain at failure
ε_{EL}	linear elastic threshold strain
ε_{SVT}	volumetric threshold strain
$\dot{\varepsilon}$	axial strain rate
ζ	curve fit parameter, hyperbolic model
κ	slope of unload-reload compression line
λ_{NCL}	slope of normal consolidation line
λ_{VT}	coefficient of strain rate effect on volumetric threshold strain
Λ	$(\lambda - \kappa) / \lambda$
μ	logarithmic rate parameter (undrained)
υ	Poisson's ratio

ρ	density
$\rho_{0.1}$	logarithmic rate parameter, Graham *et al*. (1983)
σ	total stress
σ'	effective stress
σ_1	axial stress
σ_3	horizontal stress
σ_{VP}	pre-consolidation pressure
τ	shear stress
τ_C	shear stress at yield
Φ'_P	effective peak friction angle
Φ'_{CS}	effective critical state friction angle
$\emptyset$	diameter
χ	fractional increase of β with log increase in strain rate
°/min	degrees/minute

Abbreviations

KSS	Kaolin - Sand – Silt (in proportion of 5 to 2.5 to 2.5).
KSS-541	Kaolin – Sand – Silt (in proportion of 5 to 4 to 1).
MCC	Modified Cam Clay
NC	Normally Consolidated
OCR	Over Consolidation Ratio
HOC	Heavily Over Consolidated
RCT	Resonant Column Test
CLTST	Cyclic Loading Torsional Shear Test
MLTST	Monotonic Loading Torsional Shear Test
Atm	Atmospheric pressure

1 Introduction

1.1 Preface

In geotechnical engineering events a wide range of strain rates are encountered. During the lifetime of embankments, the rate of strain is expected to be very low, whilst during dynamic events such as earthquakes or landslides the rate of strain can be orders of magnitude higher than during normal service. The response of fine grained soils varies significantly with the corresponding strain rate, displaying a drained response to slow events, and responding with undrained behaviour during rapid events. From an engineering perspective, the implications of either a drained or undrained response have important implications for the properties of soils. At strain rates where the response of fine grained soil is undrained, an increase in strain rate result in a significant increase in strength. This phenomenon is not well understood, and thus the potential for a soil to display undrained strain rate effects cannot currently be predicted with certainty.

The use of modern geotechnical events to determine the capacity of soils, such as rapid pile testing and field penetrometer tests may involve high strain rates. These types of tests are becoming increasingly attractive because of the economic advantage they have over classical techniques such as static pile testing which is time consuming. However the use of parameters from high strain rate testing in current “static” design is inhibited by the development of large strain rate effects on the measured strength. To use the high strain rate test techniques in design requires a site specific study of the strain rate effect to be conducted. This may be reliant on the use of highly specialised research apparatus which is outside of the realms normal commercial soil testing. Thus an improved understanding of the nature of strain rate dependence of soils is required to allow assessment of their potential to display strain rate effects based upon simpler testing (e.g. soil index tests) without the need for site specific advanced testing.

To improve the understanding of strain rate effects in fine grained soils a programme of research was conducted at the University of Dundee. The research involved strain rate testing over a wide range of strain rates where the behaviour of soil can be

examined from the slow strain rate partially drained response, to the high strain rate induced undrained response. The research was conducted using drained test conditions to determine the strain rate corresponding to the true undrained response of the soil. The key aspects of the strain rate dependent behaviour are examined; (1) the partially drained response, where increasing strain rate results in a decrease in strength (2) the transition to undrained behaviour where the minimum strength is expected in normally consolidated fine grained soils (3) the increase in strength with increasing strain rate where the response of the soil is undrained.

The strain rate dependence in multiple model fine grained soils is evaluated. The composition of the model soils is varied to enable a comparison of index properties and the corresponding strain rate dependence. The model soils are also tested at different initial states, to determine the influence this has on the strain rate dependent behaviour. The information collected on the strain rate dependent behaviour is then compared to a database from published literature, to develop rate potential models of fine grained soils.

1.2 Aims and Objectives

The overall aims of this project was to improve current understanding of strain rate effects in fine grained soils and in doing so, develop a rate potential framework where the potential strain rate dependency of fine grained soils can be assessed using standard geotechnical laboratory techniques.

To achieve these aims the following objectives were set out;

1. To investigate the behaviour of fine grained soils over a wide range of strain rates, from partially drained into undrained behaviour.

2. To evaluate the influence index properties of fine grained soils have on the strain rate effects on both strength and stiffness.

3. Develop a rate potential framework, from which the potential strain rate dependency (on strength or stiffness) of fine grained soils can be evaluated

from index properties, determined from standardised testing available in commercial geotechnical laboratories.

1.3 Structure of thesis

The thesis is presented in 7 Chapters;

Chapter 2 presents a review of literature related to current understanding of strain rate effects on strength, and factors which have been found to affect both partially drained and undrained strain rate effects. Previous studies where relationships between strain rate effects and index properties of fine grained soils are discussed. The effects of strain rate on stiffness are also reviewed. A summary of previous triaxial studies on undrained strain rate effects is also presented.

The methods used to determine strain rate effects on strength are presented in Chapter 3, detailing the dynamic electromechanical triaxial system used to test soils from strain rates of 1%/hr to 180,000%/hr. The reconstitution process of the fine grained soils is also described. The fine grained soils used in this study and their standard characteristics are also presented in Chapter 3.

The shearing behaviour of soils at different strain rates is described in Chapter 4, with emphasis on the effects of strain rate on the stress-strain, excess pore pressures, effective stress and volumetric strains. The behaviour of over consolidated soils at increased strain rate is also compared.

The results of strain rate effects are discussed in Chapter 5, with particular focus on behaviour at large strain (>1%). Factors that affect the partially drained as well as undrained strain rate effects are discussed and compared. Points raised in the literature review are discussed with regard to the results of this study. Relationships between strain rate effects on fine grained soils and their index properties are presented.

In Chapter 6 the strain rate effects on stiffness (strains <1%) are discussed, where relationships between various facets of the non linear behaviour of fine grained soil

are presented. Relationships between the strain rate dependence and index properties of fine grained soils are also presented and discussed.

Chapter 7 presents a summary and conclusions of the findings of this research, and discusses some potential avenues for further research of strain rate effect in fine grained soils.

2 Literature Review

2.1 Introduction

In geotechnical engineering a wide range of strain rates are encountered either through field and laboratory testing of soils, through to the lifespan of geotechnical structures. The potential for soils to display strain rate effects may have implications for the choice of field testing techniques, as well as how these techniques are factored to account for strain rate effects. To account for strain rate effects in geotechnical engineering requires testing of site specific strain rate dependence. Relating strain rate effects to fundamental soil properties would provide industry with the means to evaluate rate potential of soils without the necessity of empirical site specific testing.

To gain some understanding on the factors which influence strain rate effects, and the behaviour of soils as they are tested at different strain rates, a review of factors involved in the strain rate dependence of soils has been conducted. Existing relationships between strain rate effects and the index properties of soils, as well as the current understanding of strain rate effects on soil behaviour at small strains has also been discussed. Previous investigations into the rate dependence of soil using the triaxial apparatus are also reviewed.

The final section of this chapter summarises the review of literature, and highlights areas of weakness in the current understanding of strain rate effects, and areas for further research.

2.2 Strain rate dependent soil behaviour in geotechnical engineering

With increasing strain rate the response of soil changes, and the subsequent effect on the strength of a soil may be very significant. Figure 2-1 presents results from Lehane *et al*. (2009) where the resistance to penetration of normally consolidated Kaolin was measured at strain rates varying over 5 orders of magnitude using a T-bar penetrometer. At lower strain rates; an increase in strain rate corresponds to decreasing resistance. With increasing strain rate, the maximum strength of the soil

continues to decrease until a minimum resistance is measured, where the response of the soil changes, and will begin to display increasing resistance with a further increase of strain rate. The behaviour of normally consolidated Kaolin shown in Figure 2-1 is consistent with results of other penetrometer studies in fine grained soils conducted in both field testing and laboratory studies (Bemben and Meyers, 1974, Roy *et al*., 1982, Randolph and Hope, 2004, Kim *et al*., 2008). The variation of resistance with increasing strain rate in Figure 2-1 reflects true strain rate dependent behaviour of fine grained soils.

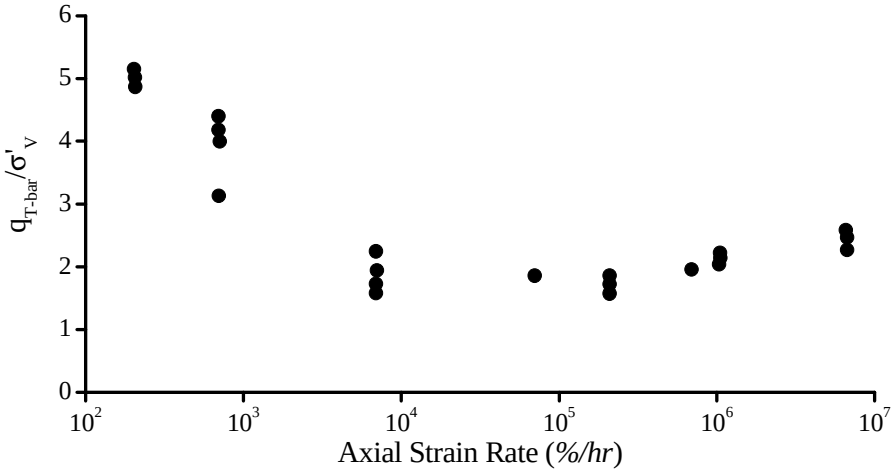

Figure 2-1 Variation of normalised T-bar penetrometer resistance in normally consolidated kaolin at increased strain rate (Lehane et al., 2009)

According to Lunne *et al*. (1997) at very slow strain rates, where the behaviour of soil is fully drained, the resistance is independent of strain rate. With increasing strain rate the effective stress reduces causing a reduction in resistance (Figure 2-1). This continues until a strain rate is reached whereby viscous effects come to influence the soil's resistance, offsetting the reduction in effective stress (and strength) and the resistance reaches a minimum. With further increase of strain rate the viscous effects come to dominate and the soil's resistance will increase.

At lower strain rates in Figure 2-1 this behaviour is consistent with the partially drained behaviour of Weald clay at different strain rates tested in a triaxial cell shown by Carter (1982). Carter (1982) conducted a numerical and experimental study on the

effect of strain rate on strength in drained triaxial tests. Carter (1982) found that with increased strain rate the strength of the soil reduces due to the development of excess pore pressures and decreasing influence (time) of consolidation. The effect of strain rate in this domain was thus termed the partially drained strain rate effect. At higher strain rates Carter (1982) found the response of the soil became undrained and the soil displayed its true minimum strength.

The increase in resistance with higher strain rates, termed the viscous effect by Lunne *et al*. (1997), has frequently been observed in undrained triaxial compression testing (Casagrande and Shannon, 1948, Lefebvre and LeBoeuf, 1987, Sheahan *et al*., 1996). These affects are significantly higher in fine grained soils than in coarse grained soils (Casagrande and Shannon, 1948, Gibson and Coyle, 1968, Vucetic *et al*., 2003). This response was often termed the viscous response (Whitman, 1957); however here it is referred to as the undrained strain rate effect because of its association with undrained soil behaviour.

An idealised version of these effects are summarised in Figure 2-2 from Quinn and Brown (2011), which highlights the four different domains of soil behaviour in relation to strain rate. The key aspects of the aforementioned studies is the apparent transition from partially drained to undrained behaviour, whereby the soil response changes from decreasing to increasing strength/resistance with an increase in strain rate. This point is labelled the transition in Figure 2-2. The potential viscous limit in the fourth domain in Figure 2-2 reflects the shear thinning behaviour (for undrained strain rate effects) of soils at increased strain rates (Guven, 1992).

The importance of understanding the strain rate dependent behaviour shown in Figures 2-1 and 2-2 is highlighted in Figure 2-3 which presents a range of strain rates associated with some important facets of geotechnical engineering. The range of strain rates shown in Figure 2-3 vary over approximately 12 orders of magnitude. The most crucial strain rates are those corresponding to building infrastructure in Figure 2-3, and those corresponding to the transition from partially drained to undrained behaviour where the minimum strength of soils would be expected. Figure 2-3 highlights the stain rates associated with the lifetime of a structure are several orders of magnitude less then those from which the capacity of the soil is determined.

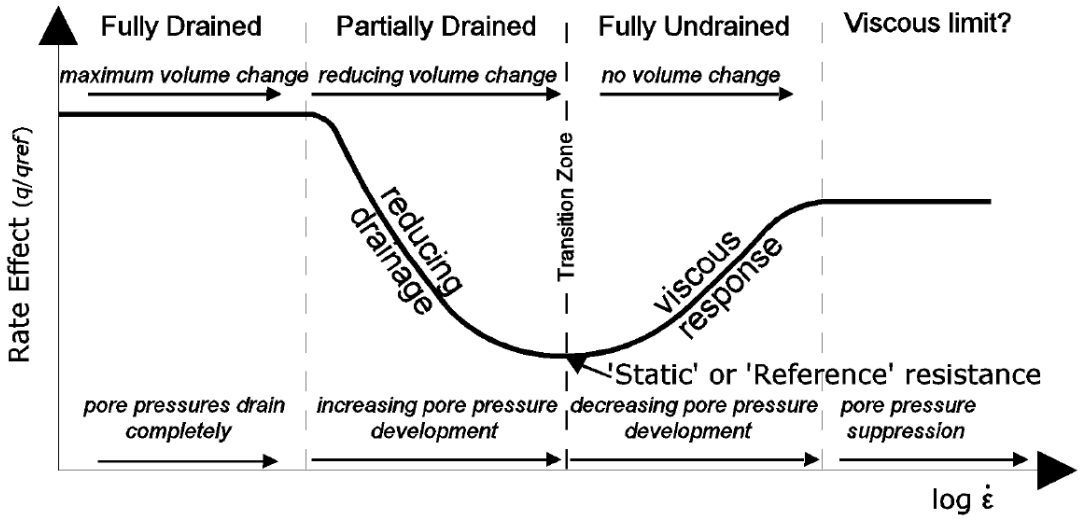

Figure 2-2 Idealised 'backbone' curve, identifying the four different domains of strain rate dependent soil behaviour (Quinn and Brown, 2011)

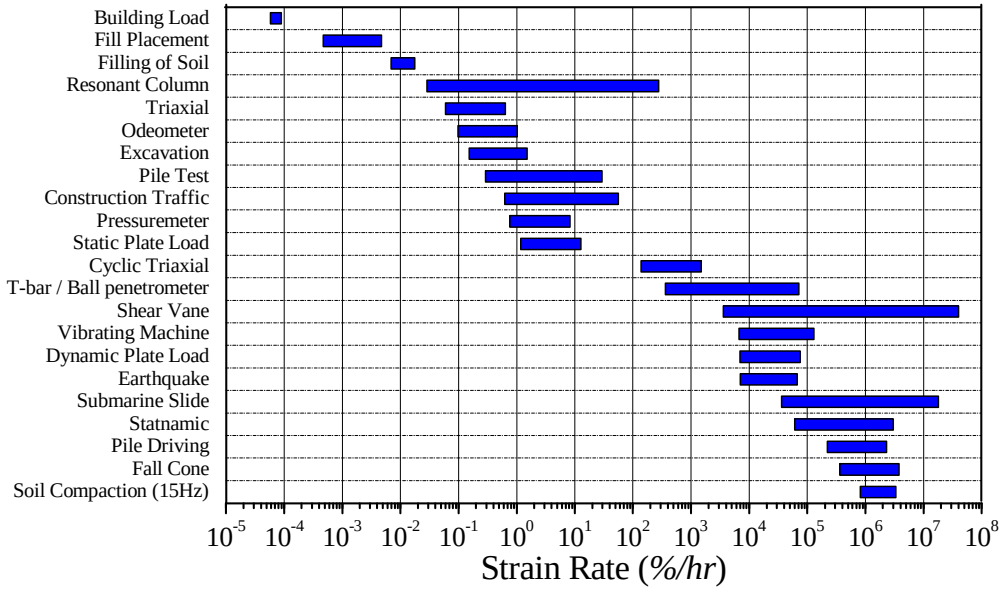

Figure 2-3 Range of rates associated with typical facets of geotechnical engineering

For tests corresponding to higher strain rates in Figure 2-3 the response of fine grained soil is expected to be undrained. For example the International Reference Test Procedure (IRTP) require a standard cone penetrometer, diameter 35.7mm, to be conducted at 20mm/s, which may be expected to give a strain rate of approximately 200,000%/hr. Specification of these rates of penetration is intended to correspond to fully drained conditions in coarse grained soils, and fully undrained conditions in fine

grained soils, however the effects of strain rate were not fully taken into account when this standard was specified (Salgado *et al*., 2013). Thus in comparison with Figure 2-1, use of the IRTP specification may inadvertently result in resistance measurements which have to some degree been affected by strain rate effects. This highlights the importance of strain rate as part of field testing techniques, and how design parameters may be affected by the strain rate effects on strength.

2.3 Factors affecting the partially drained strain rate effect on strength

The partially drained strain rate effect, corresponding to the second domain in Figure 2-2 discussed previously, has been related to decreasing effective stress due to increasing excess pore pressure development (Carter, 1982, Randolph and Hope, 2004, Kim *et al*., 2006, Salgado *et al*., 2013). The increase in excess pore pressures is due to the decrease in consolidation with increased strain rate. Finnie and Randolph (1994) found for model foundations tested at various penetration rates in calcareous sediments, the partially drained strain rate effect could be accounted for by normalising the velocity of penetration using the coefficient of consolidation;

$$V = \frac{vd}{c_v} \qquad (2\text{-}1)$$

Where v is the velocity of penetration, d is a characteristic length (often assumed as the drainage path length) and c_v is the coefficient of consolidation. This method of normalising the penetration rate has been successfully used in several studies to account for the effects of partial consolidation at increased rate (Randolph and Hope, 2004, Kim *et al*., 2006, Lehane *et al*., 2009). An example of the effect of the normalised velocity is shown in Figure 2-4 which presents the effect of strain rate on the strength of Kaolin from Lehane *et al*. (2009). The results from Lehane *et al*. (2009) are from T-bar penetration tests in a centrifuge, where the tests were conducted at various strain rates and depths.

Figure 2-4 shows that normalisation of the strain rate using Equation 2-1 reduces the variation of the results considerably for the partially drained strain rate effects. It was suggested by Lehane *et al*. (2009) that use of Equation 2-1 is not appropriate for strain rate effects in the undrained domain, where consolidation does not occur.

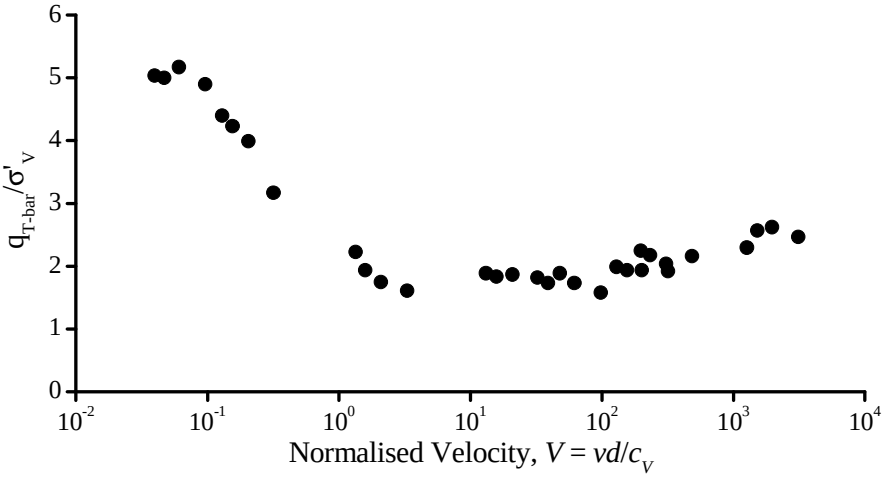

Figure 2-4 Effect of normalised velocity on normalised T-bar penetrometer resistance measurements in Kaolin (Lehane *et al.*, 2009)

2.4 Factors affecting the undrained strain rate effect on strength

Although the factors affecting the partially drained rate effects have been related to the coefficient of consolidation, the factors which affect the undrained strain rate effect are not well understood. Because an increase in shear strength with increasing shear rates is characteristic of viscous materials it is often considered that undrained strain rate effects are due to the viscosity of soils (Whitman, 1957, Lunne *et al*., 1997). Tatsuoka *et al*. (2008) attributes the response of soil to stepwise changes in strain rate to the type of inter particle contacts, whilst others postulate it may be influenced by the viscosity of absorbed water (Richardson, 1963, Briaud and Garland, 1985). Observations of soil behaviour in stepwise changes to strain rate and the viscosity of water in soils are reviewed here. Observations regarding the effect of strain rate on effective stress are discussed, as well as how over consolidation effects the undrained strain rate effect on strength.

2.4.1 Effects of stepwise change in strain rate

The behaviour of both fine grained and coarse grained soils subjected to stepwise change in strain rate has been investigated in several studies (Richardson and Whitman, 1963, Graham *et al*., 1983, Oka *et al*., 2003, Sorensen *et al*., 2007, Tatsuoka *et al*., 2008). An example of the effects of stepwise change in strain rate of undrained monotonic triaxial testing in reconstituted London clay is shown in Figure 2-5 from Sorensen *et al*. (2007). The range of strain rates, in comparison with those discussed in Section 1-2, are relatively narrow. However some interesting observations are noted, including that fine grained soils subjected to a stepwise change in strain rate will tend to a unique, strain rate dependent stress-strain curve. The stress-strain curves from stepwise changes in strain rate agree with those from constant strain rate tests at their respective strain rates (Richardson and Whitman, 1963).

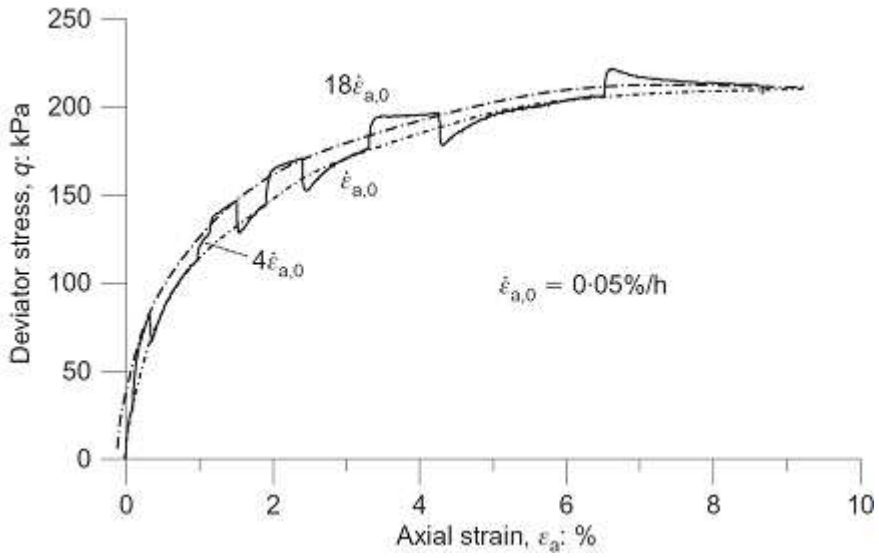

Figure 2-5 The stress strain behaviour of London clay subjected to stepwise changes in strain rate (Sorensen *et al*., 2007)

Sorensen *et al*. (2007) found the behaviour of the normally consolidated, reconstituted London clay subjected to step-wise changes in strain rate depended on strain level, displaying isotach behaviour (following unique stress-strain paths for each strain rate) at lower strains, and increasingly TESRA (Temporary Effect of Strain Rate and strain Acceleration) type behaviour (a temporary increase in stress-strain path followed by a return to the original path) at higher strain. These effects are compared by Tatsuoka *et*

al. (2008) in Figure 2-6. Tatsuoka *et al*. (2008) labelled the transition from isotach behaviour to TESRA type behaviour as described by Sorensen *et al*. (2007) as "combined" (Figure 2-6).

The combined type behaviour, which is isotach at low strains before becoming TESRA with increased strain, is associated with fine grained soils. Oka *et al*. (2003) describes how in fine grained soils, the isotach behaviour changes to the TESRA type as the soil approaches critical state. The purely TESRA and P & N (Positive & Negative) type behaviour (a positive increase in stress-strain path, followed by a decrease from original curve) in Figure 2-6 reflect behaviour of coarse grained material and is not discussed further here.

Sorensen *et al*. (2007) attributed the behaviour of reconstituted London clay shown in Figure 2-5 to the soil matrix because excess pore pressure appeared to be largely independent of strain rate. Based upon the various types of behaviour as summarised in Figure 2-6 and how they relate to different types of soils, Tatsuoka *et al*. (2008) postulated that isotach behaviour is due to inter particle contacts becoming stiffer and stronger with strain rate. The transition to TESRA type behaviour in fine grained soils is due to changes in the soil fabric from the development of irrecoverable plastic strains, which increase as the soil approaches critical state.

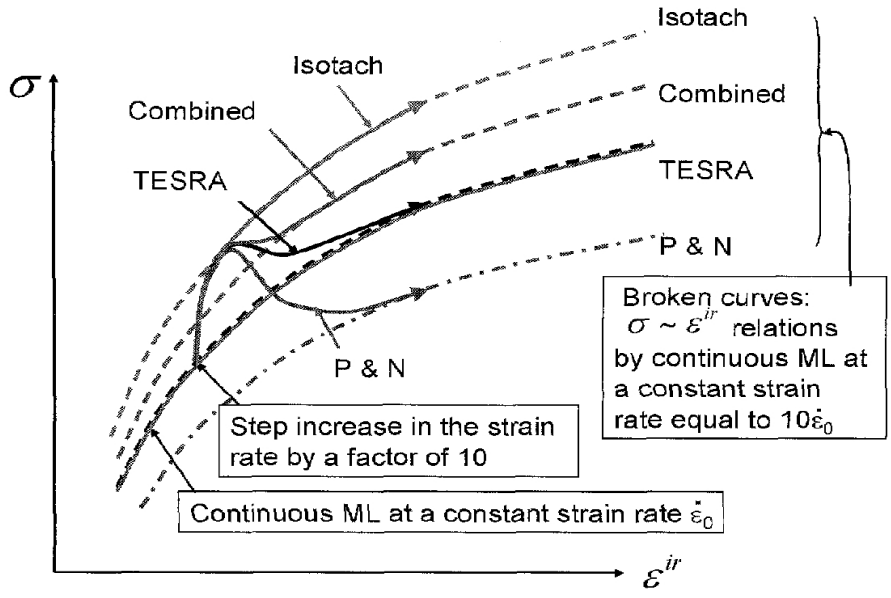

Figure 2-6 Various responses to stepwise change in strain rate (Tatsuoka *et al*., 2008)

As mentioned Tatsuoka *et al*. (2008) attributed the different types of behaviour to the inter-particle contacts. Thus changes of this type would presumably be related to the plasticity index of soil because at clay content above 35% the clay matrix dominates the mechanical behaviour of fine grained soils (Kumar and Muir Wood, 1999). The strain dependent behaviour of the effects of strain rate discussed above could also imply different strain rate effects between those measured at lower strains (< pre failure) and those at large strains (~ maximum strength or critical state).

2.4.2 Viscosity of absorbed water in fine grained soils

In some literature it is suggested that strain rate effects on strength are due to the viscosity of the water micelle enveloping the soil particles (Briaud and Garland, 1985, Rattley *et al*., 2011). This would imply that strain rate effects on strength are related to the moisture content, activity and clay fraction of fine grained soils.

Water within saturated, fine grained soils can vary in form as summarised below from Heuckel (1992);

1. Free or Bulk Water, which is able to flow due to hydraulic gradient at room temperature.
2. Intercluster absorbed water, enveloping clusters (when formed) of Kaolinite. This water is restricted from flow in normal conditions.
3. Intracluster absorbed water, at typical porosities only a few molecular sheets of water can fit in the available interlamellar space. The intracluster water cannot flow in ambient conditions.
4. Structural water, or hydroxyl, which is part of the structural lattice of the clay mineral. This water does not leave the solid below 350 degrees C.

Heuckel (1992) described how the intercluster and intracluster absorbed water can have significantly different properties than free water, specifically a higher viscosity. Thus if in soils of higher moisture content, the absorbed layers increase in size, then more water is influenced by the clay particle. The effective area of the clay particle would increase in size, and possibly give the soil greater viscosity or result in a greater strain rate effect.

There is currently no standard method of measuring the viscosity of clays at moisture content less then the liquid limit (Mahajan and Budhu, 2009). Research into the viscosity of clays (rather then simply absorbed water in clays) is generally conducted at very high moisture content, with clays taking the form of liquid suspensions. These studies typically use a rheometer, generally employing parallel plate (Low, 1976) or shear vane methods (Ghezzehei and Or, 2001). Mahajan and Budhu (2009) employed a fall cone test, however this was done again in clay suspensions of high liquidity index (>1).

Previous research has shown the viscosity of soil to decrease with increasing moisture content (Low, 1976, Allam and Sridharan, 1984, Ghezzehei and Or, 2001, Karmakar and Kushwaha, 2007, Mahajan and Budhu, 2009). This appears contrary to suggestions from Briaud and Garland (1985) and Rattley *et al*. (2011).

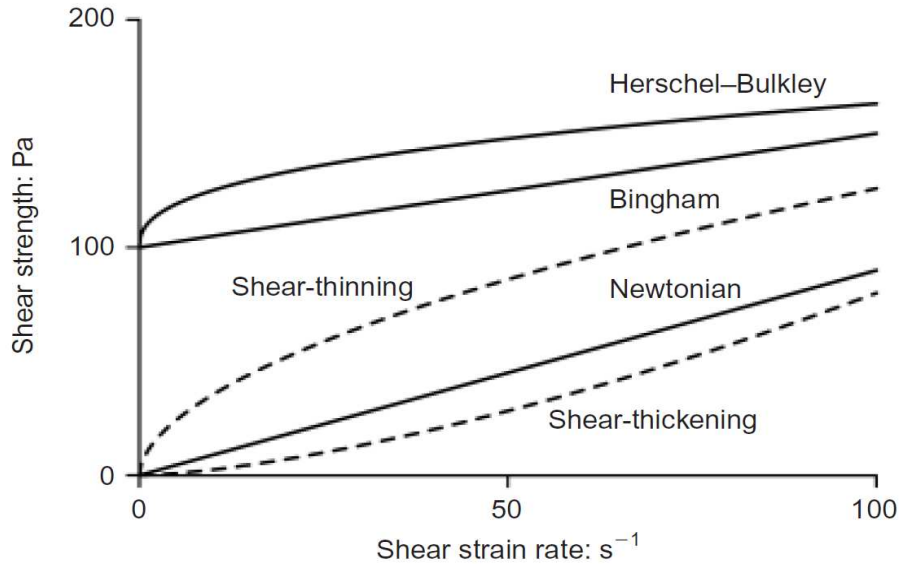

Figure 2-7 Models for viscous flow (Boukpeti *et al*., 2012)

As described by Guven (1992) soils display shear thinning behaviour in terms of their viscous flow behaviour (Figure 2.7). The viscosity of the soils, is controlled by the shear modulus, the yield stress and the coefficient of plastic viscosity (Ghezzehei and Or, 2001). Therefore for a given soil, the viscosity will increase as the shear modulus increases. The Herschel-Bulkley model in Figure 2-7 is thus most representative of the viscous behaviour of soil, which is a function of its yield stress. The strain rate effect on strength is thus the ratio of the increase in strength in the viscous domain, at

a particular yield stress. Therefore although viscosity increases, this ratio might not increase with decreasing moisture content. As shown in Figure 2-7 the viscosity (and thus strain rate effect on strength) would decrease at higher shear strain rates for a material displaying shear thinning properties. This suggests a potential limit to viscosity at very high strain rates.

Although the overall viscosity and yield stress decrease with increasing moisture content, the larger absorbed layers may influence the strength to a greater proportion. Thus the ratio of viscosity to yield stress would increase as per Figure 2-7. This would result in higher strain rate effects on strength.

2.4.3 The effect of strain rate on effective stress

As described previously the partially drained strain rate effect corresponds to increased excess pore pressure and reducing effective stress with increased strain rate (Figure 2-2). Regarding undrained strain rate effects on strength, reports in literature are often contrary to each other in terms of how increased strain rate affects excess pore pressures. Some studies report excess pore pressures are independent of strain rate (Akai et al., 1975, Soga and Mitchell, 1996), whilst other studies report the magnitude of excess pore pressures reduce with increasing strain rate (Sheahan et al., 1996). It appears that no studies on strain rate effects have observed increasing excess pore pressures with strain rate where the response of the soil is undrained.

Both Soga and Mitchell (1996), who tested natural Pancone clay at strain rates from 0.3 to 3%/hr, and Lefebvre and LeBoeuf (1987) who tested several natural clays from Eastern Canada at strain rates from 0.05 to 132%/hr, found that excess pore pressures were independent of strain rate. These findings are in agreement with Graham et al. (1982) who also tested a variety of natural soils at strain rates from 0.002 to 10%/hr. However these observations that excess pore pressures are independent of strain rate are possibly linked to the presence of an intact natural structure; tests on the same soils without their natural structure showed a dependence of excess pore pressures on strain rate (Lefebvre and LeBoeuf, 1987).

Akai *et al*. (1975), who conducted monotonic triaxial compression tests in remoulded Fukakusa clay at strain rates up to 3000%/hr, assumed there was no obvious effect of strain rate on excess pore pressures (Figure 2-8). For the majority of tests shown in Figure 2-8, no distinct relationship emerges between the magnitudes of excess pore pressures and increasing strain rate (0.0109-14.81%/min). Akai *et al*. (1975) assumed the variability of excess pore pressures indicate independence of strain rate. However, the fastest strain rate test (49.4%/min) displays significantly lower excess pore pressures. Notably Akai measured pore pressures at the base of the sample. Measurements of pore pressure taken at the base of the sample may be subject to end effects, which may be responsible for the variability in the magnitude of excess pore pressures at lower strain rates (0.0109 - 14.81%/min) in Figure 2-8.

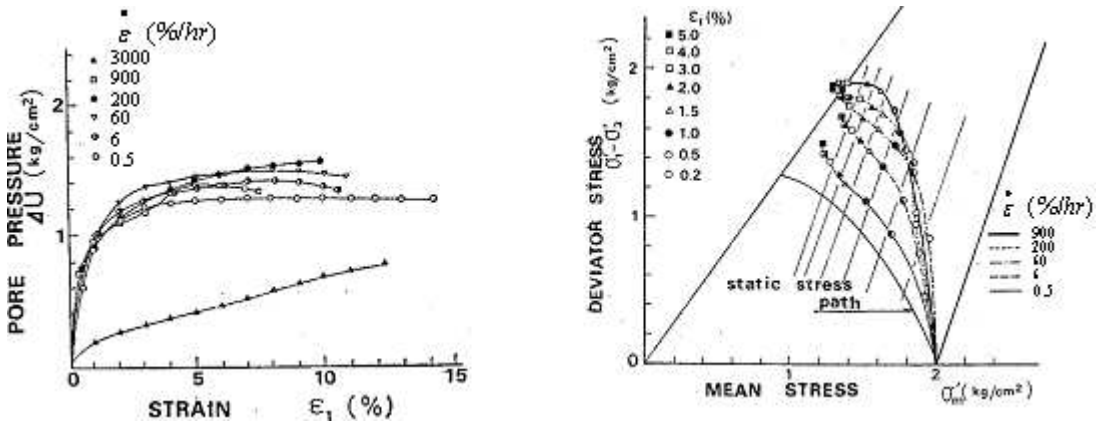

Figure 2-8 Excess pore pressures measurements from tests at various strain rates and the corresponding effective stress paths (Akai et al., 1975)

Decreasing excess pore pressures with increasing strain rate are widely reported in the literature (Richardson and Whitman, 1963, Lefebvre and LeBoeuf, 1987, Sheahan *et al*., 1996, Balderas-Meca, 2004). Lefebvre and LeBoeuf (1987) who tested natural fine grained soils from Eastern Canada found that when these soils were destructured, the magnitude of excess pore pressures decreased when tested at higher strain rate. As mentioned above, when the same soils were tested with their natural structure the excess pore pressures did not display a dependence on strain rate. A decrease in excess pore pressure with increased strain rate (at maximum strength) is often described as pore pressure suppression, and is cited as the primary mechanism responsible for strain rate effects in reconstituted soils in both normally consolidated (Lefebvre and LeBoeuf, 1987) and over consolidated state (Sheahan *et al*., 1996).

For normally and lightly over consolidated soils Sheahan *et al*. (1996) also measured an increase in the effective stress friction angle at maximum deviatoric stress. Other studies including Bjerrum *et al*. (1958), Alberro and Santoyo (1973), Hight (1983), O'Reilly (1989) and Crawford (1959) all report slight increases in peak angle of friction with increasing strain rate. The aforementioned studies however also found at higher strains the tests tend to the critical state. Therefore the position of the critical state line appears to be unaffected by strain rate. This is the case in Figure 2-9 for two strain rates, 0.12%/hr and 60%/hr, from Richardson and Whitman (1963). Figure 2-9 shows the effective stress path at the faster strain rate diverges from the slower stress path throughout. As shown in Figure 2-9 these normally consolidated soils reach failure on the critical state line.

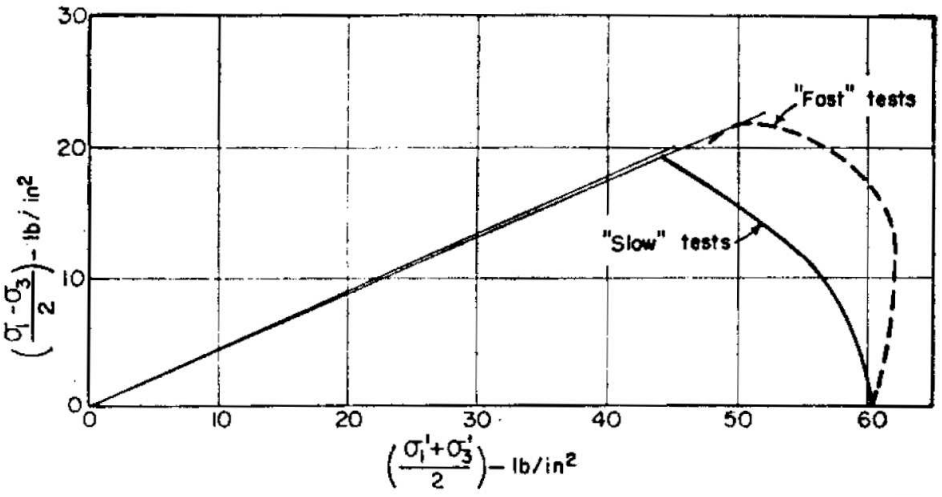

Figure 2-9 Effective stress path at slow and high strain rates (Richardson and Whitman, 1963)

Figure 2-10 presents excess pore pressure measurements from Sheahan *et al*. (1996) who conducted monotonic triaxial compression tests in anisotropically consolidated reconstituted Boston blue clay (OCR 1) at strain rates from 0.05 to 50%/hr. As shown in Figure 2-10 the excess pore pressures decrease consistently with increased strain rate. Notably at the higher strain rate tests (>0.5%/hr) at the beginning of shear the excess pore pressures tend to negative values before turning positive at higher strain levels. Similar behaviour has also been noted in monotonic triaxial testing from Zhu and Yin (2000), and Balderas-Meca (2004) who tested at considerably higher strain rates (up to 350,000%/hr) as well as in Statnamic model pile testing (Brown, 2004 & Brown *et al*., 2004). The development of negative excess pore pressures could be

caused by a time lag in excess pore pressure measurement, however it may also indicate effects due to the soil's response, such as dilation at the beginning of shear.

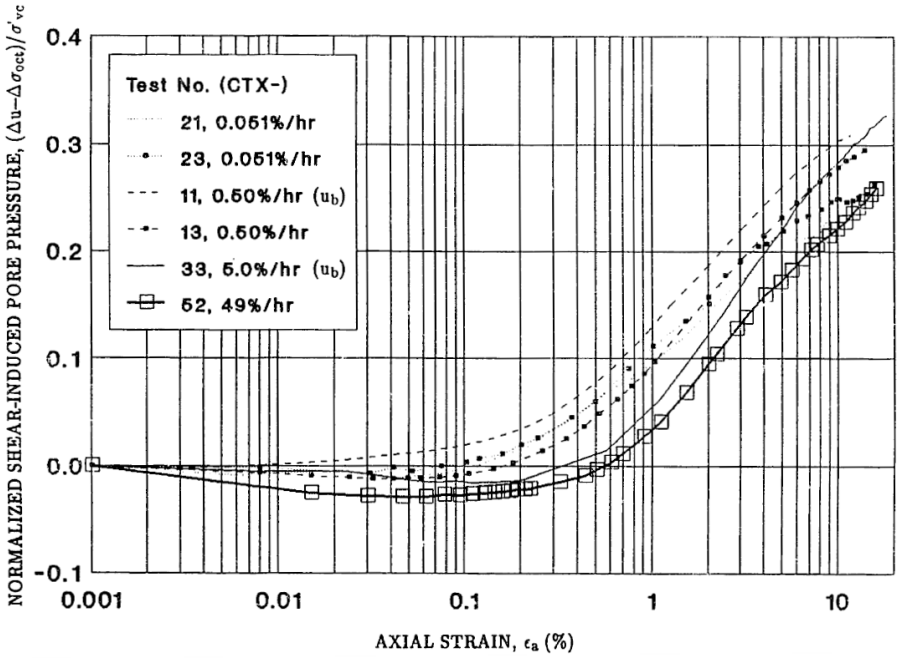

Figure 2-10 Normalised excess pore pressures measured during monotonic triaxial testing in reconstituted Boston blue clay at various strain rates (Sheahan *et al.*, 1996)

Based on excess pore pressure measurements, Richardson and Whitman (1963) cite two separate mechanisms as responsible for the rate effect, each taking effect at different levels of strain. They compared results taken from tests over a range of strain rates, giving particular attention to two strain rates, 0.12%/hr and 60%/hr. At strains less than 1% the pore pressures appeared to be independent of strain rate. At strains greater than 1%, the higher strain rate test displayed lower excess pore pressures. It was also mentioned that the measurement of pore pressures may have been in error at strains less that 1% due to a time lag with the transducer. However it was felt that any error could not have been too large, and it was safe to conclude that pore pressures were independent of strain rate to 1% strain. Therefore it was concluded that at small strains (<0.5%) the increase in shear stress with strain rate is due to an increased resistance to distortion, whereas at large strains during faster strain rates the soil particles find it more difficult to move relative to each other, and unless restricted by a change in effective stress they will attempt to compress or dilate. This suggests at large strains the strain rate effect is related to an attempt from the soil mass to change

volume. These points are explained further in Richardson (1963) with reference to the illustration in Figure 2-11.

In Figure 2-11 (a), the relationship between the soil particles is illustrated at small strains, where it was proposed that due to shear displacement particle A and B will be forced closer as the bonds at point 1 and 2 are not broken, causing rotation of particle C, thus compressing pore fluid between particle A and B. As the bonds are not broken the magnitude of the pore pressures would be a function of the shear displacement. The increase in strength would be due to viscous behaviour of the bonds, which would be a function of the rate of shear displacement, with a greater shearing force necessary to cause the same shear displacement within a shorter period of time. However, since negative excess pore pressures have been shown to manifest at small strains (Figure 2-8), it suggests these unbroken bonds referred to above become stiffer at the higher strain rate to the extent the particles may dilate when sheared.

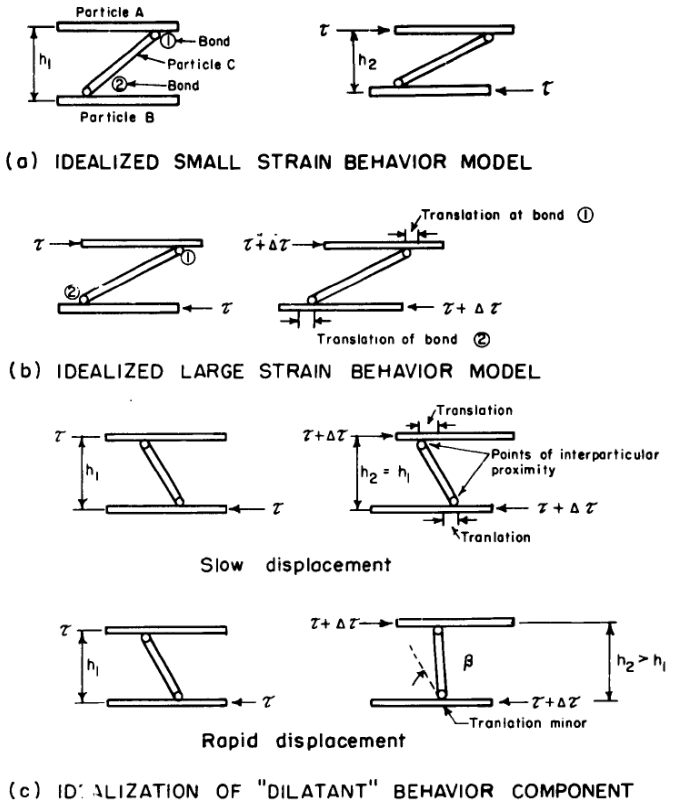

Figure 2-11 Idealisation of soil behaviour at the micro-scale during shear (Richardson, 1963)

Regarding the large strain behaviour idealised in Figure 2-11 (b) it is assumed the bonds at points 1 and 2 are broken, or possibly breaking and reforming, and thus play

a relatively minor role in the overall behaviour. Whereas at small strains Figure 2-11 (a) idealises what may be rotational forces, it is postulated that translational forces at point 1 and 2 are occurring. The effect of increased rate for large strain (>4%) behaviour is idealised in Figure 2-11 (c), where it is thought a viscous resistance to translation may be enacted due to rapid displacement, causing rotation of the diagonal particle. The rotation of this particle would in turn cause an increase of particle spacing which would result in decreasing pore pressures. This can be thought of as an increased resistance to compression or an increased tendency to dilate (Sathringam, 1991). This is an interesting mechanism which would appear to relate to the viscous properties of absorbed water of clay particles discussed earlier.

Notably, most of the studies which measured excess pore pressures during increased strain rate testing are of limited range of strain rates in comparison to the range of strain rates involved in geotechnical engineering. It is also apparent from the literature of the lack of studies which incorporate multiple soils, which could help clarify which properties govern the wide variations of soil behaviour reported in previous studies regarding development of excess pore pressures at higher strain rates.

2.4.4 The influence of over consolidation on strain rate effects

The effects of OCR on strain rate effects have been studied by Sheahan *et al*. (1996) Zhu and Yin (2000), Lehane *et al*. (2009) and Sorensen *et al*. (2007). Sheahan *et al*. (1996) conducted tests in monotonic triaxial compression tests on reconstituted Boston blue clay at OCR 1, 2, 4 and 8. Figure 2-12 presents the normalised undrained shear strength at each strain rate and OCR. With increasing OCR the overall strain rate effect reduced. However a threshold strain rate was identified by Sheahan *et al*. (1996) below which the strain rate effects vanished. This threshold strain rate increased with OCR. Between the two highest strain rates, the rate effects were very similar for each OCR. Lehane *et al*. (2009) conducted tests using a T-bar and ball penetrometer in Kaolin over consolidated to OCR 2 and 5 in a centrifuge. The range of strain rates was between 200 to $6x10^6$ %/hr. The undrained strain rate effects in Kaolin were almost identical at OCR 1, 2 and 5, which agrees with findings from Sheahan *et al*. (1996) at their highest strain rates.

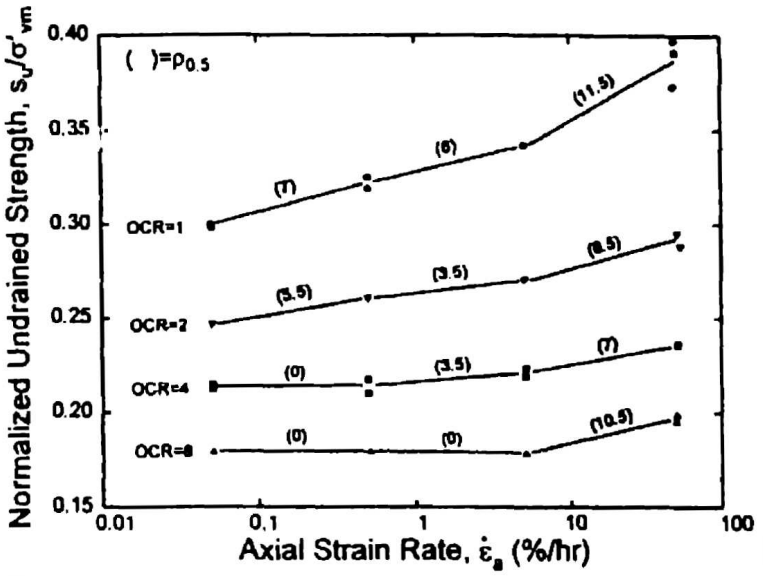

Figure 2-12 Effect of strain rate and OCR on normalised shear strength (Sheahan *et al.*, 1996)

These observations are contrary to those from Mitchell and Soga (2005) that strain rate effects will decrease with OCR due to the counter effects of dilation in over consolidated soils. Sorensen *et al*. (2007) found that over consolidation decreased the magnitude of strain rate effects in reconstituted London clay; however this is in the pre failure domain whereas the observations from Sheahan *et al*. (1996) and Lehane *et al*. (2009) are at maximum strength.

Zhu and Yin (2000) conducted monotonic triaxial compression tests in reconstituted Hong Kong marine clay at OCR 1, 2, 4 and 8 at strain rates from 0.15 to 15%/hr. The relationship between strain rate effects and OCR were inconclusive. The results from Zhu and Yin (2000) were possibly influenced by the selection of method to over consolidate the soils. The tests at each OCR were conducted at the same initial effective stress, over consolidated from different pre-consolidation pressures. This method was also chosen by Sorensen *et al*. (2007) to over consolidate their soil. In contrast, Sheahan *et al*. (1996) and Lehane *et al*. (2009) over consolidated their soils from the same pre-consolidation pressure. This may suggest that strain rate effects at maximum strength are related through the pre-consolidation pressure of over consolidated soils.

2.5 Relating undrained strain rate effects to index properties

It has been proposed, as discussed previously, that undrained strain rate effects are typically associated with fine grained soils as a result of the type of inter particle contacts and viscosity of the absorbed water of clay particles. The plasticity index has often been mentioned in the literature as an indicator of the potential rate dependence of a fine grained soil. Some models used to describe the rate dependence of undrained strength from the literature are summarised in Table 2-1. As well as plasticity index, as shown in Table 2-1 some attempts have been made to relate the rate dependence to moisture content and liquidity index.

Model	**Rate Parameter**	**Test**	**Ref.**
$(S_u)_{Field} = (S_u)_{Vane} * \gamma$	γ, See Figure 2-13	Field Vane	Bjerrum (1972)
$\frac{q}{q_{ref}} = 1 + Jv^N$	$J = I_L + 0.6$ N = 0.18	Triaxial, unconsolidated undrained tests	Gibson & Coyle (1968)
$S_U = S_{Uref}\left(1 + I_V \ln\left(\dot{\gamma}/\dot{\gamma}_{ref}\right)\right)$	$I_V = \frac{C_\alpha}{C_C}$	Rapid Pile Testing	Rodriguez *et al*. (2008)
$S_U = S_{Uref}\left(1 + I_V \ln\left(\dot{\gamma}/\dot{\gamma}_{ref}\right)\right)$	$I_V = -7 + 2.55\ln(w_L)$	Multiaxial testing	Triantafyllidis (2001)
$\frac{q}{q_{ref}} = 1 + \alpha\left(\frac{\Delta v}{v_0}\right)^\beta - \alpha\left(\frac{v_{\min}}{v_0}\right)^\beta$	$\alpha = 0.033I_P + 0.55$ $\alpha = 0.027w_L + 0.25$ $\beta = 0.2$	Statnamic Pile testing	Brown and Powell (2013)
$\frac{S_{u1}}{S_{u2}} = \left[\frac{t_2}{t_1}\right]^m$	$m = 0.036 + 0.046I_L$ $m = 0.035 + 0.00066I_p$ $m = 0.028 + 0.00060w$	Triaxial testing, Pile testing	Briaud & Garland (1985)
$\frac{\sigma_{vp}}{\sigma_{vp(ref)}} = \left[\frac{\dot{\varepsilon}}{\dot{\varepsilon}_{(ref)}}\right]^{m_\alpha}$	$m_\alpha = \frac{C_\alpha}{C_C - C_r}$	Triaxial and Oedometer testing	Soga and Mitchell (1996)
$\frac{\sigma_{vp}}{\sigma_{vp(ref)}} = \left[\frac{\dot{\varepsilon}}{\dot{\varepsilon}_{(ref)}}\right]^{m_{\alpha 2}}$	$m_{\alpha 2} = \frac{C_\alpha}{C_C}$	Oedometer	Leroueil *et al*. (1985)

Table 2-1 Strain rate effect models from studies incorporating the influence of index properties

2.5.1 Plasticity index

Bjerrum (1972) proposed the well known correction factor for field shear vane tests based on plasticity index (Figure 2-13). The rate correction from Bjerrum (1972) was developed from documented cases of the failure of embankments and excavations. Several factors other than the rate of shearing were found to influence the correction factor (Figure 2-13) including anisotropy, and chemical changes in the soils, however Bjerrum (1972) pointed to the rate of loading as the dominant factor in discrepancy between field vane strength and strength mobilised in the field.

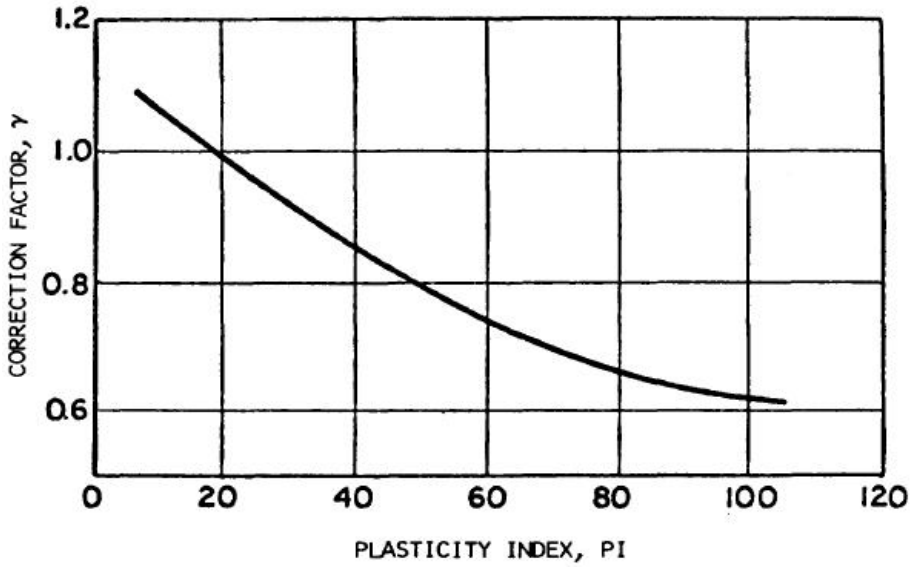

Figure 2-13 Field vane correction factor from Bjerrum (1972)

Figure 2-13 implies that strain rate effects may be expected to be greater in fine grained soils of greater plasticity index. However as highlighted by Muir Wood (2004) use of this correction factor is limited to field shear vane testing, in situations of similar characteristics from which the rate correction factor was determined. The rate correction factor from Bjerrum (1972) is also ambiguous in that the rate factor is to correct for strength derived at a time to failure of a “few minutes” and applied to embankments which are loaded over a “few months”. Nonetheless, it is still commonly referred to, and appears to be adequate for correction of strength derived from field shear vane testing (Terzahgi *et al*., 1996).

Since the work of Bjerrum (1972), other studies have also compared the strain rate effect on strength with plasticity index, and contrary to Bjerrum could not determine a

relationship between plasticity index and the strain rate effect on strength (Graham *et al*., 1983, Lefebvre and LeBoeuf, 1987). Graham *et al*. (1983) compiled results of the strain rate effect on undrained shear strength for a variety of fine grained soils, tested in triaxial compression at strain rates varying between 0.003 to 10%/hr. In comparison to Figure 2-1 as discussed previously, these strain rates are significantly lower then may be expected for a true undrained soil response. The increase in strength was linear on a semi logarithmic scale and therefore could be presented as a single rate dependent parameter (μ), describing the percentage increase in strength for a logarithmic increase in strain rate defined from a reference strain rate of 0.1%/hr. As noted by Graham *et al*. (1983) most of the results display strain rate effects on strength of between 10-15% per logarithmic increase of strain rate.

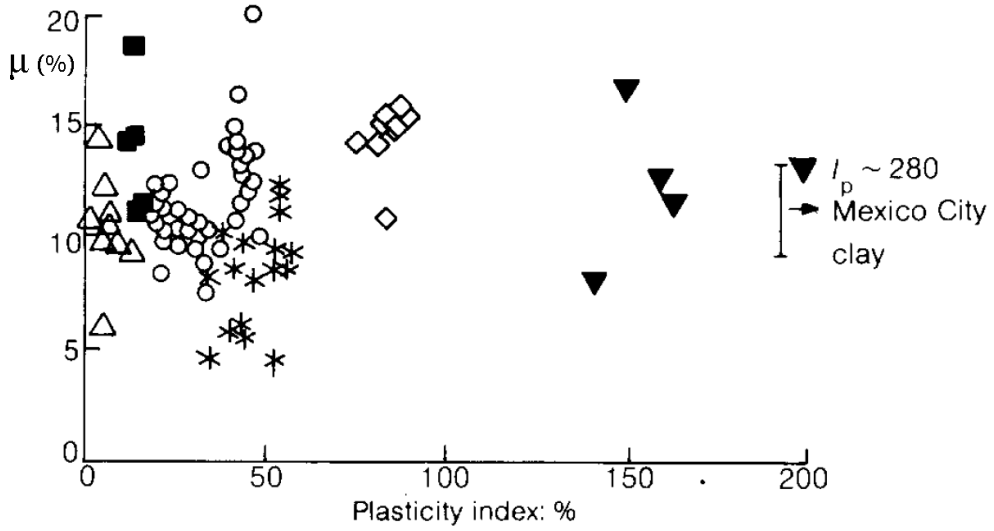

Figure 2-14 Variation of undrained rate effects for a variety of soils compiled by Graham *et al*., (1983)

Graham *et al*. (1983) also noted the significant scatter, which as shown in Figure 2-14 can vary for a soil of particular plasticity index, suggesting an influence of other factors, however this was not addressed. It is noted that much of the results compiled by Graham *et al*. (1983) were in natural soils of varying sensitivity. It is unclear as to the effect of sensitivity has on the undrained strain rate effect on strength. However Lefebvre and LeBoeuf (1987), who conducted both monotonic and cyclic triaxial testing at strain rates from 0.05 to 6000%/hr, also conducted tests on natural soils, which were tested both with inherent structure intact and when destructured by consolidation. It was found that structure had little effect on the magnitude of the

strain rate effect. This may suggest that other factors, such as the current state of the soils may influence the strain rate effects in a particular soil shown in Figure 2-14.

Figure 2-15 compiles the strain rate effect on strength from several studies to compare how the strain rate effect varies with plasticity index. Figure 2-15 compares results from Graham *et al*. (1983) and Lefebvre & LeBoeuf (1987) (destructured strain rate effects) with some other results from subsequent triaxial undrained compression studies (Sheahan *et al*., 1996, Shibuya *et al*., 1996, Soga & Mitchell, 1996, Zhu & Yin, 2000, Balderas-Meca, 2004), as well as a relationship between strain rate effects and plasticity index, taken from Triantafyllidis (2001) shown in Table 2-1. The strain rate parameter (μ) defines the percentage increase in strength for a logarithmic increase of strain rate from a reference strain rate between 0.1 to 1%/hr.

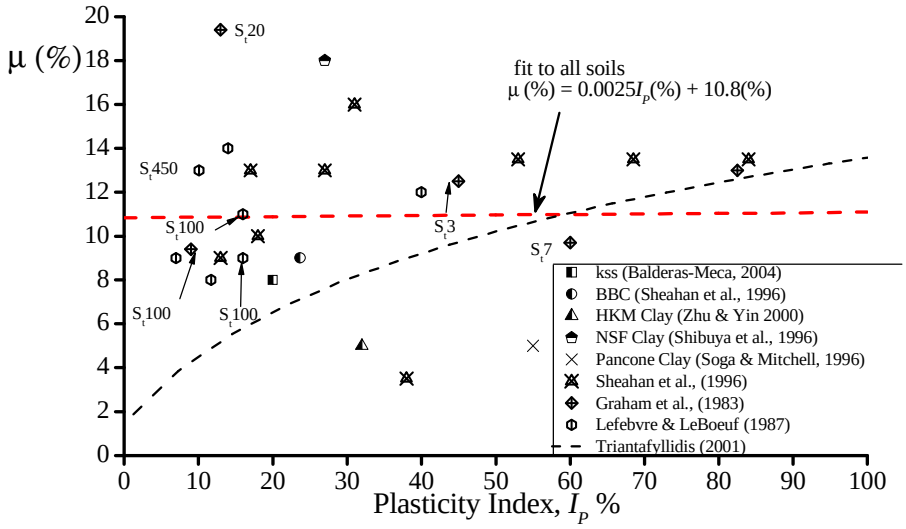

Figure 2-15 The undrained strain rate effects (%) reported in soils of different plasticity

Note; Values of sensitivity (S_t) shown adjacent to relevant data.

Most of the results in Figure 2-15 are from normally consolidated soils. Linear regression of the data shows that strain rate effects do not vary with plasticity index. The results in Figure 2-15 display scatter, and for a particular plasticity index the strain rate effects on strength can vary significantly. Most of the values in Figure 2-15 fall between 8 and 14%. Linear regression shows the value of the strain rate effect is

10.8% which is consistent with the proposed value of 10% from Kulhawy and Mayne (1990) who compared the strain rate effects of 26 natural soils from various studies.

Also included for comparison in Figure 2-15 is a proposed relationship from Triantafyllidis (2001) which relates the liquid limit (w_L) to the strain rate effect on strength (through a proxy term; the viscosity index, I_V);

$$I_V = -7 + 2.55\ln(w_L) \quad (2\text{-}2)$$

The relationship from Triantafyllidis (2001) was converted to plasticity index using the relationship from the A-line as per Casagrande (1947) shown in Equation 2.3;

$$I_P = 0.73(w_L - 0.2) \quad (2\text{-}3)$$

Equation 2-2 from Triantafyllidis (2001) is based on work by Leinenkugel (1976) who conducted biaxial testing in saturated cohesive soils at various rates. Equation 2-2 predicts increasing strain rate effects at higher plasticity index which is consistent with Bjerrum (1972), but it does not reflect general trends shown by other soils in Figure 2-15. The relationship from Triantafyllidis (2001) also does not tend to agree with the magnitude of strain rate effects from other studies shown in Figure 2-15.

The relationship between the strain rate effect and the liquid limit from Triantafyllidis (2001) and Kreig (2000) which is shown in Figure 2-16, are almost identical. The relationship proposed by Kreig (2000) in Figure 2-16, which related the ratio of secondary compression (C_α) to the primary compression index (C_C), is the same as that used by Leroueil *et al*. (1985) to describe the effect of strain rate on pre-consolidation pressure. Therefore the relationship from Triantafyllidis (2001) shown in Equation 2-2 could be more applicable to strain rates where creep effects may be more important to the strain rate on strength. Note the relationship from Kreig (2000) in Figure 2-16 has been used successfully to back figure the static capacity of piles from rapid loading tests (Rodriguez *et al*., 2008).

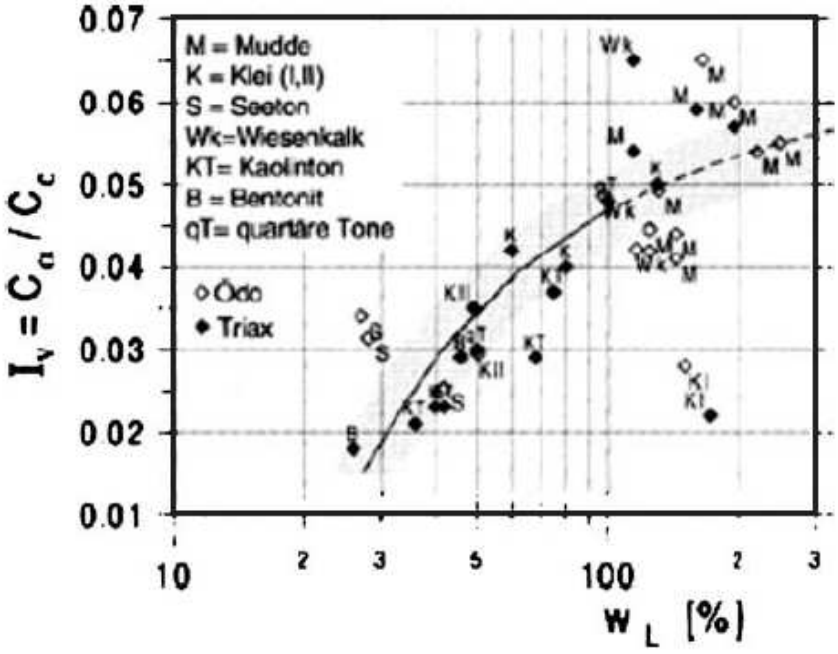

Figure 2-16 Variation of viscosity index (C_α/C_C) with liquid limit (Kreig, 2000)

The relationship between the pre-consolidation pressure and strain rate during oedometer tests has been addressed by Leroueil *et al*. (1985) amongst others including Graham *et al*. (1983) and Soga and Mitchell (1996). As mentioned, Leroueil *et al*. (1985) related the effect of strain rate on the pre-consolidation pressure to ratio of secondary compression to the compression index. Both the works of Leroueil *et al*. (1985) and Soga and Mitchell (1996) described the strain rate effect on the pre-consolidation pressure in an exponential form (Table 2-1). Soga and Mitchell (1996) postulated that strain rate effects on undrained strength and the pre-consolidation pressure may be described by a single mechanism of time dependent softening, i.e. the compression indices can be used to describe the increase in undrained strength with strain rate. Rattley *et al*. (2011) verified the correspondence between the increases in strength with strain rate and the ratio of secondary to primary compression index in direct simple shear testing at strain rates from 0.002-300%/hr in Angola marine clay. Note Angola marine clay is a structured (sensitive) soil.

To compare the theory from Soga and Mitchell (1996) with reported strain rate effects on undrained strength the compression indices are converted to plasticity index by making some assumptions between the relationships between plasticity and the

compression index. From Muir Wood (1990) the compression index can be related to the plasticity index by;

$$C_c = 0.5 G_S I_p \quad (2\text{-}4)$$

From Muir Wood (1990), assuming G_S = 2.7, the primary compression index is related to the recompression index by assuming that;

$$\Lambda = \frac{\lambda - \kappa}{\lambda} = 0.8 \quad (2\text{-}5)$$

From Kulhawy and Mayne (1990) the recompression index (C_r) can be related to the compression index (C_C) as;

$$C_r = C_C (1 - \Lambda) \quad (2\text{-}6)$$

This can then be rewritten as;

$$C_r = \frac{I_P}{370} \quad (2\text{-}7)$$

By assuming the relationship from Mesri and Castro (1987) shown in Equation (2-8) the values of primary, secondary and the reload-unload compression indices can be obtained and related to plasticity index;

$$m_{\alpha 2} = \frac{C_\alpha}{C_C} = 0.04 \pm 0.01 \quad (2\text{-}8)$$

From the Equation 2-4 to 2-8 described above, the range of strain rate exponent, *m* (as per Soga and Mitchell (1996), Table 2-1) is from 0.0375 to 0.0625. Included in Figure 2-17 are results of the effect of rotation rate using a shear vane (rotation rates typically between 6-600°/min) from Biscontin and Pestana (2001). The relationship proposed by Kreig (2000) and another relationship between the strain rate exponent

on undrained strength from Briaud and Garland (1985) are also included in Figure 2-17.

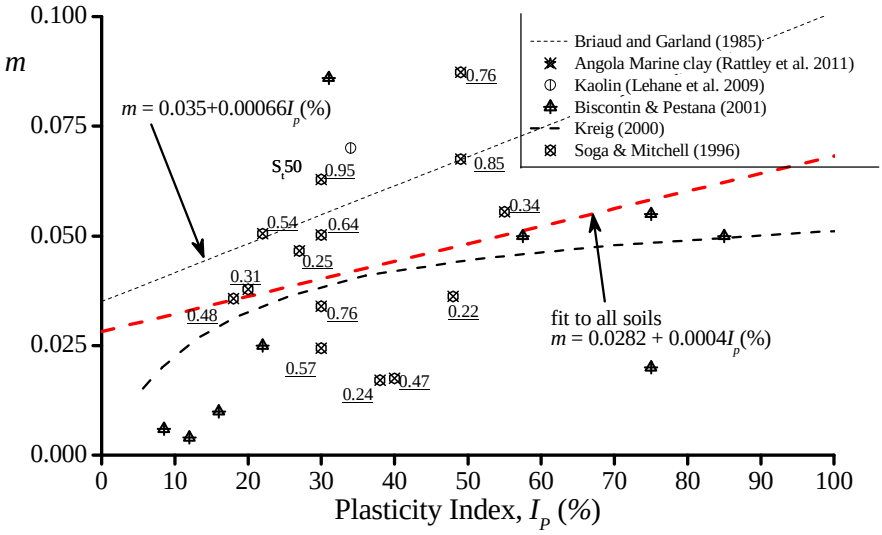

Figure 2-17 The undrained strain rate effects on strength (exponential form) reported in the literature for soils of differing liquidity index

Note the values of metastability are shown underlines adjacent to relevant data, e.g. 0.50

The relationship from both Kreig (2000) and Soga and Mitchell (1996), (m = 0.0375 – 0.0625) when converted to plasticity index, tend to a narrow range in comparison with other results shown in Figure 2-17 and do not relate well to the magnitude of strain rate effects on undrained strength from other studies. It should be noted however that Soga and Mitchell (1996) who also compiled results of the strain rate effect on strength did mention that the state of soil can be important to the strain rate effect, and strain rate effects tended to increase with metastability index, defined as the difference in liquidity index between the soil at the pre-consolidation pressure to the fully destructured (remoulded) state;

$$MI = I_{LP} - I_{L0} \qquad (2\text{-}9)$$

The values of metastability index are also presented in Figure 2-17. Increasing metastability index corresponds to higher strain rate effects, and as these occur over a

relatively narrow range of plasticity, this suggests other factors have some influence on the magnitude of the strain rate effect.

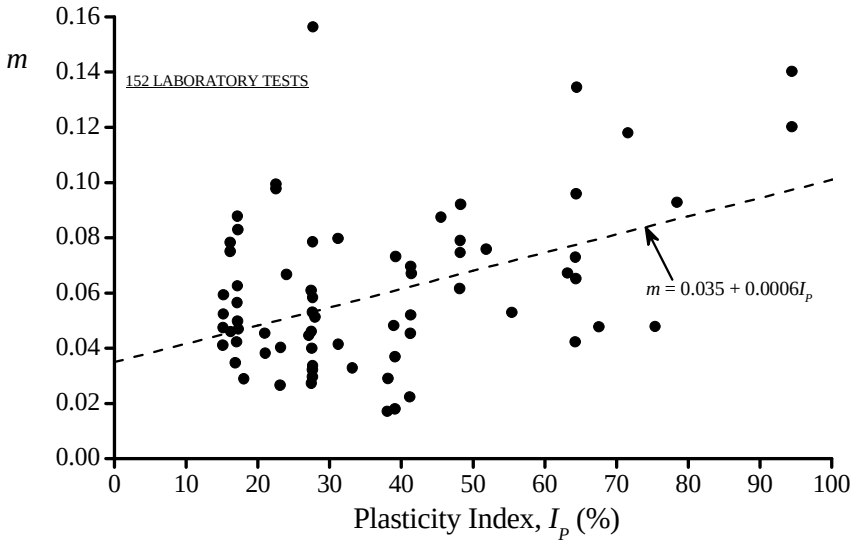

Figure 2-18 Variation of the undrained strain rate effect on strength (exponential form) with plasticity index (Briaud and Garland, 1985)

Therefore it seems from Figure 2-15 that plasticity index does not affect the strain rate effect on undrained strength. It is also apparent from Figure 2-17 that strain rate effects on other aspects of soil behaviour such as the pre-consolidation pressure may not be directly comparable (in terms of magnitude) to the effect of strain rate on undrained strength. This is particularly clear when comparing the relationships from Kreig (2000) and Briaud and Garland (1985) who tend to display much larger strain rate effects. Briaud and Garland (1985) compared results of strain rate effects from over 152 laboratory tests and 61 pile tests. There was significant scatter noted by Briaud and Garland (1985) in development of their relationship with plasticity index (R^2=0.18), as shown Figure 2-18. It was also noted there is significantly less data available for comparison at higher plasticity index which may devalue their proposed relationship.

2.5.2 Moisture content and liquidity Index

Because the magnitude of strain rate effects on undrained strength for a given plasticity index has been shown to vary significantly, this would suggest other factors

may influence the strain rate effect on strength. Because plasticity index is an indicator of the properties of soil (independent of state), studies have focused on the effect of moisture content (for a given soil), which reflects the current state of soil, and its liquidity index, which scales the moisture content in a meaningful way between its relative Atterberg limits (Muir Wood, 1990).

Brown and Hyde (2008a) conducted rapid load tests in a stiff Grimsby clay on a pile instrumented with strain gauges at various sections throughout the depth of the pile. Velocities of pile tests ranged from 0.01mm/s to 364mm/s. A strong correlation was found between the measured rate effect on pile shaft resistance along segments of the pile which increased with increasing moisture content (Figure 2-19).

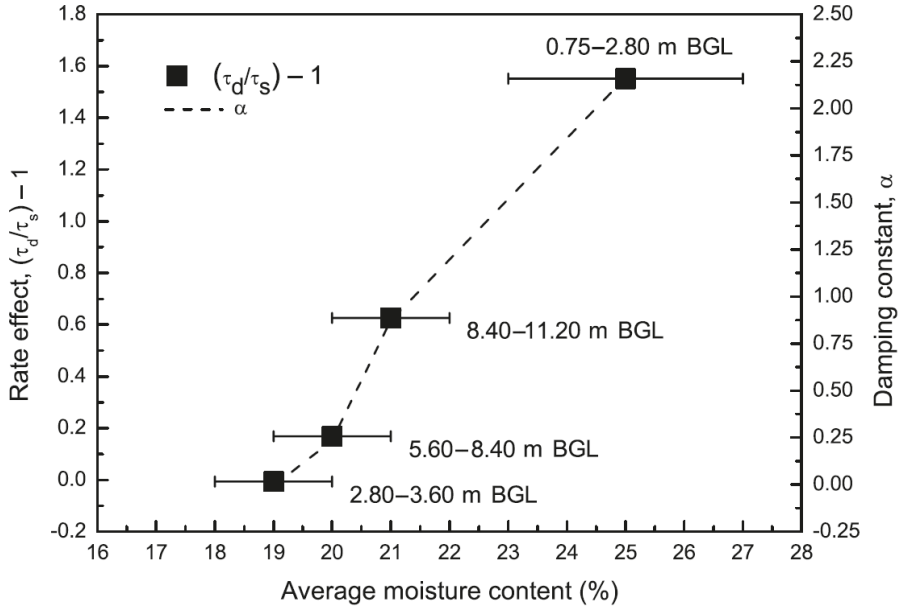

Figure 2-19 Variation of rate effects with moisture content for Rapid load testing of piles in Grimsby Till (Brown and Hyde 2008)

The observation that strain rate effects on strength increase with moisture content is consistent with results presented in Figure 2-20 from Briaud and Garland (1985) (who again noted significant scatter in the proposed relationship, R^2=0.323). Diaz-Rodriquez *et al*. (2009) also confirmed this finding with monotonic triaxial testing in Mexico City soil at strain rates from 1 to 800%/hr. Monotonic triaxial tests from Chow and Airey (2013) also found a clear relationship between the strain rate effect in Kaolin with increasing moisture content at strain rates from 5 to 480%/hr.

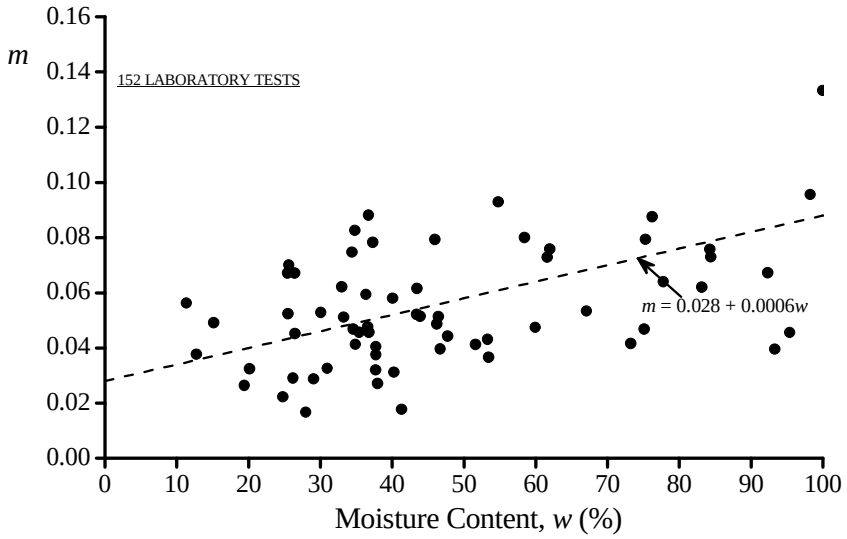

Figure 2-20 Variation of the undrained strain rate effect on strength (exponential form) with moisture content (Briaud and Garland, 1985)

The relationship proposed by Briaud and Garland (1985) shown in Figure 2-20 presumably reflects the likelihood that soils of higher plasticity index will potentially exist in situ at higher moisture content. It is an interesting observation that strain rate effects on undrained strength increase with moisture content as the viscosity of soils has been shown to decrease with increasing moisture content as discussed in Section 2.4.2. Therefore, although a soil of lower moisture content has a higher viscosity, the strain rate effect on strength is lower. Increasing moisture content (for a given normally consolidated soil) corresponds to lower effective stress and thus lower static strength, which is consistent with observations on strain rate effects from Casagrande and Shannon (1948). As viscosity is a function of effective stress (the yield stress) it appears the ratio of viscosity to the yield stress reduces as moisture content reduces, subsequently reducing the strain rate effect on strength.

With increasing moisture content in a given soil the liquidity index increases. Figure 2-21 from Briaud and Garland (1985) presents a relationship between liquidity index and the strain rate effect expressed as an exponent *m*. Much of the scatter noted in the relationship between plasticity index and the strain rate effect (Figure 2-19) from Briaud and Garland (1985) appears to have reduced in Figure 2-21, although the coefficient of determination of a correlation (R^2=0.24) has not increased greatly. Thus

Figure 2-21 merely gives a tentative suggestion that liquidity index may be a good indicator of the strain rate effects on undrained strength.

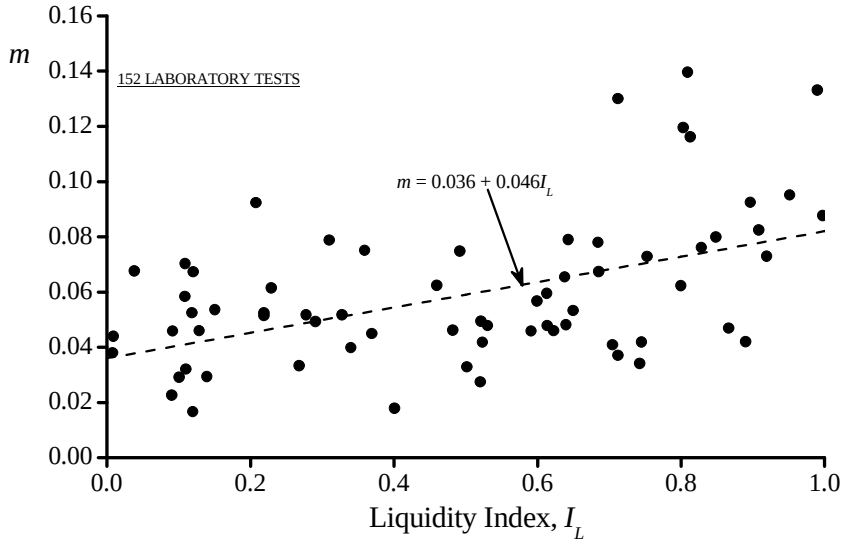

Figure 2-21 Variation of the undrained strain rate effect on strength (exponential form) with liquidity index (Briaud and Garland, 1985)

The most comprehensive report of the undrained strain rate effect on strength incorporating both soils of different plasticity index and moisture content was conducted by Gibson and Coyle (1968). In their study four fine grained soils were tested in undrained unconsolidated compression tests. The soils were loaded using a drop hammer from various heights, allowing testing to be conducted at velocities of deformation from standard unconsolidated undrained strain rates up to 3600mm/s ($15x10^6$%/hr). The resulting rate effect on strength was defined as a damping parameter J, which was found to relate well to liquidity index (Figure 2-22).

The findings from Gibson and Coyle (1968) reflect those from previously mentioned studies. To compare these findings Figure 2-23 is compiled, which compares data from various studies in Figure 2-23 (a) as the percentage increase per logarithmic increase in strain rate and (b) as exponential form.

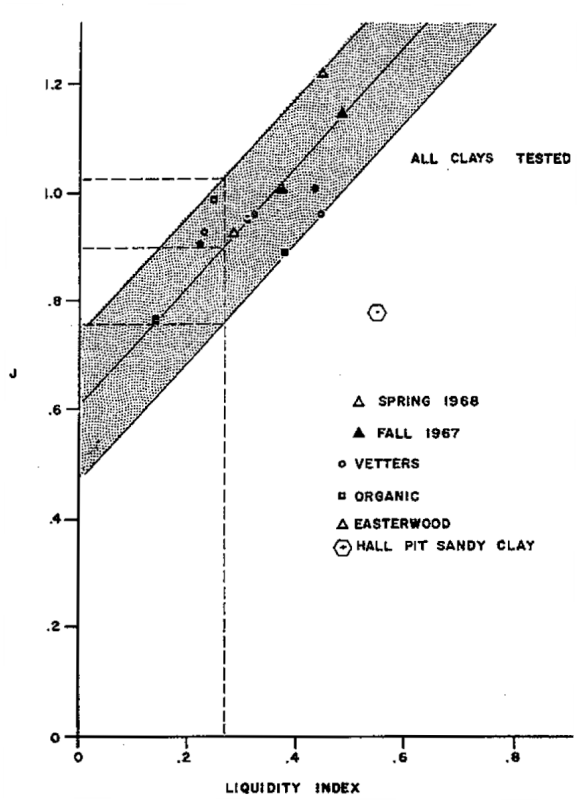

Figure 2-22 Relationship between liquidity index and rate coefficient *J* (Gibson and Coyle, 1968)

The results in Figure 2-23 display increasing strain rate effects with liquidity indices. With the exception of Mississippi and Pancone clay in Figure 2-23 (a) the soils tend to similar strain rate effects when compared with liquidity index. In Figure 2-23 (b) the three separate studies of Briaud and Garland (1985), Soga and Mitchell (1996), and Gibson and Coyle (1968) each show similar rate of increase of strain rate effects with strength with liquidity index however the magnitude of each study differs. The magnitude of the strain rate effects may differ depending on the interpretation of results from each study, or due to different techniques used to define the strain rate effects, however it is encouraging to note that each display a similar increase in strain rate effects on strength with increasing liquidity index. The metastability index of each of the soils from Soga and Mitchell (1996) in Figure 2-23 also appear to increase with liquidity index, possibly suggesting liquidity index has greater influence on strain rate effects then credited by Soga and Mitchell (1996).

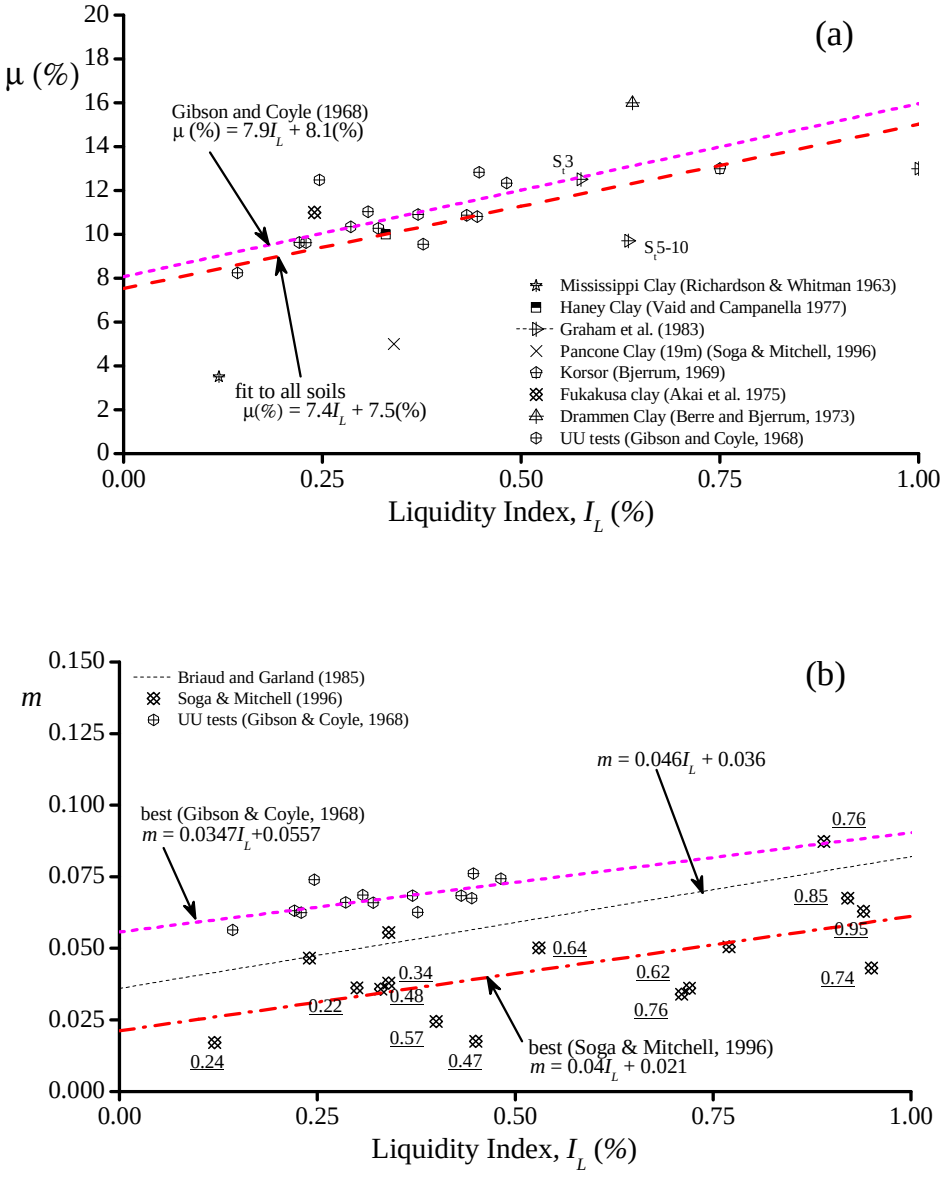

Figure 2-23 Effect of liquidity index on the rate effect for undrained strength (a) Percentage increase with log strain rate (b) strain rate effect in exponential form

2.6 Strain rate effects at small strains

The behaviour of soil at small strains is important for applications of geotechnical engineering such as those shown in Figure 2-24. Further to this the dynamic behaviour of soils at small strains is also important, particularly for events such as earthquakes. When these occur in areas of high plasticity clay, such as Mexico City, the linear nature of these soils can result in amplification of ground motions (Dobry and Vucetic, 1987).

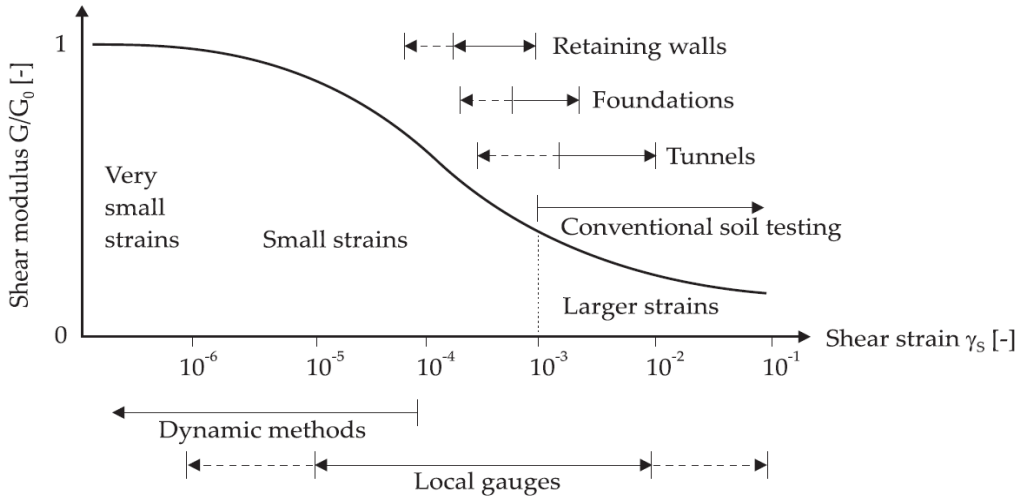

Figure 2-24 Variation of characteristic stiffness of soils with shear strain (Atkinson, 2000)

The advent of high quality strain measurements from local instrumentation developed by Burland and Symes (1982), Jardine *et al*. (1984) and Clayton and Khratush (1986) among others, allowed investigators to better determine strains without interference from triaxial compliance issues such as bedding errors. The main benefit of local instrumentation was increased accuracy at strains below 0.1%, which is typically the limit of external triaxial instrumentation. This has enabled quantification of the non-linear behaviour of soils at very small and small strains as shown in Figure 2-24.

2.6.1 Non linear behaviour of soils at small strains (<1%)

The behaviour of soils at strains approximate to those in Figure 2-24 has been extensively studied since the development of high quality strain instrumentation. Kokusho *et al*. (1982), Vucetic and Dobry (1991), Darendeli (2001) and Vardanega and Bolton (2011) have related the normalised shear modulus degradation curve to plasticity index and effective stress. However the effect of strain rate on stiffness at small strain is not well understood, and has rarely received attention.

The following sections describe the current understanding of the non linear behaviour of soils, with focus on particularly important aspects. To describe the non linear behaviour of soil, Jardine (1992) proposed the concept of kinematic sub-yield

surfaces, defining separate characteristics of non linear soil behaviour which are highlighted in comparison to a non linear stiffness degradation curve in Figure 2-25.

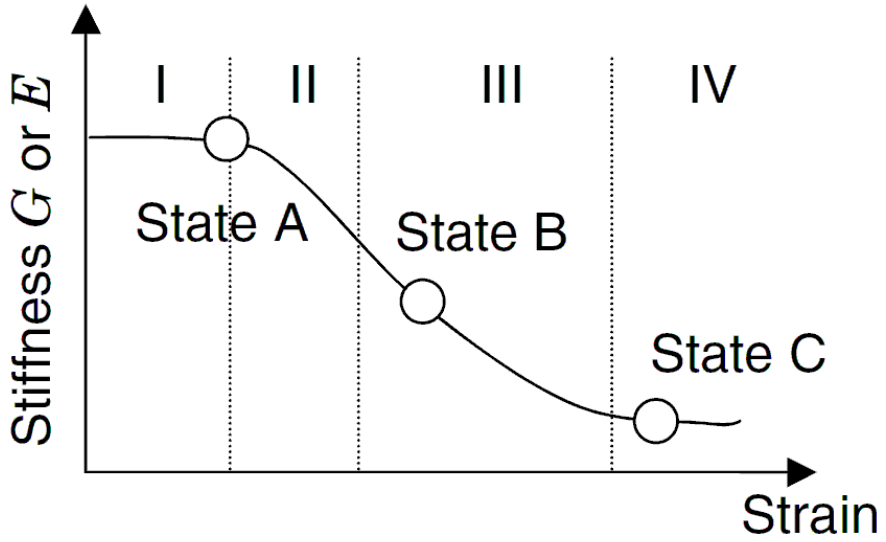

Figure 2-25 Zones of deformation characterisation, Soga and Mitchell (2005) after Jardine (1992)

I. The linear elastic zone; limited by the elastic threshold strain (Vucetic, 1994, Shibuya *et al*., 1996). Within this zone the soil particles do not slide relative to each other and the stiffness of the soils is determined from the particle packing of the solids. The stiffness remains fully elastic within this zone.

II. Recoverable zone; The soil exhibits some non-linear behaviour with increasing strain, however the degradation is fully recoverable. The boundary defining the recoverable zone is defined as the strain at which plastic strains begin to develop, as evidenced by volumetric strains, and is thus known as the volumetric threshold strain (Vucetic, 1994).

III. The pre-yield plastic zone; The zone at which irrecoverable strains begin (volumetric threshold strain) and are increasingly more important as the soil particles slide relative to each other, breaking force chains and continuously reforming to accommodate stress change (Mitchell and Soga, 2005).

IV. The full plastic zone; Signified by a distinct kink in the stress strain curve as plastic strains fully develop. If the soil reaches critical state it is considered to have reached failure (Mitchell and Soga, 2005).

The strain rate effects in the fourth zone in Figure 2-25 have been discussed previously. The other three aspects of soil non linearity, the initial elastic stiffness, the linear elastic threshold strain which defines the boundary between zone I and II (Figure 2.25), and the volumetric threshold strain which is the boundary between zone II and III (Figure 2-25) are discussed below with regard to their respective dependence on strain rate.

2.6.2 Effect of strain rate on the initial elastic modulus, G_{max}

The initial elastic stiffness and its relationship with strain rate have been investigated in numerous studies. Tatsuoka *et al.* (1997) summarised the strain rate dependence of initial Young's modulus for a variety of materials including kaolin (Figure 2-26). Tatsuoka *et al*. (1997) explained that the rate dependency of the initial Young's modulus appears to be greater at lower strain rates. This likely reflects findings from Sorensen *et al*. (2010) that creep can affect the initial elastic stiffness.

Leroueil and Marques (1996) also summarised results from several studies on fine grained soils. They noted strain rate effects on the initial elastic shear modulus (at close to very small strains) are less than 6% per logarithmic increase in strain rate, and have a tendency to decrease at very small strains less than 0.001%. It was also noted that coarse grained soils display lower strain rate effects in comparison to fine grained soils. Similarly Vucetic and Tabata (2003), who conducted tests using a simple shear device found the initial shear modulus to increase by between 2-6% per logarithmic change in strain rate for clayey soils, whereas for sandy soils this effect was between 0.5-3%. From monotonic and cyclic torsional shear tests in Vallericca clay, d'Onofrio *et al*. (1999) found the initial shear modulus (G_{max} or G_0) to increase by 5% per logarithmic change in strain rate over a limited range of strain rates, however at higher strain rates their results suggested an upper bound to the rate dependence of the initial elastic stiffness. The data from d'Onofrio *et al*. (1999) was shown to agree with the SAB (Simple Asymptotic Body) model from Di Benedetto and Tatsuoka (1997) (Figure 2-27). Notably Tatsuoka and Shibuya (1992) found no rate dependence of the initial modulus of kaolin at strain rates between 0.12%/hr and 30%/hr.

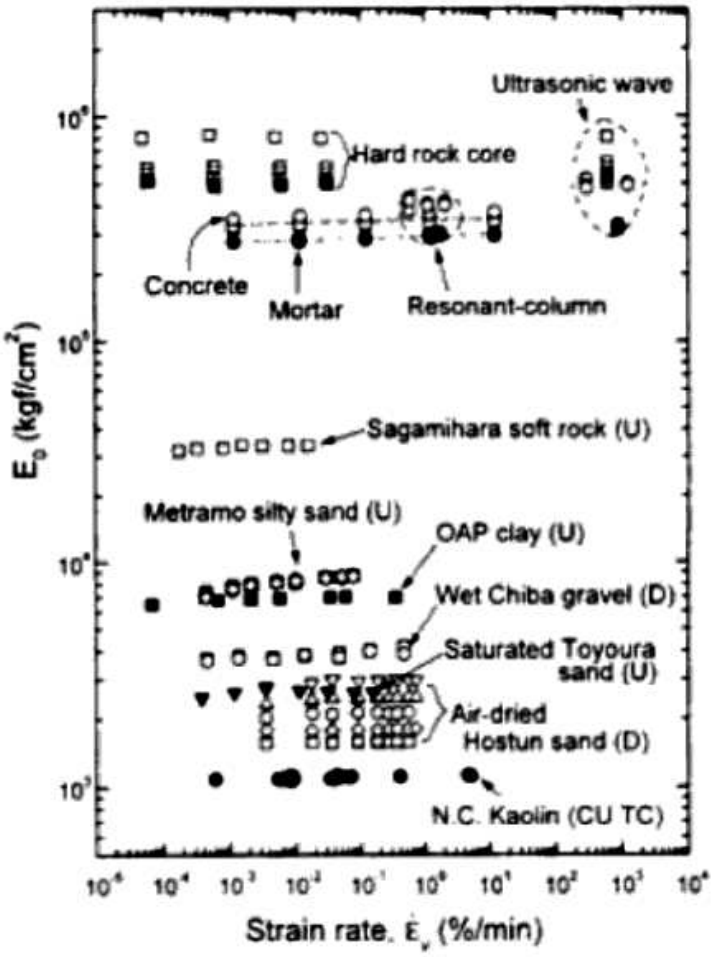

Figure 2-26 Variation of initial elastic one dimensional stiffness with strain rate for variety of materials (Tatsuoka *et al.*, 1997)

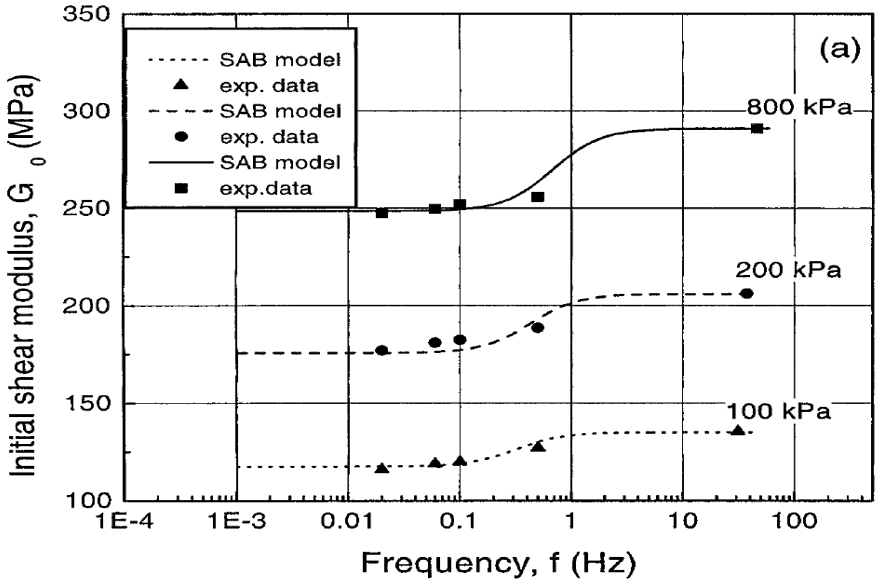

Figure 2-27 Variation of initial elastic shear modulus with frequency (d'Onofrio *et al.*, 1999)

Figure 2-28 from Mukabi (1995) presents the variation of stiffness with strain rate from cyclic triaxial compression tests in both undrained and drained conditions. Two levels of strain are compared in Figure 2-28, and for both the undrained and drained tests the stiffness is relatively similar, particularly at higher strain rates. This appears to confirm findings discussed above that for higher strain rates the rate dependence of the initial elastic stiffness disappears.

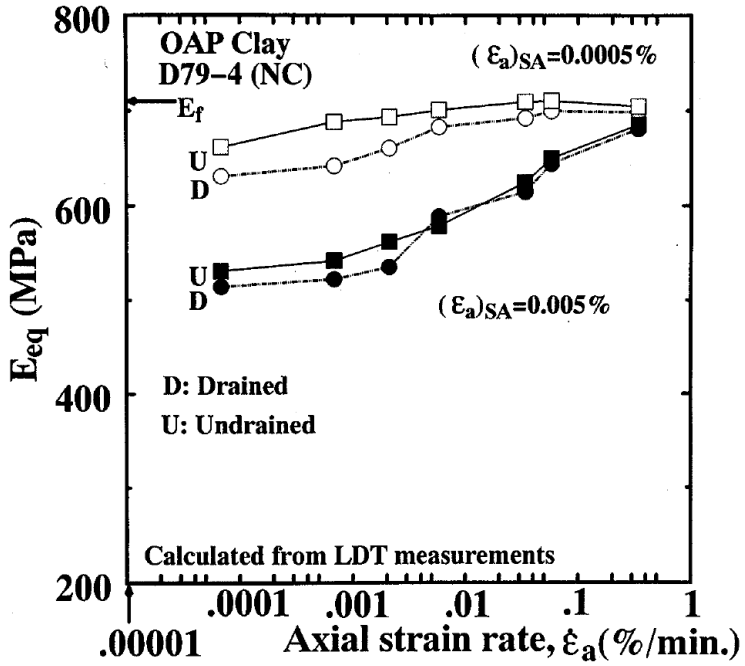

Figure 2-28 Stiffness at different strains of OAP clay at increased strain rate in both drained and undrained triaxial monotonic compression testing (Mukabi, 1995)

2.6.3 Effect of strain rate on the linear elastic threshold strain

Figure 2-29 presents stiffness degradation curves from three different strain rate tests in NSF clay from Shibuya *et al*. (1996). Clearly shown in Figure 2-29 is an effect of strain rate on the linear elastic threshold strain.

The strain rate effect on the linear elastic threshold has shown to be similar in both reconstituted Boston blue clay and reconstituted NSF clay by Santagata *et al*. (2007) and Shibuya *et al*. (1996) respectively. For both studies the elastic threshold strain increased in proportion to the square root of the strain rate. This is despite the large difference in strain rates, which were 0.5 to 4%/hr (Santagata *et al*., 2007) and 0.7 to

84%/hr (Shibuya *et al.*, 1996). In comparison with dynamic strain rate tests these strain rates are relatively low (Section 2.2.2). However Lo Presti *et al.* (1996) who conducted monotonic, cyclic triaxial as well as resonant column tests in Augusta clay at strain rates from 4%/hr up to 48,000%/hr, shows a linear elastic threshold relating to strain rate through an exponent of approximately 0.2. This indicates strain rate effects on the linear elastic threshold are comparatively higher at lower strain rates. It may also indicate a limit to the linear elastic threshold strain at higher strain rates.

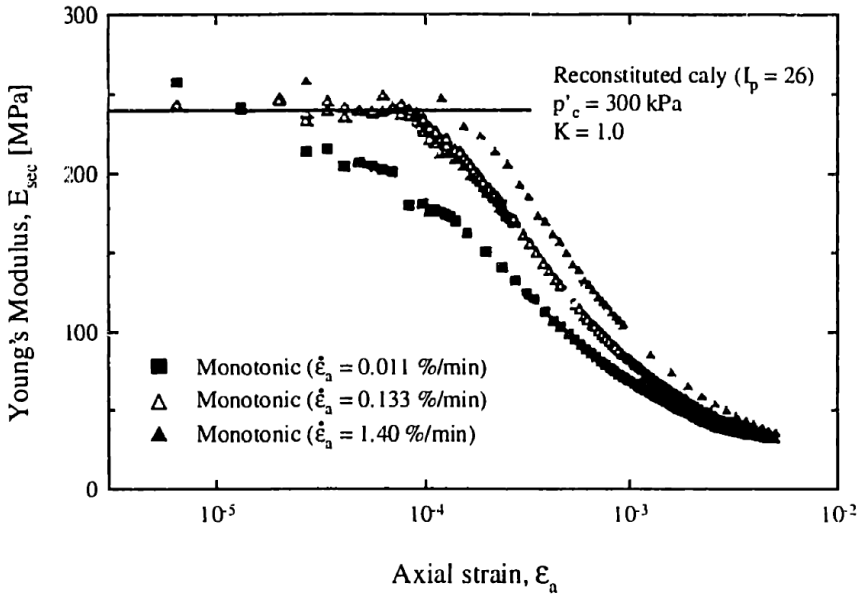

Figure 2-29 Effect of strain rate on stiffness in triaxial compression (Shibuya *et al.*, 1996)

2.6.4 Effect of strain rate on the volumetric threshold strain

There is very little information regarding the volumetric threshold strain at high strain rates. This is maybe due to difficulty in measuring the volumetric threshold strain even in static strain rate conditions (Santos and Correia, 2000). Measurement of excess pore pressures at high strain rate may be further complicated due to non-equalisation of excess pore pressures at higher strain rates. This may discourage previous research from analysing the volumetric threshold strain at high strain rate. For example Shibuya *et al.* (1996) and Santagata *et al.* (2007) both report excess pore pressures but do not compare the corresponding volumetric threshold strain which appears to vary significantly with strain rate. Santagata *et al.* (2007) appears to show a volumetric threshold strain quite close to the elastic threshold at strain rate tests between 0.5 to 4%/hr in reconstituted Boston blue clay. In contrast, results reported at

high strain rates from Shibuya *et al*. (1996) whom conducted tests in NSF reconstituted clay at strain rates from 0.7 to 84%/hr appear to display much greater degradation of stiffness at high strain rate (apparently close to failure) before a response in excess pore pressures is measured. Both the aforementioned studies were in normally consolidated soils tested in monotonic triaxial compression.

Lo Presti *et al*. (1996) tested various clays in both cyclic and monotonic triaxial compression, as well as with resonant column tests at strain rates from 4 to 48,000%/hr. It was noted the volumetric threshold strain increased with strain rate, yet no observations were made regarding the corresponding value of normalised shear modulus at this strain. It was noted by Lo Presti *et al*. (1996) that the possible effects of the magnitude of excess pore pressures on stiffness were negligible. These pore pressures were measured at the base of the samples, and thus may be subject to end effects. Lo Presti *et al*. (1996) did however note excess pore pressures decreased in magnitude with increasing strain rate.

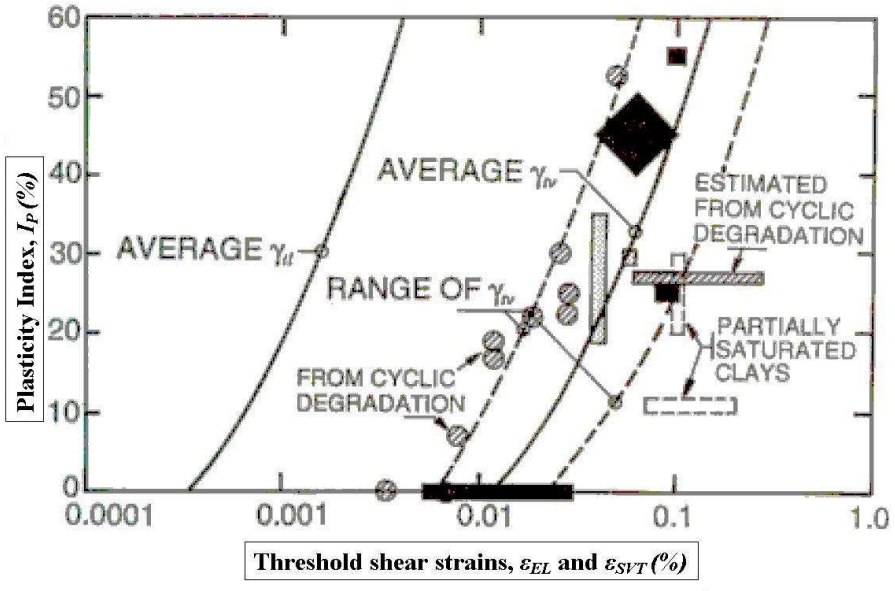

Figure 2-30 Variation of elastic and volumetric threshold strains with plasticity (Vucetic, 1994)

Thus there is little information on the effect of strain rate on the volumetric threshold strain; other then that it may be expected to increase. Vucetic (1994) compiled a range of average volumetric threshold strain rates based on plasticity index from a variety of studies (Figure 2-30). Much of the information compiled in Figure 2-30 appear to be

from cyclic triaxial, resonant column, and torsional shear tests, and may include some degree of strain rate dependence. The significance of the relationship between plasticity index and volumetric threshold strain is highlighted when the values of the volumetric threshold are related to the classical shear modulus degradation curves from Vucetic and Dobry (1991) in Figure 2-31.

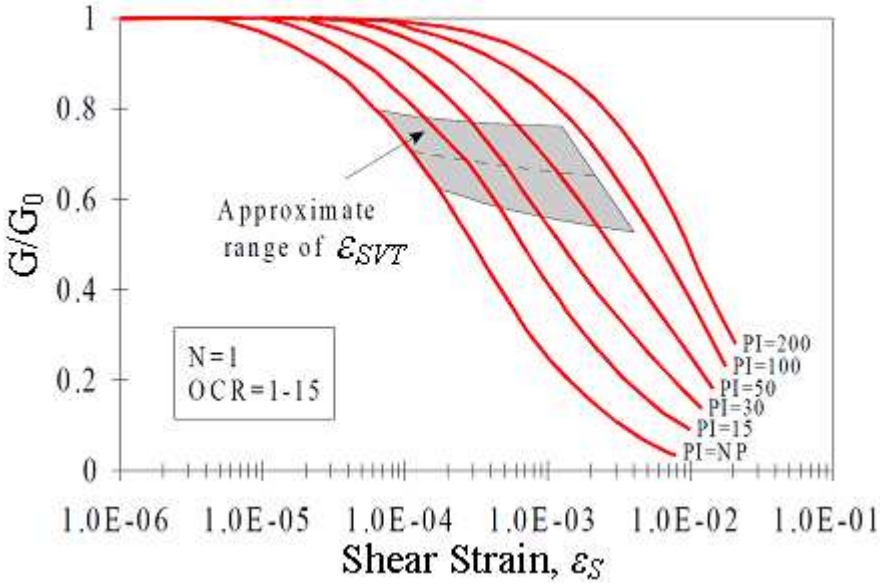

Figure 2-31 Stiffness degradation curves from Vucetic and Dobry (1991) with overlain volumetric threshold strain from Vucetic (1994), as per Santos and Correia (2000)

Figure 2-31 shows the corresponding volumetric threshold strain is approximately horizontal on the shear modulus degradation curve. As mentioned by Vucetic (1994) this could mean that regardless of soil type, the shear modulus reduces by the same amount before the volumetric threshold strain is reached. The range of normalised shear modulus at the volumetric threshold strain shown in Figure 2-31 is consistent with Ishihara (1996).

As was discussed previously the volumetric threshold strain increases with strain rate, however it is unknown how the volumetric threshold strain (ε_{SVT}) at the corresponding value of normalised shear modulus would be affected by strain rate. If it increased with strain rate (G/G_0 at ε_{SVT}) this would suggest that increased strain rate induces a more plastic response from soils, whilst the opposite would suggest higher strain rates induce a more "elastic" response. However it could also be possible strain rate does not affect the value of normalised shear modulus at the volumetric threshold.

Unfortunately there doesn't appear to be any further development of the relationship between plasticity index (or other factors) and the corresponding normalised shear modulus in the literature. Information on this matter could add value to the understanding of the plastic behaviour of soils at small strains.

2.6.5 Effect of strain rate on stiffness

The effect of strain rate on the shear modulus degradation is generally described with a strain rate coefficient of the form shown in (Equation 2-10).

$$\alpha(\varepsilon_S) = \frac{G\left(\varepsilon_S, \dot{\varepsilon}_{high}\right) - G\left(\varepsilon_S, \dot{\varepsilon}_{low}\right)}{\left(\log \frac{\dot{\varepsilon}_{high}}{\dot{\varepsilon}_{low}}\right).G\left(\varepsilon_S, \dot{\varepsilon}_{ref}\right)} \qquad (2\text{-}10)$$

Where ε_S is shear strain. Note; Equation 2-10 is defined at equal levels of shear strain (ε_S). Yong and Yapp (1969) quantified the strain rate coefficient $\alpha(\varepsilon_S)$ as the change in stiffness with a logarithmic cycle change in strain rate, normalised by a reference stiffness which is defined at a reference strain rate ($\dot{\varepsilon}_{ref}$).

Lo Presti *et al*. (1996) and Tatsuoka *et al*. (1997) brought together results from several studies (Figure 2-32). Note that Figure 2-32 presents data from studies using a variety of laboratory methods including triaxial compression, both monotonic and cyclic, and torsional shear.

As shown in Figure 2-32 the strain rate coefficient (Equation 2-10) typically increases with level of shear strain. This also agrees with findings of Akai *et al*. (1975), whom also found at higher strains the strain rate coefficient tended to a constant value. As strains approach 10^{-5} the strain rate coefficient becomes very small (Tatsuoka *et al*., 1997). This reflects the strain rate independence of the initial elastic shear modulus as discussed previously. Lo Presti *et al*. (1996) mentioned that the strain rate coefficient tended to increase more significantly with strain from approximately 0.01% upwards

as shown in Figure 2-32. This could appear to represent the interaction with the volumetric threshold strain as described earlier from Vucetic (1994).

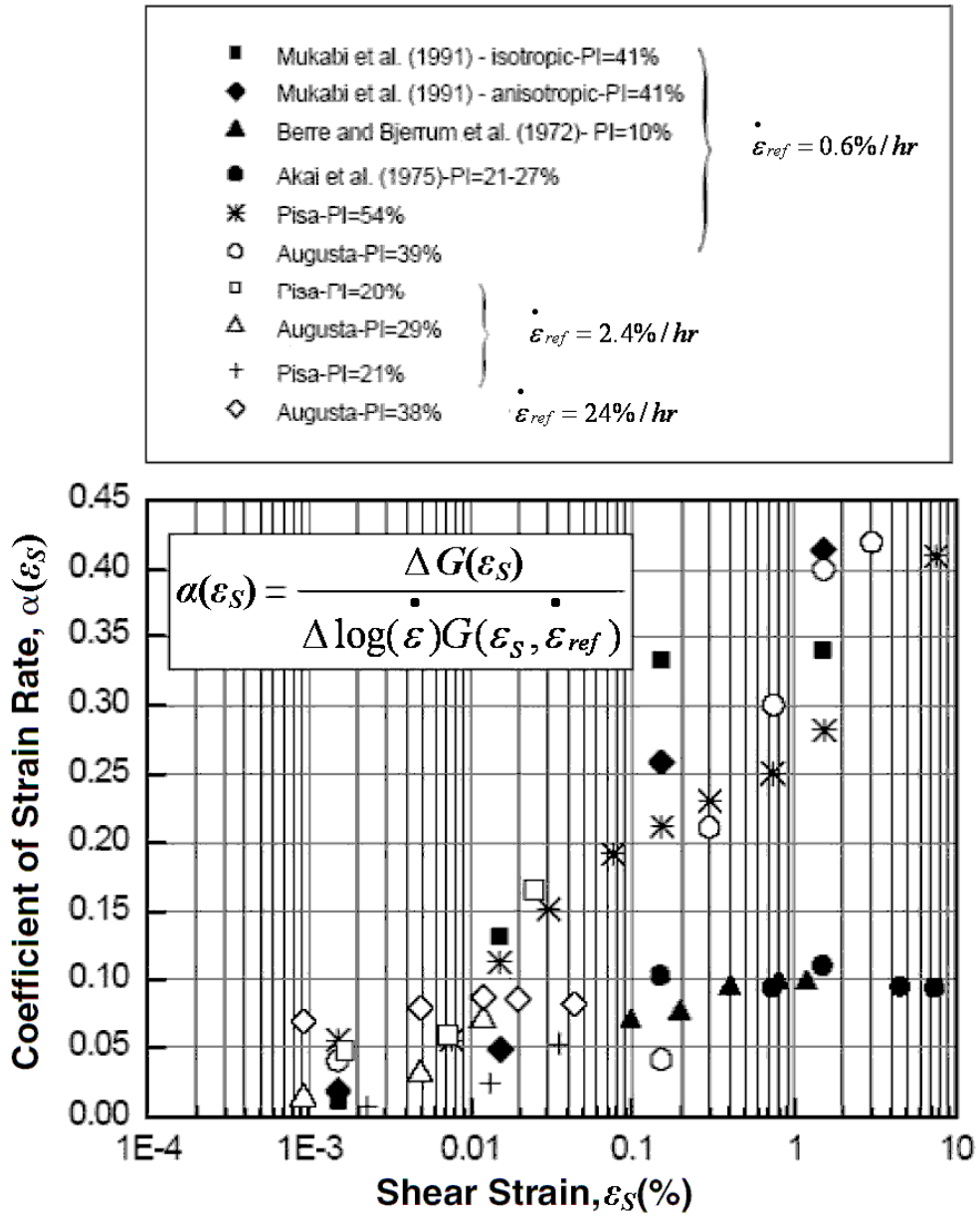

Figure 2-32 Strain rate coefficient from various soils (Lo Presti *et al.*, 1996)

Lo Presti *et al*. (1996) also mentioned that plasticity index appeared to affect the strain rate coefficient (Figure 2-32), however there was not enough data to describe a relationship. It was noted that the strain rate dependence of soil stiffness is dependent on the viscosity of the soil; a larger plasticity index is expected to display a greater effect of strain rate (Lo Presti *et al*., 1996).

2.7 Triaxial studies on strain rate effects

This section reviews and discusses some previous investigations into undrained strain rate effects with triaxial systems. Some key aspects of each study are highlighted in the historical review to give a perspective of previous investigations of strain rate effects.

Some difficulties with high strain rate testing are also highlighted. In particular the effects of non-uniform distribution of stress and strain during triaxial testing are discussed.

2.7.1 Historical review of high rate testing with triaxial based apparatus

Casagrande and Shannon (1948) conducted one of the first triaxial based studies into the relationship between soil strength and the time to failure. A specialised triaxial apparatus was required to perform high speed monotonic loading. To do this three separate loading systems were used, a pendulum, falling beam and hydraulic apparatus. Times to failure ranged over 6 orders of magnitude from 10,000 seconds to 0.01 seconds. Four natural soils were studied, three of which were fine grained and one coarse grained. It was found that the strength of all cohesive soils tested displayed a dependence on the time to failure; however the non cohesive soil displayed minor rate effects. Some of the fine grained soils were air dried to lower their water content and thus provide a range of strengths for each soil. The samples with a lower static strength displayed higher rate effects.

Richardson and Whitman (1963) compared triaxial undrained compression tests on normally consolidated Mississippi River valley clay at strain rates between 0.12%/hr and 60%/hr. Of particular note, an objective of this study was to address water migration and non uniformity (as well as strength increase) during high strain rate triaxial compression testing. A mid height pore pressure transducer as well as a typical base pore pressure measurement was incorporated. With increasing strain rate an increase in strength was accompanied by a decrease in excess pore pressures. A comparison of the pore pressures measured at the base and mid height showed that with increasing strain rate the base transducer consistently measured higher pore

pressures, highlighting the effect of non uniformity of stress distribution with increasing strain rate. However no redistribution of water was observed in the post test samples. To address possible effects of moisture distribution during shear at higher strain rate, a step-changing technique was used where the strain rate was suddenly increased from 0.12%/hr to 60%/hr. The results from step changed tests agreed well with those from steady strain rate tests (in terms of measured strength and excess pore pressure). This is today referred to as isotach behaviour. Thus the isotach behaviour indicated that migration of moisture was not responsible for the increase in strength seen at higher strain rate.

Akai *et al*. (1975) conducted normally consolidated undrained triaxial tests on remoulded Fukakusa clay using a loading system capable of delivering stable and constant rates of strain at rates from 0.12%/hr to 3000%/hr. The strength was found to be proportional to the strain rate however the excess pore pressures were found to be independent of strain rate, although notably pore pressure was measured at the base of the sample. It is possible the excess pore pressures measured by Akai *et al*. (1975) were likely were artificially large due to the effects of end restraint. The resulting effective stress path increasingly diverged from the static stress path with strain rate, tending towards the total stress path. Akai *et al*. (1975) also conducted tests on other time dependent soil mechanical phenomena including stress relaxation tests and creep tests. Empirical formulations for these phenomena and constant rate of strain tests were shown to be equivalent.

Lefebvre and LeBoeuf (1987) conducted undrained triaxial tests with monotonic and cyclic loading on three natural clays in both structured and destructured states. The monotonic tests were strain controlled at rates ranging from 0.05%/hr to 132%/hr and the stress controlled cyclic tests were conducted at 1 – 2 Hz, equivalent to strain rates of up to 6000%/hr. The magnitude of the strain rate effect for the clays in structured and destructured state was found to be almost identical, however the mechanisms attributed to the strain rate effect on strength for each state was different. For destructured soils a decrease in excess pore pressures was measured with increasing strain rate and thus the shear resistance is attributed to the change in effective stress. For structured clays the excess pore pressures was independent of strain rate and the shear resistance was attributed to the bonding within the clay skeleton. It is noted that

no mention of the location of the excess pore pressure transducer was made by Lefebvre and LeBoeuf (1987). Therefore these findings on excess pore pressures may be suspect if they were recorded at the base transducer. However the general trends of their results tend to agree with those from studies incorporating mid height excess pore pressure measurement.

Sheahan *et al*. (1996) compared the effect of strain rate on reconstituted Boston blue clay anisotropically consolidated to OCR from 1 to 8. Lubricated ends and a mid height excess pore pressure transducer were incorporated to address the issue of non uniform distribution of strains. However a relatively narrow range of strain rates from 0.05%/hr to 50%/hr were studied, which is considerably lower then used by Akai *et al*. (1975) or Lefebvre and LeBoeuf (1987). With increasing OCR the effect of strain rate was seen to generally reduce. Sheahan *et al*. (1996) found that at OCR 1 and 2 the strain rate effect on strength was caused by both suppression of shear induced pore pressures and an increase in effective stress (friction angle), however at OCR 4 and 8 the effect was entirely due to a decrease in shear induced pore pressures.

Balderas-Meca (2004) conducted tests at strain rate tests from approximately 2%/hr to 350,000%/hr, far in excess of previous studies, using a pneumatically loaded triaxial system with an artificial soil (referred to as KSS) which was designed to model the mechanical behaviour of a natural fine grained soil. The strain rate effect increased linearly with the logarithm of strain rate. However the rapid introduction of the displacement piston into the triaxial cell caused a significant increase in cell pressure during shear. The deviatoric stress and excess pore pressures were thus corrected for differences cause due to the rapid increase in cell pressure. Despite this the excess pore pressures were found to decrease significantly with increased strain rate.

In summary these studies each found significant difficulties in measurement of excess pore pressures during shear. As discussed previously, with increasing strain rate excess pore pressures are generally seen to reduce. The effects of non uniformity were addressed by Richardson and Whitman (1963) and Sheahan *et al*. (1996) using step changing techniques and lubricated ends respectively. Nonetheless the shear strength increased with an increase in strain rate and a decrease in excess pore pressures was still observed. Unfortunately most of the studies described previously utilised a

narrow range of strain rates, typically quite low in comparison to those in other geotechnical applications (Section 2.2). The study from Balderas-Meca (2004) could unfortunately suffer from cell pressure changes during shear, masking true effective stress behaviour as well as possibly influencing the shear strength.

This summary of previous triaxial studies highlights the necessity for a high strain rate investigation of strain rate effects on strength, where difficulties noted in previous investigation are addressed. Further to the works of Casagrande and Shannon (1948) and Lefebvre and LeBoeuf (1987), there is also a necessity for a triaxial investigation incorporating a variety of soils, with the purpose of defining the dependence of strain rate effects on soil properties.

2.7.2 Non uniformity in triaxial testing

As discussed previously a major concern with triaxial testing is the adverse effects of boundary conditions on the distribution of stress and strain throughout the sample. Manifesting through a variety of effects, non uniformity of stress and strain may influence the measured deformations, effective stress measurements, and shear strength of the specimens. The effects of non uniformity can arise due to natural in-homogeneities within the specimen itself, and also due to compliance issues with the triaxial system. The problem of in-homogeneities within test specimens is generally a concern for tests on undisturbed natural clays and the sampling techniques involved in obtaining such specimens. However this is not pertinent to this study, and is not discussed further here, instead concentrating on the problem of compliance issues with the triaxial system.

For triaxial tests, significant effects may arise due to non uniformity from the end restraint of the samples brought about from friction induced with use of rough porous stones (Rowe and Barden, 1964), and the restriction of lateral expansion with use of membranes (Carter, 1982).

Triaxial systems are intended to allow samples to deform radially upon axial deformation. Calculations of the cross sectional area and the subsequent stresses are ideally dependant on the assumption that the specimens deform as perfect cylinders.

The friction between the ends of the specimen and the rough porous stones can lead to a disturbance of the ideal stress field and subsequent strain within the specimen (Rowe and Barden, 1964). Additionally as the membrane encasing the samples is required to be sealed, the membrane is fixed at the base pedestal and top cap, thus restricting the expansion of the samples at these locations (Carter, 1982). The disturbance to the stresses and strains at the ends of the samples thus prevents the sample deforming as a perfect cylinder, which can lead to irregular deformations, typically seen as barrelling, and also a concentration of stresses at the end of the samples. Figure 2-33 from Rowe and Barden (1964) illustrates the potential disturbance to a triaxial specimen with affected areas labelled as “dead zones”.

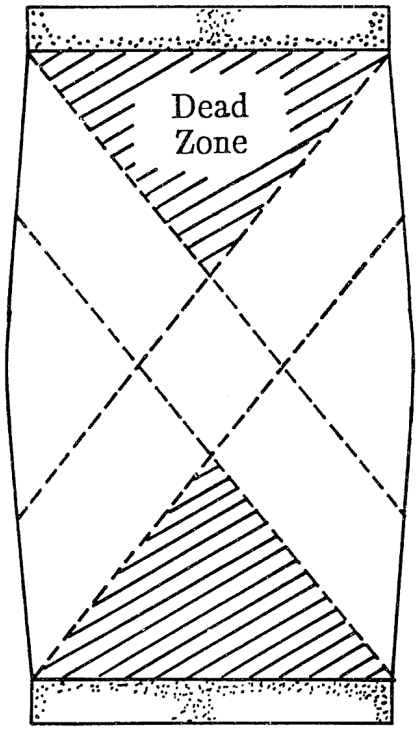

Figure 2-33 Illustration of "dead zones" within a triaxial specimen (Rowe and Barden, 1964)

Due to the concentration of stresses within these zones the pore pressures may be higher relative to the rest of the specimen, which may lead to migration of pore water. When excess pore pressures are measured at the base of the specimen this may lead to effective stress measurements that do not reflect the true behaviour of the specimen.

To overcome the effects of non uniformity lubricated ends are recommended to reduce friction. The main benefit of the use of lubricated ends is the reduction of pore

water migration. Olsen and Campbell (1964) measured lower pore pressures and a drop of the peak angle of friction in kaolin tested with lubricated ends, however found no change in the degree of sample bulging. Duncan and Dunlop (1966) found that lubricated ends did not significantly affect the strength of fine grained soil, but provided improved measurements of volume change in the case of drained testing and pore water migration in undrained tests. However Germaine and Ladd (1988) found that due to the additional effort of using lubricated ends the only tangible net benefits of their use are when reliable data is required at large strains (>15%) and in soils of OCR>6 where reliable pore pressure measurements are required. Additionally Germaine and Ladd (1988) also mention that lubricated ends can reduce the precision of small strain measurements, whilst Duncan and Dunlop (1966) found that use of lubricated ends reduced the stress-strain moduli.

Sheng *et al*. (1997) conducted finite element modelling of the response of a normally consolidated fine grained soil under different drainage conditions (drainage via top and bottom, and undrained) with three different conditions of contact between the soil and platen;

1. Perfectly smooth contact (SC); No friction between specimen and end platens, representing perfect lubricated ends.
2. Frictional contact (FC); Soil-platen friction angle of 20 degrees, representing enlarged rough end platens.
3. Completely rough contact (RC); No sliding was allowed at the contact surfaces, representing rough end platens where the specimen is restrained by a membrane fixed with seals at the sample ends.

Figure 2-34 show the effects of these criteria on the distribution of axial stress and axial strain throughout a specimen (modelled) in drained conditions. The maximum stresses shown in Figure 2-34 are at the ends of the specimen. The minimum stresses are at the centre towards the outer edge of the specimen, where mid height pore pressure transducers are typically located. The non uniformity of the strains was found to be more pronounced than the stresses, with the ends of the specimen showing the smallest axial compression and radial extension. The centre showed the largest axial and radial strains. Assuming the axial strain differences shown in Figure

2-35 reflect similar differences in excess pore pressures, the effects of non uniformity can be significant for measurements of pore pressures at the edge (mid or base) of triaxial specimens. Note both drained and undrained modelling was conducted at a strain rate of approximately 0.2%/hr.

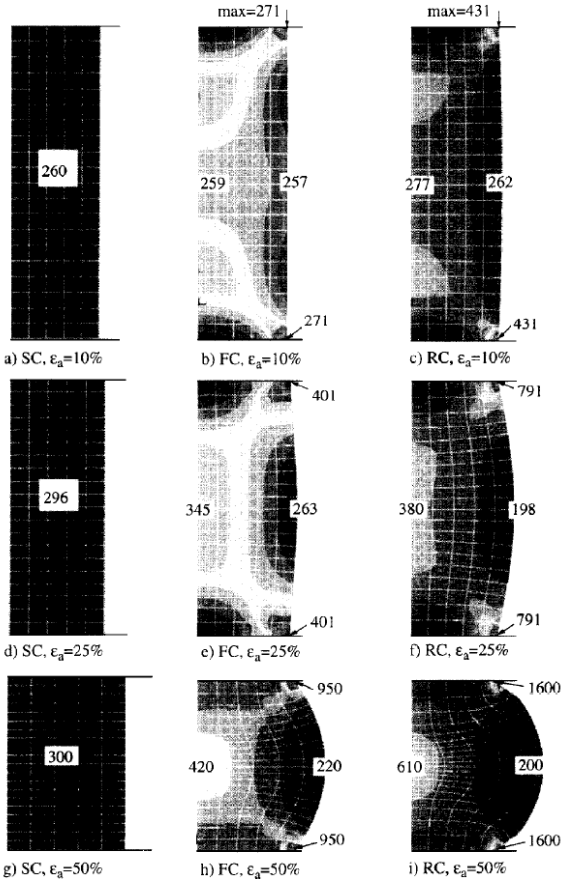

Figure 2-34 Axial stress distribution during simulated loading of clay (Sheng *et al*., 1997)

The local volumetric strains of the specimens for the undrained test is shown in Figure 2-36; where it is shown that to satisfy the constant volume condition some areas of the specimen contract while others swell. The local volumetric strains show compression at the ends of the specimen and extension at the outer part of the mid section of the specimen. Although undrained (constant volume) tests will not display volumetric strain through global measurements, Figure 2-36 highlights this can occur in local measurements.

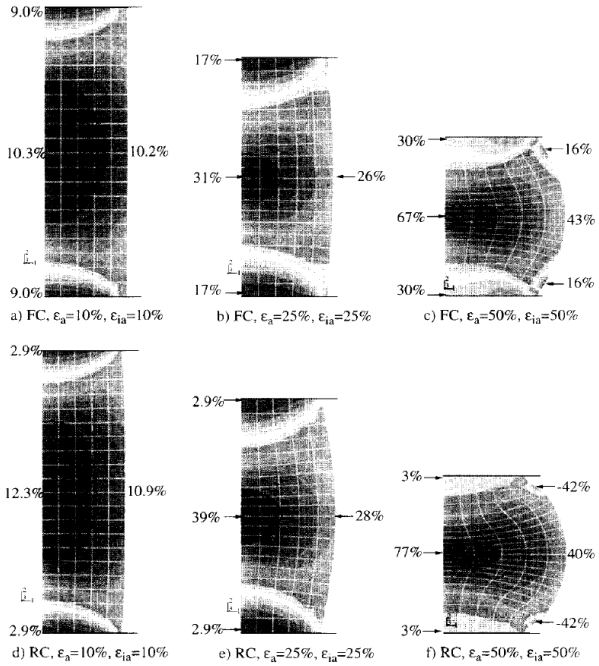

Figure 2-35 Effect of strain on distribution of axial strains during simulated loading of clay (Sheng *et al.*, 1997)

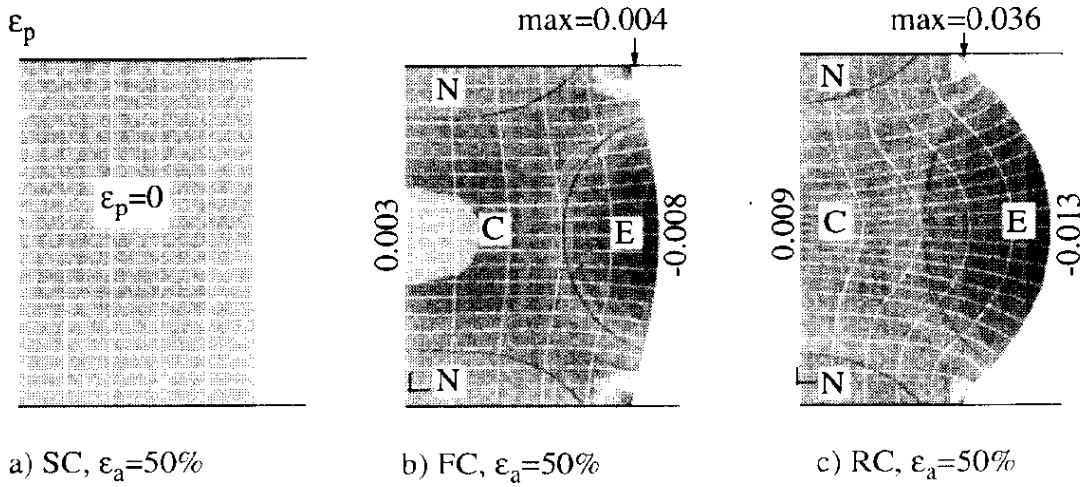

Figure 2-36 Distribution of volumetric strain with different end restrain conditions in simulated undrained tests (Sheng *et al.*, 1997)

Thus the non uniform development of stress and strain can be severely affected by non uniformity in triaxial testing. To avoid non uniformity during shear tests using fixed ends, Germaine and Ladd (1988) made recommendations on the selection of appropriate rates of strain to achieve full equalisation of pore pressures based on the coefficient of consolidation. Similar recommendations are made in BS 1377-8:1990, where for example a fine grained soil with a coefficient of consolidation of 20m^2/year, 200mm in length and a diameter of 100mm, tested in undrained triaxial compression

with radial drains and an expected strain at maximum deviatoric stress of 2%, the maximum specified rate of strain (for acceptable levels of non uniformity) is approximately 0.15%/hr.

During high strain rate testing, and presumably in general soil behaviour, where a true soil response is undrained there will be some degree of non uniformity within the stress and strain distribution throughout the soil unless considerations are on an infinitely small element.

2.8 Findings from literature and areas for further research

This chapter is a literature review of strain rate effects in fine grained soils. In particular this chapter focused on strain rate effects on strength and stiffness. The variation of soil behaviour in comparison to the range of strain rates involved in geotechnical engineering is presented. Literature which report relationships between index properties and strain rate effects on strength are compared. The effect of strain rate on different aspects of the stiffness degradation curve is discussed. Some aspects of the viscosity of soils, the influence of over consolidation on strain rate effects, and effects of increased strain rate on excess pore pressures are also discussed. A list which summarises some of the aspects discussed in this chapter as well as some of the findings and areas of weakness within the current understanding of strain rate effects in fine grained soils is presented below;

1. There are a wide range of strain rates encountered in geotechnical engineering. Soil behaviour can vary with strain rate, from drained to partially drained, before becoming fully undrained at higher strain rates. Each different response from soils results in significantly different strength.

2. In many studies the magnitude of excess pore pressures reduce with increased strain rate during undrained (constant volume) soil testing. This is often considered suppression of excess pore pressures. This has often been cited as the primary mechanism involved in undrained strain rate effects on strength (Sheahan et al., 1996). However there are contrary reports on the effect of strain rate on the development of excess pore pressure with some studies

reporting excess pore pressures are independent of strain rate (Soga and Mitchell, 1996). Notably most of the studies which measured excess pore pressures during increased strain rate testing are of limited range of strain rates in comparison to the range of strain rates involved in geotechnical engineering. There is a need for a greater understanding of the effective stress regime during high strain rate testing in particular.

3. The effect of over consolidation may reduce the strain rate effects at lower strains (Sorensen *et al*., 2007). However the undrained strain rate effect on strength may not be affected by over consolidation at maximum strength (Sheahan *et al*., 1996, Lehane *et al*., 2009). There is little information on the influence of over consolidation on strain rate effects on strength. Some differences in the method of over consolidation are also evident in the literature. It is unclear how this may affect the strain rate effect. Further study of the influence of the OCR on strain rate effect is needed, and particularly at higher strain rates.

4. Plasticity index does not appear to be sufficient in describing strain rate effects on strength for a wide variety of soils; however there appears to be some correlation between undrained strain rate effects, moisture content and liquidity index, with an increase in these parameters related to increased strain rate effects. There is a need for a systematic approach into the investigating how strain rate effects vary with index properties of fine grained soils. Current models which propose relationships between strain rate effects and fine grained soils do not relate well to much of the other reported strain rate effects in the literature. The previous investigations into strain rate effects on strength have been conducted over a limited range of strain rates, and at magnitudes of strain rate far less then those experienced during many geotechnical events. There is a need for greater understanding of the factors involved in strain rate effects in fine grained soils, which may explain much of the discrepancies between reports in the literature.

5. Strain rate effects do not affect the initial elastic stiffness at high strain rates, and appears to be limited to an increase up to 6% (from a reference strain rate)

at lower strain rates. It is not clear as to the exact range of strain rates although this is likely related to soil type and susceptibility to creep.

6. Increased strain rate has been shown to increase the linear elastic threshold; however this has been shown for a limited range of strain rates. There is need for testing of this aspect of soil behaviour at a greater range of strain rates, and in a variety of different soils to determine the influence of soil properties on the rate dependence of the linear elastic threshold strain.

7. There is limited data on the relationships between strain rate effects and other factors such as the volumetric threshold strain. This aspect of soil behaviour appears to be relatively ignored in research. This important aspect of the non linear behaviour of soils should be investigated in terms of strain rate.

8. The effects of strain rate on stiffness are typically compared as a simple strain rate coefficient. It has been suggested that the strain rate coefficient is related to plasticity index (Lo Presti., 1996), however there is currently insufficient data to develop a relationship. A greater volume of data is required to determine the relationship between fine grained soils and the effects of strain rate on stiffness. The strain rate coefficient is also typically defined over a relatively narrow range of strain rates, far less then the higher strain rates involved in geotechnical engineering.

3 Methodology

3.1 Introduction

This chapter presents the test methods and soil characterisation procedures and test data information which has been used to determine the effects of strain rate on fine grained soils. Triaxial testing was carried out at a range of strain rates, on three different model soils. This was applied to determine how strain rate effects vary in different soils. The main focus of this chapter is to describe the specialised triaxial apparatus used to conduct high strain rate testing and to characterise model soils, which were used in this research to compare the effects of strain rate on soil types.

The reconstitution process of the model soils and preparation of the test samples are described. The characteristics of the model soils, and how their properties compare to other soils in literature has been discussed.

Specifications of the specialised triaxial system which includes local axial and radial Hall effect instrumentation, mid and base excess pore pressure transducers, and axial bender elements are outlined. A description of the hardware and software used during testing, testing procedures and the performance of the system during high strain rate testing are presented and discussed.

3.2 Testing programme

The testing programme was developed taking the following objectives into consideration;

- To conduct triaxial compression tests at strain rates ranging from slow ‘static’ rates of strain to rapid ‘dynamic’ strain rates. This would allow for an assessment of the strain rate effect to be undertaken.
- Quantify strain rate dependent behaviour in terms of effective stress.
- Assess the effect of strain rate on soil stiffness at small strains.

- To compare variations of strain rate effects in soils with differing composition and state.
- To develop a framework to describe the potential of soil to display strain rate effects, accessible through soil parameters determinable from standard laboratory classification testing.

To compare the factors which influence the magnitude of the of strain rate effect, three different soils are tested at identical axial strain rates. These soils are reconstituted from the same batches of materials at different compositions to provide a variance for comparison. Each soil was of different plasticity. The three soils are tested at the same liquidity index (I_L = 0.22) over the entire range of strain rates. Two soils are further tested at another identical liquidity index (I_L = 0.11) over the entire range of strain rates. The rate dependence of Kaolin was evaluated at three different levels of initial effective stress (300kPa, 720kPa, 1150kPa). Another model soil, KSS, which is composed of a mixture of Kaolin with sand and silt, is tested at an effective stress of 560kPa. The third soil, KSS-541 is composed of the same materials as KSS, however the proportion of the materials is different that in KSS. KSS-541 is tested at an effective stress of 300kPa and 600kPa. All tests are normally consolidated unless otherwise stated.

Standard soil laboratory classification was conducted in unison with the specialist high speed triaxial testing. Standard classification tests were conducted in accordance with BS 1377-2:1990. The equipment used to determine soil characteristics include a standard GDS instruments Triaxial Testing System (GDSTTS), and standard Atterberg limit testing.

The following soil characteristics were determined from standard laboratory equipment, with their associated index properties presented in Table 3-1;

- The Atterberg Limits
- Permeability
- Coefficients of consolidation
- Consolidated drained and undrained shear strength
- Particle size distribution

Soil	**Effective stress, p'_0 (*kPa*)**	**Plasticity Index, I_P (*%*)**	**Critical state ratio, *M***	**Number of tests**	**Range of strain rate (*%/hr*)**
Kaolin	300	45	0.875	4	300-180,000
Kaolin	720	45	0.875	7	1-180,000
Kaolin	1150	45	0.875	7	1-180,000
Kaolin OCR 4	300	45	0.875	2	300-180,000
Kaolin OCR 10	115	45	0.875	2	300-180,000
KSS	560	23	0.933	7	1-180,000
KSS-541	300	20.5	0.95	7	1-180,000
KSS-541	600	20.5	0.95	7	1-180,000

Table 3-1 Summary of soils, their properties, and strain rate tests used in this study

To determine the strain rate effects, an electromechanical computer controlled triaxial loading system was used. Rees (2003) reported that this system provides greater control of displacement and strain rate in comparison with hydraulic and pneumatic loading systems. This testing device was capable of applying constant rates of strain over a larger range of strain rate than that of the conventional triaxial systems. To this end, constant rates of strain were applied at 1%/hr, 5%/hr, 10%/hr, 300%/hr, 1,800%/hr, 18,000%/hr and 180,000%/hr. Ranges of strain rates and the number of tests are included in Table 3-1. The 1%/hr strain rate test was selected to comply with typical static strain rate laboratory triaxial testing. This strain rate was also close to the recommended reference strain rates as used in other triaxial undrained strain rate effect studies (Lefebvre and LeBoeuf, 1987, Sheahan *et al*., 1996).

To assess strain rate effects in terms of effective stress, two pore pressure transducers were used. The effect of non uniformity can lead to non-uniform stress distribution within the specimen. To address this issue, a pore pressure transducer was positioned at sample mid height, outside the regions of the dead zone, as discussed previously in Chapter Two, Section 2.7. Additionally, pore pressures are measured at the base of the sample. Comparison was made of the pore pressures measured at each transducer to give insight of the effect of strain rate on non-uniformity effects.

Axial and radial Hall effect transducers are used to measure displacements locally on the sample. These allow for the assessment of soil deformation free of error due to bedding effects. These measurements are used to determine soil stiffness, and are compared with initial stiffness measured with an axial bender element system.

3.3 Reconstitution

3.3.1 1-Dimensional Consolidometer

A one dimensional consolidation apparatus as shown in Figure 3-1 was purpose built to reconstitute the soils from slurry to solid states. The consolidation apparatus was designed around standard U100 aluminium sampling tubes (460mm × Ø105mm). This system allows for a vertical stress to be applied to the slurry whilst enabling drainage from both ends of the U100 tubes to take place.

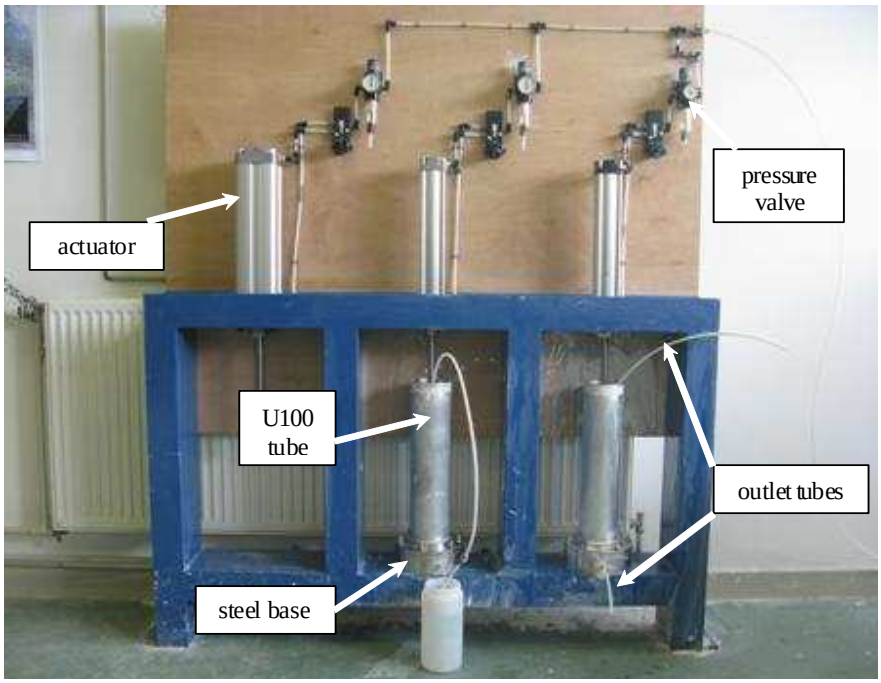

Figure 3-1 The 1-dimensional consolidation rig for reconstitution of samples

A stainless steel base (Figure 3-1) was designed to which one end of the U100 sampling tube were securely fixed. The base housed a 100mm diameter porous stone through which water was expelled from slurry under pressure from a pneumatic piston, actuated from the other end of the U100 tube. The stainless steel piston head also housed a 100mm diameter porous stone through which drainage was permitted

during consolidation. Both the base and piston head consisted of machined stainless steel. The porous stones in both the base and piston head were connected to outlet valves from which the expelled water was collected in external containers. The piston head was driven though an actuator connected to an external air supply. The air supply to the actuators was controlled with a pressure valve. Switches were also provided to control the direction of the actuator. The consolidation moulds were designed to provide a seal through the provision of O-rings at the connection points of the U100 to the base and piston head. A Wykeham Farrance WF17060 pore pressure transducer was used to measure the vertical stress placed on the slurry before consolidation began.

This was to be undertaken with the assumption being that that total stress would equal pore pressures when the soil was in the slurry state. It was assumed that in-homogeneities would occur due to friction at the sides of the consolidation moulds. To reduce this problem the U100 tubes were lined with a thin layer of silicone grease. Preliminary tests indicated that the plasticity index throughout the reconstituted samples was uniform. Several preliminary tests were undertaken to check for voids (by dissection) in the samples. These may occur from trapped air in the slurry however after optimisation of the slurry placement technique voids were eradicated from the consolidated test samples.

Soil reconstituted in this way would also be anisotropic. As the tests in the triaxial system were required to be isotropic, the consolidation pressures (140kPa) were selected to be low to allow the effects of anisotropy to be overcome with isotropic recompression at an effective stresses of at least 300kPa in the triaxial cell. Rossato *et al*. (1992), reporting on other literature noted that consolidating to double the pre-consolidation pressure proved sufficient to erase any memory of past stress history.

3.3.2 Preparation of soil slurry

Soil slurries were prepared by mixing quantities of each model soil with de-aired/de-ionized water. The quantities of each slurry mix are detailed in Table 3-2. To ensure homogeneous slurry mixtures the slurries were first mixed gently by hand using a spatula before full mixing in a mixing apparatus. The mixing apparatus was a BEAR

varimixer with an auger type mixing blade. De-aired and de-ionized water was obtained from natural tap water, firstly through a deioniser under vacuum and then drawn into a reservoir under vacuum of minus 1 Atm.

Name of model soil	% of Speswhite Kaolin	% of HPF5	% of HST95	Mixing moisture content (%)
Kaolin	100	0	0	125
KSS	50	25	25	80
KSS-541	50	10	40	80

Table 3-2 Batch proportions (% mass) of each soil and moisture content (mixing)

To produce uniform clay slurries Sheeran and Krizek (1971) recommend mixing at moisture contents of 1.5 to 2 times the liquid limit of the clay. The value of 80% mixing moisture content was used for KSS as recommended by Balderas-Meca (2004). This value was also used for KSS-541. The ratio of slurry moisture content to liquid limit is thus 2 for both KSS and KSS-541.

Samples of Kaolin are mixed at 125% moisture content as it has a significantly higher liquid limit and requires a higher moisture content to achieve a level of workability suitable for pouring into the consolidation moulds. The moisture content of the Kaolin slurry could not be increased further due to the high compressibility of the slurry, which if mixed at higher moisture content would not leave enough solid material at the end of consolidation for samples of correct dimensions for triaxial testing. For Kaolin the ratio between slurry moisture content and liquid limit was approximately 1.7 which was within the limits as recommended by Sheeran and Krizek (1971).

The components of each mixture were first organised into their relevant quantities by percentage mass. At the beginning of the mixing process the Kaolin component was firstly mixed by hand in the mixing bowl with an increasing quantity of water to ensure the mixture was relatively homogeneous and had not segregated to the bowl. The other constituents were carefully added to the Kaolin and gently mixed with remaining water. Once the full quantities of each material were added to the bowl and hand mixed the mixture was placed in a mixing apparatus. The mixing apparatus was set to the slowest speed setting and mixed for 1 hour. During the mixing process the

apparatus was frequently stopped and hand stirred to ensure segregation had not occurred between the mixture and the base and sides of the bowl. At 1 hour the mixture was homogeneous.

3.3.3 Consolidation of the soil slurry

To prepare the consolidation moulds to accept the slurry, the porous discs of the consolidation apparatus are prepared by saturation under vacuum for 1 hour. Once saturated the base porous stone was placed into the steel base and covered with a water soaked filter paper. The inside of the mould which has been lined with a smear of silicone grease was immediately fitted to the steel base. The mould was then partially filled with de-aired water which was then used to force out trapped air through the base drainage lines, as well as flushing the pore pressure transducer which was placed on the base drainage line. Water was continuously drawn out until a final level of approximately 40mm was left over the base porous stone at which point the outlet valve on the pore pressure transducer is closed. A Wykeham Farrance WF17060 pore pressure transducer was used to measure the pore pressures with a local electronic display.

The slurry was then slowly poured into the consolidation mould. A tremie pipe system was experimented with however this was found to be less effective at removing trapped air during the pouring process. As the slurry is poured in, the water in the mould was displaced upwards preventing air from becoming trapped in the mould. Once filling of the mould was complete the excess water was removed.

The piston head was removed from the saturation tank and attached to the actuator. Another filter paper was placed on the porous disc in the piston head which was then lowered gently via the actuator into the mould. When the piston head has entered the mould the water was forced through the porous piston head releasing any trapped air. When water was seen in the drainage line the upper valve is closed and pressure applied. At this point the system was sealed and via the pressure valve controlling actuator it was lowered further into the mould at approximately 1kPa/second until the pore pressures reach 140kPa. The applied vertical stress was further checked by the gauge reading on the pressure valve to the actuator. The pore pressure was monitored

for 15 minutes to ensure it was stable before the valves are opened and the slurry was then allowed to consolidate for three days. The vertical stress was frequently checked on the actuator pressure valve to ensure stable pressures were transmitted to the slurry during consolidation.

3.4 High speed computer controlled triaxial testing device

3.4.1 Overview

A bespoke triaxial system was purpose built by GDS Instruments. It was modified from a GDS Instruments Electromechanical Dynamic Triaxial Testing System (DYNTTS) which in normal circumstance was a 5Hz cyclic triaxial testing system. In this instance it was upgraded to allow rapid application of monotonic displacement. The system was capable of axial strain rates up to 180,000%/hr (100mm/s), on samples of 100mm in diameter, and 200mm in length. The system consists of the built-in loading system with load measured at the top of the sample by a submersible load cell. Pore pressures are measured at the base and mid heights of the test samples where, local Hall effect transducers and axial bender elements are installed. Back pressure and cell pressure was controlled via separate GDS standard pressure controllers.

3.4.2 Displacement control

Axial deformation was achieved through the base pedestal from a screw driven sub system. The built in dynamic axial loading system was driven by a brushless dc servomotor which are controlled through feedback from a remote transducer. In this case feedback was taken from the axial motor high speed shaft controller. Measurements of global (external) displacement were taken from the shaft controller. The displacement range was 100mm, with an accuracy of 0.07% and a resolution of 0.208μm.

To compensate for volumetric displacements caused by the loading ram entering the cell, a balancing mechanism within the ram was provided. This operates via a hydraulic connection though the centre of the ram, connecting the cell fluid to an

annular piston which provides equal and opposite reactions to the movement of the ram within the cell. This system provides for a zero net volume change within the cell brought about due to the ram movement.

3.4.3 Data acquisition and control

The GDS Digital Control System (GDSDCS), which is housed underneath the triaxial cell (Figure 3-2), provides 16 bit acquisition and 16 bit control output with closed loop feedback of displacement or load. The GDSDCS runs at 10 kHz per channel, providing 2000 control points when running at 5Hz. All transducers were operated through eight channel 16-bit data acquisition hardware.

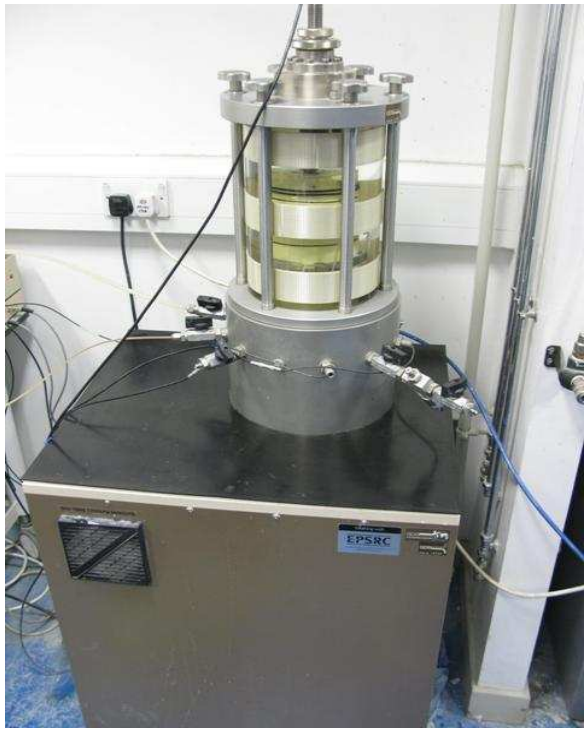

Figure 3-2 Electromechanical Triaxial Testing Device

The entire system (including cell and base controllers) was connected to a PC and a user interface was provided through the GDSLAB software package from which all aspects of the test can be controlled from saturation and consolidation to shearing. GDSLAB also allows configuration of the hardware through the GDS Dynamic Control System (GDSDCS) to provide better control during static or rapid triaxial testing. For rapid triaxial tests the system allows for user defined input of displacement waveforms using a 1,000 point ASCII file. In this case the input axial

displacement ramp has minimal acceleration and deceleration zones to maximize the zone of constant velocity (strain rate).

Figure 3-3 presents the input and output displacement ramps with time for an 180,000%/hr test, which was the fastest used in this study. The triaxial system responds well to this velocity input, and achieves a stable constant velocity. The corresponding load cell measurements were noted to occur once constant velocity had been achieved in the output displacement ramp, and therefore deformation of the samples are at constant velocity.

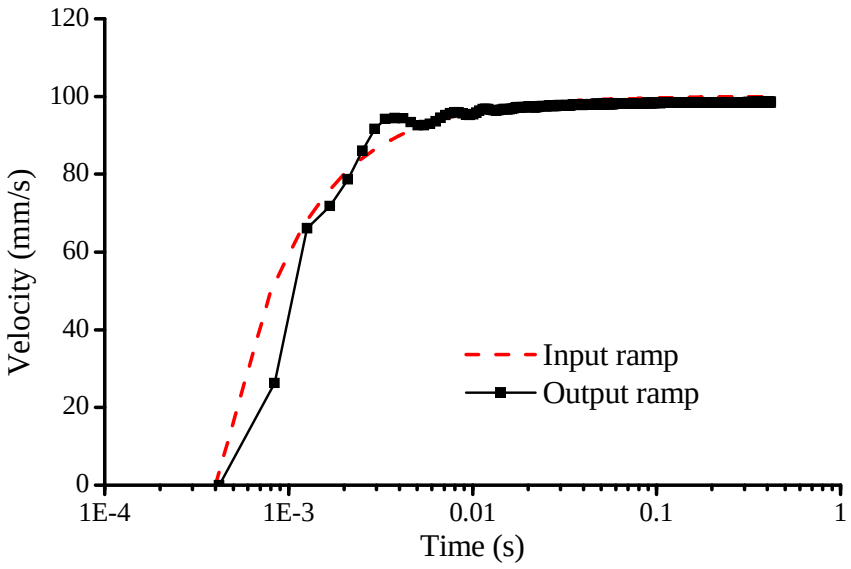

Figure 3-3 Input and output velocities during a 180,000%/hr (100mm/s) strain rate test

The minimal rate of strain used in rapid configurations from the dynamic control modulus (GDSDCS), was approximately 700%/hr for a range of axial strain to approximately 20%. A maximum number of 1,000 points was recorded during the rapid tests. At lower rates of strain the static configuration was used, although the static setting had difficulty achieving desirable levels of control at rates of strain greater than 300%/hr. The maximum rate of points recorded using the static configuration was 1 point per 4 seconds.

3.4.4 Pressure/Volume controllers

The cell pressure was controlled using a GDS standard volume/pressure controller (STDDPC). The device was connected via a USB directly to the PC and control and acquisition was via the GDSLAB software. The device has a capacity of 200cc and an operating range of 3MPa. The accuracy was to ±1kPa with a resolution of ±0.15%. The device functions by pressurizing de-aired water with a piston. The piston is actuated by a ball screw which is turned in a captive ball nut by an electric motor and gearbox. This assembly moves rectilinearly on a ball slide as shown in Figure 3-4.

Volume was measured by an incremental motor, by monitoring the number of steps used. Pressure was measured by an integral solid state transducer. The same supply of water that was used for the cell pressure controller, was used as triaxial cell fluid and for reconstitution of the soils. The water within the pressure controller was changed frequently during the consolidation stages of the samples due to the volume change of the soils. The outlet end of the controller was elevated to promote the escape of any air which may have entered the system. Connection of the cell pressure controller was achieved via tubing connections. The outlet of the cell pressure controller was located at the same level as the inlet to the triaxial cell to minimize head pressure differences.

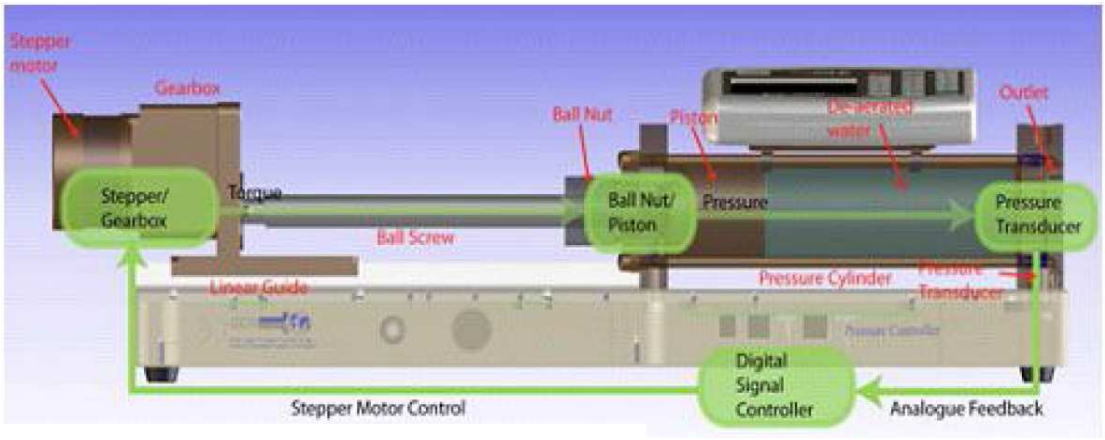

Figure 3-4 Schematic of GDS Instruments standard controller (GDS instruments datasheet – STDDPC:1, 2010)

The back pressure controller was the same type as the cell pressure controller (STDDPC) and was also connected to a PC via a USB connection. In addition, it was controlled using GDSLAB. The base controller was connected to the triaxial sample

through the top cap via 3mm internal diameter plastic tubing. Again de-aired and de-ionized water was used.

The controllers were frequently emptied and refilled due to the volumes of water expelled from each soil during consolidation. During the process of emptying or refilling the controllers, the drainage lines were monitored to avoid influx of entrapped air. Before reconnecting to the cell the controllers were flushed through and also used to flush the connection valves forcing out air before the lines were connected to the cell. The performance of the controllers in terms of pressure measurements were regularly checked by running tests in a cell filled with water alone. These were then calibrated against the measurements of the pressure transducers.

3.4.5 The triaxial cell

The triaxial cell was made from thick Perspex, reinforced laterally at three locations. The operational pressure rating capacity of the cell was 1700kPa. The cell was sealed by tightening six vertical screws onto a compressible rubber O-ring. The cell was filled via an inlet at the base. This was also used as a drain at the end of the tests.

The Perspex unit, and the base unit were cleaned frequently to remove any contaminants and after cleaning refilled with de-aired water before set up of the sample to flush trapped air out from the base of the cell and from the base pedestal. When filling the cell for testing the inflow of cell water takes place slowly to remove trapped air. Thereafter, stepped increments of cell pressure were applied through the difference in head from the reservoir of de-aired water, and any remaining trapped air was forced out of the top of the cell.

3.4.6 Measurement of excess pore pressures

Pore pressures were measured at mid height and at the base. The mid height pore pressures transducer was a Druck PDCR 81 as shown in Figure 3-5. This was the same as that used by Bond and Jardine (1991), Brown (2004) and Balderas-Meca (2004). They found that the response time to a step of 100kPa was 10-24ms

(Balderas-Meca 2004). The pressure range of the transducer was up to 1500kPa. The base pore pressure transducer was a p102 Sherborne, connected via plastic tubing through the base pedestal to the sample. The base pore pressure transducer was flushed during the preparation of the cell before each test. The mid height pore pressure transducer was saturated under vacuum for as long as possible between tests, and when removed from vacuum the transducer head was kept in de-aired water.

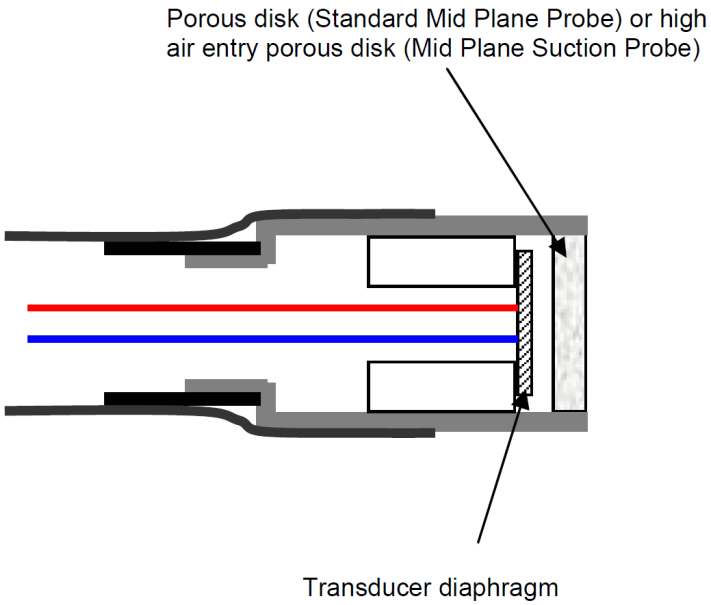

Figure 3-5 Schematic of mid height pore pressure transducer (GDS Instruments datasheet M4P:1, 2005)

To determine if leaks were occurring on the line between the pore pressure transducer and the inlet through the base pedestal, a fixed membrane was used to monitor pressure/volume changes between the transducer and the cell.

The installation of the mid height pore pressure transducer involved penetration through a pre-cut hole in the membrane. A grommet was placed with its flanges located between the membrane and the sample. The mid height probe was then taken from de-aired water and pushed through the grommet taking care to ensure the probe was in contact with the sample.

Four O-rings were fixed around the grommet tightening the contact with the probe. To avoid leaks in this area of weakness the connection between the mid height pore pressure transducer and the membrane was reinforced with several layers of liquid

latex during the setup of the sample. The latex was applied with a fine brush and only to areas immediately around the point of connection.

During initial tests the latex was allowed to cure overnight. The connection to the sample and the membrane had been sealed with O-rings to avoid evaporation of moisture and pore pressures were seen to reduce slightly during the curing process. To expedite the curing process, an air current was passed over the latex with a fan immediately upon application. This reduced the time required to cure each layer of latex allowing testing to commence within hours.

3.4.7 Sample centre pore pressure measurement

To gain a better understanding of the pore pressure response in the sample during high speed tests, a hollow aluminium tube was designed to attach to the mid height pore pressure transducer. This protruded from the face of the transducer to the centre of the sample. Due to inevitable changes in stress and likely expected localisation of strains within the centre of the sample during shearing, it was decided not to place the mid height pore pressure transducer into the sample. This was decided to avoid the risk of damage to the transducer.

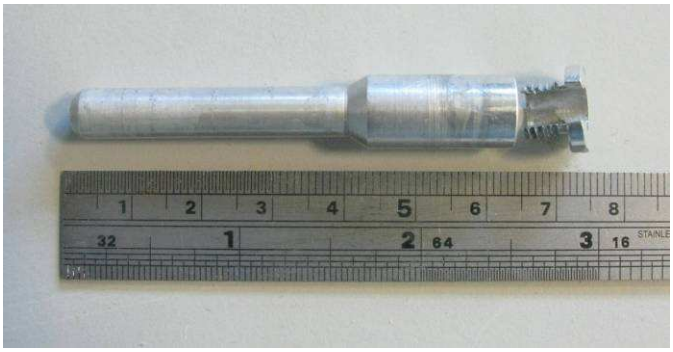

Figure 3-6 The mid height pore pressure transducer extension tube

This test arrangement is shown in Figure 3-6 with the objective being to measure pore pressures generated directly at the centre of the sample. The mid height pore pressure transducer, located at the edge of the samples would not be expected to sustain shear stresses and strains. It was also considered that stresses within the sample may be non-uniform and thus could result in concentration of pore pressures in the centre of

the sample exceeding the range of the transducer. The hollow aluminium device was selected as it would allow transfer of pressures through the soil to the transducer from a smaller area connected directly to the centre of the sample. The dimensions of the hollow section of the tube was 40mm in length, 6.9mm O.D., 1mm wall thickness, with an increased in diameter at the connection point to house the transducer (9.8mm O.D. and 10mm in length).

The test where this attachment was used was a repeat of a standard high strain rate test (180,000%/hr) conducted in normally consolidated Kaolin (p'_0 = 720kPa). The installation of the pore pressure extension device was similar to that of the regular mid height pore pressure device. A specially prepared grommet was used to fit the enlarged outer diameter of the extension device. The mid height probe was fixed into the extension device whilst submerged, before most of the water was removed and the entire system was inserted into the sample. Preliminary tests demonstrated that good contact could be achieved between the sample and the transducer as the face of the transducer was now at least 15mm inside the edge of the sample. The entire connection between the sample and the extension device was than sealed with several layers of latex in the same way as the standard mid height pore pressure transducer and Hall effect instrumentation.

3.4.8 Measurement of local strains

Local displacements were measured by both axial and radial Hall effect transducers (Clayton and Khratush 1986). The arrangement of the transducers on the sample is shown in Figure 3-7. The displacement range of the local transducers was 6mm, with a resolution using a 16bit data acquisition system of 0.1μm, and an accuracy of 0.8%. Using Equation 3-1, shear strain (ε_S) is defined from axial (ε_A) and radial strains (ε_R);

$$\varepsilon_S = \left(2/3\right)\left(\varepsilon_A - \varepsilon_R\right) \qquad (3\text{-}1)$$

The arrangement of each axial Hall effect gauge requires fixing two independent holding pads to the specimen. Each holding pad was fixed with pins which are inserted through the membrane approximately 20mm into the soil sample. Adhesive

and latex are then used to bond the membrane to the fixing pads to provide a seal. A spring mounted pendulum was fixed to the upper pad which holds a magnet. The lower holding pad was used to mount a semi-conductor plate housed in a smooth titanium unit, over which the pendulum holding the magnet was free to pass during axial deformation. The spring system provides contact between the magnet and the semi-conductor whilst ensuring friction remains low. As the magnet passes over the semi-conductor a change in voltage was produced in a direction normal to the current flow. The weight of the axial Hall effect gauge was approximately 21 grams.

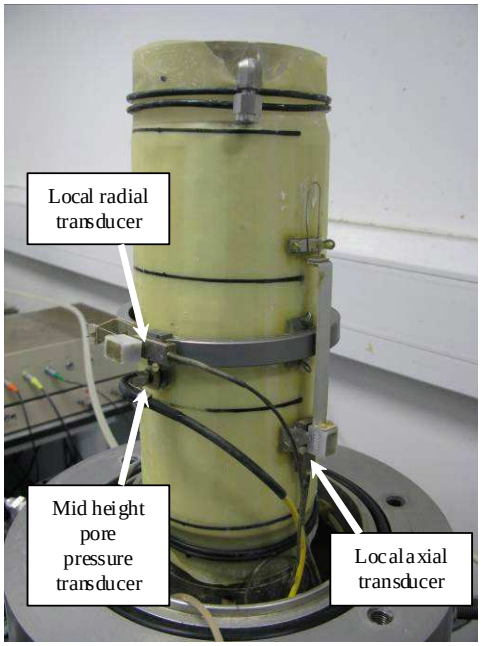

Figure 3-7 100mm diameter triaxial sample prior to testing

The radial Hall effect gauge consists of a radial calliper fixed at the mid point of the specimen. The calliper was fixed at the centre of each arm by two pins protruding into the sample by approximately 20mm which are then sealed with adhesive and latex during the set up of the sample. Identical magnets and titanium semi-conductors are used as for the local axial Hall effect gauge. The measurements are taken at the opening of the calliper as the unit opens or closes. The total weight of the radial Hall effect gauge was approximately 70 grams. Both the axial and radial devices are designed so the self-weight was partially counteracted by buoyancy uplift. During initial tests adhesive (Bostick adhesive 2402) was applied between the fixing pads and the membrane before the connection was sealed with several layers of latex.

Although the local Hall effect devices are designed to reduce friction as much as possible it was found that at high strain rates there was an apparent delay in local deformation registering. It is assumed that this was due to friction occurring at the commencement of the shearing stage. The delay in local deformations was corrected by comparing the derivative of each transducer with respect to time to the derivative of the deviatoric stress with respect to time and matching points of correspondence for each curve (peaks) as shown in Figure 3-8.

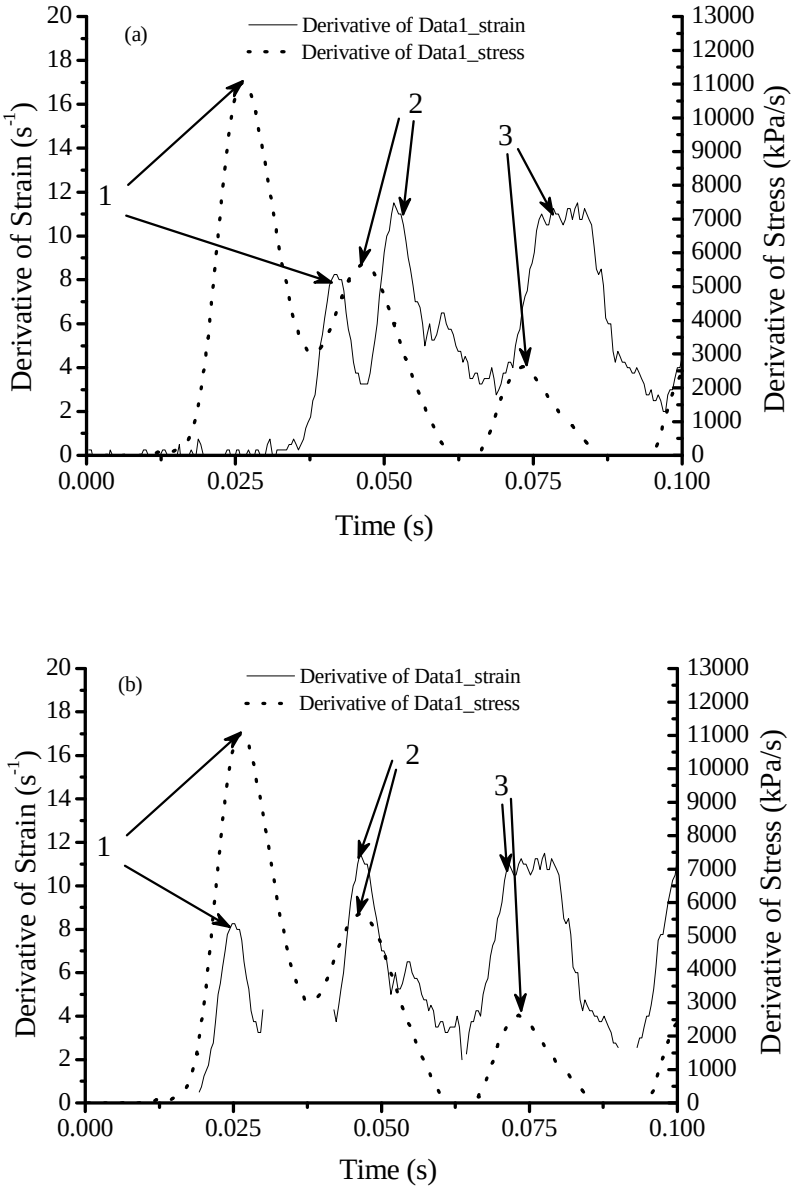

Figure 3-8 Correction to the derivative of local strain measurements to align the derivative of deviatoric stress measurements (a) uncorrected (b) corrected

An example is shown for Kaolin at p'_0=720kPa sheared at a strain rate of 18,000%/hr in Figure 3-9. This test in particular had difficulty in maintaining smooth control of axial displacement during the shearing process and was relatively simple to correct. For other tests the control was far superior and the resulting comparison of derivatives with respect to time was difficult, required intensive inspection of the recorded points and care during the correction process to avoid inducing errors into the results.

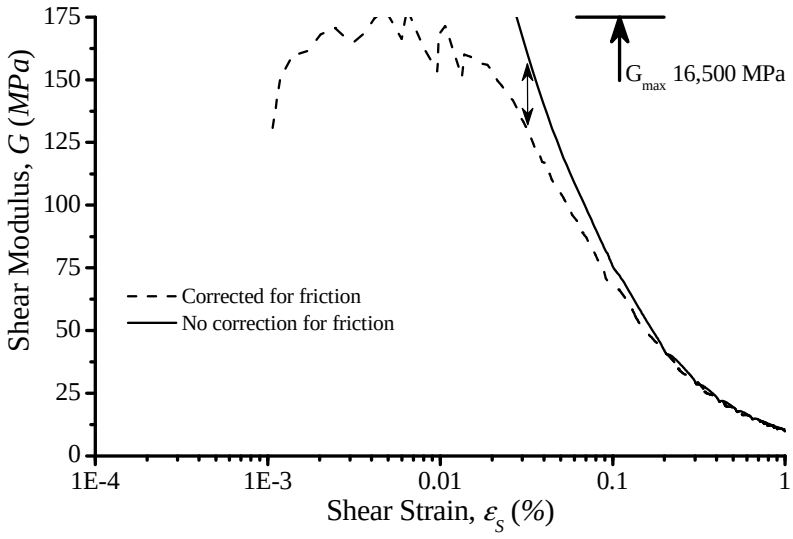

Figure 3-9 Normalised shear modulus degradation curves, uncorrected and corrected for friction on local hall effect measurements during a 18,000%/hr strain rate test in Kaolin-720kPa

3.4.9 Dynamic small strain measurements

Axial bender elements were incorporated into the base pedestal and top cap. The porous discs at the ends of the sample have a hollow recess to allow the bender elements to protrude into the sample. Each bender element consisted of a ceramic plate, which extended 1.5 mm into the sample. A single sinusoidal pulse was used for generating a shear wave. The bender element system was operated via the GDSBES software, running independently of GDSLAB. The bender elements system was connected to the PC via a USB connection to a master control box operating solely for the bender elements. The resolution of the data acquisition was 16bit. The speed of data acquisition is 2M samples per second with simultaneous sampling of both the source and received signals.

Measurements of the shear wave velocity were taken at the end of consolidation. The input sinusoidal pulse had a wave period of 0.2ms, with amplitude of 14 volts. For each measurement of the shear wave velocity an average of 30 input waves were stacked by GDSBES with a time between each wave of 0.1 seconds. The velocity of the shear wave can then be taken from user defined selection of points of source and received signals within GDSBES or from an ASCII data file to which the acquired stack of data was written. Sample heights used in shear modulus calculations were taken as tip to tip as recommended by Viggiani and Atkinson (1995a). The received shear wave signal was easy identifiable and therefore, the velocity of each shear wave was calculated with a cross correlation of characteristic points as recommended by Sorensen (2006) and shown in Figure 3-10. The points picked were the first peak of both the sent and received signals.

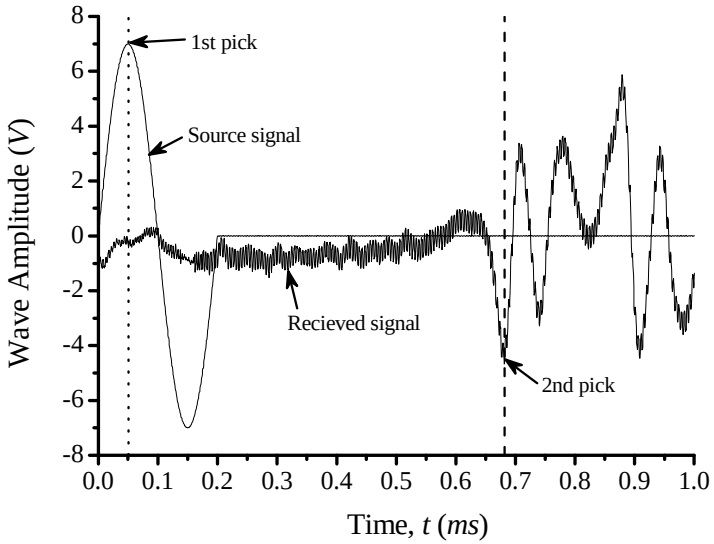

Figure 3-10 Cross correlation of input and output shear waves of typical Bender Element signal

3.4.10 Load cell and top cap connection

Load was measured with a 5kN submersible load cell, with accuracy to ±0.1% and a resolution to ±0.2N. Initial tests were conducted with contact between the top cap and load cell through a fixed, rounded adaptor screwed directly into the base of the load cell. The sample was seen to tilt during consolidation due to alignment problems, offsetting the ram from its groove fitting in the top cap.

Although the tilting was minor the resulting volume change during consolidation created an increasing gap between the alignment of the load cell ram and its corresponding insert groove in the top cap. The docking procedure with that arrangement would induce shear stress on the sample, possibly resulting in strains throughout the sample. To avoid such a situation the docking ram connection to the load cell was replaced by a half ball seated in the insert groove in the top cap as shown in Figure 3-11, similar to Gasparre (2005). During docking the half ball was allowed to rotate freely between the load cell and top cap, avoiding transmitting stress until full contact was made thus ensuring no disturbance to the sample during docking. The half ball was manufactured from stainless steel and its surface was polished.

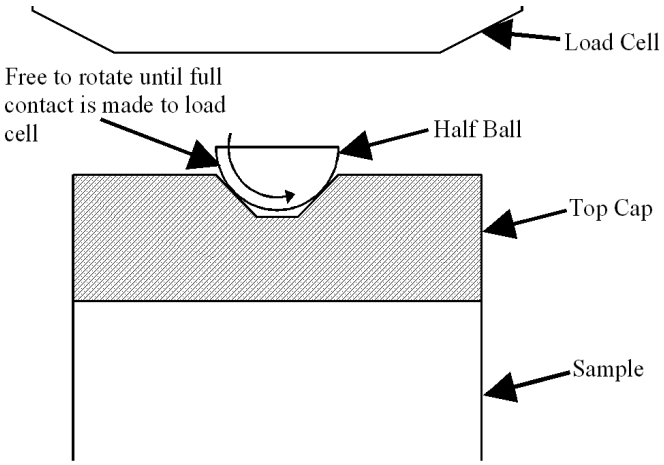

Figure 3-11 Arrangement of half ball in top cap for connection to load cell (during shear) for isotropic tests as per Gasparre (2005)

3.4.11 K_0 tests

The K_0 values were found for each soil in the triaxial cell using 100mm diameter samples with a length to height ratio of 2. The test was controlled via GDSLAB under conditions of zero lateral strain using the radial Hall effect device. The samples were loaded with a cell pressure ramp at a rate of approximately 3kPa/hour which was sufficient to keep excess pore pressures below 5%. Drainage of water was through the top of the specimen. Radial filter strips were also used. The connection of the top cap to the load cell was made via a vylastic sleeve which, was placed around the top cap and also to a Perspex connection to the load cell. This arrangement is shown in Figure

3-12. The connection between the top cap and load cell was supported by a vacuum between the top cap extension and the vylastic sleeve.

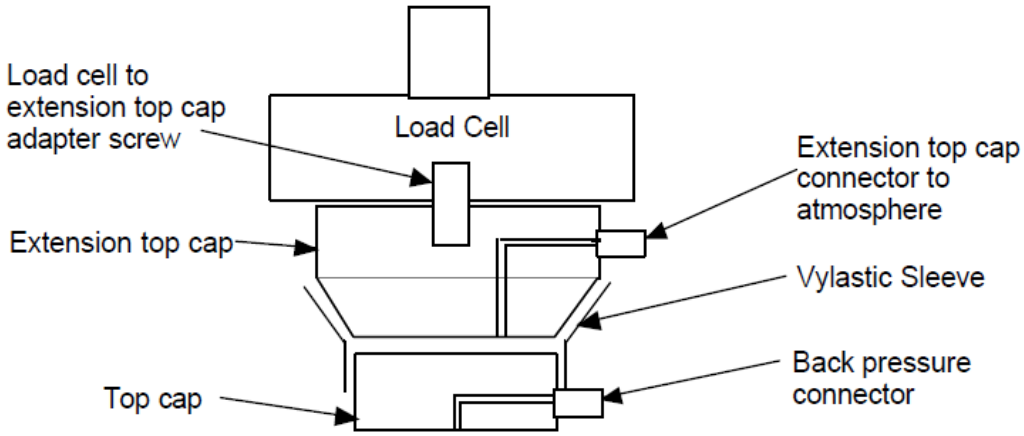

Figure 3-12 Arrangement of top cap connection to load cell during anisotropic tests

3.4.12 Sample set up

In preparation for testing the soil was very slowly extruded from the one dimensional consolidation and trimmed to remove any silicone grease. The sample was then trimmed to approximately 205mm in length. The trimmings are weighed to determine moisture content and the final sample dimensions and weight were recorded.

The connection between the base pore pressure transducer and the pedestal was flushed with de-aired water using the standard GDS controller through the pore pressure transducer itself to ensure the system was free of trapped air. The top cap drainage lines are also flushed through the standard GDS back pressure controller to ensure no air was trapped within the drainage lines. When the systems have been flushed they are placed at the same level within the lower section of the cell which has been filled with de-aired and de-ionised water to benchmark the controllers and both mid height and base pore pressure transducer.

Whilst the base pedestal was submerged at this level the porous stone was placed on the pedestal to avoid trapping of air between the porous stone and the base pedestal. The porous stones and mid height pore pressure transducer are saturated under vacuum for 1 hour prior to testing.

The sample was then located on the porous stone whilst still submerged to avoid trapping air at the stone-soil interface. Side filter drains are placed onto the specimen. The filter papers as well as the membrane had previously been prepared for the mid height pore pressure transducer insertion and placed in de-aired water for several hours prior to testing. The membrane was placed onto the sample using the membrane expander. Once the membrane has been placed onto the sample the upper porous stone was located and the top cap was attached with a small amount of water used to ensure the system was as free as possible of trapped air. Double o-rings are fixed to the base pedestal. The grommet and the mid height pore pressure transducer are then located through the hole made in the membrane whilst ensuring the transducer face was inserted well into the sample, whilst avoiding air pockets which may occur at the interface. Four O-rings are placed over the grommet. Any trapped air between the membrane and the sample was removed by stroking the air pockets out before double O-rings were fixed to the top cap and membrane. At this stage the first coat of liquid latex was applied to the grommet and mid height pore pressure transducer.

The axial and radial local transducers pads are then located and fixed using pins approximately 20mm long and Bostick adhesive 2402. Once the axial and radial local transducer pads are fixed into position they, as well as the mid height pore pressure transducer are coved with a layer of latex. After this had cured the semi-conductor chips of the Hall effect sensors were fixed into position. Several more layers of latex were then applied. Each layer of latex was applied with a fine brush to ensure as little surface area of the membrane was covered to avoid any issue with flexure between the latex and membrane during consolidation. Each layer of latex was cured by running an air current using a fan to expedite the drying process. The sample was sealed within the membrane and would not be affected by the fan.

Once the application of latex seals was complete the connection between the top cap drainage line and the back pressure controller was made whilst ensuring the line remains free from trapped air. The upper Perspex cell was attached and the entire cell was filled slowly using a reservoir of de-aired and de-ionised water. During this process the cell controller empties into the cell to remove any trapped air into the cell. Air was released from the cell during filling via a valve located at the top of the cell.

3.4.13 Saturation and consolidation

The soil was saturated according to BS 1377-6:1990, with increments of cell and back pressure of 25kPa/hr applied until the cell pressure reached 325kPa. The B-value test was performed where cell pressure was increased to 350kPa. A minimum B of 0.96 was required before progression to consolidation. Volume changes during saturation were recorded and used to determine changes to the sample for follow-on calculations of moisture content.

The samples are consolidated incrementally to a particular effective stress corresponding to a particular value of liquidity index. The increments of cell pressure were never greater than 150kPa. The change in moisture content was calculated through the volume of expelled water at the end of the consolidation process to allow comparison of soils at the same value of liquidity index to be undertaken. The sample was considered consolidated once 95% of the excess pore pressure had dissipated.

The change in void ratio was determined from volume change measurements taken from the back pressure controller. The dimensions of the sample were then derived with the Equations (3-2) and (3-3);

$$A = A_0\left[1-\frac{2}{3}\frac{\Delta V_C}{V_0}\right] \tag{3-2}$$

$$L = L_0\left[1-\frac{1}{3}\frac{\Delta V_C}{V_0}\right] \tag{3-3}$$

Where A, is the cross sectional area of the sample, L is the length, and V is the volume. The subscript 0 denoted initial conditions.

Once the change in void ratio was determined several shear wave tests are conducted using the bender element system and used with the density of the soil which was derived based on the volume change methods. Docking of the sample to the load cell was via movement of the piston upwards, where the half ball connects with the load cell without transmitting load by rotating within a groove until contact was made. Full

contact was assumed via visual inspection of the contact area to avoid any stressing/straining before the shear stage.

3.5 Standard triaxial apparatus

3.5.1 Hardware

The standard triaxial system was a fully automated GDS Instruments Triaxial Testing System (GDSTTS). The GDSTTS was designed for 38mm diameter samples. The system consists of a Bishop and Wesley type stress path triaxial cell with hydraulic loading or displacement control using an Advanced Pressure/Volume controller (ADVDPC). An additional two advanced controllers were used to control back and cell pressures. The pressure capacity of both the Bishop and Wesley cell and the controllers was 200kPa. The volume capacity of each controller was 200cc, with volume resolution to ±0.001cc and pressure resolution to 0.1kPa.

Load was measured with a 5kN submersible load cell accurate to ±0.1% and a resolution of ±0.2N. Drainage was through the back pressure line connected to the top cap of the specimen. Pore pressures were measured at the base with a P102 Sherburne transducer. Axial displacements were measured externally with a calibrated LVDT connected to the loading ram through a side arm. All instrumentation was logged and managed through a National Instruments Data Acquisition card resident in a PC.

3.5.2 Control and acquisition

Data acquisition was through a 16 bit serial pad connected to the PC through a National Instruments Data Acquisition card. The instrumentation and each test was managed using GDSLAB software. During displacement controlled testing, the loading of the axial ram with the advanced controller was dependant on a feedback loop from the axial LVDT. During tests points are recorded at a maximum rate of 1 point per 4 seconds, which was written to an ASCII file.

3.5.3 Consolidated undrained triaxial tests

For each soil at least three consolidated undrained shear tests were conducted at increasing initial effective stress to determine the slope of the isotropic compression and the critical state line. 38mm diameter samples were used (rather then other dimensions) as this was the specification for this triaxial apparatus. The 38mm specimens were sampled directly from U100 consolidation moulds which were used to reconstitute the 100mm sample as used for the high speed tests. The process of reconstitution was the same as discussed in Section 3.3 for 100mm diameter samples used in the Electromechanical Triaxial system tests. Once the 38mm samples were taken from the U100 moulds they were sealed with wax. With the exception that side drains were not used, the samples were prepared in the same way as the 100mm diameter tests described in previously in Section 3.4.12.

Saturation of the 38mm samples was in accordance with BS 1377-6:1990 by ramping the cell and back pressure at 25kPa/hr until the cell pressure reached 325kPa with an effective stress of approximately 25kPa. When the cell pressure reached 325kPa a B check was performed where the cell pressure was increased 25kPa. If the saturation value were less than 0.96 the test was discarded. Following saturation the samples were consolidated with increments of cell pressure increasing up to a maximum of 150kPa in accordance with BS 1377-6:1990.

Once 95% of the excess pore pressures had dissipated the samples were deemed consolidated. During consolidation the base pedestal was raised as the specimen decreases in volume to prevent the possibility of tilting of the sample. The base pedestal was raised with manual input of displacements or automatically with rates corresponding to those slow enough to ensure deviatoric stresses do not develop. This was to prevent non uniform stress distribution to the sample at the start of shear. During consolidation the volume change in the sample was measured by the back pressure controller.

3.5.4 Triaxial permeability tests

For permeability testing the hardware of the standard triaxial system was reconfigured. Axial displacements were not required during permeability testing

therefore the advanced controller originally used for axial displacements in the Bishop and Wesley cell was utilised to provide a pressure differential through the sample to the base of the triaxial sample. The other aspects of the standard triaxial system remain unchanged. The GDSLAB software was reinitiated to configure the hardware to a permeability module to provide control of the rearrangement of the hardware.

The entire process of preparation for the 38mm samples to full saturation remains unchanged from consolidated undrained tests. When fully saturated the samples were incrementally consolidated in accordance with BS 1377-6:1990 to initial effective stresses corresponding to those of each sample used in the strain rate dependence tests in the electromechanical triaxial testing system. To initiate upward flow through the specimen the valve to the base pressure line was closed and its pressure increased to give the desired pressure differential. The base pressure line was then opened. The flow of water through the specimen and the pressures at the ends of the specimen were measured continuously by the advanced controllers and also at the base with the pore pressure transducer. The acquired data was written to an ASCII file for further processing.

3.6 Materials

Model soils rather than sampled natural clays have been selected for this study. A commonly used material in geotechnical research is Kaolin, also known as china clay. The main mineral in this clay is Kaolinite, which has few or no exchangeable cations and strong interlayer bonding. Kaolinite is also relatively inactive compared to other clay minerals. For these reasons Kaolinite may be described as the least clay-like of the clay minerals (Powrie, 2004).

In comparison with other clays of a similar clay fraction, Kaolin has a relatively high permeability which allows for shorter tests under drained conditions (Sorensen, 2006). Kaolin clays are thus attractive for research in geotechnical engineering, and are easily commercially available (Rossato *et al.*, 1992). A disadvantage of Kaolin is that its clay fraction is higher than typical natural soils, which may promote particle orientation during sedimentation, consolidation and shearing, and thus Kaolin has an

unusual tendency (in comparison with destructured clays) to quickly develop residual strength.

Rossato *et al*. (1992) compared the mechanical behaviour of a wide variety of natural soils taken from several studies with that of reconstituted Kaolin, and found that Kaolin displayed non typical behaviour to that of natural cohesive soils. To address the difference between natural soils and Kaolin, they developed a compound model soil known as KSS (Kaolin-Silt-Sand). By mixing Kaolin with fine sand and silt, it was possible to better reflect the mechanical behaviour of some soils, including glacial tills of southern England. KSS compromises 50% Kaolin, 25% sand and 25% silt, and although the addition of the larger particles reduces the plasticity from that of Kaolin, KSS retains cohesive properties.

Compared to Kaolin the overall clay fraction of KSS is reduced, resulting in lower coefficient of compressibility and comparatively higher strength. Due to the inclusion of larger particles in KSS it will also be more permeable than Kaolin, and may subsequently allow for different inter-particle response to stresses. KSS has been successfully used in similar studies involving increasing rates of strain (Balderas-Meca, 2004) and also in rapid loading of model piles (Brown, 2004) where its mechanical response has been found to be comparable to that of lodgement Tills such as Cowden and Grimsby Till.

Thus a comparison between the strain rate dependence of Kaolin clay and KSS will provide clarity on the relationship between strain rate effects and fundamental soil properties which are altered due to the inclusion of the larger particles in KSS. In this study the components of KSS are 50% Speswhite Kaolin, 25% fine Congleton Sand (HST95), and 25% fine silica flour (HPF 5) which was taken as the silt component.

To contrast the influence of the sand and silt components used in KSS a third soil was introduced by altering the proportion of these components. The Kaolin proportion of the third soil was maintained at 50% however the sand content was increased to 40% and the proportion of silt was reduced to 10%. Thus the third soil was named KSS-541 to distinguish the proportions of each constituent in the soil. The aim of increasing the proportion of sand was to increase the permeability of the soil, whilst

the proportion of Kaolin was maintained to retain the cohesive characteristics of KSS-541. The comparison of KSS and KSS-541 will provide information on the influence of sand content in particular. Each soil was expected to be dominated by the clay matrix of the sample based on the clay fraction of the samples (Kumar and Wood, 1999).

3.6.1 Soil description and classification

The particle size distribution (PSD) was determined separately for each material and these are presented in Figure 3-13. The PSD for sand was determined using the dry sieving method as per BS1377-2:1990. The PSD for both Speswhite Kaolin and the HPF5 silt were determined by laser diffraction using a Malvern Hydro 2000MU, where they were tested in suspension and dispersed by ultrasonication.

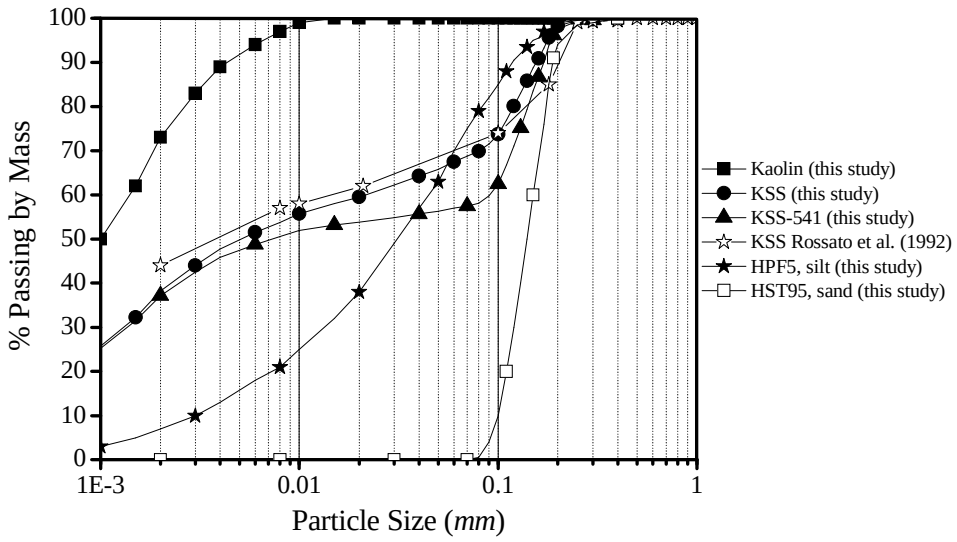

Figure 3-13 Particle Size Distribution of model soils as well as their individual constituent materials used in this study, compared with Rossato *et al.* (1992)

PSD curves for the compound materials (KSS and KSS-541) are shown in Figure 3-13 which are based on the percentage mass of each material used for the model soils. Figure 3-13 also illustrates PSD curves for the KSS as per Rossato *et al*. (1992). These are almost identical to that from Brown (2004) and Balderas-Meca (2004). The influence of marginally different materials in the composition of KSS does not appear to affect the PSD greatly.

From Figure 3-13 the clay fraction of the Speswhite Kaolin is approximately 73% which was lower when comparisons are made to the findings of Rossato *et al*. (1992). The clay fraction of the silica flour and the fine sand are minimal. The effect of mixing fine sand and silt with Kaolin to develop KSS reduces the clay fraction to approximately 38%, and 37% for KSS-541 (Table 3-3).

The plasticity index was determined for each soil as per BS 1377-2:1990. The liquid limit was determined using the cone penetrometer method. The plastic limit was determined using the rolling thread method. The results are shown in Figure 3-14 and Table 3-3. In Figure 3-14 KSS and KSS-541 soils are relatively close in comparison with Speswhite Kaolin. With increasing sand content the liquid limit was seen to reduce and subsequently the plasticity index also reduces. Similar plastic limits were measured for KSS and KSS-541.

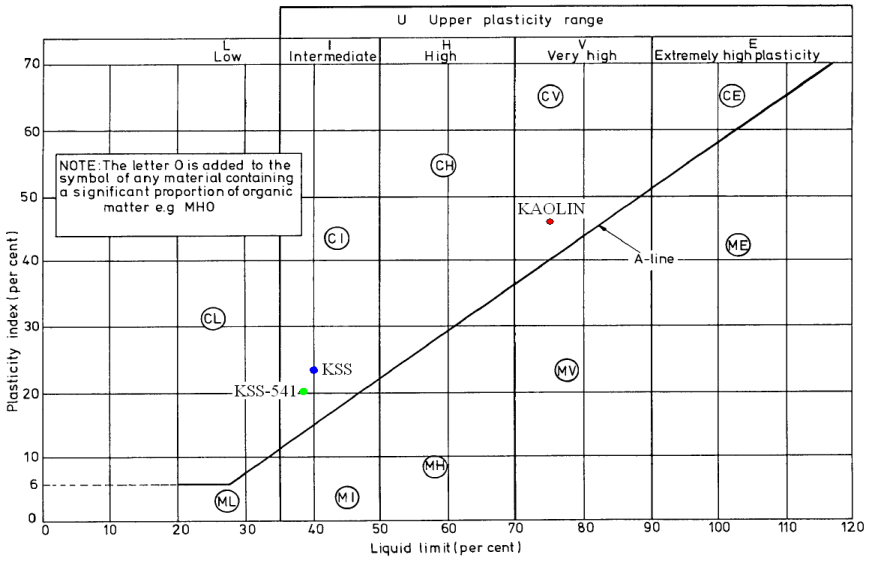

Figure 3-14 Model soils used in this study overlain on classification chart for cohesive soils from BS 5930

The ratio between the plasticity index and the clay fraction is known as the activity (Equation 3-4), which is closely related to the specific surface and the mineralogy of the clay (Skempton, 1953).

$$A = \frac{I_P\%}{CF\%} \qquad (3\text{-}4)$$

Where *A* is the activity of the soils, I_P is the plasticity index and *CF* is the % mass of particles less than 2 microns. The values of the activity (Table 3-3) are typical of those of Kaolinite based soils.

Soil	**Plastic Limit, w_P (%)**	**Liquid Limit, w_L (%)**	**Plasticity Index, I_P (%)**	**Clay Fraction, *CF* (%)**	**Activity**
Kaolin	30	75	45	73	0.61
KSS	17	40	23	38	0.60
KSS-541	18	38.5	20.5	38	0.55

Table 3-3 Summary of model soils used in this study and their index properties

3.6.2 Primary consolidation

The behaviour of each soil in drained compression was determined in both isotropic and 1-dimensional conditions. Each test was conducted on samples reconstituted from slurry in a 1-dimensional consolidation apparatus where the slurry was consolidated under a vertical effective stress of 140kPa. The isotropic consolidation line was defined in the standard triaxial apparatus using 38mm samples which are re-consolidated to an effective stress of 250, 500 and 750kPa. These stresses were selected with the assumption that when reconsolidation was complete the soil will be normally consolidated.

1-dimensional consolidation lines were defined with 100mm diameter samples in the electromechanical triaxial apparatus under anisotropic test conditions using a radial local hall effect to maintain zero lateral strain. Figure 3-15 presents the isotropic consolidation line from the standard triaxial apparatus tests and the K_0 tests in v-lnp' space. The slopes of the 1-dimensional and isotropic consolidation lines are shown in Table 3-4. The values of the Compression Index (C_C), (Equation 3-5), for each soil are compared to those from Rossato *et al*. (1992) and typical ranges from other soils in Figure 3-16. The values of Compression Index appear to be similar to those from the range found by Hight *et al*. (1987).

$$C_C = \frac{\Delta e}{\Delta \log \sigma_V'} \qquad (3\text{-}5)$$

Where e is void ratio and σ'_V is the vertical effective stress.

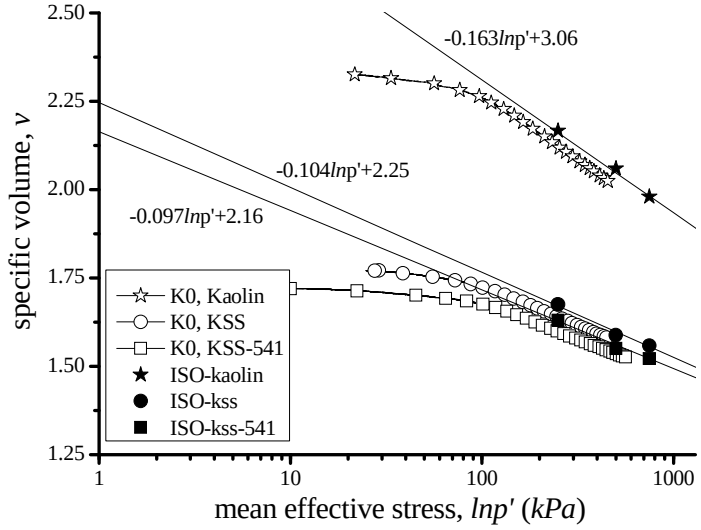

Figure 3-15 Effective stress paths during K_0 consolidation

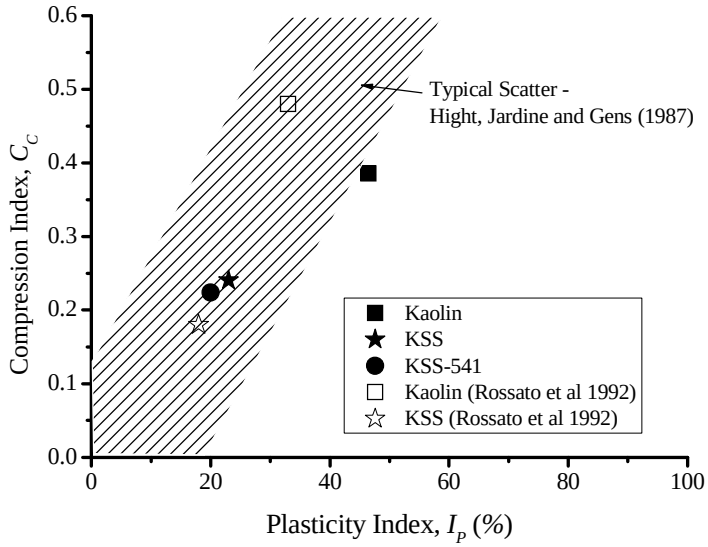

Figure 3-16 Comparison of compression indices with Rossato *et al*. (1992)

Soil	**Compression Index, C_C**	**λ_{NCL}**	**N**	**Γ**
Kaolin	0.385	0.1630	3.06	2.93
KSS	0.24	0.1044	2.25	2.17
KSS-541	0.22	0.0971	2.16	2.08

Table 3-4 Consolidation properties of soils used in this study

3.6.3 Secondary consolidation

The coefficient of secondary compression for each soil was determined at the end of isotropic consolidation in the standard triaxial apparatus. Notably little deviation of the coefficient of secondary compression was seen from approximately 5 days. The coefficient of secondary compression was defined as;

$$C_\alpha = \frac{\Delta e}{\Delta \log t} \qquad (3\text{-}6)$$

Where *e*, is voids ratio and *t* is time in minutes. The values of secondary compression are shown in Figure 3-17.

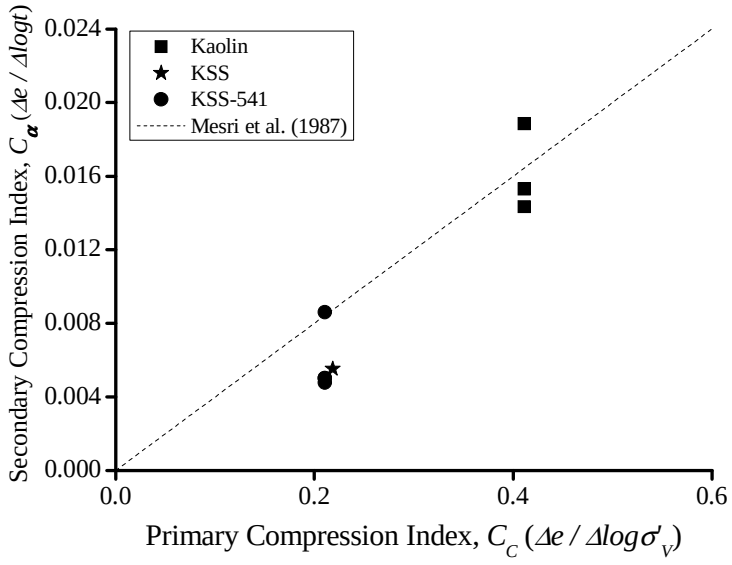

Figure 3-17 Secondary compression values from triaxial isotropic creep tests, compared with Mesri and Castro (1987)

Mesri and Castro (1987) compared results of several soils and found the ratio of C_α/C_C to be approximately constant for a particular soil. It was also found that the ratio of secondary compression to the compression index were quite similar for particular class of soil, with inorganic soft clays averaging with ratios of 0.04±0.01. This relationship as determined by Mesri and Castro (1987) is compared to the results of these soils in Figure 3-17. The three soils in this study compare well with the range of values as described by Mesri and Castro (1987).

3.6.4 Critical state line

The critical state line has been defined from undrained triaxial compression tests on 38mm diameter samples in the standard triaxial device. The samples were isotropically consolidated to an initial effective stress of 250, 500 or 750kPa. The effective stress ratio (*q/p'*) at critical state for each model soil are compared in terms effective angle of internal friction at critical state in Figure 3-18 with results from Rossato *et al*. (1992). The Kaolin used in this study develops higher angles than the Kaolin used by Rossato *et al*. (1992); however the values for KSS and KSS-541 are similar to the KSS as per Rossato *et al*. (1992).

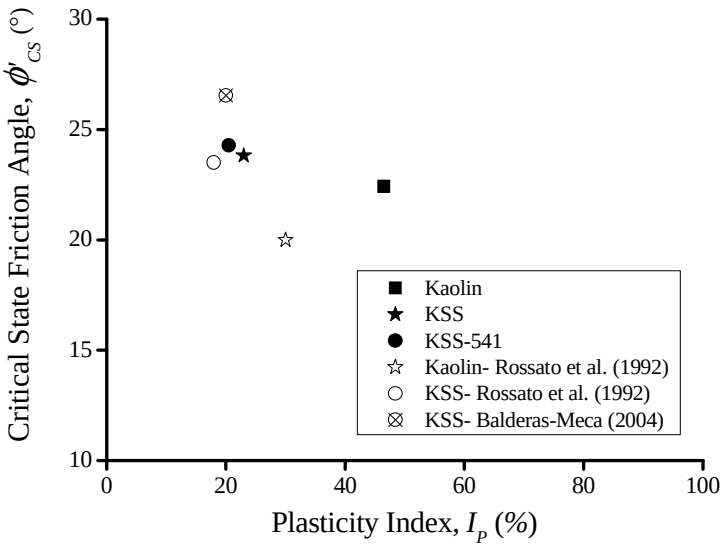

Figure 3-18 Comparison of the critical state frictional angle of soils used in this study with Rossato *et al.* (1992)

3.6.5 Permeability

Permeability tests were conducted in the standard triaxial apparatus using 38mm diameter samples, with a length to height ratio of 2:1. The soils were consolidated to effective stresses corresponding to those used during high strain rate tests before a hydraulic gradient was applied using advanced GDS controllers. An hydraulic gradient was achieved by applying upward differential pressures of 10kPa.

The permeability (*k*) of each soil was calculated as;

$$k = \frac{1.63qL}{A\Delta p} * 10^{-4} \qquad (3\text{-}7)$$

Where q, is the mean rate of flow through the sample, L is the length of the sample, A is the cross sectional area and Δp is the pressure difference applied to the top and bottom of the sample.

Permeability was shown to vary with void ratio. Figure 3-19 compares permeability with those of Kaolinite as determined by Al-Tabbaa and Wood (1987). The relationship between permeability and void ratio was almost identical for KSS and KSS-541, indicating for that for these soils void ratio has a greater influence than plasticity index.

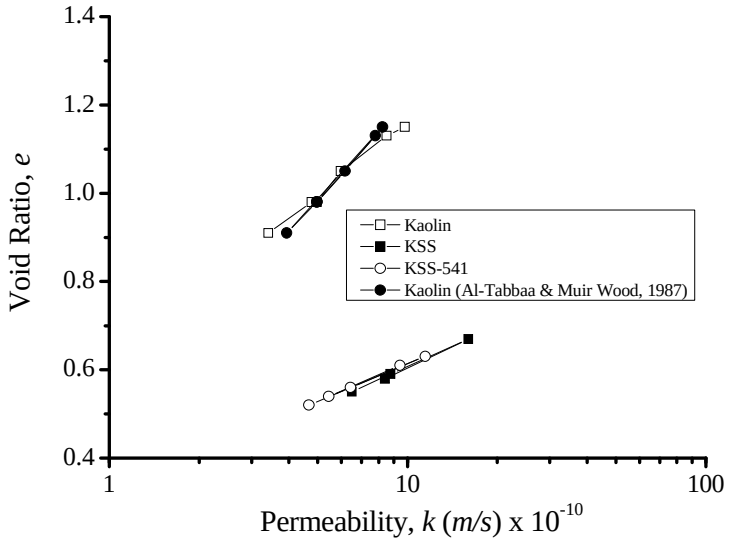

Figure 3-19 Variation of permeability with void ratio for each soil used in this study

The results for each soil are shown in Table 3-5 along with coefficients of consolidation that were calculated as per Equation 3-8.

$$C_V = \frac{k}{m_V * \gamma_W} \qquad (3\text{-}8)$$

Where $m_{V,}$ is the coefficient of volume compressibility as defined as;

$$m_V = \frac{\Delta V_{e2} - \Delta V_{e1}}{V_{e0} - \Delta V_e} * \frac{1000}{p'_2 - p'_1} \quad (3\text{-}9)$$

Where V_{e1} and V_{e2} describe the change in volume from the initial volume of the sample V_{e0} corresponding to the change in effective stress (p'). The values of m_V were taken from 100kPa increments (to the pre-consolidation pressure) in the normally consolidated range of compression.

Soil	λ_{NCL}	Coefficient of Compressibility, m_v (m^2/MN)	Permeability, k (m/s)x10^{-10}	Coefficient of Consolidation, C_V (m^2/year)
Kaolin 720kPa	0.1634	0.12	4.96	13.9
Kaolin 1150kPa	0.1634	0.075	3.71	14.7
KSS 560kPa	0.1044	0.12	8.4	23
KSS-541 300kPa	0.0971	0.2	9.43	15
KSS-541 600kPa	0.0971	0.11	5.44	16.6

Table 3-5 Summary of the hydraulic properties of soils used in this study

3.6.6 Initial small strain shear modulus

The initial shear modulus was derived from measurements of shear wave velocity taken from axial bender elements incorporated into the top cap and base pedestal of the electromechanical GDS apparatus. The velocity of the shear wave was taken from the time to travel the distance between the tips of the bender elements. The initial shear modulus was related to the shear wave velocity through the density of the soil through Equation 3-10.

$$G_0 = \rho V_S^2 \quad (3\text{-}10)$$

Where $V_{S,}$ is the velocity of the shear wave and ρ is the density of the soil at the time the shear wave was recorded.

The velocity of the shear wave was taken at the end of isotropic consolidation, and at various effective stresses for each soil. The variation of the initial shear modulus with

mean effective stress as is shown in Figure 3-20 where both axis have been normalised by a reference pressure of 1kPa. This has being done to make the relationship between shear modulus and effective stress dimensionless (Viggiani and Atkinson, 1995b).

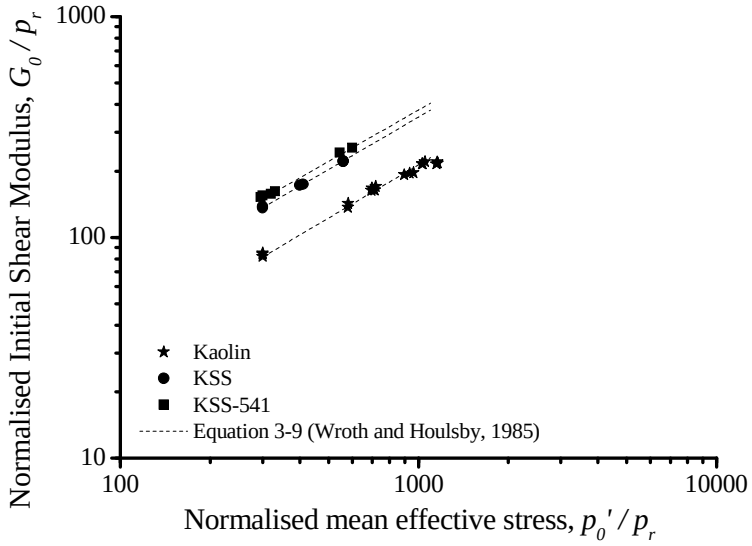

Figure 3-20 Variation of normalised initial shear modulus with initial effective stress for soils used in this study

Wroth and Houlsby (1985) proposed Equation 3-11 to describe the relationship between shear modulus and mean effective stress.

$$\frac{G_0}{p_r} = A\left(\frac{p'}{p_r}\right)^n \qquad (3\text{-}11)$$

Where p_r is a reference pressure of 1kPa, and A and n are dimensionless material parameters dependent on the nature of the soil (Viggiani and Atkinson, 1995).

Viggiani and Atkinson (1995b) compared the initial shear modulus from several soils and found that plasticity index has an effect on both coefficients A and n. Figures 3-21 and 3-22 compares values of A and n for each soil taken from Figure 3-20 where, it is shown that the initial shear modulus of the soils from this study compares well with the general trend suggested by Viggiani and Atkinson (1995b). Note the dashed lines

in Figures 3-21 and 3-22 are not best fit lines but trends taken from Viggiani and Atkinson (1995b).

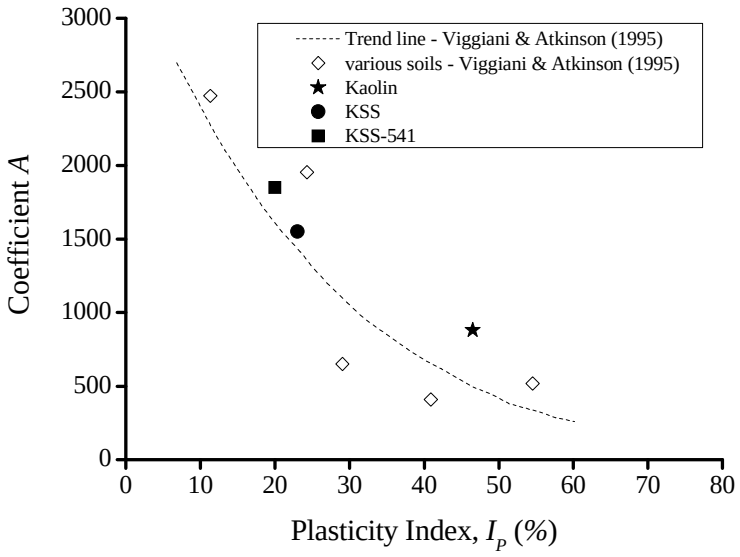

Figure 3-21 Variation of coefficient *A* (Equation 3-11) for soils used in this study

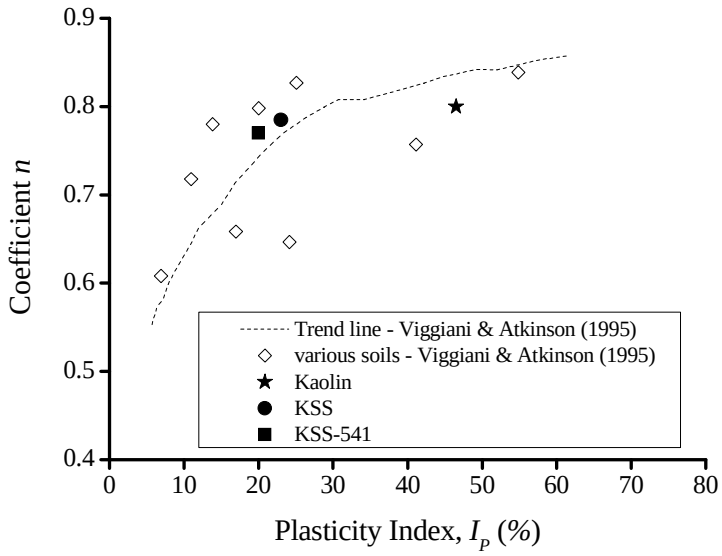

Figure 3-22 Variation of coefficient *n* (Equation 3-11) for soils used in this study

4 Results and Discussion of Shearing Behaviour

4.1 Introduction

This chapter describes the shearing behaviour of soils during the triaxial shear tests. The majority of tests conducted in this study and discussed here are on normally consolidated samples. Additionally, four tests on over consolidated samples are also described and compared to the behaviour of normally consolidated samples. The constant rate of strain tests were conducted at one of seven axial strain rates including; 1%/hr, 5%/hr, 10%/hr, 300%/hr, 1,800%/hr, 18,000%/hr and 180,000%/hr. Each strain rate test was conducted without physical restriction on drainage and therefore these are drained triaxial compression tests in terms of the test configuration. Table 4.1 lists the soils and corresponding number of tests on each that were analysed for the results presented in this chapter.

Soil	**Initial effective stress, p'_0 (kPa)**	**Plasticity Index, *Ip* (%)**	**Critical State ratio, *M***	**Void ratio, *e***	**Number of tests**
Kaolin	300	45	0.875	1.13	4
Kaolin	720	45	0.875	1.00	7
Kaolin	1150	45	0.875	0.90	7*
Kaolin OCR 4	300	45	0.875	0.95	2
Kaolin OCR 10	115	45	0.875	0.99	2
KSS	560	23	0.933	0.59	7
KSS-541	300	20	0.95	0.60	7
KSS-541	600	20	0.95	0.54	7

Table 4-1 List of soils, their characteristics and number of tests used in Chapter 4

Note; * number of tests presented here is two

The effect of strain rate (each of the abovementioned strain rates) on normally consolidated soil is presented for one soil in particular (KSS consolidated to 560kPa) for brevity. This soil displayed shearing behaviour typical of the other normally

consolidated soils in regard to aspects discussed in this chapter. The behaviour of over consolidated Kaolin (OCR 1, 4 and 10) at high strain rate (300%/hr and 180,000%/hr) is also compared.

4.2 Constant strain rate tests in normally consolidated soils

Results of constant strain rate tests in KSS consolidated to 560kPa (KSS 560kPa) are presented here to highlight and discuss typical strain rate dependent behaviour observed of normally consolidated soils. The behaviour of the soils is discussed with particular emphasis on the effect of strain rate on shear stress at strains in excess of 1% shear strain.

The main focus of this section is normally consolidated soils over a wide range of strain rates, tested in drained conditions to avoid forcing artificially undrained behaviour from the soil. Therefore it is expected where the transition to undrained behaviour occurs is reflective of real soil behaviour in situ.

The behaviour of the soil is addressed, with focus on strain rate dependent aspects and how they may relate to geotechnical engineering; in particular, capacity testing. The main aspects of soil shear behaviour in a triaxial system and their dependence on strain rate are presented; the stress-strain curves, excess pore pressures, volumetric strains, and typical effective stress paths.

4.2.1 Stress-strain

Figure 4-1 presents the deviatoric stress–strain curves for strain rates between 1-180,000%/hr in KSS-560kPa. The deviatoric stress has been normalised by the initial effective stress at the end of consolidation (p'_0) in Figure 4-1. An effect of strain rate and strain is evident on the deviatoric stress shown in Figure 4-1. At low strains (<1%); a faster strain rate results in an increase in deviatoric stress. However at higher strains it can be seen that the samples display different behaviour depending on strain rate, ranging from apparent strain hardening to clearly identifiable maximum/peak deviatoric stresses.

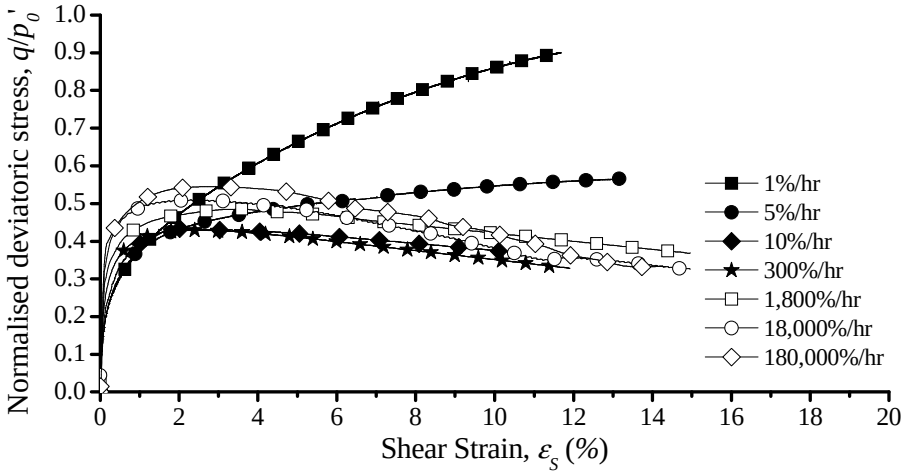

Figure 4-1 Normalised deviator stress-strain curves at increased strain rate for KSS at 560kPa

The test undertaken at the slowest strain rate of 1%/hr displays no peak in deviatoric stress as the soil work hardens under continued strain. The 1%/hr tests developed the greatest maximum deviatoric stress. The 1%/hr test was prematurely halted because the gain in strength displayed by the soil at this strain rate was sufficient to threaten the capacity of the load cell. With continued strain the 1%/hr test would presumably display a higher strength.

As the samples were tested at increasing strain rates from 5%/hr to 300%/hr the maximum deviatoric decreased, and the samples began to display a more clearly defined peak deviatoric stress. At strain rates from and in excess of 10%/hr; the sample shapes changed, and began to display early barrelling before clear development of slip planes as evidenced by softening in the stress strain curves (Figure 4-1). The 300%/hr test developed the lowest overall deviator stress shown in Figure 4-1, identifying it as close to where the transition from partially drained to undrained behaviour occurs as discussed in Section 2.2.2. Each test at strain rates in excess of 300%/hr displayed an increase in maximum deviatoric stress, as well as higher deviatoric stress over the entire range of strain. However with increasing strain, softening of the sample occurs (at strain rates of 300%/hr to 180,000%/hr), which tend to similar values of deviatoric stress at higher strain (>10%). Figure 4-1 thus highlights the effect of strain rate on deviatoric stress, as well as highlighting that strain rate effects on deviatoric stress cannot be considered independently of strain,

particularly at lower strain rates. Figure 4-2 presents how strain rate and level of strain affect the deviatoric stress for KSS-560kPa.

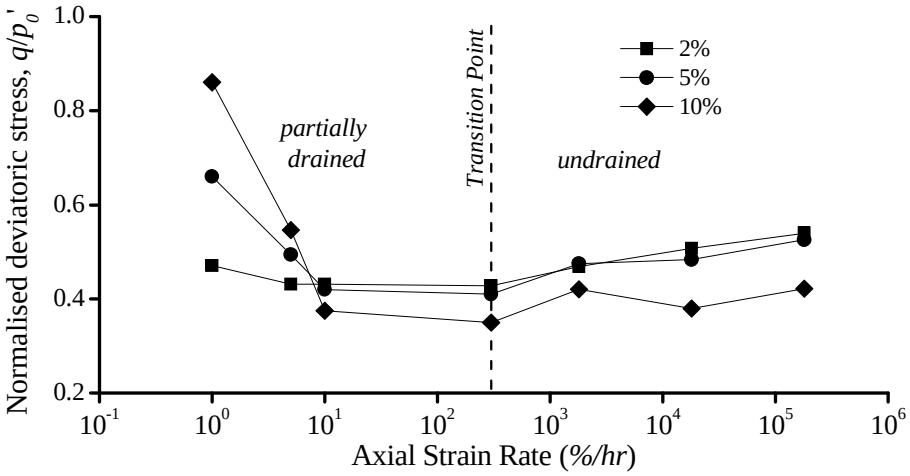

Figure 4-2 Variation of normalised deviatoric stress with strain rate and strain in KSS 560kPa

The deviatoric stress measured at each strain rate is presented for 2%, 5%, and 10% strain (Figure 4-2). A virtual boundary is shown in Figure 4-2, labelled as the transition point, dividing the domain where a decrease in strain rate results in an increase in strength from that where increasing strain rate results in an increase in strength. The transition is shown corresponding to a value of 300%/hr. Figure 4-2 shows that with increasing strain the tests at strain rate less then the transition display increasing strength indicating strain hardening. This reflects behaviour seen by Carter (1982) in a numerical and experimental study on strain rate effect on the strength of a fine grained soil in drained triaxial tests. At strain rates to the right of the transition point an increase in strain rate results in an increase of strength. This reflects behaviour seen in undrained triaxial testing at increased strain rates (Lefebvre and LeBoeuf, 1997, Sheahan *et al*. 1996). As clearly visible in Figure 4.2, there is a much larger increase in strength (strain rate effect) in the partially drained domain in comparison to the undrained domain.

4.2.2 Excess pore pressure

The corresponding excess pore pressures for KSS-560kPa are shown in Figure 4-3 for measurements at the mid height excess pore pressure transducer.

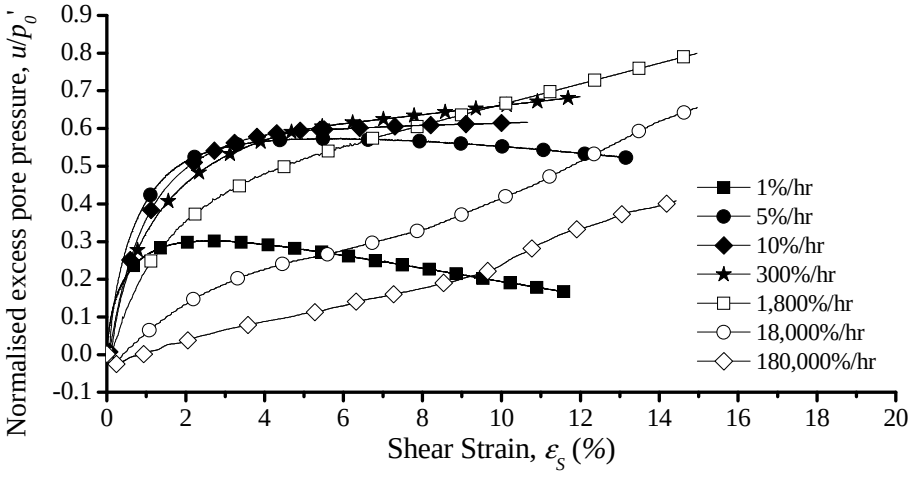

Figure 4-3 Normalised mid height excess pore pressure measurements at increased strain rate in KSS 560kPa

The excess pore pressures which developed during the early part of shearing during the 1%/hr test begin to dissipate due to consolidation at later stages and the soil strain hardens. Increased excess pore pressures were measured from 5%/hr to 300%/hr tests. These tests displayed similar magnitudes of excess pore pressures. With increasing strain rates from 300%/hr the magnitude of the excess pore pressures continually reduced for each test at increased strain rate. This may indicate suppression of excess pore pressures consistent with behaviour of normally consolidated at increased strain rate as noted by Lefebvre and LeBoeuf (1987), Sheahan *et al.* (1996), and Balderas-Meca (2004). This may also indicate a time lag in excess pore pressure measurements at high strain rate.

At the beginning of shearing for the 18,000%/hr and 180,000%/hr tests slightly negative excess pore pressures are measured before they become positive at higher level of strain. The development of some negative excess pore pressure at the beginning of shear was also evident in results from Sheahan *et al.* (1996) and Balderas-Meca (2004). This may suggest some dilation is occurring at the beginning

of shear at higher strain rate tests, which is unexpected due to the association of contraction during shear in normally consolidated soil. Suppressed or dilative excess pore pressures would result in an increase in mean effective stress. This is often cited as the mechanism to which the strain rate dependent strength increases are attributed.

Figure 4-4 presents the variation of excess pore pressures with strain rate measured at the mid height of the sample.

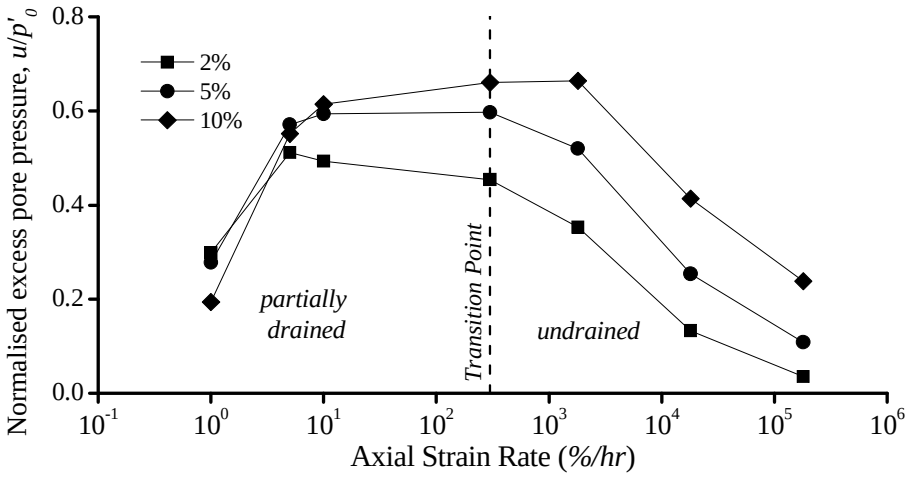

Figure 4-4 Variation of normalised excess pore pressures (mid height) with strain rate and strain in KSS 560kPa

Figure 4-4 shows that excess pore pressures are dependent on both the magnitude of strain and strain rate, which is in contrast to Akai *et al*. (1975) and Soga and Mitchell (1996) who found that pore pressures (in increased strain rate testing) were a function of strain and not strain rate. In comparison with this study the aforementioned studies used a limited range of strain rates, although Akai *et al*. (1975) tested at strain rates up to 3,000%/hr. The excess pore pressure measurements from Akai *et al*. (1975) were taken from the base of samples, which may be subject to end effects.

At strain rates in excess of 300%/hr, there is a similar magnitude of increase in excess pore pressure between 2%, 5%, and 10% strain. In terms of percentage increase, there is a much larger increase in excess pore pressures with strain for faster tests. The decreasing excess pore pressure with increasing strain rate is typical for each other

series of tests in the other normally consolidated soils. Behaviour shown in Figure 4-4 may simply reflect the strain softening seen in the corresponding stress strain curves discussed previously.

4.2.3 Volumetric stress path

The volumetric strain-effective stress paths are shown in Figure 4-5 for KSS 560kPa at strain rates between 1%/hr to 300%/hr. The effective stresses in Figure 4-5 were derived using mid height excess pore pressure measurements.

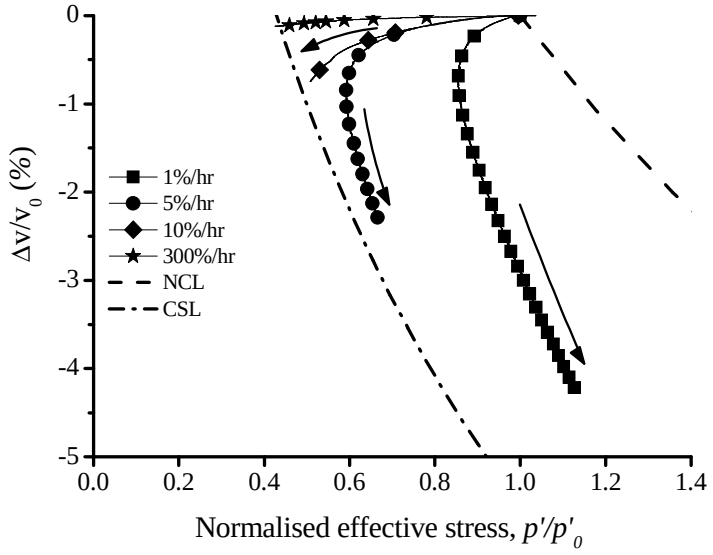

Figure 4-5 Variation of volumetric strain with strain rate in KSS 560kPa

With increasing strain rate a reduction in the volumetric strain is evident in Figure 4-5. Data from tests at strain rates above 300%/hr are omitted from Figure 4-5 because they do not display a change in volume.

The stress paths in Figure 4-5 convey how with increasing strain rate the corresponding magnitude of volumetric strain occurs at significantly lower effective stress. This reflects the decreasing influence of consolidation with increasing strain rate, and the transition to increasingly undrained behaviour. With the reduction in effective stress (seen for increasing strain rate) the soils tend closer to critical state,

and thus the potential increase in strength due to consolidation effects (potential volumetric strain) reduce.

This is particularly evident between strain rates of 5 and 10%/hr where the strain rate is doubled; the soil displays much lower volumetric strain and hence lower maximum strength. There is little difference between 5 and 10%/hr volumetric strain-effective stress paths at the early stage of shear ($p'/p'_0 > 0.7$). During construction (where excess pore pressure and settlement are monitored) it would be indecipherable whether the soil will improve in terms of strength (as at 5%/hr) or tend to critical state at lower strength (as at 10%/hr). Prior knowledge of the strain rate dependency of the soil could allow more efficient construction practise, allowing works to continue if as at 5%/hr the factor of safety would improve during construction.

As shown in Figure 4-5, the test at 300%/hr displays almost no volume change during shear in comparison with lower strain rate tests and is thus considered practically undrained. Coupled with classification of the soil in terms of critical state, determination of the strain rates corresponding to fully drained, partially drained and undrained response prior to construction would allow engineers to better understand the likely behaviour of soil in working conditions, making efficiencies in construction practises possible.

4.2.4 Effective stress path

The effective stress paths of KSS-560kPa for strain rate tests between 1%/hr to 180,000%/hr as shown in Figure 4-6. The effective stress paths are derived using mid height excess pore pressure measurements.

Figure 4-6 (a) shows that effective stress paths for 1%/hr and 5%/hr change direction at higher strain, and tend towards the critical state line. It is expected these tests would intercept the critical state line at higher strain. The 1%/hr test was halted to avoid over rating the capacity of the load cell as previously mentioned. The 5%/hr tests were typically halted due to leakage in the sample membrane, which at higher strain levels was caused by a flex in latex seals which ruptured. The 10%/hr and 300%/hr tests are assumed to intercept the critical state line, with minor differences between effective

stress paths and critical state line due to the proximity of the mid height pore pressure transducer to the shear plane (Sheng *et al*., 1997). At the 0.25% strain contour in Figure 4-6; the 10%/hr and 300%/hr tests have diverged from the 1%/hr and 5%/hr tests indicating the transition to undrained behaviour at these strain rates. The effective stress paths in Figure 4-6 of KSS 560kPa at strain rates between 1%/hr and 300%/hr are expected behaviour of soils displaying partially drained to undrained behaviour.

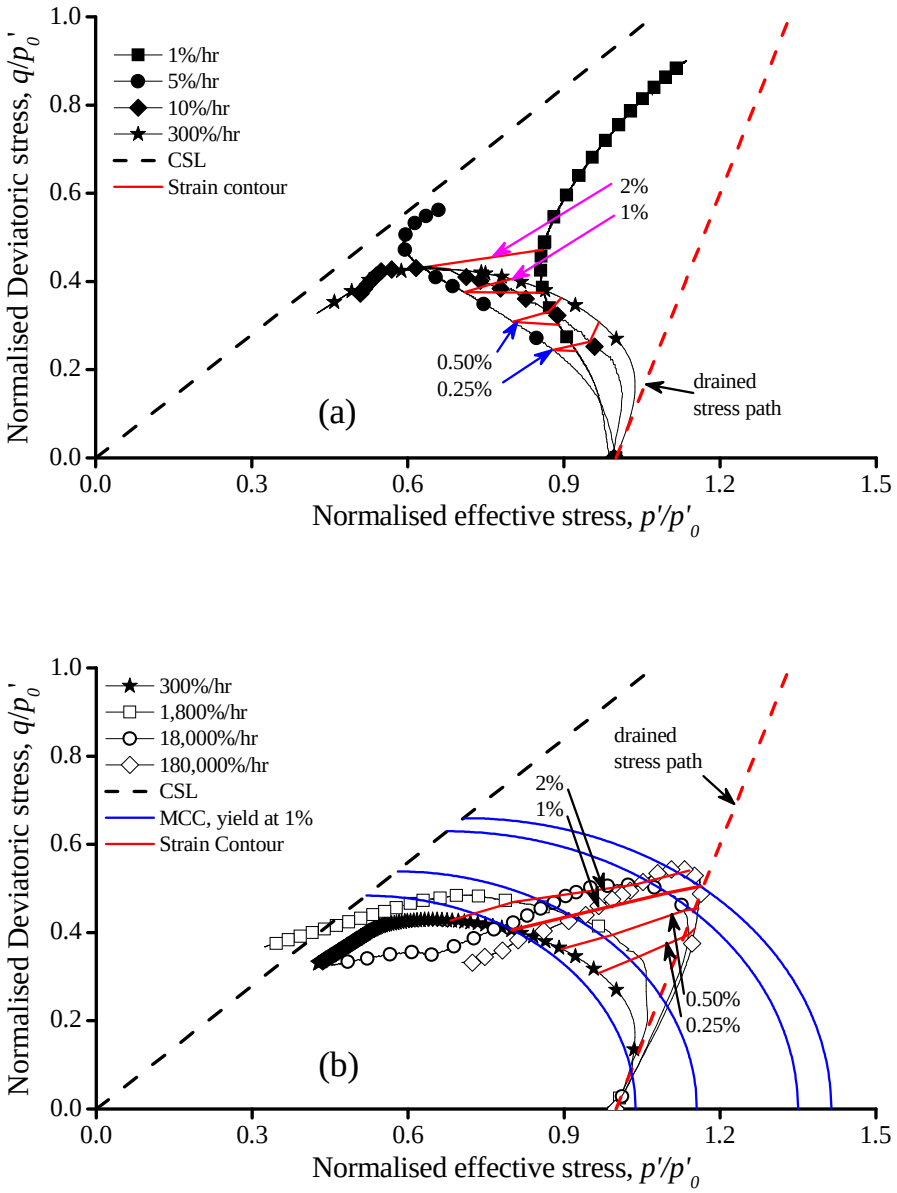

Figure 4-6 Effective stress path of KSS 560kPa derived using mid height excess pore pressure measurements during tests at (a) 1-300%/hr (b) 300-180,000%/hr

With increasing strain rates from 300%/hr the effective stress paths diverge further, tending towards the drained effective stress path with increased strain rate (Figure 4-6 (b)). This observation was also found in similar studies such as Sheahan *et al*. (1991) and Balderas-Meca (2004). Notably the stress paths lay outside the state boundary surface as described in the Modified Cam Clay (MCC) and Original Cam Clay (OCC) models for isotropic normally consolidated soil, as can be inferred from the initial effective stress ($p'/p'_0 = 1$). Balderas-Meca (2004) also noted this, and suggested the existence of a dynamic boundary surface as originally mentioned in research by Akai *et al*. (1962), Richardson and Whitman (1963) and Yong and Japp (1969) among others. Kutter and Sathringam (1992) mentioned in constitutive modelling the increase in undrained strength due to strain rate can be accommodated as an apparent increase in OCR. Figure 4-6 (b) shows a Modified Cam Clay (MCC) yield locus (Equation 4-1) for each strain rate test where the initial effective stress (p'_0) is increased to form a new yield locus for each strain rate test.

$$\frac{p'}{p'_0} = \frac{M^2}{\left(M^2 + \eta^2\right)} \qquad (4\text{-}1)$$

Where M is the slope of the critical state line, and η is the stress ratio. Each yield locus is defined at 1% strain. As shown in Figure 4-6 (b) the yield locus expands with increased strain rate. The increase in initial effective stress (Equation 4-1) used to develop the yield surface at 1% strain is 13% per log cycle increase in strain rate (from the p'_0 used for 300%/hr).

The MCC yield locus intercepts the critical state line at higher deviatoric stress than each strain rate test shown in Figure 4-6 (b). The critical state line is thought to be independent of strain rate (Richardson and Whitman, 1963, Lefebvre and LeBoeuf, 1987, Sheahan *et al*. 1996, Soga and Mitchell, 1996), although this observation was at strain rates significantly lower then those used in this study. These studies typically found the maximum strength close to or coincident with the critical state line, which is anticipated from normally consolidated soils. The results from this study (Figure 4-6 (b)) display maximum strength at a stress ratio less then critical state, which indicates the excess pore pressure measurements at maximum strength are less then

those expected from normally consolidated soils. It may also be possible that at higher strain rate the soils will develop peak strength before critical state is reached, as was noted by Sheahan *et al*. (1996) in normally consolidated reconstituted Boston blue clay. The effective stress paths tend towards the critical state line after the maximum strength has been displayed.

The aforementioned studies typically cite pore pressure suppression and the subsequent increase in effective stress as the mechanism involved in strength increasing with strain rate. Significant differences to previous studies may exist due to issues with measurement of excess pore pressures, as well as the strain rate at which tests are conducted, which are typically two to three orders of magnitude lower then the maximum strain rate used here. Balderas-Meca (2004) conducted tests at strain rates in excess of this study; his results did not display a maximum/peak in deviatoric stress, and effective stress paths at high strain rate did not intercept critical state. Notably the tests from Balderas-Meca (2004) suffered from cell pressure changes during high strain rate testing.

The effective stress paths for high strain rate tests (300%/hr to 180,000%/hr) thus display interesting behaviour which is contrary to expected frictional behaviour of normally consolidated soils. Although there is some consistency with literature (reduced excess pore pressure with increased strain rate), the correspondence with the critical state line at maximum/peak strength is not consistent with previous research, although notably previous studies utilised considerably lower strain rates.

4.3 Constant strain rate tests in over consolidated soils

In total four tests were conducted in Kaolin in an over consolidated state. Two tests were conducted at OCR 4 and two at OCR 10. The pre-consolidation pressure for these tests was 1150kPa, which was also used as the consolidation pressure for a series of normally consolidated tests in Kaolin. Thus in total 6 tests can be compared, two at each of OCR 1, OCR 4 and OCR 10. For each OCR, a test is compared at 300%/hr and 180,000%/hr. The 300%/hr strain rate was chosen because as discussed previously it was the lowest strain rate which is considered to be fully undrained. The 180,000%/hr test is the fastest strain rate used in this study.

4.3.1 Stress-strain

Figure 4-7 compares the deviatoric stress normalised by the initial effective stress at the end of consolidation for OCR 1, 4 and 10, at strain rates of 300%/hr and 180,000%/hr. Each OCR displays an increase in normalised deviatoric stress with increasing strain rate.

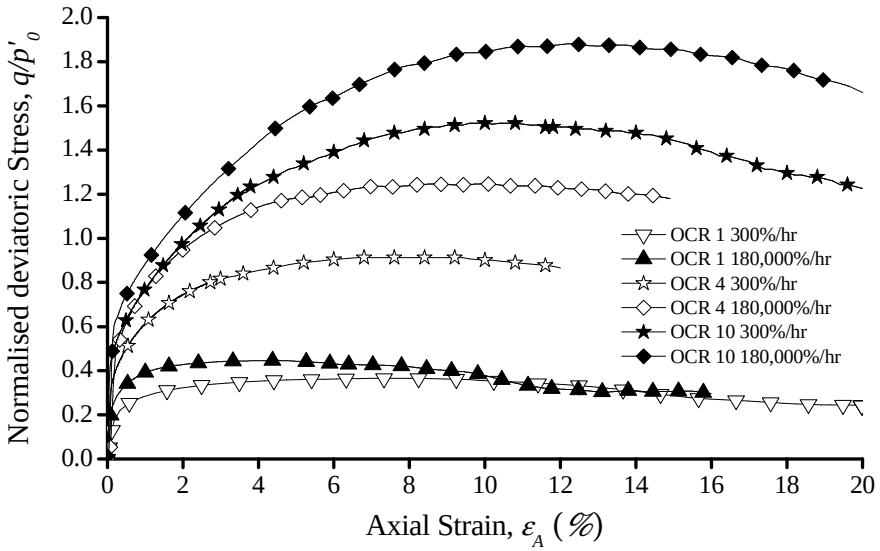

Figure 4-7 Normalised deviatoric stress-strain curves in Kaolin at OCR 1, 4 and 10

The increase in deviatoric stress at maximum strength (irrespective of strain) is 22% at OCR 1, 36% at OCR 4, and 23% at OCR 10. This increase in deviatoric stress in OCR 4 appears to be unrealistically high in comparison to that from OCR 1 and 10.

Previous research has shown that strain rate effects do not vary with OCR (Sheahan *et al*. 1996, Lehane *et al*. 2009). In considering this, the similarity between strain rate effects measured in OCR 1 and 10, and the unusually high increase in strength displayed by OCR 4 it appears OCR 4 may be in error. However to develop the strain rate effect on strength from the results shown in Figure 4-7, and correct for the possibly erroneous result of at least one of the OCR 4 tests, Equation 4-2 from Ladd and Foot (1974) which links the undrained strength and OCR may be used. Equation 4-2 describes the increase in strength as a function of the OCR and the corresponding normally consolidated value of strength;

$$\frac{Su}{p'_0} = \left(\frac{Su}{p'_0}\right)_{NC} (OCR)^{\Lambda} \qquad (4\text{-}2)$$

Where S_u is the undrained strength, p'_0 is the mean effective stress at the end of consolidation, and the exponent Λ is used as a curve fit parameter. Figure 4-8 presents the fit of Equation 4-2 to the 300%/hr and 180,000%/hr results in OCR 1, 4 and 10.

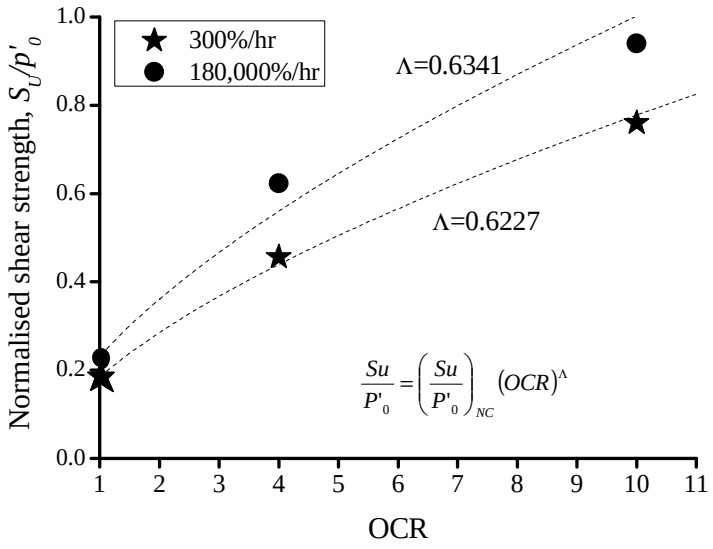

Figure 4-8 Normalised shear strength in Kaolin at OCR 1, 4 and 10, measured with 300%/hr and 180,000%/hr tests

From the results of the curve fit shown in Figure 4-8, the strain rate effects on maximum strength for the over consolidated tests are then re-evaluated. The strain rate effect on strength, defined at the ratio of strength measured between 300%/hr and 180,000%/hr is then 25% at OCR 1, 27% at OCR 4, and 28% at OCR 10. Thus the results from this study appear to show little variation in strain rate effect with OCR. This confirms the findings from Lehane *et al*. (2009) and Sheahan *et al*. (1996).

Sheahan *et al*. (1996) found that with increasing OCR there was no effect of strain rate on strength below a particular threshold strain rate, which increased with OCR as discussed in Chapter Two, Section 2.4.4. From Sheahan *et al*. (1996) the threshold strain rate increased from 0.5%/hr at OCR 4, to 5%/hr at OCR 8. Because the threshold strain rate is lower for normally consolidated soils these will display

comparatively greater strain rate effects on strength if the threshold strain rate is not exceeded for the over consolidated soil. This would be represented in the value of Λ from Equation 4-2 in Figure 4-8. If as shown in Figure 4-8 the normally consolidated soil displays greater strain rate effects on strength, the intercept with the axis (at OCR=1) will increase, yet if the over consolidated soil does not display the same strain rate effects on strength the curve fit exponent Λ will decrease. Sheahan *et al*. (1996) found at strain rates in excess of the threshold strain rate the ratio of increase in strength with strain rate was similar for each OCR and subsequently the value of Λ was similar for these strain rates (> threshold rate). The existence of a threshold shear strain has also been mentioned in other studies involving the rate dependence of fine grained soils (Dayal and Allen, 1976, Skempton, 1985).

For isotropic over consolidated soils the exponent Λ from Equation 4.2 is related to the slope of the normal consolidation line and the unload-reload consolidation line (for static strain rates) with Equation 4-3 (Muir Wood, 1990).

$$\Lambda = \frac{\lambda - \kappa}{\lambda} \qquad (4\text{-}3)$$

Where λ is the slope of the normal consolidation line, and κ is the slope of the unload–reload line. From Equation 4-3 the value of Λ in Kaolin is approximately 0.78. Figure 4-8 shows that between 300%/hr and 180,000%/hr the exponent Λ increased marginally from 0.6227 to 0.6341. Yet differences between Λ from Equation 4-8 for both sets of strain rate tests are small in comparison with the differences between Λ from Equation 4-3. Although the maximum strength occurs at different strain levels; deriving the exponent Λ at the same strain does not give improved agreement between Equation 4-2 and 4-3. Using Equation 4-3 the values of Λ from Sheahan *et al*. (1996) is approximately 0.8.

As mentioned Sheahan *et al*. (1996) found that Λ continually reduced with each logarithmic increase in strain rate between 0.05%/hr to 50%/hr (Λ=0.757-0.686) at OCR 1, 2, 4, and 8 in Boston blue clay. However once the threshold strain rate for all OCR (5%/hr at largest OCR=8) was exceeded the value of Λ became very similar for each OCR. Thus the parameter Λ varies with strain rate, and the threshold strain rate.

This trend is in agreement with results from this study. Thus it appears that similar to Boston blue clay, these results in Kaolin appear to reflect an existence of a threshold strain rate, which has been exceeded by the minimum strain rate test of 300%/hr. These results show that strain rate effects in Kaolin at different OCR can be the same, with the caveat that a threshold strain rate must be exceeded. It is also noted that previously Zhu and Yin (2000) confirmed that the exponent Λ changes very little over a range of strain rates between 0.15 to 15%/hr in Hong Kong marine clay at OCR 1, 2, 4 and 8, which suggests the threshold strain rate may be significantly different in different soils.

4.3.2 Excess pore pressure

Figure 4-9 presents the excess pore pressure measurements measured at the mid height of the samples during both 300%/hr and 180,000%/hr tests. With increasing strain rate and OCR the magnitude of excess pore pressures reduce. This is consistent with observations on both normally consolidated and over consolidated soils in other studies involving increased strain rate and OCR (Sheahan *et al*. 1996, Zhu and Yin, 2000, Balderas-Meca, 2004). With increasing OCR the excess pore pressures tend to negative values. This is consistent with effects of dilation on heavily over consolidated soils.

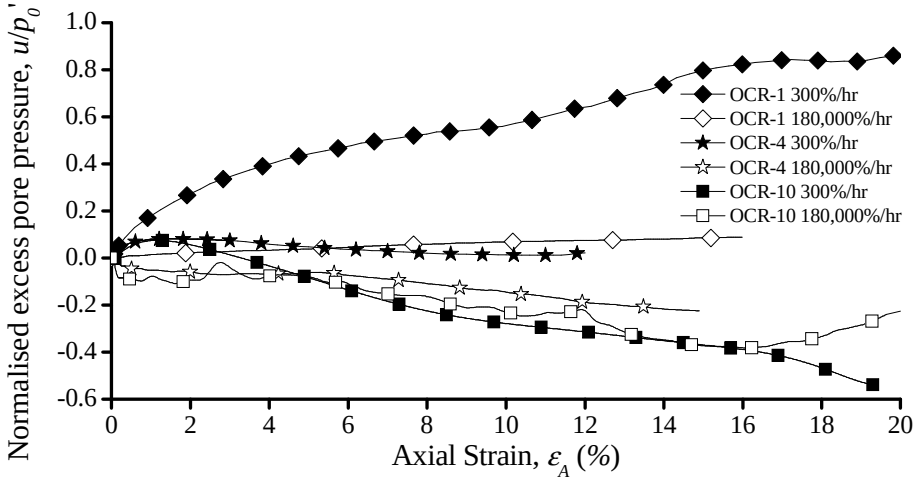

Figure 4-9 Normalised mid height excess pore pressures for Kaolin at OCR 1, 4 and 10, at 300%/hr and 180,000%/hr

It is difficult to interpret the results shown in Figure 4-9. The observations may reflect the difficulty with measuring excess pore pressures at high strain rate (180,000%/hr). Based upon previous research it may be expected that excess pore pressures would become increasingly negative with OCR and strain rate. In considering this it seems possible the excess pore pressures at OCR 10 in Figure 4-9 may not reflect the pore pressures on the shear plane.

Future testing may include a larger number of lower strain rate tests (<180,000%/hr), as well as possibly a larger number of pore pressure transducers to help interpret how excess pore pressure varies with OCR and strain rate. It is possible that effects of non uniform excess pore pressures and subsequent localisation may have influenced excess pore pressure measurements to the extent that the proximity of the mid height transducer to the shear plane may be a significant factor in the results shown in Figure 4-9, particularly regarding the OCR 10 results. As mentioned previously the 180,000%/hr test at OCR 4 also displayed a larger then expected deviatoric stress, thus this test may also display unusual excess pore pressures.

4.3.3 Effective stress path

The effective stress paths of the 300%/hr and 180,000%/hr tests at each OCR are shown in Figure 4-10. The drained effective stress paths, defined from the initial effective stress at the end of consolidation for each soil is also shown in Figure 4-10. The results shown in Figure 4-10 are normalised by the effective stress at the equivalent specific volume on the critical state line (p'_e).

As shown the effective stress paths of 180,000%/hr tests diverge from those of the 300%/hr tests for each OCR. With the exception of the 300%/hr test at OCR 1, all effective stress paths in Figure 4-10 tend towards the drained effective stress path. Thus these effective stress paths (with the exception of 300%/hr at OCR 1) appear as though these are drained tests. However during these tests there was no recorded change in volume, and therefore the response of the soil is undrained.

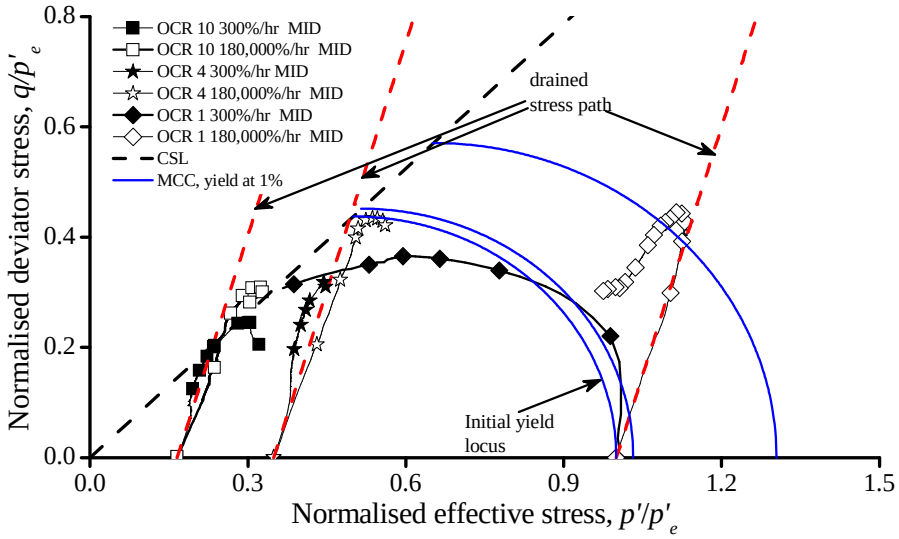

Figure 4-10 Effective stress paths (mid height pore pressures) for Kaolin at OCR 1, 4 and 10

As mentioned in Section 4.2.1, Yong and Japp (1969) proposed a dynamic state boundary surface to account for increasing deviatoric stress due to strain rate. A Modified Cam Clay (MCC) initial yield locus (Equation 4-1) is shown in Figure 4-10 to highlight the feature of the normally consolidated soils diverging from typical normally consolidated behaviour assumed in well known elastic plastic models.

The yield point used to define the locus is at 1% strain. The increase in effective stress (p'_0) in Equation 4-1, describing the increasing yield locus increases by approximately 10% per logarithmic increase in strain rate. However the MCC yield locus does not capture the strength of the soils displayed at maximum strength, which as shown for normally consolidated soil occurs at a stress ratio less than critical state.

According to Cam Clay theory the heavily over consolidated soils will develop positive excess pore pressures before the initial yield locus is reached, thereafter developing negative excess pore pressures to soften towards the critical state line. At maximum deviatoric stress the effective stress paths of heavily over consolidated soils (OCR 4 and 10) are expected to be on the dry side of the critical state line in Figure 4-10. Some softening is seen in the over consolidated stress paths, however they appear to show little correspondence with the critical state line. Significantly higher excess pore pressures are required to bring the effective stress paths to the dry side of the

critical state line in Figure 4-10. Therefore it may be the case that effective stress paths shown in Figure 4-10 do not reflect the true soil behaviour because of uncertainty over the validity of excess pore pressure measurements discussed previously.

Because of the comparatively similar measured stress paths of the heavily over consolidated tests, it is assumed there may be a lag in the measurement of excess pore pressures, or a misrepresentation of true excess pore pressures due to localisation which is more prevalent in heavily over consolidated soils, and the subsequent distance of the mid height transducer from the shear plane.

4.4 Limitations of triaxial testing at high strain rates

Prior to this point in the chapter the results of triaxial tests have been presented and discussed with emphasis on how strain rate affects the behaviour during shear. Here some shortcomings of triaxial testing at high strain rates are discussed to highlight the potential adverse effects and how these relate to the results presented in the previous sections. The effect of strain rate on triaxial tests in the literature are primarily discussed in relation to the possible adverse effect of uneven pore pressure distribution, pore water migration, and subsequent non uniform development of stress and strain throughout the samples.

4.4.1 Strain rates, and equalisation of pore pressures

Non uniform distributions of excess pore pressures are a concern in triaxial testing. The equalisation of excess pore pressures throughout a soil subjected to shear is dependent on the coefficient of consolidation and dimensions of the samples. As the rate of strain increases the time available for the soil to equalise excess pore pressures reduces. Table 4-2 presents the approximate time taken to reach a strain of 2% for each particular strain rate test.

Axial Strain Rate (%/hr)	Time to 2% axial strain		
	(hours)	(minutes)	(seconds)
1	2	120	7200
5	0.4	24	1140
10	0.2	12	720
300	0.066	0.4	24
1,800	0.0011	0.066	4
18,000	0.00011	0.0066	0.4
180,000	0.000011	0.00066	0.04

Table 4-2 Variation of time to 2% axial strain for strain rates used in this study

Estimating the time for the equalisation of excess pore pressures based upon values of the coefficient of consolidation and the maximum drainage path available within the samples (diameter 100mm, length 200mm) using Equation 4-4 gives values for each soil as shown in Table 4-3.

$$t = \frac{H^2}{c_V} \tag{4-4}$$

Where H is the maximum drainage path length, and c_v is the coefficient of consolidation.

Soil	Coefficient of consolidation, c_v (m^2/year)	Time for equalisation	
		Radially (minutes)	Axially (minutes)
Kaolin-300kPa	10.69	123	490
Kaolin-720kPa	13.94	94	376
Kaolin-1150kPa	14.71	89	357
KSS-560kPa	23.02	57	228
KSS-541-300kPa	15.04	87	349
KSS-541-600kPa	16.62	79	316

Table 4-3 Variation of time for equalisation of excess pore pressures based upon coefficient of consolidation for soils used in this study

Thus based on a comparison of the time to reach 2% strain and the coefficient of consolidation of each soil it suggests that pore pressures may not equalise though the soils at strain rates in excess of 1%/hr. Although the equalisation of excess pore pressures could improve with increasing strain, this raises three issues in relation to excess pore pressures for high strain rate triaxial tests;

- The effect of non uniform excess pore pressure development.
- The effect the coefficient of consolidation of each soil may have on the quality of excess pore pressure measurements and subsequent effective stress measurements.
- Localisation of strains due to uneven pore pressure distribution and subsequent development of discontinuities within the sample.

The triaxial tests were conducted with fixed ends, therefore some effects of non uniformity were expected despite the low coefficient of consolidation of the soils used in this study. Fixed end platens may reduce the lateral deformation at the ends of triaxial samples due to increased friction, causing a concentration of stress at the ends of sample. Subsequently pore pressures measured through the base of the sample may be adversely affected. The use of lubricated ends was not possible due to incorporation of axial bender elements into the end platens.

However the adverse affects of localisation due to fixed ends on measurements of pore pressures were expected to be avoided by incorporating a mid height pore pressure transducer into the triaxial system. The mid height pore pressure transducer is located at the edge of the samples to avoid disturbance to the soil. A similar device was also used in other high strain rate triaxial studies (Richardson and Whitman, 1963, Sheahan *et al*. 1996, Balderas-Meca, 2004), each of which found excess pore pressures decreased with increasing strain rate. The same type mid height transducer was used in this study as that from Balderas-Meca (2004) whom measured the response of the transducer to a 100kPa increase in pressure to be between 0.01-0.024 seconds which is faster than the time to 2% strain as shown in Table 4-2.

4.4.2 Localisation of samples during high strain rate tests

Figure 4-11 presents images of selected samples at the end of shear to illustrate how localisation and the development of shear planes become more evident at higher strain rates. Each test is from kaolin normally consolidated to 1150kPa and sheared at a strain rate of 1%/hr, 300%/hr or 180,000%/hr. The test conducted at a strain rate of 1%/hr (Figure 4-11-a) appeared to allow pore pressures to dissipate (to some extent) during shearing. Tests at this strain rate did not display localisation/development of a distinct failure plane. Samples tested at strain rates above 10%/hr display some localisation during shear. The tests at 300%/hr (Figure 4-11-b) show a distinct localisation at the centre of the samples, an effect which became more evident with increased strain rate as evidenced by the 180,000%/hr test (Figure 4-11-c).

The effect of localisation (as post peak strain softening) was also evident in the stress strain curves as shown in Figure 4-12, which presents three stress strain curves from tests in Kaolin, each of which is at a different consolidation pressure but sheared at the same rate (1,800%/hr). There is agreement between tests that display localisation/development of discontinuities (as per Figure 4-11) and post peak strain softening (as per Figure 4-12).

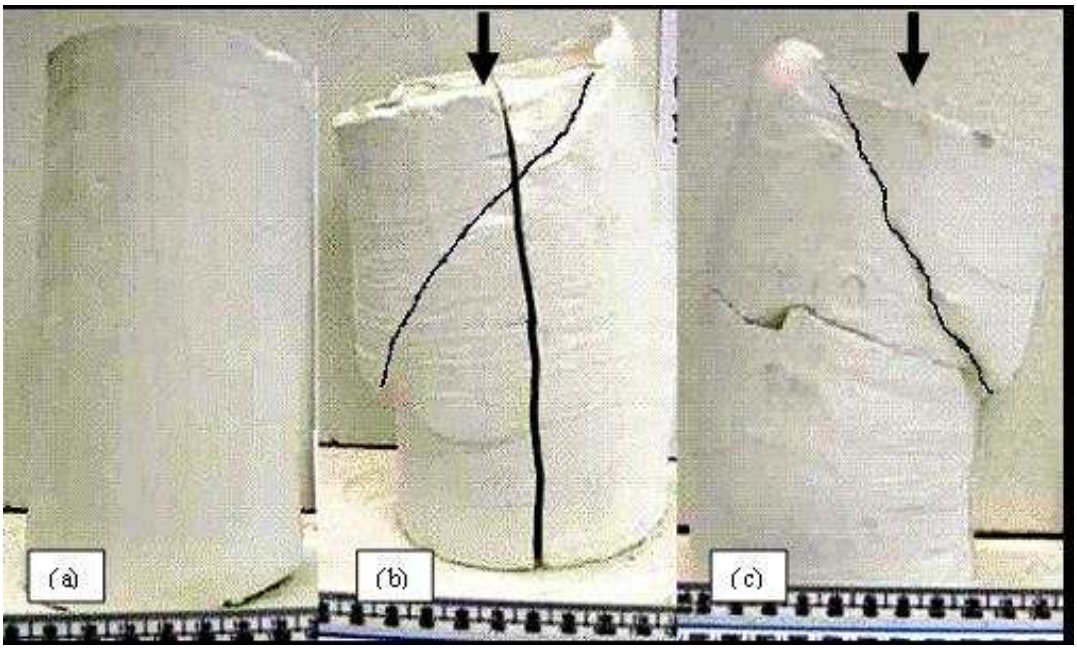

Figure 4-11 Kaolin-1150kPa samples after shear stage (a) 1%/hr (b) 300%/hr (c) 180,000%/hr

Note; samples are photographed up-side down. Direction of loading shown as arrow

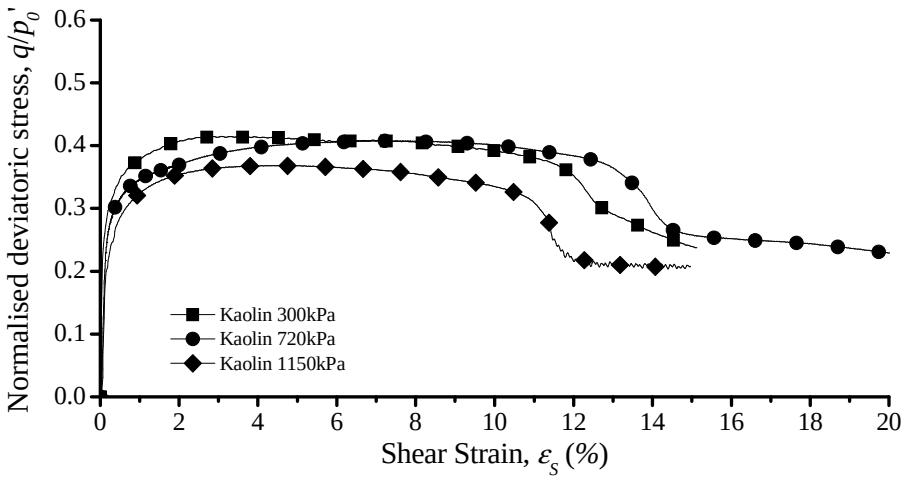

Figure 4-12 Normalised deviatoric stress strain curves in Kaolin consolidated to different effective stresses, sheared at 1,800%/hr

4.4.3 Measurement of effective stress at maximum strength

Effective stress friction angles determined using measurements from the mid height pore pressure transducer are shown in Figure 4-13 for Kaolin consolidated to 720kPa sheared at axial strain rates from 1%/hr to 180,000%/hr.

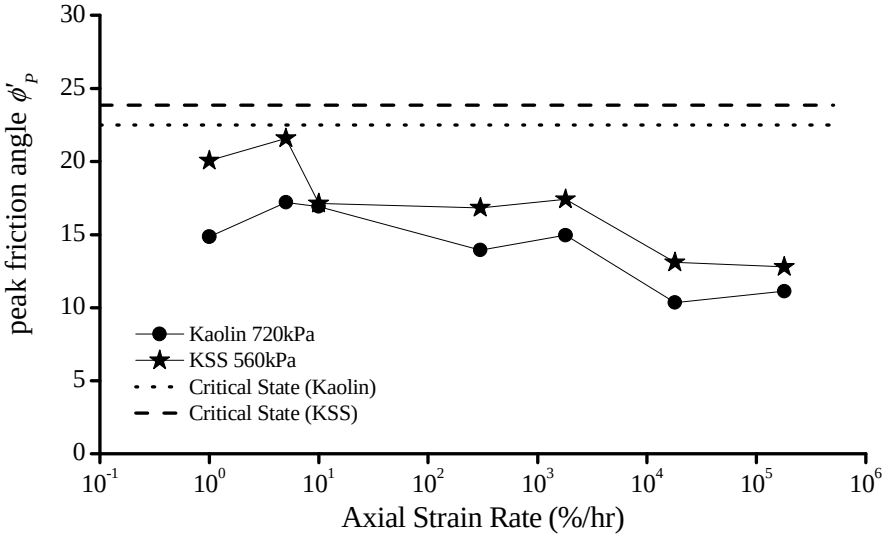

Figure 4-13 Effective stress friction angle at maximum deviatoric stress using mid height pore pressure measurements

Note; The results presented for 1%/hr and 5%/hr tests are at 10% strain.

The friction angles in Figure 4-13 are those corresponding to the maximum/peak deviatoric stress. Equation 4-5 is used to determine the friction angle from the corresponding stress ratio;

$$\sin\phi_P^{'} = \frac{3\eta_P}{6+\eta_P} \qquad (4\text{-}5)$$

Where η_P is the stress ratio at maximum strength. Figure 4-13 shows that with increasing strain rate the friction angle at maximum deviatoric stress reduces. Figure 4-13 also shows the friction angle is significantly lower then that expected at critical state.

As discussed in Section 4.2.4; the 1%/hr and 5%/hr results are assumed to reach critical state at higher magnitude of strain as these tests are strain hardening. The 10%/hr results also intercepting the critical state line slightly after peak strength due to increasing excess pore pressure. The results presented in Section 4.2.4 showed that with increasing strain rate from 300%/hr the effective stress paths increasingly show less tendency (at peak strength) towards the critical state line. Because at strain rates from 300%/hr the results shown in Figure 4-13 are from isotropic normally consolidated soil behaving in an undrained manner it is expected that maximum strength will correspond to the critical state strength. Therefore some of the results shown in Figure 4-13 (>300%/hr) appear to contradict some basic assumptions of behaviour of undrained triaxial tests on normally consolidated soils.

Sheahan *et al*. (1996) and Richardson and Whitman (1963) found the critical state line was independent of strain rate using measurements of effective stress in tests with a mid height pore pressure transducer. The relationship between the strain rate and effective friction angle in Figure 4-13 are contrary to findings from Sheahan *et al*. (1996) and Richardson and Whitman (1963). In addition to the effect of decreasing excess pore pressures Sheahan *et al*. (1996) also found that increasing strength with strain rate for reconstituted Boston Blue clay (RBBC) of OCR 1 and 2 was due to an increase in the effective stress friction angle at peak strength. It is noted the aforementioned studies utilised a maximum strain rate between 50%/hr to 60%/hr, which is significantly lower then those shown in Figure 4-13. Unfortunately results of

normally consolidated soils from Balderas-Meca (2005) which achieved axial strain rates in excess of this study did not display a peak or critical state strength. The excess pore pressure measurements from Balderas-Meca (2005) were also thought to suffer from changes in cell pressure during shear, which was not an issue for the tests in this study.

Assuming the critical state line is independent of strain rate, and coincides with the maximum strength measured during normally consolidated undrained compression tests (Atkinson, 2007); the effective stress peak friction angles from soils tests in this study (Figure 4-13) can only be in disagreement with critical state due to the magnitude of excess pore pressures measured at the mid height of the samples at the maximum strength. It is also counterintuitive that normally consolidated soils would display reducing effective stress friction angles with increasing strain rate whilst also displaying an increase in strength. Thus the magnitudes of excess pore pressures measured at the mid height of the sample are considered unrepresentative for high strain rate tests (>300%/hr).

4.4.4 Comparison of mid height and base pore pressure measurements

To compare mid height and base pore pressures Figure 4-14 presents the difference between excess pore pressures by subtracting the measurements of the base transducer from those recorded at the mid height of the sample. The excess pore pressures are compared at maximum deviatoric stress for each test.

Figure 4-14 shows that with increasing strain rate that generally the mid height pore pressure transducer begins to display higher excess pore pressures. Effective angles of friction derived using base pore pressure measurements thus would provide no better agreement to the expected critical state values than pore pressures measured at the mid height. That pore pressures are greater in magnitude for mid height measurements than base measurements is contrary to the observations made by Richardson and Whitman (1963). It appears from Figure 4-14 that once the strain rate is sufficient the stresses at the centre of the samples become more concentrated then those at the ends.

Akai *et al*. (1975) and Lefebvre and LeBoeuf (1987) used base excess pore pressure measurements to develop effective stress paths for tests at strain rates up to 3000%/hr.

As highlighted here the use of measurements taken from the base pore pressure transducer may not be suitable at such strain rates. These studies (as well as Richardson and Whitman (1963) and Sheahan *et al*. (1996)) showed that the gradient of the critical state line is not affected by strain rate. For those studies the effect of strain rate was attributed to decreasing excess pore pressures and the corresponding increase in effective stress. From the results of this study it is unclear how preceding studies into strain rate effects measured excess pore pressures at the base of samples of sufficient magnitude at high strain rate tests (>300%/hr) to make this conclusion. It would appear most likely that either there was an affect of end restraint in previous studies which caused an artificial increase in excess pore pressures or the soil was sufficiently permeable to allow transient movement of excess pore pressures to the transducer. Therefore caution is advised when using base pore pressure measurements particularly in soils of low permeability or relatively low coefficient of consolidation.

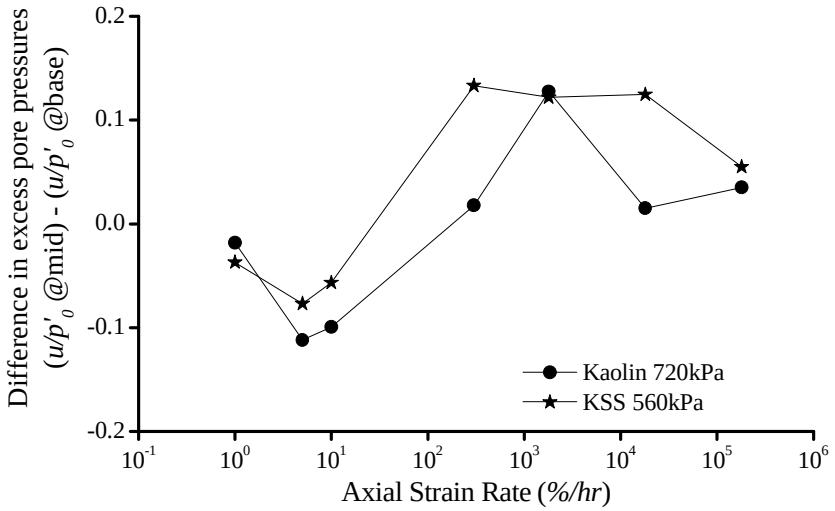

Figure 4-14 Difference between normalised excess pore pressures measured at sample mid section and base for Kaolin and KSS at increasing strain rate. The excess pore pressures are those corresponding to maximum deviatoric stress

The level of normalised difference between pore pressures measured at the two locations was not related to the soil type or the conditions at which the soils were tested. It therefore is concluded that the magnitude of difference in excess pore pressures may be due to the location of mid height transducer, and its proximity to the shear plane as it develops.

4.4.5 Measurement of excess pore pressures at sample centre

To gain a better understanding of the pore pressure response in the sample during high speed tests a hollow aluminium tube was designed to attach to the mid height pore pressure transducer and protrude from the face of the transducer to the centre of the sample as described in Chapter three, Section 3.4.7. The objective of this was to measure pore pressures that were generated directly at the centre of the sample. The non-uniformity of pore pressure development in a triaxial sample where drainage was allowed has been investigated both numerically and experimentally in several studies (Carter, 1982, Sheng *et al*., 1997, Liyanapathirana *et al*., 2005). However little is known about the non-uniformity of pore pressures within undrained samples tested at greatly increasing strain rate.

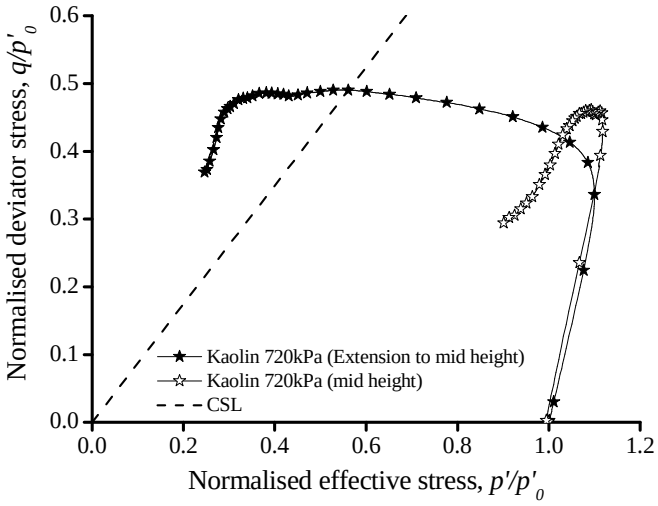

Figure 4-15 Effective stress paths for Kaolin 720kPa, sheared at 180,000%/hr using mid height pore pressure transducer extension piece

The mid height extension tube was used in a repeat of the 180,000%/hr test in Kaolin normally consolidated to 720kPa. Use of the extension device resulted in a large increase in the measured excess pore pressure, whilst the overall strength and base pore pressure measurements were almost identical to those from the original test. The resulting effective stress paths are compared in Figure 4-15. The effective stress path developed with the extension piece is similar to the original test at lower strain, however as excess pore pressures increase the effective stress path travelled past the critical state line. The magnitude of excess pore pressures measured with the mid

height transducer extension tube are likely influenced by the relatively stiffer aluminium used to block surrounding pressures. This may explain why the effective stress path from the extension tube test passes the critical state line to such an extent.

The effective stress path from the test incorporating the extension piece does not make it any clearer as to which part of the stress strain curve corresponds to the critical state line. However the potential variability of excess pore pressures towards the central axis of the sample is highlighted. The development of excess pore pressures within a triaxial sample at high strain rates requires further investigation.

4.5 Summary

The behaviour of normally consolidated and over consolidated model soils subjected to a range of strain rates have been discussed in this chapter. The behaviour of normally consolidated soils has been considered at a range of strain rates from 1%/hr to 180,000%/hr. The behaviour of over consolidated Kaolin has been compared at OCR 1, 4 and 10 at strain rates of 300%/hr and 180,000%/hr. Each of the strain rate tests have been conducted with drainage permitted from the samples; however at higher strain rates the response of the soil became undrained (no volume change). The effects of strain rate have been presented and discussed in terms of the response of deviatoric stress, excess pore pressures, the change in volume and the effective stress path. Some difficulties encountered in high strain rate testing were also discussed. A summary of findings are outlined below;

1. An effect of strain rate and strain is evident on the deviatoric stress. At low strains (<1%) a faster strain rate results in an increase in deviatoric stress. At higher strains the samples display different behaviour depending on strain rate, ranging from strain hardening to clearly identifiable maximum/peak deviatoric stresses.

2. At lower strain rates (1-300%/hr) the effects of strain hardening reduce with an increase in strain rate, resulting in a decrease in strength. Increasing strain (in this range) corresponds to an increase in excess pore pressures and

reduction in volume change as with increased strain rate the response of the soil becomes increasingly undrained.

3. The response of the soil is considered fully undrained at strain rates of 300%/hr. At strain rates in excess of 300%/hr; increasing strain rate results in an increase in deviatoric stress. This also corresponds to decreasing excess pore pressure and thus increasing effective stress.

4. The effective stress paths from slower strain rate tests (1-10%/hr) appear to tend towards critical state. At strain rates of 10%/hr and 300%/hr the effective stress paths tend towards critical state slightly after the maximum deviatoric stress. At strain rates in excess of 300%/hr the stress paths follow the drained effective stress path, appearing as though drained stress paths (note no change in volume) expanding the state boundary surface with increased strain rate.

5. The over consolidated soils display similar strain rate effects at maximum strength. This may only be valid once a threshold strain rate (as per Sheahan *et al*. (1996)) is exceeded. A threshold strain rate appears to exist in Kaolin, although it is exceeded by 300%/hr

6. Over consolidated stress paths follow the total stress path even at 300%/hr tests (unlike normally consolidated tests) and thus appear as drained stress paths.

7. For normally consolidated soils it was found that at higher strain rates excess pore pressures were higher in the mid section of the sample then at the base, contrary to findings from Richardson and Whitman (1963). The friction angle measured at maximum deviatoric strength also decreased with increasing strain rate (300%/hr to 180,000%/hr), although shear strength was found to increase.

8. A pore pressure extension device was used to measure excess pore pressures at the centre of the sample, which highlighted the potential for variable excess pore pressures towards the central axis of the sample.

5 Strain Rate Effects at Large Strains (>1%)

5.1 Introduction

The shearing behaviour of both normally consolidated and over consolidated samples has been discussed previously in Chapter Four. This chapter describes strain rate effects on strength during triaxial shear testing. The effect of strain rate on strength is compared with particular focus on behaviour at large strains as discussed in Chapter Four.

In this Chapter, separate analysis and discussion are presented for both partially drained and "viscous" type undrained responses with increasing strain rate. The influence of soil properties on partially drained and undrained strain rate effects are presented and analysed, and where possible compared to previously published findings. The outcomes of this analysis are then used to develop rate effect prediction models which may be of benefit to industry. For convenience, Table 5-2 presents a summary of the soils and the number of tests at different strain rates which are considered during this chapter.

Soil	**Initial effective stress, p'_0 (kPa)**	**Plasticity Index, I_P (%)**	**Critical State ratio, M**	**Void ration, e**	**Number of tests**
Kaolin	300	45	0.875	1.13	4
Kaolin	720	45	0.875	1.00	7
Kaolin	1150	45	0.875	0.9	7
Kaolin OCR 4	300	45	0.875	0.95	2
Kaolin OCR 10	115	45	0.875	0.99	2
KSS	560	23	0.933	0.59	7
KSS-541	300	20	0.950	0.60	7
KSS-541	600	20	0.950	0.54	7

Table 5-1 List of soils and their characteristics used in Chapter 5

5.2 Quantification of the strain rate effect

To define the strain rate effect on strength requires normalisation of rate dependent strength by a reference strength obtained at a reference strain rate. Figure 5-1 presents the normalised maximum deviator stresses obtained from tests in Kaolin-1150kPa and KSS-560kPa over the complete range of strain rates tested.

The maximum deviator stress from each strain rate test in Figure 5-1 have been normalised by a reference value of maximum deviator stress (q_{ref}), to derive the rate effect (q/q_{ref}). The reference values of strength (q_{ref}) are taken here as the results from the 300%/hr tests. This is the lowest strain rate at which the soils display what is considered practically fully undrained behaviour and is for this reason labelled the transition point in Figure 5-1. This strain rate test also develops the lowest maximum deviatoric stress. For these reasons the strength of each soil measured at this strain rate (300%/hr) is considered to correspond to the static strain rate undrained strength of each soil. The coincidence of the soil transitioning to fully undrained behaviour and the development of the lowest strain rate dependent strength at the same strain rate is consistent with findings from Carter (1982) as well as observations from Randolph and Hope (2004) and Lehane *et al.* (2009).

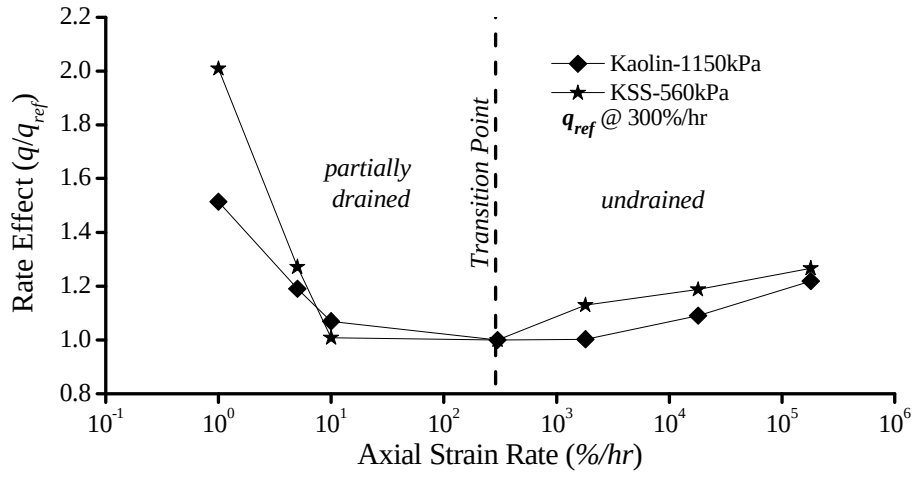

Figure 5-1 Strain rate effect (q/q_{ref}) at maximum deviatoric strength with increasing strain rate for normally consolidated soils

Normalisation of the maximum strength from each strain rate test with the strength from 300%/hr (transition point), distinguishes a partially drained strain rate effect from an undrained strain rate effect in Figure 5-1. The increase in strain rate effect (q/q_{ref}) in the partially drained domain (Figure 5-1) is consistent with the behaviour observed by Carter (1982). Carter (1982) did not conduct tests at strain rates greater than those needed for the response of soil to become undrained.

However, several studies on the effect of rate of penetration on strength of fine grained soil have been conducted at a wide range of rates to observe both partially drained and fully undrained soil response (Bemben and Meyers, 1974, Randolph and Hope, 2004, Lehane *et al*., 2009). These studies have shown that at rates of penetration beyond the soil transition to an undrained response the strength of fine grained soils increase. This reflects the behaviour shown in the undrained domain in Figure 5-1. Similarly to that done in Figure 5-1, Randolph and Hope (2004) also normalised the rate effect on strength by the minimum strength which was measured at the transition from partially drained to fully undrained behaviour. Variation in the rate effect (q/q_{ref}) in Figure 5-1 reflects the true rate dependent soil behaviour, which ranges from strain hardening in the partially drained domain to what is often termed a viscous effect (Lunne *et al*., 1997) in the undrained domain.

Previous research into the strain rate dependence of strength in triaxial compression tests used lower reference strain rates. The range of reference strain rates used in previous studies is from ≈0.1%/hr (Graham *et al*., 1983, Zhu and Yin, 2000) to ≈1%/hr (Lefebvre and LeBoeuf, 1987, Kulhawy and Mayne, 1990, Sheahan *et al*. 1996). Previous investigations into the strain rate effect on strength with the triaxial apparatus were typically undertaken in constant volume/undrained compression conditions. Each of these studies found that strength increased at a strain rate in excess of the reference strain rate. It is shown in Figure 5-1 that at strain rates of less than 300%/hr, a decrease in strain rate is accompanied by increase in strength.

Thus Figure 5-1 is thought to present a more realistic view of the true rate dependence of soil strength at lower strain rates. Furthermore, Figure 5-1 highlights the importance of selecting a suitable strain rate to determine the strength most relevant for a particular aspect of geotechnical design. Because of the bilinear nature of the

strain rate effect, and the different nature of the response of soil and the corresponding strength, factors controlling the strain rate effect in the drained and undrained domains are discussed separately.

5.3 Factors affecting the partially drained strain rate effect

Partially drained conditions are displayed during the shearing stage for each test conducted at strain rates of 1%/hr, 5%/hr and 10%/hr. Tests at strain rates corresponding to partially drained conditions were conducted in three different types of soil. The effect of current state on strain rate effects in the partially drained domain was investigated for two soils which were consolidated to higher effective stress before shear.

In total five series of tests were conducted, each series comprising of tests at a strain rate of 1, 5, and 10%/hr. The soils include Kaolin consolidated to 720kPa and 1150kPa. The KSS was consolidated to 560kPa and the KSS-541 to 300kPa and 600kPa. All the results considered in this section are for normally consolidated soils. A selection of the soil properties are listed in Table 5-2.

Soil	**Plasticity Index, I_P (%)**	**Void Ratio, e**	**Permeability, k (m/s)x10^{-10}**	**Coefficient of Consolidation, C_V (m^2/year)**
Kaolin 720kPa	45	1.00	4.96	13.9
Kaolin 1150kPa	45	0.90	3.71	14.7
KSS 560kPa	23	0.59	8.40	23.0
KSS-541 300kPa	20	0.60	9.43	15.0
KSS-541 600kPa	20	0.54	5.44	16.6

Table 5-2 Properties of soil tested at partially drained strain rates

As discussed previously in Section 4.2, with increasing strain rate the time available for consolidation reduces. This is due to the lower time available for drainage and pore pressure equalisation to occur. With increasing strain rate and decreasing availability of time for consolidation, a build up of excess pore pressure occurs and the soil develops lower strength. This is consistent with findings of a triaxial study

reported by Carter (1982), and is well documented in the case of the rate dependence of strength using various types of penetrometer (Bemben and Meyers, 1974, Randolph and Hope, 2004, Kim *et al*., 2006, Lehane *et al*., 2009).

Figure 5-2 presents the partially drained strain rate effect at maximum strength for each soil. The partially drained strain rate effect is defined using the strength from the 300%/hr strain rate test. Although tests at this strain rate are considered to have displayed undrained behaviour, it is used here for continuity with the undrained strain rate effect. Figure 5-2 illustrates that with reducing strain rate each soil displays an increase in strength. At 1%/hr, the most permeable soils, KSS 560kPa and KSS-541 300kPa display the largest increase in strength with reducing strain rate ($q/q_{ref} \approx 2$). KSS 560kPa also has the largest coefficient of consolidation, and therefore it could be expected this soil would display the largest strain rate effect on strength in the partially drained domain. Despite scatter of the strain rate effect in Figure 5-2, at strain rates of 1%/hr and 5%/hr the strain rate effect on maximum strength relates to the coefficient of consolidation. However, at 10%/hr the strain rate effect does not relate with the coefficient of consolidation. This is likely due to effects of non-uniform excess pore pressures, which are expected to increase with strain rate.

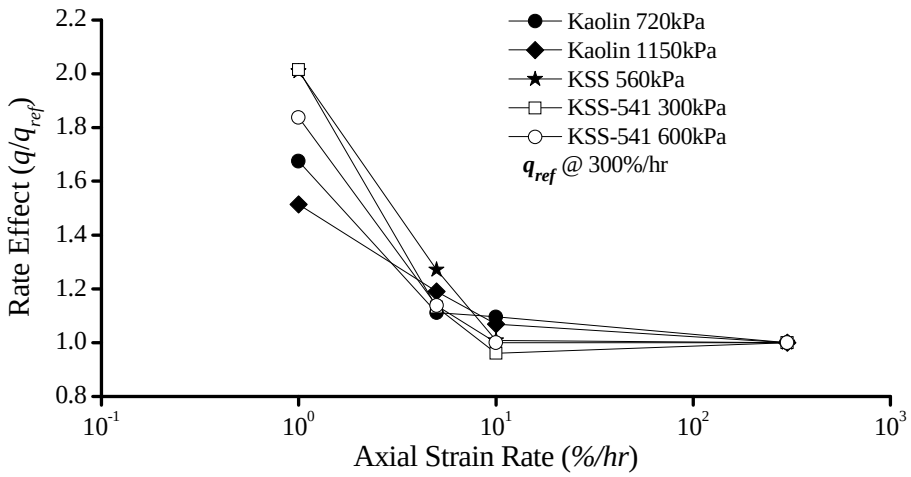

Figure 5-2 Variation of partially drained strain rate effect at maximum deviatoric stress with increasing strain rate

Using dimensional analysis Finnie and Randolph (1994) found that a normalised velocity *V*, was more appropriate then strain rate or velocity for analysis where consolidation effects are important;

$$V = \frac{vd}{c_v} \tag{5-1}$$

Where *v*, is velocity, *d* is a characteristic length (often assumed as the drainage path length) and c_v is the coefficient of consolidation. Subsequently, the use of the normalised velocity has been used to compare effects of partial consolidation during penetration testing at different rates (House *et al*., 2001, Randolph and Hope, 2004, Kim *et al*., 2006, Lehane *et al*., 2009).

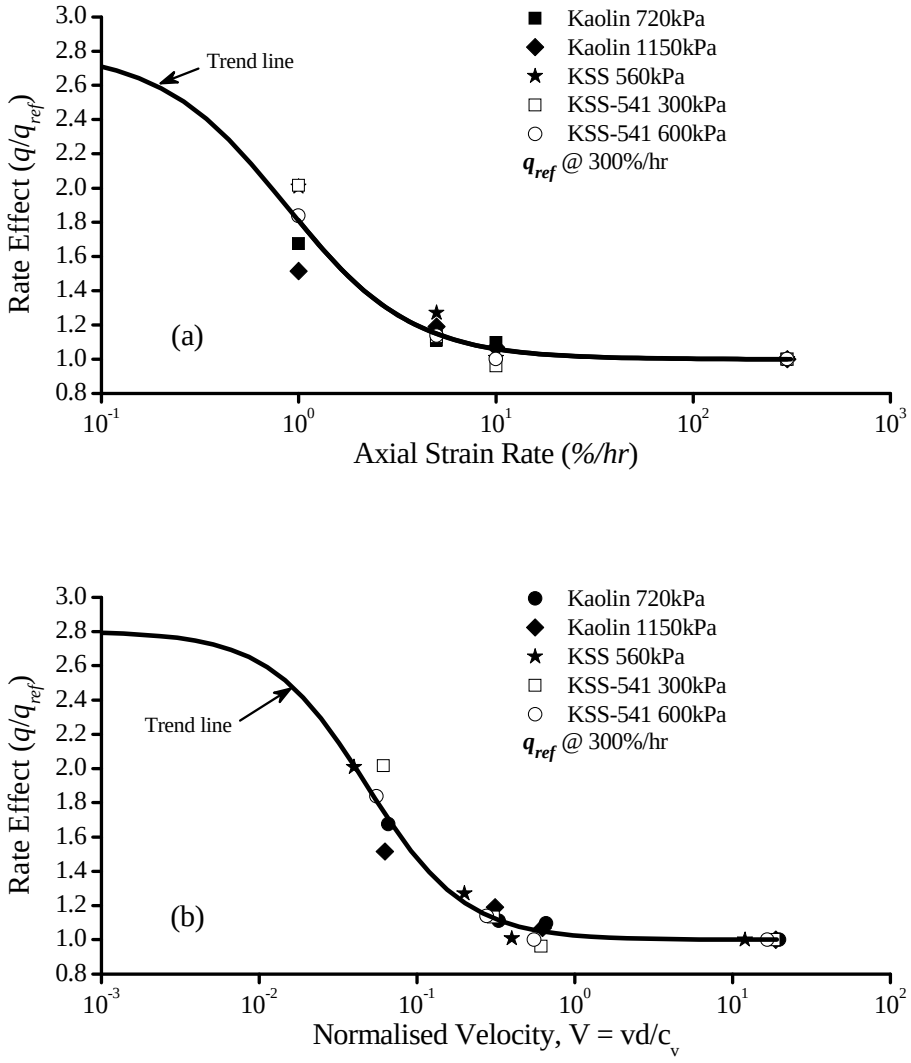

Figure 5-3 Variation of strain rate effect on maximum strength for (a) axial strain rate (b) normalised velocity, *V*

Figure 5-3 compares the strain rate effect on maximum strength with both strain rate (Figure 5-3 a) and with normalised velocity (Figure 5-3 b). The strain rate effect in Figure 5-3 is derived using 300%/hr as the reference strain rate. Normalisation of the velocity of deformation using Equation 5-1 shows that the rate effect tends towards a single curve. This indicates that the coefficient of consolidation is suitable for describing the strain rate effect in partially drained domain for the results of different soil used in this study.

The trend lines shown in Figure 5-3 (a) and (b) are best fit lines to the full set of data included in each Figure. The form of the trend lines is taken from a simple hyperbolic equation used by Chung *et al.* (2006) to describe the partially drained rate effect on strength from penetration at different rates:

$$\frac{q}{q_{ref}} = \left(1 + \frac{b}{1 + cV^{d}}\right) \qquad (5\text{-}2)$$

Where *b*, *c* and *d* are curve fit parameters and *V* is the normalised velocity, which is taken as strain rate for the trend line in Figure 5-3 (a). The values of the curve fit parameters, which were developed using the least squares method in OriginPro 7.5 are shown for each method in Table 5-3. For Figure 5-3 (a) the strain rate is used rather then normalised velocity *V* in Equation 5-2.

Method	***b***	***c***	***d***
Axial Strain Rate (%/hr)	1.80	1.23	1.37
Normalised Velocity, *V*	1.80	69.8	1.40

Table 5-3 Values for curve fit parameters (Equation 5-2) as shown in Figure 5 (a) and (b)

The percentage difference from each soil to the trend line reduces with use of the normalised velocity *V*. The average difference of all soils from the trend line in Figure 5-3 (a) was approximately 8%, which reduces to approximately 3.5% in Figure 5-3 (b). This further emphasises the appropriateness of the normalised velocity *V* to describe the partially drained strain rate effect on strength.

The minimum value of normalised V in Figure 5-3 (b) ranges from approximately 0.04 to 0.06. The values of normalised velocity for each soil are presented in Table 5-4. Finnie and Randolph (1994) suggested that fully drained conditions exist at normalised velocity of $V \approx 0.01$ (Table 5-5). Salgado *et al.* (2013) stated that the transition from drained to partially drained occurs at $V \approx 0.05$, which is similar to Lehane *et al.* (2009).

Based on the observations from these penetrometer studies the soils tested at 1%/hr ($V \approx 0.04$-0.06) should correspond to drained conditions. However Randolph and Hope (2004) found that reducing the normalised velocity to $V \approx 1$ for both the T-bar and cone penetrometer resulted in a doubling of the rate effect ($q/q_{ref} \approx 2$). Figure 5-3 (b) shows that to achieve double the rate effect a normalised velocity of approximately $V \approx 0.04$ is required. Thus the strain rate effects (at this particular value of normalised velocity, V) for this study are far lower than those reported in previous penetrometer studies (Randolph and Hope, 2004, House *et al*., 2001).

Soil	**Coefficient of Consolidation, C_V (m^2/year)**	**Normalised velocity, V at 1%/hr**	**Normalised velocity, V at 300%/hr**
Kaolin 720kPa	13.9	0.066	20
Kaolin 1150kPa	14.7	0.062	19
KSS 560kPa	23.0	0.040	12
KSS-541 300kPa	15.0	0.061	18
KSS-541 600kPa	16.6	0.055	16

Table 5-4 The range of partially drained normalised velocity, V for each soil

This is likely due to the fact that the 1%/hr and 5%/hr tests were halted prematurely and they would likely display greater strength at higher strain. The strength (strain rate effect) for 1%/hr and 5%/hr tests in Figure 5-3 is taken at 10% strain. It was reported in Chapter Four, Section 4.2 that the tests at slowest strain rates (1%/hr and 5%/hr), displayed an increase in excess pore pressures during shear before these were dissipated with continued strain. Soils tested at this strain rate are thus strain hardening. The 1%/hr tests were halted to avoid over-rating the load cell however,

they were expected to continue to strain harden. The 5%/hr tests would also be expected to continue to increase in strength at higher strain, although to a lesser extent then the 1%/hr tests.

The strain rate effect shown for these tests does not reflect the true maximum drained strength of each soil, although the normalised value of V suggest they may be attenuating to where drained values of strength may be expected. The values of strain rate effect at 1%/hr and 5%/hr tests would most likely develop greater strength (strain rate effect) then those presented in Figure 5-3. Thus, the gradient of the trend lines shown in Figure 5-3 would increase. This would improve the correspondence with values of strain rate effect at these normalised velocities shown in previous studies.

Test Type	Drained V	Undrained V	Reference
Model Foundation	0.01	30	Finnie & Randolph (1994)
CPT	-	30	Randolph & Hope (2004)
T-bar PT	-	11	Randolph & Hope (2004)
CPT	0.05	10	Kim *et al.* (2006)
CPT	0.04	100	Schneider *et al.* (2007)
T-bar PT	0.05	~7	Lehane *et al.* (2009)
Ball PT	-	~14	Lehane *et al.* (2009)
CPT	0.01	20	Jaeger *et al.* (2010)
CPT	0.05	10	Salgado *et al.* (2013)

Table 5-5 The range of normalised velocity, V from literature

Finnie and Randolph (1994), from tests with model foundations in calcareous sediments suggested that the response of soil becomes undrained at $V \approx 30$. As mentioned previously the 300%/hr strain rate tests are taken as that which corresponds to the transition from partially drained to undrained. The range of normalised V corresponding to the reference strain rate (300%/hr) in this study ranges from 12 to 20 (Table 5-4). Some differences between the normalised velocities at the transition are expected due to differences between triaxial and penetrometer testing. Randolph and Hope (2004), measured the transition between partially drained to undrained behaviour occurred as $V \approx 11$ for T-bar, and $V \approx 30$ for a cone penetrometer in Kaolin.

It may be expected that the normalised velocity at the transition to undrained behaviour would depend on the test at which it is conducted. As shown in Figure 5-3 (b), the value of strain rate effect reaches a plateau from normalised velocity between 0.6-1.

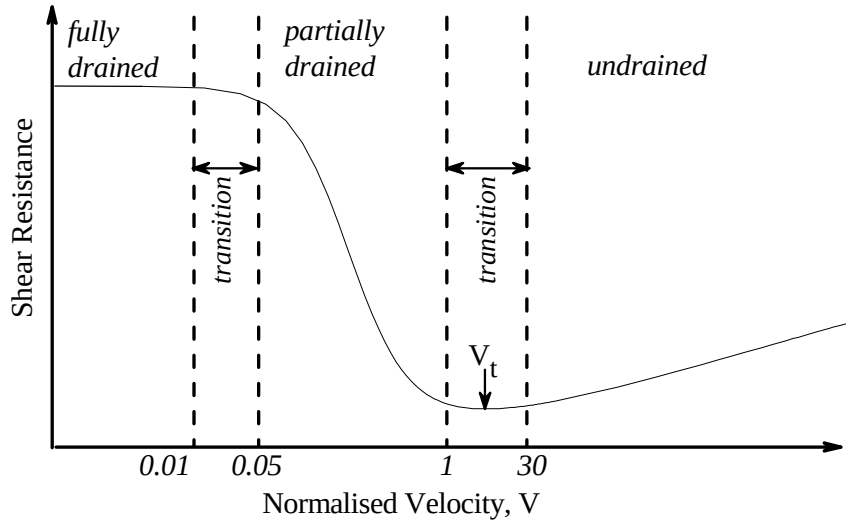

Figure 5-4 Illustration of the variance of soil resistance with increased normalised velocity, *V*

These values of normalised velocity correspond to a strain rate of 10%/hr for this study. In contrast to the 1%/hr and 5%/hr tests which strain harden to some extent as discussed previously, the 10%/hr tests display significant effects of non uniformity, as evidenced by localisation and strain softening discussed in Section 4.2. If the effects of non-uniform excess pore pressure equalisation are significant at this strain rate (normalised $V \approx 1$), the strength of the soil may reflect that of an undrained sample. Although the soils tested at 10%/hr displayed volume change (thus are partially drained) this may not have been significant to the strength of the sample once the shear plane began to develop. The value of normalised velocity for tests at this strain rate thus may not reflect the true behaviour of the soil. The drainage path length included in the normalised velocity should account for this, however it may not be as suitable due to non uniformity in the triaxial specimen. If effects of non-uniform excess pore pressure equalisation are expected to be pronounced, the strain rate effect at a corresponding value of normalised V may be significantly reduced. Assuming a larger drainage path length (as opposed to the radius as done here) would increase the

normalised velocity, which would improve correspondence with findings from House *et al.* (2001) and Randolph and Hope (2004). Figure 5-4 presents a typical bilinear backbone curve based on the values of normalised velocity *V* measured in the current study, including the lower drained and upper undrained values from previous investigations presented in Table 5-5.

Although the non-uniform excess pore pressure equalisation could explain why the strain rate effect at $V \approx 1$ is lower than expected, Salgado *et al.* (2013) found that at $V \approx 1$ the strain rate effect tended to plateau to the minimum strength, similar to that noted in Figure 5-3 (b). They attributed this behaviour within the plateau to an offset between partially drained and viscous undrained behaviour, noting that the transition to fully undrained behaviour did not occur until $V = 10$. The observations from Salgado *et al.* (2013), reflect the behaviour shown in Figure 5-3 (b) well. It is therefore inconclusive as to the exact nature of soil behaviour between normalised $V \approx 1$ to where the undrained transition is thought to take place, i.e. whether the response is due to non uniformity or true soil behaviour as per Salgado *et al.* (2013).

The transition to fully undrained behaviour was deemed by Salgado *et al.* (2013) to occur where rate dependent excess pore pressures reached a maximum, at $V = 10$. However, as shown in Figure 5-5, the excess pore pressure measurements from this study do not reflect their reported findings.

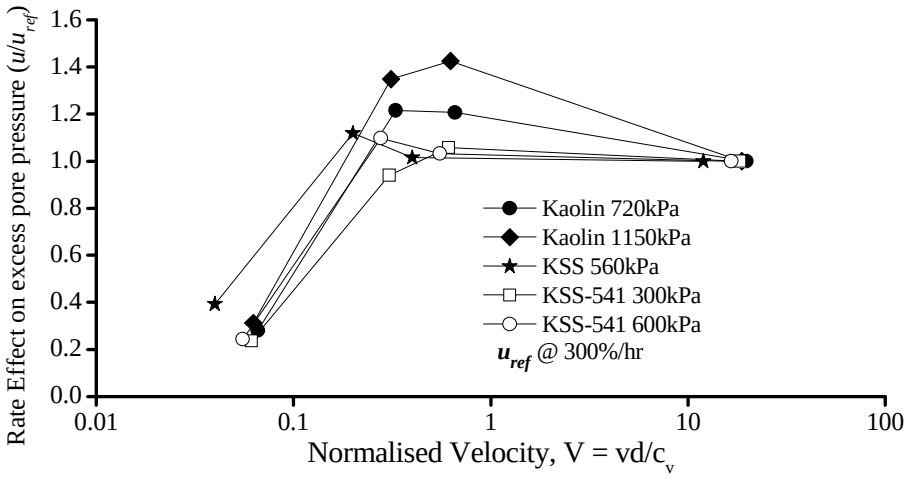

Figure 5-5 Variation of excess pore pressure rate effect (mid height) with normalised velocity, *V*

Figure 5-5 presents the rate effect on excess pore pressures from mid height transducer measurements. The rate effect in Figure 5-5 is defined using the measurements of excess pore pressures at maximum deviatoric stress for each strain rate test. Each measurement of excess pore pressure is normalised by the reference strain rate result, taken as 300%/hr, to define the rate effect (u/u_{ref}). Figure 5-5 highlights that significantly lower excess pore pressures were measured at the 300%/hr results (Normalised velocity ≈ 12-20).

The maximum excess pore pressures measured at strain rates between 5%/hr to 300%/hr were very similar in magnitude for each soil. It could be expected that the largest excess pore pressures are developed at the transition of the soil response to undrained behaviour. The excess pore pressure corresponding to the maximum deviatoric stress decreased significantly from 10%/hr to 300%/hr with a difference in one instance of over 40%. This likely is due to a lag in excess pore pressure measurements at the higher strain rate. Therefore assessment of the transition to undrained behaviour is made based on the shape of the strain rate effect from deviatoric stress measurements.

5.3.1 Transition from partially drained to undrained

Another method to determine the transition point from partially drained to undrained behaviour is by including undrained strain rate effects in the process. Through comparison of the partially drained and undrained strain rate effect the transition point is interpolated. Because the soil in question is normally consolidated it is assumed the minimum strength (no strain rate effect) corresponds to where the soil transitions from partially drained to undrained. To describe the relationship between the strain rate effect in the partially drained and undrained domain Equation 5-3 from Lehane *et al.* (2009) is used;

$$\frac{q}{q_{ref}} = \left[a + \frac{b}{1 + \mathrm{cV}} \right] \left[\frac{v/d}{(v/d)_{ref}} \right]^{m} \qquad (5\text{-}3)$$

Where *a*, *b* and *c* are curve fit parameters, *V* is the normalised velocity, *v* is the velocity in mm/s (taken as axial velocity), and *d* is the penetrometer diameter (assumed in this study as drainage path length), and *m* is an exponent describing the increase of strength with increased stain rate.

The value $(v/d)_{ref}$ represents the minimum value at which viscous rate effects are occurring, which was taken at 0.0001%/s (Rattley *et al.*, 2008), corresponding to 3×10^{-6}/s in Lehane's study, and 1×10^{-6}/s for use in this study. The fit of Equation 5-3 to Kaolin consolidated to 720kPa are presented in Figure 5-6. The equation fits the results well, particularly in the partially drained domain at higher strains, and in the undrained domain at lower strains.

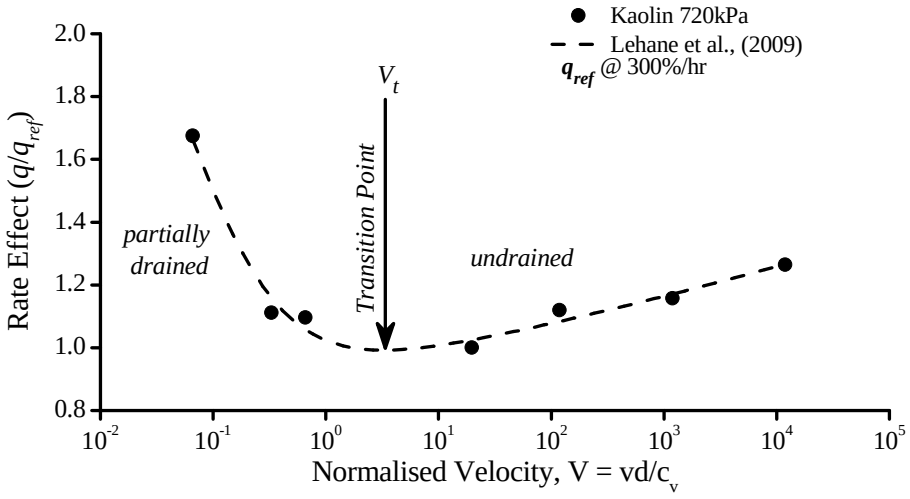

Figure 5-6 Fit of Equation 5-3 to the strain rate effect (q/q_{ref}) in Kaolin 720kPa

Table 5-6 presents the curve fit parameters from the fit to the strain rate effect on each soil. The *b* parameter was taken at the value of strain rate effect at 1%/hr (Normalised velocity, $V \approx 0.04$-0.06). The *c* parameter represents the drainage conditions of each soil. A decrease in *c* reflects faster drainage. The value for the KSS 560kPa is the largest, yet corresponds to the highest value of coefficient of consolidation and therefore may be erroneous. The *a* parameter represents the breadth of the transition from partially drained to undrained.

Soil	Plasticity Index, *Ip* (%)	*a*	*b*	*c*	*m*	V_t
Kaolin 720kPa	45	0.77	1.67	18.3	0.034	3.48
Kaolin 1150kPa	45	0.79	1.51	20.4	0.028	3.30
KSS 560kPa	23	0.68	2.00	21.3	0.044	3.11
KSS-541 300kPa	20	0.65	2.00	15.1	0.048	4.18
KSS-541 600kPa	20	0.69	1.83	18.0	0.044	3.32

Table 5-6 Curve fit parameter from Equation 5-3

As shown in Table 5-6, the *a* parameter relates strongly to soil type, with a higher *a* parameter shown for Kaolin. This reflects the lower permeability of this soil. Each of the curve fit parameters shown in Table 5-6 are strongly linked to permeability. This seems intuitive for the partially drained strain rate effect. The undrained rate effect (i.e. the *m* parameter) which also shows some correspondence to permeability decreases with plasticity index. Thus the undrained rate effect at maximum strength is shown here to correspond to lower plasticity index. This also influences the *a* parameter, which increases (with I_P). This is indicating a broader transition between partially drained to undrained conditions. The parameter V_t in Table 5-6 represents the normalised velocity at the projected minimum strain rate effect. Lehane *et al.* (2009) describe how by differentiation of Equation 5-3 with respect to velocity (v) can be used to define the parameter V_t resulting in Equation 5-4 below;.

$$V_t = \frac{b}{acm} \qquad \text{for } m < 0.1 \tag{5-4}$$

Lehane *et al*. (2009) reported V_t values of between 5 and 9 for the T-bar, and 11 and 17 for the Ball penetrometer. This was in both normally and over consolidated Kaolin (V_t decreasing with OCR). Danziger and Lunne (1997) reported that the transition from partially drained to undrained, and subsequently the minimum strength would vary with different rates depending on the plasticity index, OCR and moisture content. Jaeger *et al.* (2010), confirmed that V_t varies in Kaolin depending on OCR, as well as with a model soil comprising Kaolin and a large component of sand (75%), as well as a mixture of silica flour and bentonite. Table 5-6 presents, with the exception of KSS-541 300kPa which, displays the largest value of V_t, that the values of V_t shown for

soils in this study do not vary greatly. This may be due to the limited range of c_V for the soils used in this study. It is therefore inconclusive from the soils in this study as to how other soil properties affect the transition to undrained behaviour.

Further research on the effects of plasticity index and other soil properties could incorporate fine grained soils of significantly different activity, as well as incorporating soils at a wider range of liquidity index to determine the effects of compressibility on the value of V_t.

5.4 Factors affecting the undrained strain rate effect

This section will compare the influence of index properties on the strain rate effect on undrained strength. The results are compared considering the effect of strain rate at tests of 300%/hr, 1,800%/hr, 18,000%/hr and 180,000%/hr. Three series of tests are carried out in normally consolidated Kaolin, each consolidated to a different consolidation pressure, enabling a comparison of effective stress, and thus moisture content, void ratio, and liquidity index on the strain rate effect in Kaolin. A further two series of tests were undertaken in KSS-541, which broadens the comparison to plasticity index, as well as the aforementioned index properties. A further series of tests was carried out in KSS consolidated to 560kPa. In total six series of tests are considered here, each in different soils, or at different state. Each series comprises of four strain rate tests, each at a different strain rate. A total of 24 tests are thus considered here.

Figure 5-7 presents the strain rate effect (q/q_{ref}) at strain rates from 300%/hr to 180,000%/hr for three soils of increasing plasticity index, each of which are normally consolidated to the same value of liquidity index (I_L = 0.22) before shear. The 300%/hr tests are used as the reference deviatoric stress (q_{ref}). Figure 5-7 shows regression lines derived with least squares method in OriginPro7.5 using Equation 5-5. The logarithmic strain rate parameter μ (Equation 5-5) is the fractional increase in deviatoric stress per logarithmic increase in strain rate.

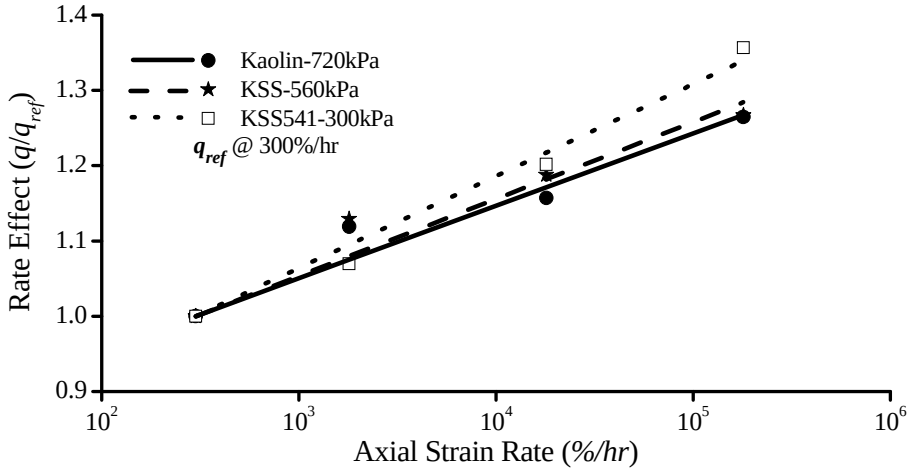

Figure 5-7 The strain rate effect (q/q_{ref}) at strain rates from 300%/hr to 180,000%/hr

$$\frac{q}{q_{ref}} = 1 + \mu \log\left(\frac{\dot{\varepsilon}}{\dot{\varepsilon}_{ref}}\right) \tag{5-5}$$

Because much of the literature describes the effect of strain rate with an exponential Equation of the form shown in Equation 5-6, this approach has also been applied to the result of this study to facilitate comparisons to be made with the respective literature.

$$\frac{q}{q_{ref}} = \left(\frac{\dot{\varepsilon}}{\dot{\varepsilon}_{ref}}\right)^{m} \tag{5-6}$$

Where *m*, is the undrained strain rate exponent. The reference strain rate in both Equation 5-5 and 5-6 is the corresponding result from the 300%/hr tests.

5.4.1 Influence of strain on undrained strain rate effects

The strain rate effect (Equation 5-5) and how it varies with increasing strain is shown in Figure 5-8. The range of strains shown in Figure 5-8 are from 0.5% to 3%. The strain at failure (maximum/peak strength) for the undrained tests used to define the logarithmic parameter in Figure 5-8 is typically between 2 and 4% as shown in Figure

5-9. Therefore at strains beyond this (identified as lower boundary in Figure 5-8), the strain rate parameter is increasingly affected by localisation and strain softening, and is excluded from analysis on this basis.

Akai *et al.* (1975) and Balderas-Meca (2004), describe similar behaviour of the variation of strain rate effect with increasing magnitude of strain (Figure 5-8). Both studies found that for a particular strain the strain rate parameter is approximately constant, although both report different values at which this occurs. Akai *et al.* (1975) report this occurs at quote 1% strain, whereas Balderas Meca (2004) report 2% strain.

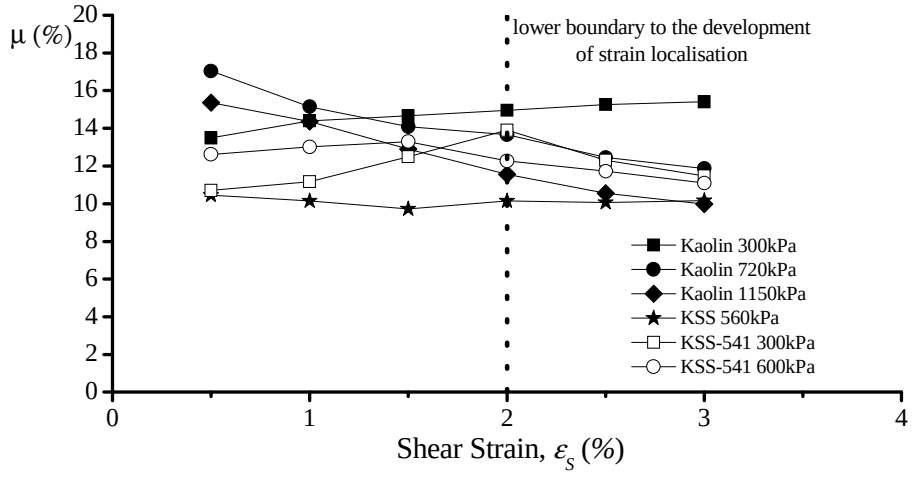

Figure 5-8 Effect of strain on the strain rate parameter (μ)

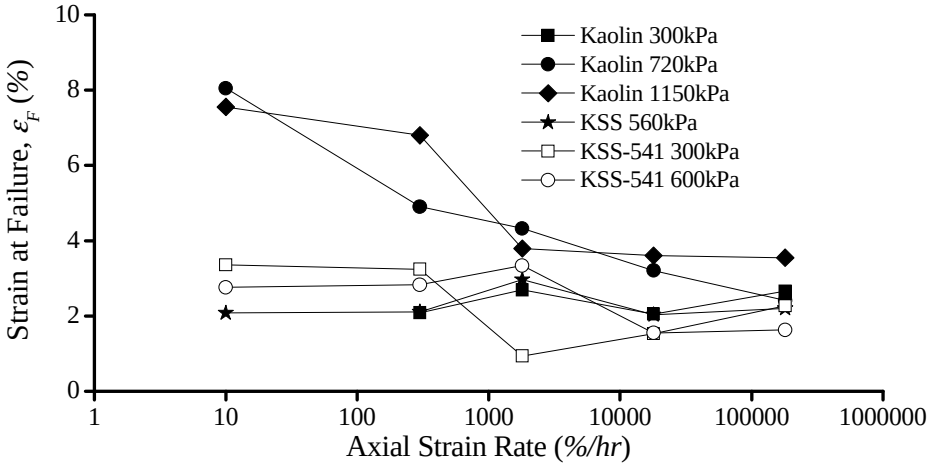

Figure 5-9 Variation of strain at failure (ε_F) at increasing strain rate

From this study it appears there is more variation in the strain rate parameter with strain level for some soils. Both Kaolin 300kPa and KSS 560kPa show approximately constant values of rate parameter from approx 0.5% strain, which reflects findings from Akai *et al.* (1975) and Balderas-Meca (2004). However, the other soils tested tend to show near constant or decreasing rate effects with increasing strain.

This may reflect findings from Balderas-Meca (2004) and how at low strains (<2%) there is a more pronounced strain rate effect, which tends to decrease to asymptotic values from 2% strain. It is noted that Akai *et al.* (1975) did not report this behaviour, finding that strain rate effects increased to a maximum at 1% strain. However, decreasing strain rate parameter shown in Figure 5-8 more likely reflects the transition to failure for some of the tests used to develop the strain rate parameter. It is possible that inherent variability is reflected in results shown in Figure 5-8, although at least four tests have been used to define each point as shown previously, with many having being repeated (for small strain data retrieval purposes) and showing strong repeatability.

Because maximum strength occurred at different strains for differing soils and tests (Figure 5-9), this parameter may be unsuitable for comparing the effect of soil type on strain rate parameter. Therefore the strain rate effect at 2% strain is chosen as the representative strain rate effect for comparison of properties which influence the strain rate effect at large strain. This value is chosen to avoid the possible effects of non-uniformity and localisation, whilst being close to the maximum yield strength of each test so as to represent the strain rate parameter at large strains. As mentioned earlier, the yielding of these soils typically occurred at strains from 2% to 4%.

5.4.2 Influence of plasticity index on strain rate effects

Figure 5-10 compares the effect of strain rate on strength in the undrained domain, with plasticity index. For reasons described in Section 5.4.1, Figure 5-10 compares the strain rate parameter for values of deviatoric stress at 2% strain. Each value of rate parameter for a particular plasticity index in Figure 5-10 are derived from a series of four tests between 300%/hr and 180,000%/hr.

Soils of the same plasticity index are connected by solid lines in Figure 5-10. The largest range of variation in rate parameter is seen for Kaolin (I_P = 45%) which displays values between approximately 11-15%. The range of values displayed by KSS-541 is 12 to 14%, notably within the range of rate parameters displayed by Kaolin. A trend line developed from linear regression to all points is included in Figure 5-10, which shows a slight increase in rate effect with plasticity index, which is approximately 0.5% ($\delta\mu$ = 0.5) for a 10% increase in plasticity index.

It should be noted that if KSS-560kPa was excluded from this interpolation the fit to the remaining points would not deviate with plasticity index (approximately $\delta\mu$ = 0.1% for plasticity index increased by 10%). Because of the variation of rate parameter displayed by Kaolin and KSS-541 and the similarity of their results when considering the full range of plasticity index, it appears that increasing plasticity index may not affect the rate parameter, and thus there is not a strong correlation between the magnitude of the strain rate effect and plasticity index for the soils tested as part of this study.

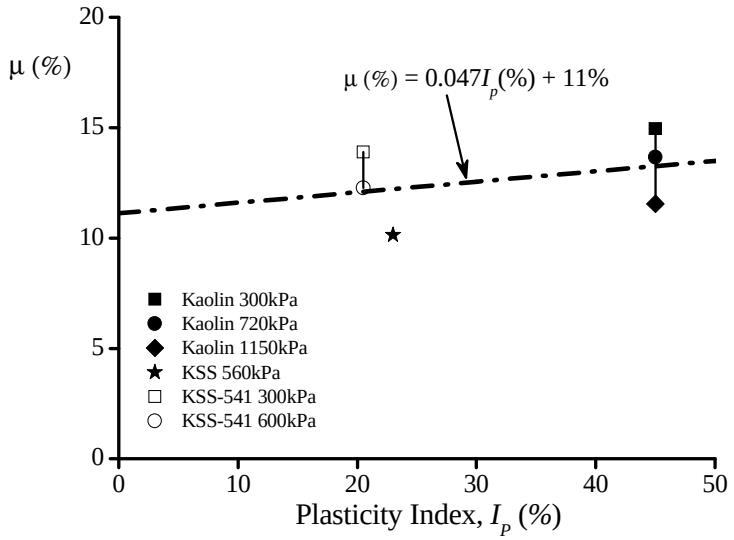

Figure 5-10 Variation of undrained rate effect (q/q_{ref}) on strength with plasticity index

To gain further perspective on the findings of this study in relation to how plasticity index may impact the rate effect, Figure 5-11 compares the undrained strain rate parameter in (a) logarithmic form and (b) exponential form with values of other soils

collated from studies of undrained strain rate effects in the literature. The majority of results collated from the literature in Figure 5-11 are taken from triaxial compression tests, from which a linear increase in strength has been observed although the range of strain rates varies between studies.

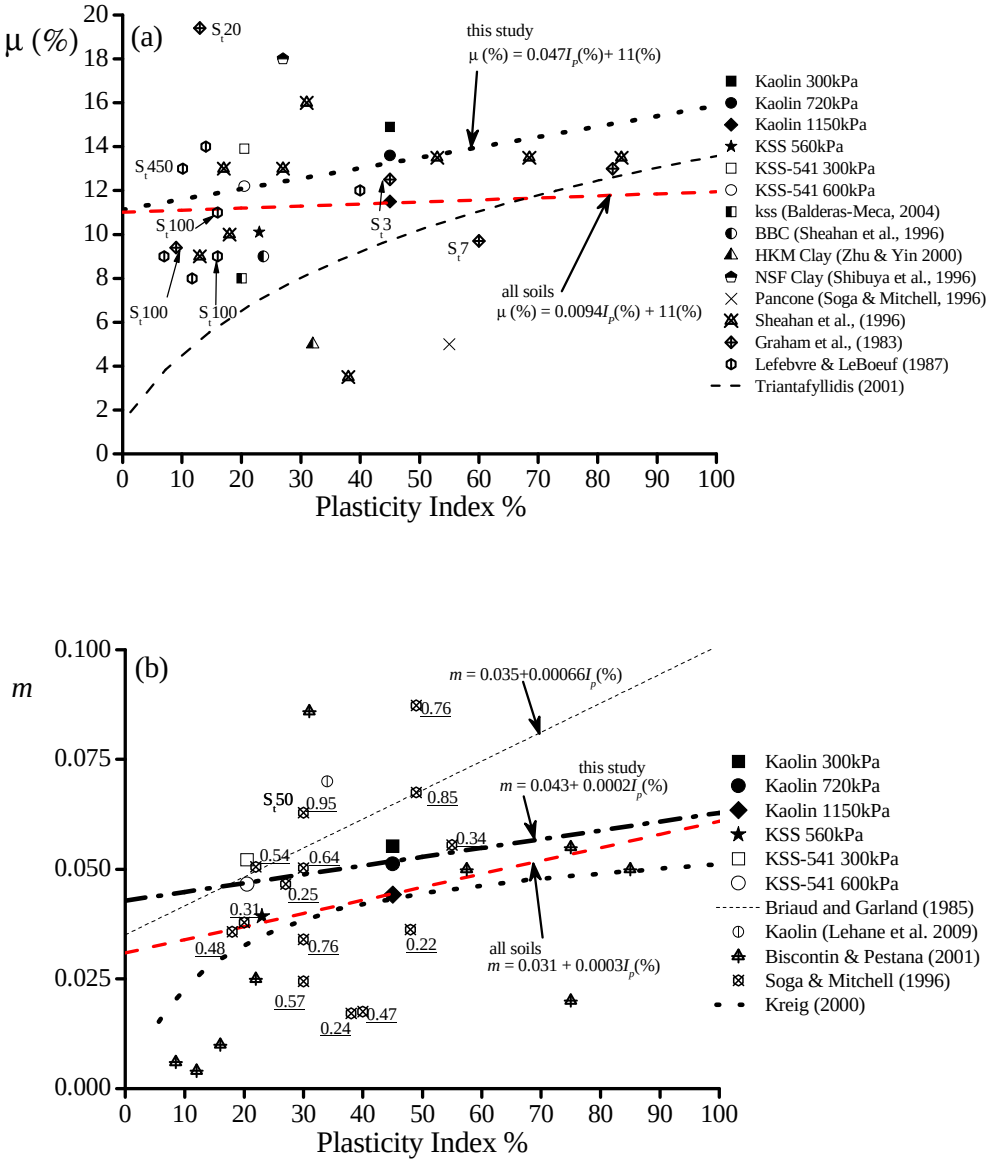

Figure 5-11 Comparison of strain rate effects on strength with plasticity index in (a) logarithmic form (b) exponential form, including data from literature

Note; Values of metastability index (Soga and Mitchell, 1996) for each soil shown underlined adjacent to data point. Values of sensitivity (S_t) shown adjacent to relevant data.

The strain rate parameter shown in Figure 5-11 (a) is dependent on the reference strain rate. The results shown in Figure 5-11 are generally taken from reference strain rates of 0.1 – 1%/hr. They are not corrected here however it is thought this would not bias the observations with plasticity index as shown in Figure 5-11.

With the exception of Balderas-Meca (2004), who tested at strain rates up to 350,000%/hr, the range of strain rates used to determine the strain rate effects on strength shown are typically lower than those used in this study. Lefebvre and LeBoeuf (1987) used the highest monotonic triaxial strain rates of other studies, testing at up to 132%/hr. Results from Biscontin and Pestana (2001) shown in Figure 5-11 (b) are from shear vane testing at rates of rotation between 6-600°/min.

Figure 5-11 (a) presents two trend lines, each constructed using the least squares method. The first trend line describes results for the soils from this study, the second describes all soils included in Figure 5-11 (a). The second trend line taken from analysis of the strain rate effect from all soils shows little variation with plasticity index ($\Delta\mu$ = 0.1% for plasticity index increased by 10%). Neither of these trend lines (Figure 5-11 (a)) relate well to a proposed relationship from Triantafyllidis (2001). Much of the results reported in the literature display greater strain rate effects than predicted by Triantafyllidis (2001). Based upon Figure 5-11 (a) the strain rate effect does not appear to relate to plasticity index.

Results of soils used in this study display an exponential strain rate parameter (m) from Equation 5-6 ranging from 0.04 to 0.055. Figure 5-11 (b) compares the results from this study with strain rate effect reported in the literature described in an exponential form. A trend line has been constructed using the least squares method to results from this study, as well as to all results in Figure 5-11 (b). Also shown in Figure 5-11 (b) is a relationship between the strain rate effect and plasticity index from Briaud and Garland (1985) and from Kreig (2000). Similarly to those presented in Figure 5-11 (a) there is a large degree of scatter in the data of Figure 5-11 (b).

Each trend line displays an increase in strain rate exponent with plasticity index, although each of the trend lines in Figure 5-11 (b) display little correspondence to each other. The increase in strain rate parameter m, expressed as a percentage to a first

degree of accuracy over a 10% increase in plasticity index varies from ≈ 1.7% from Briaud and Garland (1985), ≈ 0.75% from all soils in Figure 5-11 (b), to ≈ 0.5% for the results in this study. The magnitude of the strain rate effect measured during the current study fall between those proposed by Briaud and Garland (1985) and Kreig (2000).

At 6% plasticity index, i.e. for non plastic soils (BS 5930:1990) both trend lines in Figure 5-11 (a) show a strain rate effect of approximately 11%. The value of 11% is close to the findings from Kulhawy and Mayne (1990). Considering results from 26 studies on the strain rate dependence of fine grained natural soils, they found that on average strength increases by 10% per logarithmic increase of strain rate from a reference strain rate of 1%/hour. These findings are widely quoted in literature on the effect of strain rate on fine grained soils and are often used as an approximation measure in the absence of further information on strain rate effects. The values of the strain rate exponent (Figure 5-11 b) at a plasticity index of 6% correspond as a first degree of accuracy to a strain rate parameter (μ) of between 7-10%. This is less than but similar to that seen in Figure 5-11 (a).

Notably, in Figure 5-11 (b) three soils (compiled by Biscontin and Pestana, 2001)), Drammen Clay (Aas, 1965), St. Alban Clay and St. Louis de Beaucours (Roy and Leblanc, 1988) with plasticity indices of 8.5, 12 and 16% (Figure 5-11 b), tend to low values of strain rate exponent as the plasticity index reduces to less then 20%. Strain rate effects on these soils are lower than those encountered at similar plasticity index in Figure 5-11 (a). Neither the relationship from Triantafyllidis (2001) nor that from Kreig (2000) which, both present decreasing strain rate effects with plasticity index describe the results presented in Figure 5-11 well. Because of the large variability in the data presented in Figure 5-11 (a) and (b) (at plasticity index less <20%) it is difficult to extrapolate how the strain rate effect varies as plasticity index reduces tending to non-plastic, where strain rate effects are not expected. It would seem likely that other factors affect the strain rate effect on strength (at least at plasticity index <20%).

The results compiled by Soga and Mitchell (1996), are from triaxial tests in normally and lightly over consolidated soil. The plasticity indices range from 18 to 55%. They

found that strain rate effects on strength may relate to a metastability index, defined as the difference in liquidity index between the current and fully remoulded state of soil. Therefore, for a given plasticity index, the results compiled by Soga and Mitchell (1996) in Figure 5-11 (b) increase with metastability. The values of metastability index are shown adjacent to their strain rate exponent in Figure 5-11 (b).

The relationship from Briaud and Garland (1985), which displays the largest increase of strain rate exponent with plasticity index is derived from 152 laboratory and both in-situ and model pile tests. They noted a large degree of scatter in their data set used to define their relationship with plasticity index shown in Figure 5-11 (b). Therefore, combining these factors with the scatter in data presented in Figure 5-11 and the observations from results of soils in this study, it is reasonable to conclude that plasticity index is not a single governing factor of strain rate effects on strength. The observation that plasticity index alone does not affect the strain rate parameter is consistent with Graham *et al.* (1983), as well as Lefebvre and LeBoeuf (1987).

5.4.3 Influence of initial effective stress on strain rate effects

To compare how the rate effect varies with the initial state of fine grained soils, multiple series' of tests were conducted in Kaolin and KSS-541 at different consolidation pressures.

Soil	Initial effective stress, p'_0 (kPa)	Plasticity Index, I_P (%)	Void ratio, e	Moisture Content, w (%)	Liquidity Index, I_L
Kaolin 300kPa	300	45	1.13	43.9	0.31
Kaolin 720kPa	720	45	1.00	39.9	0.22
Kaolin 1150kPa	1150	45	0.90	34.9	0.11
KSS 560kPa	560	23	0.59	22.1	0.22
KSS-541 300kPa	300	20	0.60	22.5	0.22
KSS-541 600kPa	600	20	0.54	20.3	0.11

Table 5-7 List of key index properties relevant to the strain rate effect

A series of four tests were conducted at three separate consolidation pressures in Kaolin, with a further two series of tests in KSS-541 and one series of tests was conducted in KSS. The range of effective stresses selected for consolidation pressures were chosen to correspond to particular void ratios and hence moisture contents, with particular moisture contents selected to allow comparison of different soils at identical values of liquidity index. Some properties of the soils for each series of tests are shown in Table 5-7.

Figure 5-12 presents the strain rate effect and the effective stress for each soil at the end of consolidation. Each point in Figure 5-12 corresponds to a linear fit of the logarithmic increase in strain rate on strength measured from four tests between 300%/hr to 180,000%/hr. The rate parameter in Figure 5-12 is the same as that compared to plasticity index in Figure 5-10. The soils of same plasticity index are connected by solid lines in Figure 5-12. With increasing effective stress for a given soil the strain rate effect in Figure 5-12 reduces. This corresponds to reducing void ratio, moisture content and liquidity index.

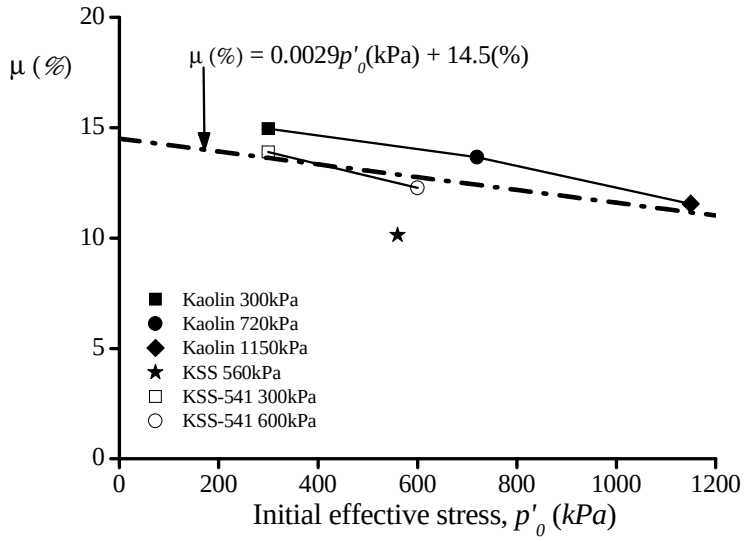

Figure 5-12 Variation of strain rate parameter with consolidation pressure in different soils

At a particular consolidation pressure and thus effective stress in Figure 5-12, making a comparison between Kaolin and KSS-541 illustrates that a higher rate parameter is measured for Kaolin. Making a direct comparison at an effective stress of 300kPa in

Figure 5-12, the strain rate effect is higher in Kaolin, which corresponds to higher plasticity index, void ratio, moisture content and liquidity index (Table 5-8).

Bjerrum (1972), developed a correction factor for strength determined using the field shear vane, which is based on the increased rate effect he measured at a higher plasticity index (Section 2.5.1). Figure 5-12 shows that if in-situ testing is conducted in different soils (different plasticity index) which are under a similar degree of effective stress (e.g. at 300kPa) the results would present themselves as showing an increase in rate effect with plasticity index.

Figure 5-12 also implies that if the current effective stress is ignored and is significantly different, when considering the strain rate effect it could be easily conceived that strain rate effects do not vary with plasticity index, i.e. a rate effect of approximately 13% is measured in KSS-541 at approximately 400kPa, whilst Kaolin also displays at strain rate effect of 13% yet at 900kPa. This may explain much of the variation between strain rate parameter and plasticity index discussed in Section 5.4.2. i.e. the strain rate effect is also dependent on state.

Because the strain rate effect reduces in soil consolidated to higher effective stress, and increases in soil of higher plasticity index (at identical effective stress) as shown in Figure 5-12, a relationship between the strain rate effect on strength and plasticity index, at identical effective stress is proposed. Equation 5-7 below describes the strain rate parameter for plasticity index between 20-45% and consolidated to an effective stress between 300 to 600kPa;

$$\mu(\%) = 0.056 I_P(\%) + 11.9(\%) \qquad (5\text{-}7)$$

Equation 5-7 is relevant to normally consolidated soils, at moisture content in excess of the plastic limit, however may only be appropriate at liquidity index in excess of approximately 0.1. This caveat is included because currently there is little understanding of strain rate effects at moisture content close to or at the plastic limit.

5.4.4 Influence of moisture content on strain rate effects

Previous investigations have found strain rate effects on strength increase with moisture content (Brown and Hyde, 2008a, Briaud and Garland, 1985, Gibson and Coyle, 1968). Figure 5-13 presents the rate parameter derived as an exponent of increasing strain rate effect with strain rate and how it varies with moisture content. The rate parameter is defined in this way to enable a comparison with findings from Briaud and Garland (1985), which used an exponential form to compare the effect of strain rate on strength. The values of rate parameter in Figure 5-13 are the same as those presented previously in Figures 5-10 and 5-12.

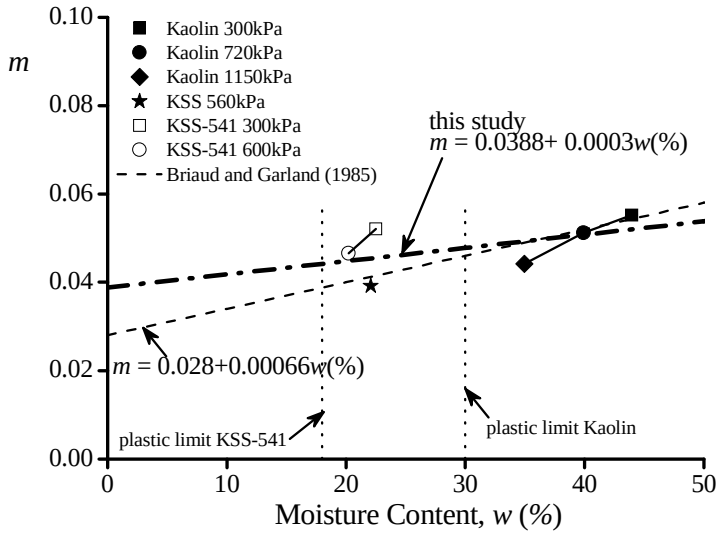

Figure 5-13 Variation of strain rate parameter with moisture content for different soils

Figure 5-13 shows that for both Kaolin and KSS-541; higher moisture content corresponds to a higher rate effect confirming observations from Brown and Hyde (2008) and Gibson and Coyle (1968) that moisture content corresponds to higher rate effects in a particular soil.

The relationship between strain rate effects and moisture content in Figure 5-13 from Briaud and Garland (1985) which is a best fit taken from over 152 tests including laboratory and pile tests, suggest that rate effects will consistently increase with moisture content. In a general way the results from Briaud and Garland (1985) correspond well to the results from this study, however similar rate effects are found in both Kaolin and KSS-541 yet there is a 50% difference in moisture content

between the different types of soils. Therefore the change in moisture content is important but not the absolute magnitude as suggested by Briaud and Garland (1985).

Figure 5-13 also presents the moisture content at the plastic limit of both Kaolin and KSS-541. Extrapolations of the relationship between moisture content and strain rate effects for both Kaolin and KSS-541 with their respective plastic limits show similar strain rate effects ($m \approx 0.04$). The decrease in strain rate effect with moisture content in Figure 5-13 also implies that KSS-541 tends to $m = 0$ at 0% moisture content, and Kaolin also tends to $m = 0$ at 0% moisture content. This implies that rate effects do not occur in fine grained soils if there is no moisture in the soil. However in practical terms the plastic limit is more relevant to industry. Future research could incorporate samples closer to the plastic limit to verify how strain rate effects vary at the plastic limit.

Briaud and Garland (1985) and Rattley *et al.* (2011) postulated that strain rate effects in fine grained soils may be due to the viscosity of the water envelope absorbed onto the surface of a clay particle. Heuckel (1992) describes various forms water can take within a fine grained soil. Relevant to here are observations that within the absorbed layer of clay particles water can have significantly different properties. In particular, water can display much higher viscosity (Heuckel, 1992). However, several studies have shown that decreasing moisture content corresponds to higher viscosity in fine grained soils (Low, 1976, Allam and Sridharan, 1984, Ghezzehei and Or, 2001, Karmakar and Kushwaha, 2007, Mahajan and Budhu, 2009). Israelachvili *et al*. (1978) showed that higher stress is required to initiate shear for a decreasing number of molecular layers of water on a clay surface. Viscosity is a function of the yield stress (Ghezzehei and Or, 2001), and thus it appears the yield stress and viscosity of soils increase with reducing number of molecular layers of water within the absorbed layer. If in soils of higher moisture content the absorbed layers increase in size, then more water is influenced by the clay particle. Thus although the viscosity and yield stress decrease with moisture content, the absorbed layers influence the strength to a greater proportion. Thus the ratio of viscosity to yield stress would increase, causing a greater strain rate effect as per Figure 5-13.

However the effects of moisture content on the strain rate effect in Figure 5-13 also reflect the void ratio of the soils. The contribution to shear resistance (strength) offered from water absorbed on the surface of clay particles has been shown to be negligible (Allam and Sridharan, 1984). Assuming a face to face contact between clay particles, the shear resistance, which would be entirely dependent on that offered from the absorbed water, would be of little consequence in comparison to the fully mobilised frictional resistance of soil in reality (Allam and Sridharan, 1984). Therefore the orientation of particles in fully saturated soils must be predominantly of edge to edge or edge to face contacts. As a soil consolidates and becomes denser the orientation of the particles will become increasingly face to face (Resendiz, 1965). As the void ratio reduces during consolidation the number of particle contacts will grow. Thus the strength of soil will increase, and in this regard the viscosity will increase. However because of the reorientation of the particles (increasingly face to face) there is comparatively less viscosity then when edge to edge contacts are prevalent. Thus the number of particle contacts influences the static strength, and the type of contacts influence the ratio of viscosity to the static strength. Thus the strain rate effect on strength and its relationship to moisture content as shown in Figure 5-13 may reflect the change in particle contacts as the soil is consolidated to higher effective stress.

5.4.5 Influence of liquidity index on the strain rate effects

Figure 5-14 presents the strain rate effect at 2% strain at the corresponding liquidity index for each series of tests used to define the rate parameter. The strain rate effect on strength is the same as that previously compared to plasticity index, effective stress, and moisture content. Figure 5-14 illustrates that for Kaolin and KSS-541 the strain rate effects on strength increase with liquidity index (Equation 5-8). This confirms findings from Gibson and Coyle (1968) as well as Briaud and Garland (1985).

$$\mu(\%) = 12.9 I_L + 10.2(\%) \qquad (5\text{-}8)$$

In this study the soils were originally tested at particular values of liquidity index with the intention of enabling a better comparison between strain rate effects, plasticity index and the current state of each soil. Early tests showed a good correspondence

between strain rate effects on strength in different soils at the same liquidity index, and the methodology was expanded to include further testing at different liquidity indices.

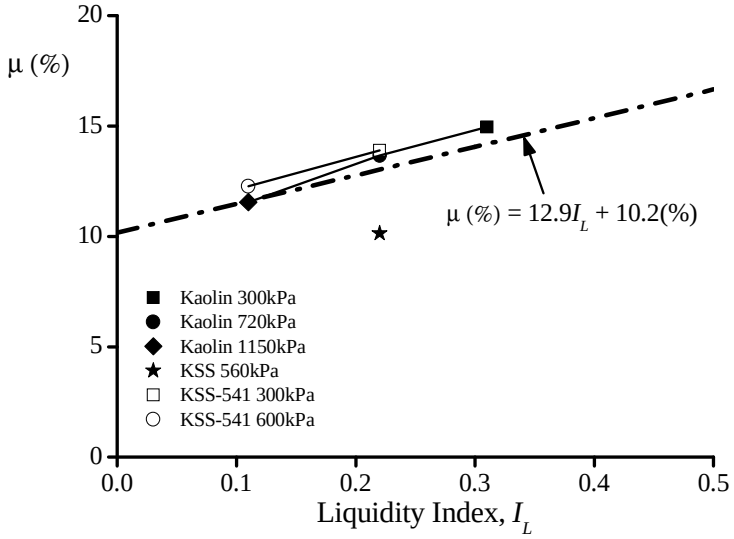

Figure 5-14 Variation of rate effect parameter with liquidity index for different soils

As shown in Figure 5-14 the strain rate parameter is very similar for Kaolin and KSS-541 soils when normalised to their respective liquidity index. The agreement between Kaolin and KSS-541 shown in Figure 5-14 suggests liquidity index is ideal to account for the strain rate effect in the soils used in this study. It is noted that KSS 560kPa may be erroneous, or could be influenced by other factors, such as higher then expected effects of consolidation during the lower strain rate tests used to define the strain rate effect in KSS. As described in Section 5.3, KSS displays a greater coefficient of consolidation then other soils used in this study.

Variation of strain rate effects for a soil of given plasticity index depending on the liquidity index may explain much of the scatter noted previously in Figure 5-11. Each soil has also shown increasing strain rate effects with increasing moisture content, yet similar magnitude of strain rate effects between soil types of very different moisture content. Thus normalisation of the plasticity index and moisture content with liquidity index reflects the variation of strain rate effect due to both soil classification and current state.

Figure 5-15 presents a comparison between the strain rate effect in (a) logarithmic form and (b) exponential form with results reported in literature. Each of the studies shown in Figure 5-15 describes increasing strain rate effects with liquidity index. The results from the literature in Figure 5-15 (a) are from triaxial studies, typically at strain rates far lower then those used in the current study. Tests from Gibson and Coyle (1968), who conducted undrained unconsolidated triaxial compression tests at velocities up to 3600mm/s ($15x10^6$%/hr) display a slightly lower increase in strain rate effect with liquidity index (Figure 5-15 (a)). Note the results from Gibson and Coyle (1968) were taken from published data, and may be subject to slight error in reinterpretation as a strain rate effect in either logarithmic or exponential form.

Figure 5-15 (b) highlights excellent correspondence with both the trends and magnitude of strain rate effects from this study with those from Briaud and Garland (1985). The trend lines from both from Gibson and Coyle (1968) and from Soga and Mitchell (1996) also show similar relationships between the increase of strain rate effect with liquidity index, however the intercept at liquidity index = 0 are slightly different.

As mentioned some differences in the magnitude of the strain rate effect may be due to the interpretation of the published data from Gibson and Coyle (1968). It is also possible there is some degree of anisotropy in the natural soil tested by Gibson and Coyle (1968), which may increase the strain rate effect (Mukabi and Tatsuoka, 1999b, Santagata *et al.*, 2007). The results from Soga and Mitchell (1996) shown in Figure 5-15 are also reported with their respective values of metastability index. Both the metastability index and strain rate effects increase with liquidity index, however there may be some influence of sensitivity within the data reported by Soga and Mitchell (1996) which may have influenced their results, however the sensitivities of those soils was not reported. The agreement between the results from this study with the relationships from both Gibson and Coyle (1968) and Briaud and Garland (1985) in Figure 5-15 (b) seems good. Therefore the relationship between the strain rate effect on strength and liquidity index from the soils used in this study seem reasonable.

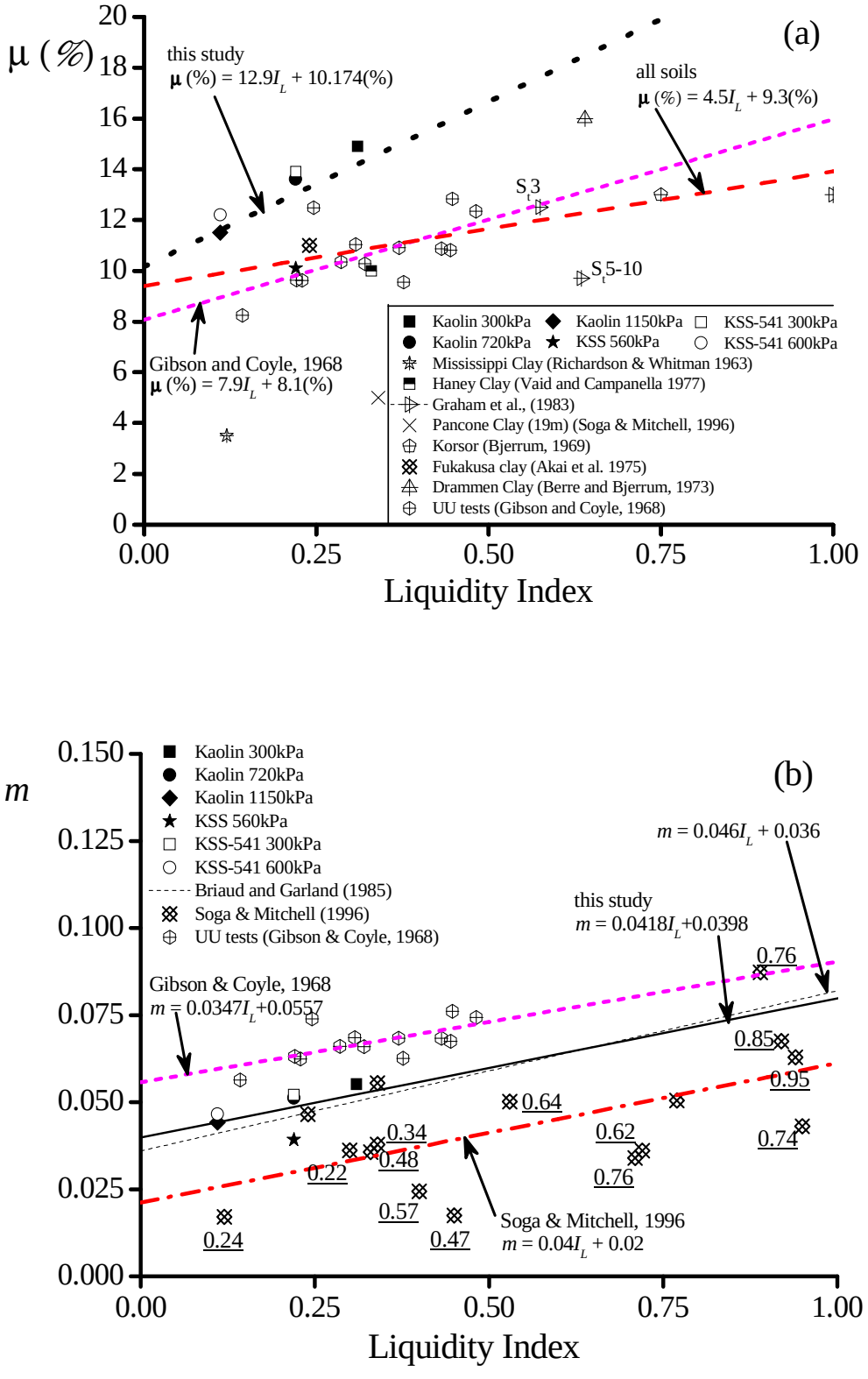

Figure 5-15 Comparison of strain rate effects on strength with liquidity index in (a) logarithmic form (b) exponential form, including data from literature

The trend line fit through all results in Figure 5-15 (a) shows the strain rate effect varies from approximately 10% at IL = 0 to 24% at IL = 1. The variation of strain rate effect with liquidity index in Figure 5-15 (a) and (b) implies that a soil of any plasticity index could display the same variation of strain rate effects on strength depending on the moisture content. Thus soils of low plasticity index may display larger strain rate effects than those of high plasticity index (depending on the liquidity index). However this would seem counter intuitive as it may be expected that strain rate effects reduce with plasticity index, to comply with observations that strain rate effects are insignificant in non plastic soil. Figure 5-15 also implies that soils with moisture contents at the plastic limit will display a strain rate effect on strength.

The relationship between the strain rate effect and liquidity index in Figure 5-15 is derived for Kaolin based soils, each with a substantial clay fraction (37-73%) and of similar activity. Kumar and Wood (1999) found that for clay fractions above 35% the mechanical behaviour is controlled by the clay matrix. At clay fractions less then this it is possible the strain rate effect on strength is significantly different. With lower clay fraction the plasticity index would also reduce (depending on activity). Future investigations could incorporate lower clay fractions to determine how this property relates to strain rate effects. This may clarify the discrepancy between the prediction shown in Figure 5-15 and expected behaviour from soils of low plasticity and liquidity indices discussed above.

At activities higher then those from soils in this study (A = 0.55-0.61) it is possible the strain rate effect and how it may relate to liquidity index may also change. Soils of significantly higher plasticity index could be expected to have higher activity. Therefore the relationship shown in Figure 5-15 may only be suitable for soils of similar activity and clay fractions of at least 35%. Future studies could involve soils at lower liquidity indices and in soil of low plasticity index yet high liquidity index to determine the suitability of the findings from the current study to a wider range of soils.

5.4.6 Influence of OCR on strain rate effects

Figure 5-16 compares the strain rate effect at each OCR with increasing magnitude of strain. Data from the equivalent pre-consolidation pressure (OCR=1) is included. Each value of strain rate effect in Figure 5-16 is defined using results of 300%/hr and 180,000%/hr tests. Figure 5-16 shows that at lower levels of strain (<6%) the strain rate effect reduces with increasing OCR. This is consistent with observations from Sorensen *et al.* (2007) that in the pre-failure domain the strain rate effect reduces with increasing OCR. However the higher OCR soils display increasing strain rate effect with increasing level of strain, whilst the OCR 1 soil displays reducing strain rate effect with increasing strain. The variation of strain rate effect with strain and OCR can be explained in Figure 5-17, which presents the strain at maximum deviatoric stress (failure) for OCR 1, 4 and 10 at 300%/hr and 180,000%/hr. With increasing OCR the strain at maximum stress increases significantly (Figure 5-17).

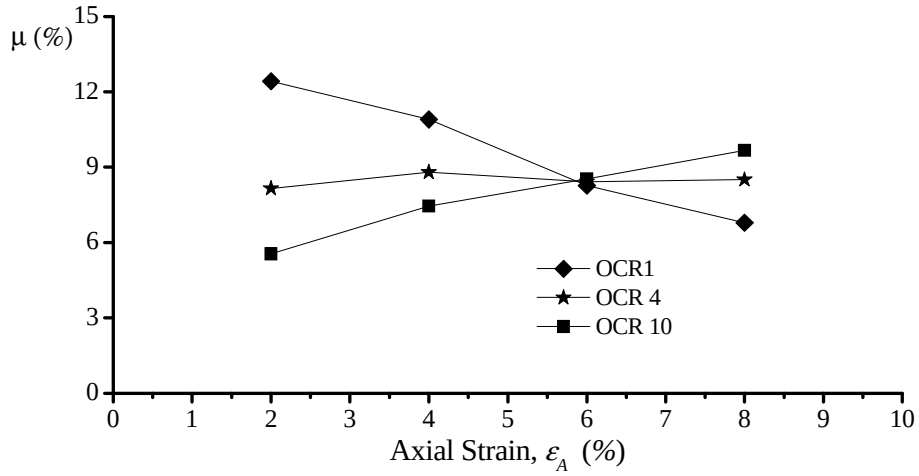

Figure 5-16 Variation of strain rate parameter and level of strain at OCR 1, 4 and 10

Thus based upon the magnitude of the strains at failure in Figure 5-17, the comparison made of the strain rate effect and strain at different OCR in Figure 5-16 represent different aspects of soil behaviour. The strain rate effect of the high OCR soils (increasing with strain) is in the pre-failure domain, whereas at the corresponding strain the OCR 1 soil (decreasing strain rate effect with increasing strain) had exceeded yield at lower levels of strain. This is illustrated in Figure 5-18, which

presents contours of strain at failure overlain on stress-strain curves for the over consolidated soils in Figure 5-18.

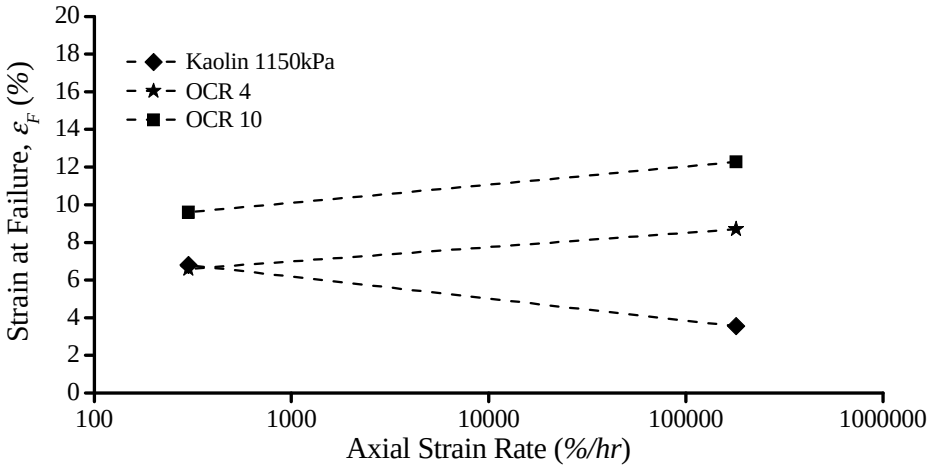

Figure 5-17 Strain at maximum stress in OCR 1, 4 and 10

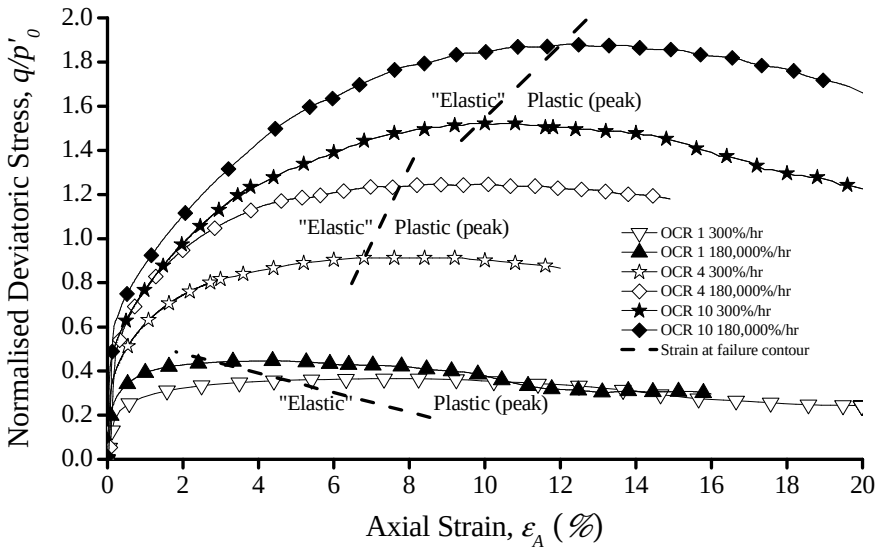

Figure 5-18 Effect of strain rate on stress-strain curves for Kaolin at OCR 1, 4 and 10

Thus it is shown that although strain rate effects on maximum strength are the same, strain rate effects in the pre-failure domain decrease with increasing OCR. That strain rate effects decreases in the "elastic" zone with increasing OCR agrees with Balderas-Meca (2004) and as mentioned Sorensen *et al.* (2007). Soga and Mitchell (2005) also mentioned that strain rate effects reduce with OCR, although they did not specify if this is at maximum strength or in the pre-failure domain.

5.4.7 Normalisation of undrained strain rate effects

Prior to this section the strain rate effect was found to increase with moisture content for both Kaolin and KSS-541. The magnitude of the strain rate effect was found to relate to the liquidity index. This section compares and discusses different methods of normalisation of the undrained strain rate effect, to provide industry a method of incorporation of strain rate effects in design.

To compare the effect of moisture content on the rate effect Figure 5-19 presents the strain rate parameter (μ) normalised by the moisture content. The normalised rate parameter is reduced to approximately constant values for each individual soil. Thus for a particular soil the moisture content is shown to be a suitable parameter to normalise the rate effect. The same effect can be achieved by normalising the rate parameter by void ratio.

As shown in Figure 5-19 the rate effect normalised by moisture content is considerably higher for KSS-541 in comparison to Kaolin. The ratio between the normalised rate parameter for KSS-541 and Kaolin is approximately the same as the ratio between the respective plasticity indices, liquid limit and clay fraction.

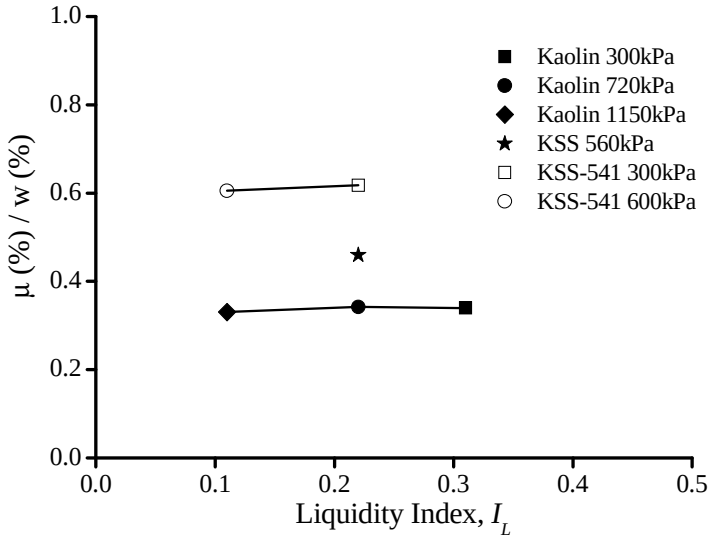

Figure 5-19 Logarithmic strain rate parameter normalised by moisture content

Therefore to determine the effect of clay fraction on the normalised rate parameter the results from Figure 5-19 are normalised by the clay fraction. By normalising by clay fraction the average difference between the normalised strain rate effect for Kaolin and KSS-541 has reduced considerably to approximately 8% in Figure 5-20.

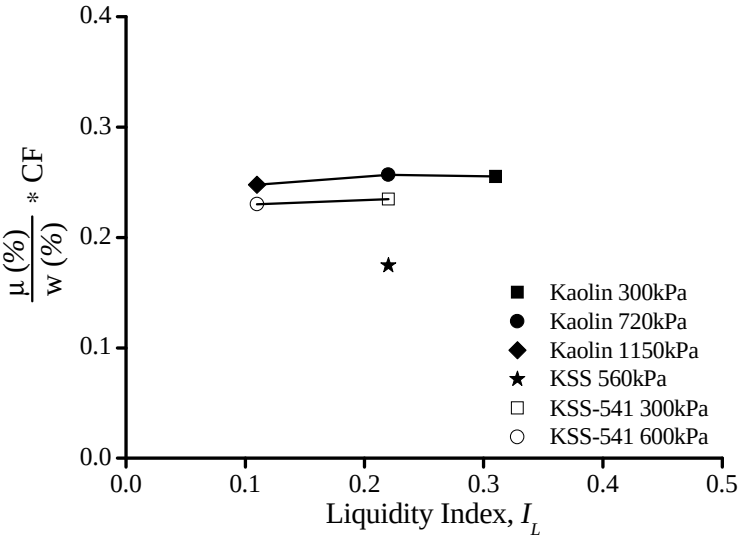

Figure 5-20 Normalisation of the logarithmic strain rate parameter by moisture content and clay fraction

Soil	Plasticity Index, *Ip* (%)	Moisture Content, *w* (%)	Clay Fraction, *CF*	Activity, *A*	Liquidity Index, I_L
Kaolin 300kPa	45	43.9	0.73	0.61	0.31
Kaolin 720kPa	45	39.9	0.73	0.61	0.22
Kaolin 1150kPa	45	34.9	0.73	0.61	0.11
KSS 560kPa	23	22.1	0.38	0.60	0.22
KSS-541 300kPa	20	22.5	0.37	0.55	0.22
KSS-541 600kPa	20	20.3	0.37	0.55	0.11

Table 5-8 List of index properties of soils relevant to normalisation of the undrained strain rate effect on strength

From Figure 5-20 the following relationship is proposed to determine the strain rate effect on strength based on moisture content and clay fraction;

$$\mu(\%) = \frac{0.235}{CF} \times w(\%) \quad (5\text{-}10)$$

Equation 5-10 describes the strain rate effect as a percentage increase per logarithmic increase in strain rate. Equation 5-11 below describes the same strain rate effect as an exponent;

$$m = \frac{0.086}{CF} \times w \quad (5\text{-}11)$$

Unfortunately the difference of 8% in Figure 5-20 cannot be easily explained. This process also does not account for the strain rate effect in KSS. As shown in Table 5-8; the lowest clay fraction for the soils used in this study is approximately 37%. It is noted that at clay fraction lower then this the mechanical behaviour of soils will change dramatically as shown by Kumar and Muir Wood (1999). Seed *et al.* (1964) and Lemos and Vaughan (2000) also noted that mechanical behaviour of soils is significantly affected at clay fractions lower then approximately 40%. It is possible the differences in the normalised strain rate effect between Kaolin and KSS-541 are due to the transition from mechanical behaviour dominated by the clay fraction to increasing influence of coarse particles. The activity of the KSS and KSS-541 soils is slightly lower then that of Kaolin (A = 0.55-0.61), indicating that the clay fraction does not influence the plastic behaviour in the soils containing coarse material to the same extent. Future investigations could incorporate a wider range of clay fraction to determine if at clay fractions lower than those used here would display lower strain rate effects.

The normalisation described above does not account for the strain rate effect in KSS. As shown in Table 5-8 the index properties of KSS are similar to those of KSS-541 and therefore similar magnitude strain rate effects may be expected. However as discussed above and shown in Figure 5-21 the strain rate effect (compared with strain rate) is lower for KSS then the other soils.

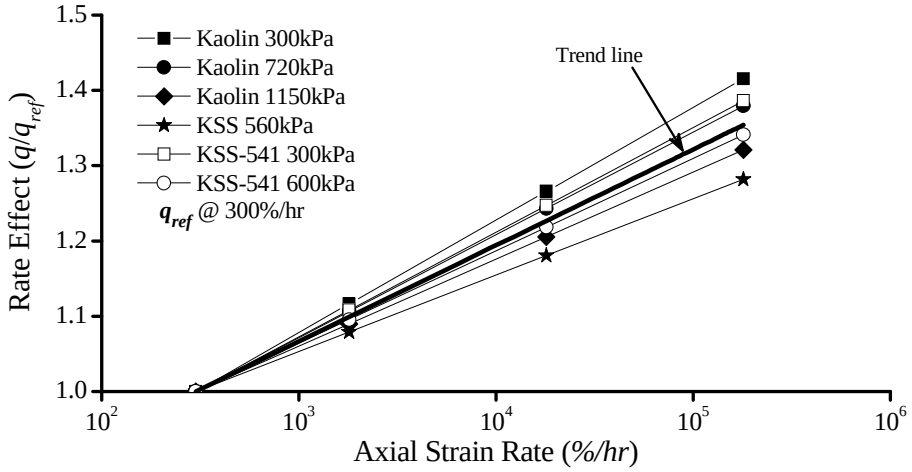

Figure 5-21 Variation of strain rate effect (q/q_{ref}) defined at 2% strain, with increasing strain rate

As shown in Table 5-9 the coefficient of consolidation is higher in KSS then the other soils, resulting in a lower normalised velocity, *V* as discussed in Section 5.3.

Soil	Coefficient of Consolidation, C_V (m^2/year)	Normalised velocity, *V* at 300%/hr
Kaolin 300kPa	10.7	26
Kaolin 720kPa	13.9	20
Kaolin 1150kPa	14.7	19
KSS 560kPa	23.0	12
KSS-541 300kPa	15.0	18
KSS-541 600kPa	16.6	16

Table 5-9 Coefficient of consolidation and corresponding normalised velocity, *V* for all soils

This suggests the effects of partial consolidation may be higher in KSS at the same axial stain rates (as other soils of lower c_V), and thus the 300%/hr strain rate test, which is used to define the strain rate effect (q/q_{ref}) may be influenced by partial consolidation in KSS. This would cause a decrease in the undrained strain rate effect and may explain why KSS displays a lower undrained strain rate effect than the other soils. Figure 5-22 presents the undrained strain rate effect with normalised velocity, *V* for each soil. The normalised velocity, *V* which normalises the velocity of the test

using the drainage path length and coefficient of consolidation, has accounted for much of the variation in the partially drained strain rate effect on strength in Section 5.3.

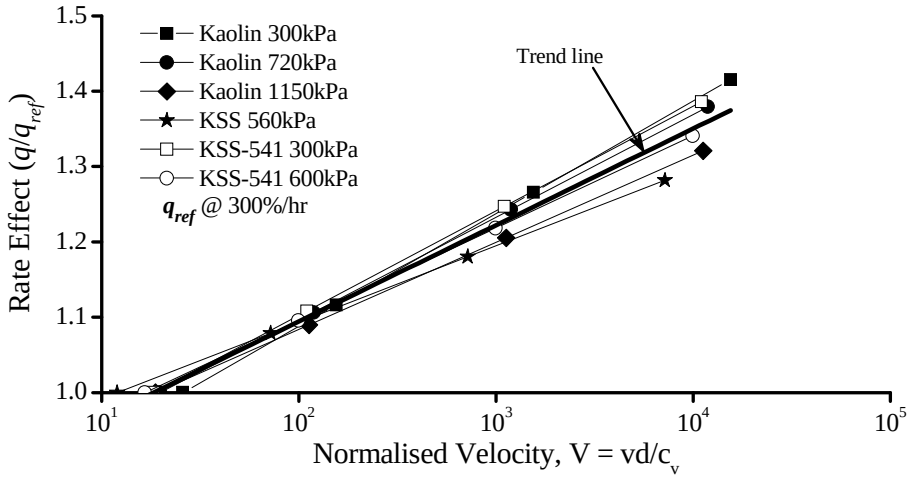

Figure 5-22 Variation of strain rate effect (q/q_{ref}) defined at 2% strain, with increasing normalised velocity *V*

A trend line has been constructed using the least squares method from the results shown in Figure 5-22. The trend line is the same form of the strain rate parameter (μ) used to describe the strain rate effect previously. The average strain rate effect for all soils is 12.8%, which is the same as that shown in Figure 5-21, which compared the strain rate effect with strain rate. The difference (averaged difference of all soils) between the strain rate effect and the average trend line has reduced in Figure 5-22 to on average less than 3%, whereas in Figure 5-21 the difference was 6%. This indicates some applicability of using the normalised velocity *V* in the undrained domain, although there is no consolidation occurring during these tests. The difference in the strain rate effect displayed by KSS from other soils has reduced at lower values of normalised velocity, *V*.

The use of normalised velocity, *V* to normalise the undrained strain rate effect may not be suitable because as mentioned there is no consolidation occurring during these tests. Lehane *et al.* (2009) also described how this parameter (normalised velocity, *V*) is unsuitable for use in the undrained domain, and instead opted to present results with

strain rate. Nonetheless, use of the normalised velocity *V* has reduced the scatter in Figure 5-22.

Ideally a single equation or non-dimensional normalisation technique could be employed by engineers to predict strain rate effects on strength in both the partially drained and undrained domain. Consideration was given to normalisation of velocity (during shear) using permeability, which would make the corresponding normalised velocity dimensionless. However in the undrained domain the use of permeability was found to be unsuitable, because it could not be used with other soil parameters to reduce the scatter between the data. Therefore the normalised velocity, *V* is retained in development of a dimensionless technique to describe the undrained strain rate effect. This also has the convenience of maintaining some correspondence with partially drained strain rate effects. To further reduce the scatter of the undrained strain rate effect shown in Figure 5-22, the normalised velocity is modified by the inclusion of the moisture content and clay fraction as discussed previously;

$$V_2 = \left(\frac{vd}{c_V}\right) / \left(\frac{CF}{w}\right) \qquad (5\text{-}12)$$

Figure 5-23 presents the undrained strain rate effect of each soil with the normalised velocity, V_2 (Equation 5-12).

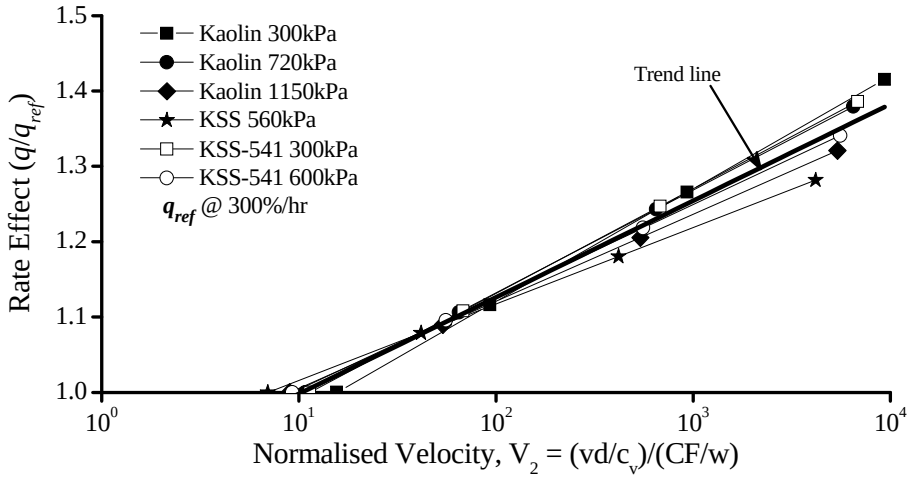

Figure 5-23 Variation of strain rate effect (q/q_{ref}) defined at 2% strain, with increasing modified normalised velocity V_2

The scatter between results and the trend line in Figure 5-23 has reduced to on average of 1.5%. This indicates Equation 5-12 provides a better method for the prediction of the potential of strain rate effects in a wider variety of fine grained soils.

At the highest strain rates used in the current study; Figure 5-23 illustrates this method of normalisation offers good agreement for three soils in particular, Kaolin 300kPa, Kaolin 720kPa, and KSS-541 300kPa. For other soils this method offers some improvement for describing the strain rate effect at a single normalised velocity V_2, although does not offer the same level of agreement seen in the aforementioned soils.

Figure 5-23 also shows the values of normalised velocity V_2 are in reasonable agreement with those corresponding to the transition strain rate (V_t) discussed in Section 5.3.1. The values of normalised velocity V_2 at where the rate effect (q/q_{ref}) = 1 vary from 7 to 15 (Figure 5-23). The values of V_t (Section 5.3.1) where the rate effect (q/q_{ref}) = 1 are typically ≈ 3 to 4 for the soils from this study, with values from approximately 7 to 30 typically reported in literature as the transitional V_t.

In industry, the normalised velocity can be calculated using the velocity, drainage path length, and the coefficient of consolidation. If the value of normalised velocity is greater then V_t, an undrained response of the soil and a subsequent increase in strength can be expected. Where the soil response is undrained the normalised velocity V_2 can be used to determine the expected difference in strength. For example if a value of normalised velocity, V_2 is calculated as 10^3, from Figure 5-23 a rate effect of approximately 25% can be expected.

5.5 Summary of effects of strain rate at large strain (>1%)

The effects of strain rate on strength, for both the partially drained and fully undrained response of fine grained soils have been discussed in this chapter. The scope of this chapter is large strains, which correspond to 10% for partially drained strain rates tests (<300%/hr) and 2% for higher strain rate tests where the response of the soil becomes undrained (≥300%/hr). This chapter compares the strain rate effects in three model fine grained soils, Kaolin, KSS and KSS-541. Soil properties which influence the magnitude of strain rate effects, for either partially drained or undrained strain rate

effects have been discussed. Particular attention has been focused on the undrained strain rate effect and how this varies with the classification of the soil (plasticity index) and the current state of the soil by conducting tests in both Kaolin and KSS-541 consolidated to a range of effective stress. A summary of findings is outlined below;

1. The partially drained rate effect on strength (compared at identical strain rate) increased in soils of higher coefficient of consolidation.

2. The partially drained strain rate effect was shown to be adequately accounted for by normalisation using a normalised velocity V (Finnie and Randolph, 1994), which makes the velocity of deformation non dimensional by taking into account the drainage path length and the coefficient of consolidation.

3. The normalised velocity, V corresponding to the transition from partially drained to undrained behaviour is from 12 to 26 at the strain rate corresponding to 300%/hr, or 3 to 4 when interpolated using Equation 5-3. These values are in reasonable agreement with those published in the literature.

4. There appears to be no affect of soil index properties on the point of transition from partially drained to undrained behaviour for the soils used in this study, which depends on the coefficient of consolidation of each soil.

5. The undrained strain rate effect on strength for different soils was analysed at equal levels of strain (2%) to avoid the effects of localisation on the strain rate effect.

6. The range of undrained strain rate effect in Kaolin was from 11-15% (per logarithmic increase in strain rate). KSS-541 displayed a range of undrained strain rate effect of 12-14%. KSS displayed an undrained strain rate effect of approximately 10%.

7. A direct comparison of undrained strain rate effects from data in the current study displayed no particular variation of undrained strain rate effects with plasticity index. In consideration of the comparison made from data of the current study with data collated from publications in the literature it was concluded that plasticity index is not a single governing factor of strain rate effects on undrained strength. However when considered in conjunction with the current state of soils, a relationship with plasticity index was determined. For example in normally consolidated soils, each consolidated to 300kPa, increasing strain rate effects were related to soil of higher plasticity which also corresponds to increased void ratio and moisture content. Therefore strain rate effects are influenced by the state of soils as well as the plasticity.

8. For a particular soil, increased strain rate effects were measured at higher moisture content. Therefore the moisture content is important to the strain rate effect of a particular soil. However the absolute magnitude of moisture content (considering multiple soils) was not related to the undrained strain rate effect.

9. The liquidity index of the soils, which scales the moisture content with the plasticity index, was strongly related to the undrained strain rate effect on strength for Kaolin and KSS-541. The increase in strain rate effect with increasing liquidity index from the current study was found to be very similar to those from the collated from the literature (Gibson and Coyle, 1968, Briaud and Garland, 1985, Soga and Mitchell, 1996).

10. The strain rate effect on maximum strength was found to be independent of OCR, for soils compared at OCR 1, 4 and 10. This is consistent with Sheahan *et al.* (1996) and Lehane *et al.* (2009). However at lower strains (<6%) comparing the strain rate effect at equal magnitude of strain showed the strain rate effect reduces with OCR, which is consistent with Sorensen *et al.* (2007).

11. The undrained strain rate effect on strength of Kaolin and KSS-541 was successfully normalised using both the moisture content and clay fraction of these soils. The undrained strain rate effect of KSS, which was lower then that of Kaolin and KSS-541, was thought to be affected by the significantly higher

coefficient of consolidation of KSS. Use of the normalised velocity, *V* which was used to account for the partially drained strain rate effect on strength was also found to offer some suitability for normalisation of the undrained strain rate effect for all soils (including KSS). The applicability of this parameter (*V*) for normalisation of the undrained strain rate effect (no volume change) is unclear. Combining the normalised velocity, *V* and the ratio of clay fraction to moisture content provided a further improvement in reducing the scatter of data (undrained strain rate effect).

6 Strain Rate Effects at Small Strains (<1%)

6.1 Introduction

The focus of this chapter, is concentrated on assessing the influence of strain rate on the behaviour of the soils at low strain levels (<1%). This chapter presents results from a total of 39 monotonic triaxial compression tests, on normally consolidated soils. The same tests as discussed in Chapter Five (at strain >1%) are presented. Table 6.1 lists the soil types and corresponding number of tests on each soil that were analysed and are discussed within this chapter.

Soil	**Effective Stress, p'_0 (kPa)**	**Plasticity Index, I_P (%)**	**Elastic Shear Modulus, G_0 (MPa)**	**Void Ratio, e**	**Liquidity Index, I_L**	**Number of tests**
Kaolin	300	45	90	1.13	0.31	4
Kaolin	720	45	170	1	0.22	7
Kaolin	1150	45	210	0.9	0.11	7
KSS	560	23	222	0.59	0.22	7
KSS-541	300	20.5	155	0.6	0.22	7
KSS-541	600	20.5	255	0.54	0.11	7

Table 6-1 List of soils and their key characteristics which are analysed in Chapter 6

The effect of soil type and current state on soil behaviour at small strains is well documented in literature, however the effect of strain rate and how it relates to different soils is not well understood.

This chapter will present and discuss observations of behaviour of soil at low strain levels and at increased strain rate. The results are then compared to standard static models of the stiffness degradation of fine grained soils. The principal aspects of small strain stiffness: (1) the initial elastic shear modulus; (2) the linear elastic threshold strain and; (3) the volumetric strain threshold strain are discussed in terms of their dependence on strain rate. The strain rate effect is then compared as a simple

strain rate coefficient which will be analysed to assess factors affecting the magnitude of the strain rate effect on stiffness degradation for different soils. A model commonly used to describe the non linear behaviour of soils is assessed (in terms of strain rate) and modified to account for factors influencing strain rate effects on stiffness degradation.

6.2 Shearing behaviour at small strains

This section presents some observations on the shearing behaviour at small strains, and how it varies with the type of soil, state and the strain rate are discussed. The results are compared to proposed relationships between stiffness degradation and index properties from the literature to gain perspective on the results of this study in comparison to previous research.

6.2.1 Effects of strain rate on stiffness and deformation

A typical example of the normalised secant shear modulus at different strain rates is shown in Figure 6-1 for Kaolin consolidated to an effective stress of 720kPa. Subsequent presentation of the stiffness degradation curves display data smoothed by adjacent averaging in OriginPro 7.5.

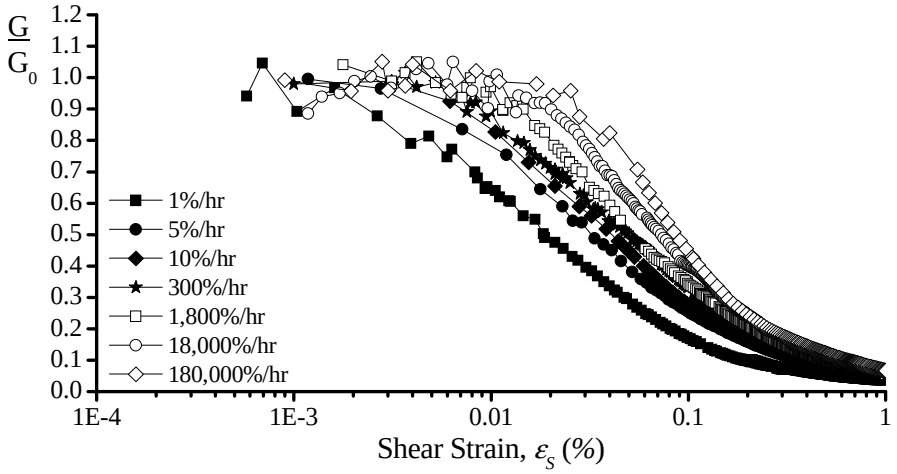

Figure 6-1 Normalised stiffness degradation curves of Kaolin-720kPa at various strain rates

Figure 6-1 highlights that at strains less than 1% an increase in strain rate results in an increase in deviatoric stress and subsequently stiffness. The secant shear modulus is derived from shear stress and strain measurements using Equation 6-1, and Equation 3-1 from Section 3.4.8.

$$G = \frac{\Delta q}{3\Delta \varepsilon_S} \qquad (6\text{-}1)$$

The normalising parameter; the elastic shear modulus (G_0) from Figure 6-1 accounts for the increase in consolidation pressure and the corresponding decrease in void ratio (Hardin and Drnevich, 1972, Tatsuoka *et al*., 1997). The value of initial or elastic shear modulus (G_0) is derived from the density of the sample as calculated from the total volume gauge of the back pressure controller during consolidation (Chapter Three, Section 3.3.9), and the shear wave velocity which is found using axial bender elements as discussed in Section 3.4.9.

With increasing strain rate an effect on the deformation of the soil under testing was established. Figure 6-2 compares the effect of strain rate on the development of radial and axial strain for KSS-541 600kPa. Increasing strain rate gives rise to comparatively higher radial strain, signifying the transition from predominantly drained to undrained behaviour with increased strain rate.

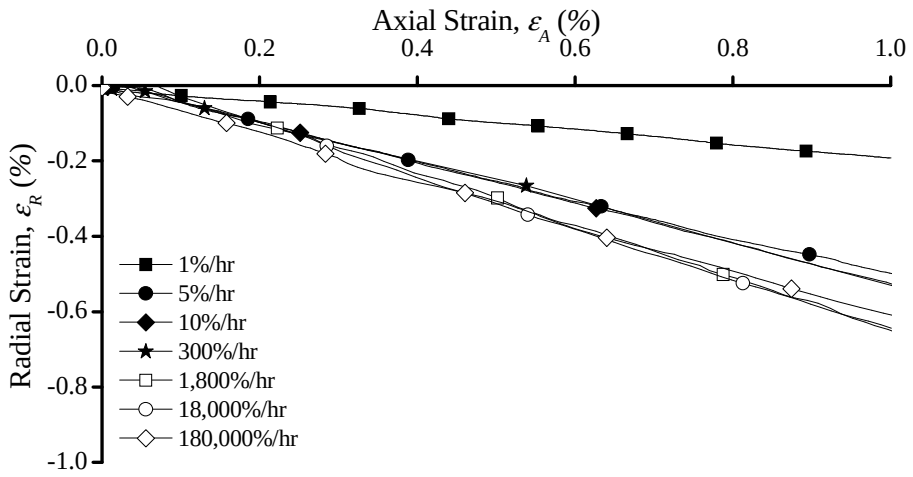

Figure 6-2 Development of axial and radial strains with strain rate for KSS-541-600kPa

The effect of strain rate on local strains is better visualised in Figure 6-3 which presents volumetric strain (ε_V) at different strain rate in KSS-541 600kPa. The volumetric strain is defined as per Equation 6-2;

$$\varepsilon_V = \varepsilon_A - 2\varepsilon_R \qquad (6\text{-}2)$$

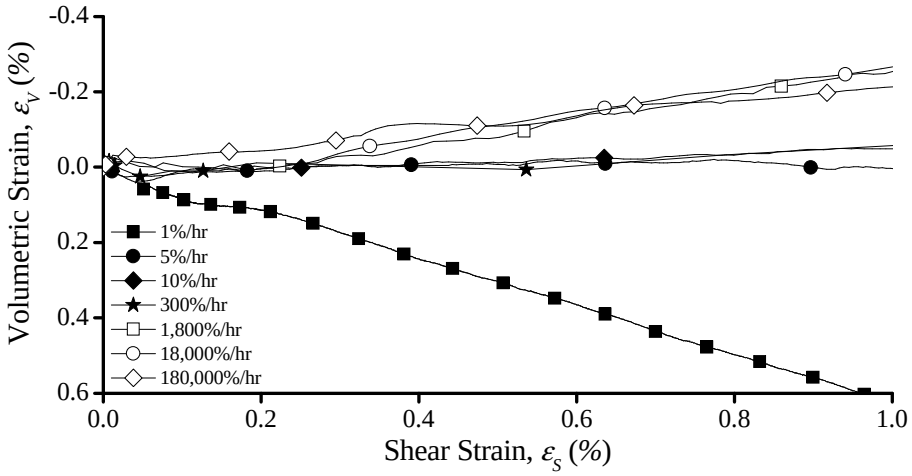

Figure 6-3 Local volumetric strains of KSS-541-600kpa at various strain rates

The 1%/hr test data displays positive volumetric strain with increasing shear strain which suggests that consolidation is taking place. Furthermore it was observed that with increased strain rate the magnitude of volumetric strain (compared at equal shear strain) reduces, representing a transition to undrained behaviour. The relatively minor volumetric strains measured during 5%/hr to 300%/hr tests indicates that at these strain rates the soils behave as though undrained (at small strains at least). Figure 6-3 shows that at strain rates in excess of 300%/hr volumetric strains become negative. Negative volumetric strains indicate expansion or dilation of the sample. This could also be interpreted as barrelling of the samples. Note; there were no volumetric strains recorded using the volume controllers during tests at strain rates at and in excess of 300%/hr.

Considering that the volumetric strains are representative of dilation, this has the potential of resulting in a reduction of excess pore pressure. The strain rate tests which display such volumetric strains are those which display increasing strength

with strain rate (Section 5.5.4). Previously published literature report the strain rate effect on strength is linked to increasing suppression of excess pore pressure (Sheahan *et al*. 1996, Lefebvre and LeBoeuf, 1987). Furthermore Richardson and Whitman (1963) proposed a schematic diagram detailing this exact effect at the micro-scale as discussed in Section 2.4.3. Thus the tests at higher strain rates illustrated in Figure 6-3 are seen to agree with such effects.

Excess pore pressures measured at the mid height of the sample are shown in Figure 6-4. Tests at strain rates greater than 1%/hr display a reduction of excess pore pressures (at these strains). At high strain rates (>300%/hr) the excess pore pressures tend to negative values. The results presented in Figure 6-3 and in Figure 6-4 tend to support the argument that strain rate effects on strength may be due to increased suppression of pore pressures, and the subsequent increase in effective stress.

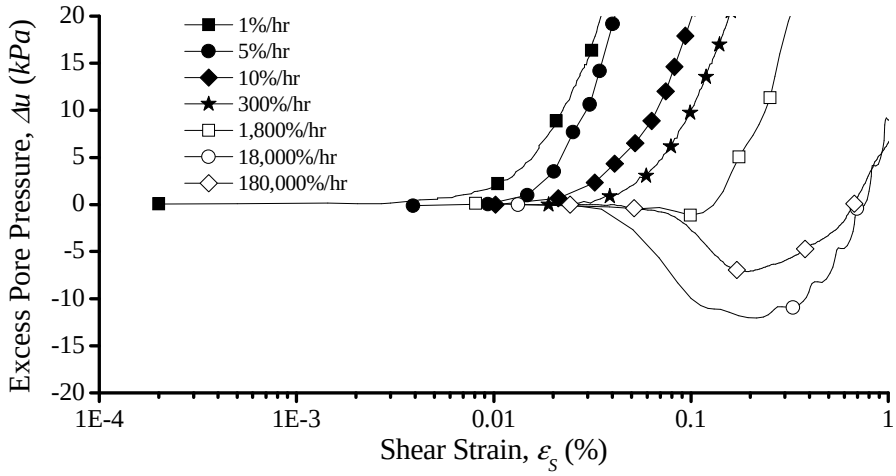

Figure 6-4 Excess pore pressures at various strain rates from mid height transducer measurements in KSS-541 600kPa, with focus on range of Δ*u*±20kPa

As negative volumetric strains could also reflect barrelling of the samples, which may occur during undrained tests (Sheng *et al*., 1997) this must also be considered. Although barrelling may be visualised easily by the magnitude of the volumetric strain, it is unclear how this would manifest in the corresponding excess pore pressure measurements. Assuming that barrelling is caused by the inability of soil to equalise excess pore pressures, which in turn induce localisation of strains, it may be possible

that the lateral deflection of the soil may cause a reduction of excess pore pressure in the region adjacent to the mid height transducer. To investigate if this is reasonable, volumetric strains are compared to properties of the soil which are linked to localisation in fine grained soils: permeability (k) and the coefficient of consolidation (c_v).

To compare the effect of strain rate on volumetric strain and how this varies with the soil properties, an apparent Poisson's ratio can be used as it conveniently represents a deformation characteristic of each test sample as a single non-dimensional parameter. It is termed the apparent Poisson's ratio (rather then simply Poisson's ratio) because of the possible influence of non uniformities on the local measurements. From the axial and radial strains the apparent Poisson's ratio is calculated as per Equation 6-3;

$$\nu = -\varepsilon_r / \varepsilon_A \qquad (6\text{-}3)$$

The apparent Poisson's ratio is compared with permeability in Figure 6-5. The same observations are observed when comparing the apparent Poisson's ratio to c_v, however the illustration with permeability is more defined.

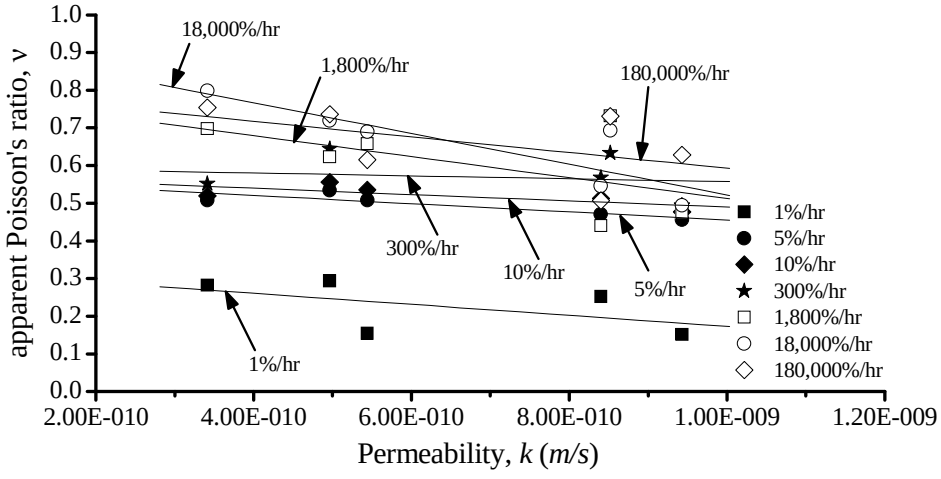

Figure 6-5 Variation of apparent Poisson's ratio with strain rate in soils of various permeability

Permeability and c_v are associated with non-uniform distribution of excess pore pressure and subsequent localisation, and consolidation. It is thought that by

comparing how strain rate and these parameters affect the apparent Poisson's ratio, insight into the possible cause of negative volumetric strain at high strain rate may be determined.

Trend lines have been constructed using linear regression of the apparent Poisson's ratio and permeability at each strain rate. Although scatter in the data presented in Figure 6-5, (particularly at higher permeability), these trend lines indicate that decreased permeability corresponds to an increase of the apparent Poisson's ratio at each strain rate. This appears to reflect the capability of soils of greater permeability to undergo drainage in at least the areas approximate to the local transducers. As the apparent Poisson ratio appears to relate to permeability in this way it suggests that localisation (Section 4.4.2) may be related to the magnitude of volumetric strains as described earlier. However it is noted that the Kaolin 300kPa test, although having a relatively high permeability, displays similarly high Poisson's ratio.

Due to the scatter in results Figure 6-5 is not conclusive. There is scatter in the data at the highest strain rate for Kaolin soils which have the lowest permeability. Therefore it is inconclusive as to whether localisation or dilation is responsible for the magnitude of negative volumetric strains observed for high strain rate testing.

Figure 6-5 also highlights how significant the differences are between the apparent Poisson's ratio measured at strain rates from 1%/hr to 5%/hr. In comparison with Wroth (1975) who predicted a drained Poisson's ratio increasing from 0.3 to 0.35 with plasticity index for these soils; the apparent Poisson's ratio measured with 1%/hr tests are lower. However Wroth (1975) is based on findings from lightly over consolidated soils.

The 5%/hr tests display an apparent Poisson's ratio nearing 0.50. Normally consolidated soils sheared in undrained conditions typically show a Poisson's ratio close to 0.50. In many instances where the Poisson's ratio cannot be measured it is taken as 0.49 or 0.50 to conform to the assumption that as a cylindrical sample in an undrained triaxial test deforms it will do so uniformly. Therefore although drainage is permitted during testing the samples appear to behave in an undrained manner according to local strain measurements. As discussed in Section 4.2.3, the 5%/hr tests

display significant volume change at larger strain. Thus the observation they display an apparent Poisson's ratio of 0.50 is only applicable at small strain. As shown in Section 6.2 the 5%/hr test also displays a greater stiffness (than the 1%/hr) at small strains. Therefore it is thought that "viscous" affects are influential, even at strain rates which are considered in terms of large strains to be partially drained. This would confirm observations from Lehane *et al*. (2009).

6.2.2 Comparison with stiffness degradation design charts

To place the results of normalised shear modulus degradation in context with existing research published in the literature, and also to show the effect that strain rate can have on shear modulus degradation, a selection of test data are compared with proposed stiffness degradation curves and models of stiffness degradation from the literature. Figure 6-6 presents a direct comparison between the 1%/hr, 300%/hr, and 180,000%/hr results of Kaolin consolidated to 720kPa and 1150kPa. These are compared to the proposed design charts developed by Vucetic and Dobry (1991) and Vardanega and Bolton (2011). The data from this study presented in Figure 6-6 has been smoothed using adjacent averaging in OriginPro 7.5. A maximum of 5 points were used in the adjacent averaging process, with care taken to ensure the crucial aspects of the stiffness degradation curve (ε_{EL}, ε_{SVT}) as well as the curve itself are maintained.

The proposed design charts from Vucetic and Dobry (1991) are widely referred to in literature on the degradation of normalised shear modulus. The stiffness degradation curves from these design charts vary with plasticity index. Figure 6-6 displays the design curves at plasticity indices of 0, 30, 50, 100 and 200%.

The proposed design charts from Vucetic and Dobry (1991) as well as Vardanega and Bolton (2011) are presented as strain rate independent and the curves shown in Figures 6-6 (a) - (c) are identical. Figure 6-6 illustrates that for the majority of strain levels the stiffness of 1%/hr tests are below those from predictions of both Vucetic and Dobry (1991) and Vardanega and Bolton (2011). At lower strains, approximate to the linear elastic threshold; Figure 6-6 indicates that results from this study display slightly higher stiffness values. However the measured stiffness tends to below

predictions from Vucetic and Dobry (1991) and Vardanega and Bolton (2011) with increased strain.

Due to the differences between the design curves from Vucetic and Dobry (1991) and Vardanega and Bolton (2011) with data from this study, the same 1%/hr, 300%/hr and 180,000%/hr results have been compared in Figure 6-6 to a model developed by Darendeli (2001) which predicts the normalised shear modulus based on plasticity index and effective stress (Equation 6- 4) and again is strain rate independent.

$$\frac{G}{G_0} = \frac{1}{1+\left(\frac{\varepsilon_S}{\varepsilon_{S-ref}}\right)^{\alpha}} \quad (6\text{-}4)$$

Where the reference shear strain $\varepsilon_{S\text{-}ref}$ (%) is derived using Equation 6-5 below;

$$\varepsilon_{S-ref} = \left(\phi_1 + \phi_2 I_P \left(OCR^{\phi 3}\right)\right)\left(p'^{\phi 4}_0\right) \quad (6\text{-}5)$$

Where $\emptyset_1$ = 0.01, $\emptyset_2$ = 0.0352, $\emptyset_3$ = 0.3246, $\emptyset_4$ = 0.3483 as determined from linear regression of over 100 tests in a variety of soils (Darendeli, 2001) and α = 0.919 is the average curve coefficient, determined from tests on a variety of natural soils.

Comparisons with Darendeli (2001) indicate better agreement with the data set of the current study. However differences were again observed at the linear elastic threshold and the magnitude of shear modulus at higher strain. Factors which may be contributing to these differences in the shear modulus degradation curves from those of the literature are discussed in the following.

The design curves from Vucetic and Dobry (1991) and Vardanega and Bolton (2011) are based on a literature review of other laboratory studies, involving monotonic and cyclic triaxial, torsional shear and resonant column testing. Notable differences between the modulus reduction curves from Vucetic and Dobry (1991) and Vardanega and Bolton (2011) have been attributed to rate effects (Vardanega and

Bolton, 2011) because much of the data used by Vucetic and Dobry (1991) involved resonant column testing.

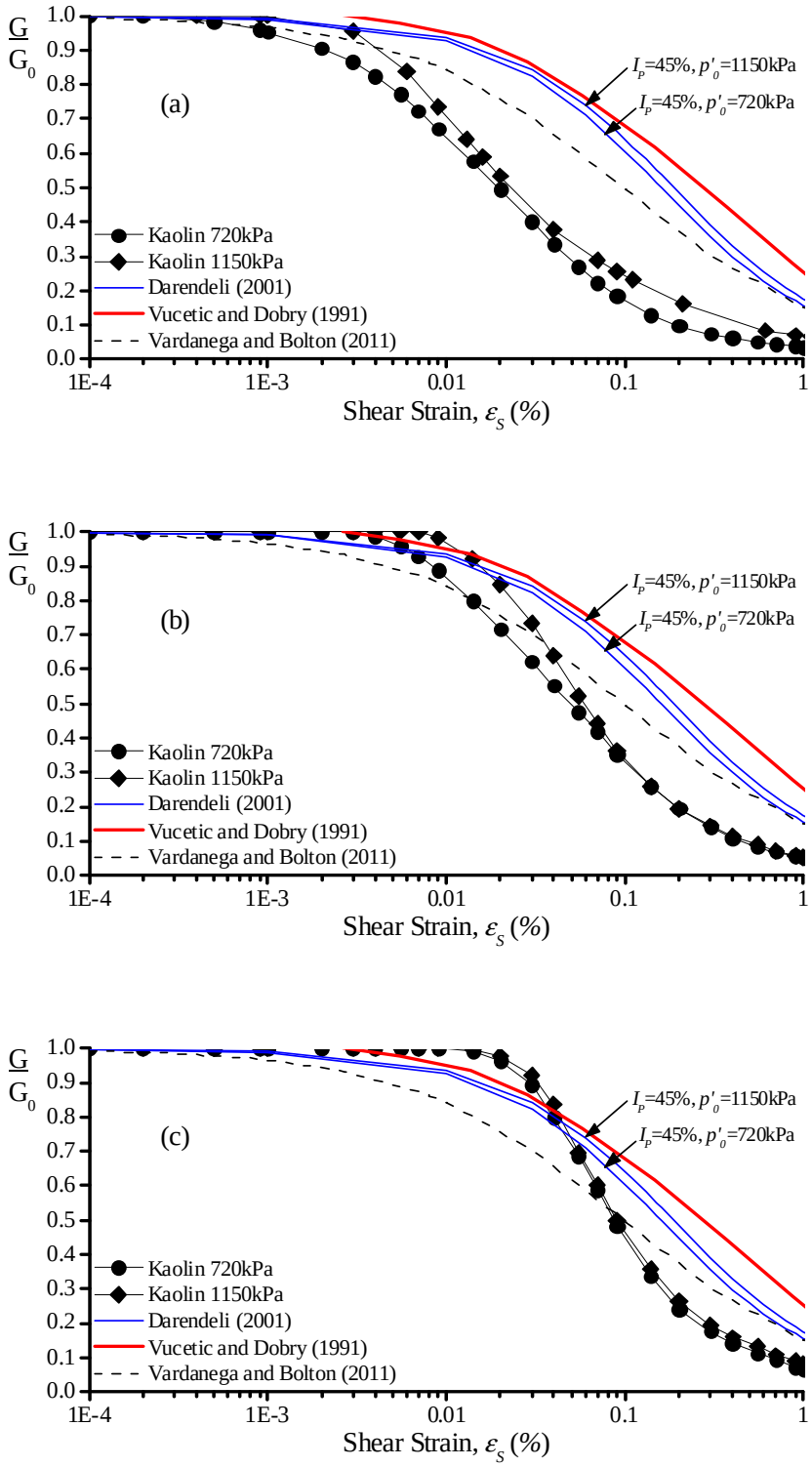

Figure 6-6 Comparison of G/G_0 for (a) 1%/hr, (b) 300%/hr, (c) 180,000%/hr results of Kaolin 720kPa and Kaolin 1150kPa with the proposed design curves from Vucetic and Dobry (1991), Darendeli (2001) and Vardanega and Bolton (2011)

Vardanega and Bolton (2011) corrected resonant column results used in their database by assuming a strain rate effect of 5% per logarithmic cycle difference in strain rate on the basis of findings from Lo Presti *et al*. (1997) and d'Onofrio *et al*. (1999) to bring their database to a reference strain rate of 0.36%/hr. Note the findings from Lo Presti *et al*. (1997) show the coefficient of strain rate increasing with strain, from which Vardanega and Bolton (2011) selected as 5% from the lower range of strains because this point was more relevant to the focus of their research.

Darendeli (2001) constructed a database from experiments on natural soils from various locations using resonant column and torsional shear tests. Darendeli (2001) attributes differences between their design curves to those from Vucetic and Dobry (1991) to accuracy problems in measurements with older equipment, and did not give significant attention to the rate dependent behaviour of the shear modulus degradation curve. Equation 6-5 from Darendeli (2001) is defined at a loading frequency of 1Hz, and subsequently the strain rate would increase with strain, meaning a logarithmic increase in strain at the same frequency would also correspond to logarithmic increase in strain rate. Thus strain rate effects would be involved to an increasing degree, and could be a greater cause of discrepancy between Darendeli (2001) and Vucetic and Dobry (1991).

Therefore significant differences between the findings from previous research may exist due to strain rate effects and due to the type of test used to determine the normalised shear modulus. Although Vardanega and Bolton (2011) applied a rate correction to their results, based on the level of disagreement with 1%/hr tests (Figure 6-6) the correction factor used could have been insufficient. It may also be the case that strain rate corrections should be applied differently depending on strain, which would be consistent with Lo Presti *et al*. (1997) as mentioned above, and the effect of testing at constant frequency if the soil is rate dependent.

Although the normalised shear modulus degradation curves from this study are different in shape from those compared in Figure 6-6 and 6-7, the effects different properties of the soils have on the magnitude of the shear modulus degradation curves relate to each other in the same way. A summary of some effects on both the initial shear modulus and normalised shear modulus degradation curve are presented in

Table 6-2 which has been compiled from Hardin & Drnevich (1976), Vucetic and Dobry (1991), and Darendeli (2001).

Increasing Parameter	**Initial Shear Modulus (G_0)**	**Normalised Initial Shear Modulus (G/G_0)**
Strain Amplitude	***	***
Plasticity Index	***	***
Strain Rate	***	***†
Frequency of loading	*‡	*‡
Effective Stress	***	***
Void Ratio	***	***
Degree of Saturation	-	***I
OCR	**	*
Structure	***	*
Coarse Grain Characteristics	***	*
Number of Cycles	-	***

*** Very important

** Important

* Relatively unimportant

† If G and G_0 are measured at different rate

‡ At frequency; >0.1Hz (Hardin & Drnevich, 1976)
>1Hz (Darendeli, 2001)

I *** (Hardin & Drnevich, 1972)
* (Darendeli, 2001)

- Unclear or not applicable

Table 6-2 The relevant importance of parameters which affect the normalised shear modulus degradation curve (Hardin and Drnevich, 1972, Vucetic and Dobry, 1991, Darendeli, 2001)

As was shown in the previous comparisons to Vucetic and Dobry (1991), Vardanega and Bolton (2011), and Darendeli (2001), Kaolin 1150kPa displayed a higher normalised shear modulus degradation curve than Kaolin 720kPa. Thus for a soil of particular plasticity index, the results of this study show that higher initial effective stress results in increasingly linear behaviour. This is consistent with Table 6-2 and Darendeli (2001)

To compare the effect of plasticity index on the normalised shear modulus degradation curve a comparison is made in Figure 6-7 between KSS, KSS 541 and Kaolin, each at liquidity index of 0.22. Figure 6-7 (a), (b) and (c) present results at strain rates of 1%/hr, 300%/hr and 180,000%/hr respectively. The trends in Figure 6-7 reflect higher normalised shear modulus with plasticity index. KSS-541 displays the lowest normalised shear modulus. In Figure 6-7 (a), with increasing strain rate the difference from KSS-541 to KSS varies from 20-50%, depending on strain, and to Kaolin is 20-35%. At 300%/hr the difference between KSS and KSS-541 is similar to that at 1%/hr, whilst Kaolin displays a much greater increase, up to 70% at higher strains. At 180,000%/hr the difference between KSS from KSS-541 is approximately 30%, whilst Kaolin again displays an increase up to approximately 70%. Thus there are reasonably similar differences between the soils at each strain rate. Therefore it is assumed this reflects a consistent influence of soil type (plasticity index) and state (effective stress) on the normalised shear modulus degradation curve. These are consistent with trends noted in Table 6-2 from previous research.

Differences in the magnitude of normalised shear modulus from results of this study and previous research were highlighted in Figure 6-6. The same trends regarding the normalised shear modulus, and how it varies with soil type are noted. Therefore relating strain rate effects on stiffness to soil index based on the data from tests conducted as part of this research should be relevant to other strain rate depending testing in fine grained soils.

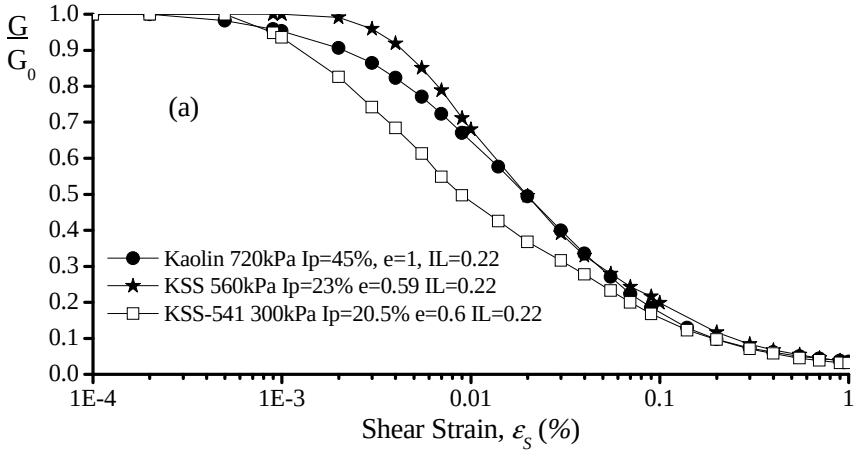

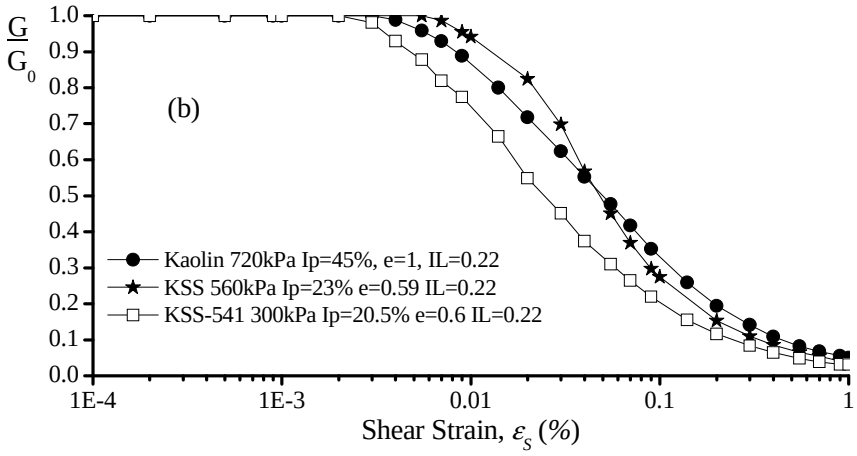

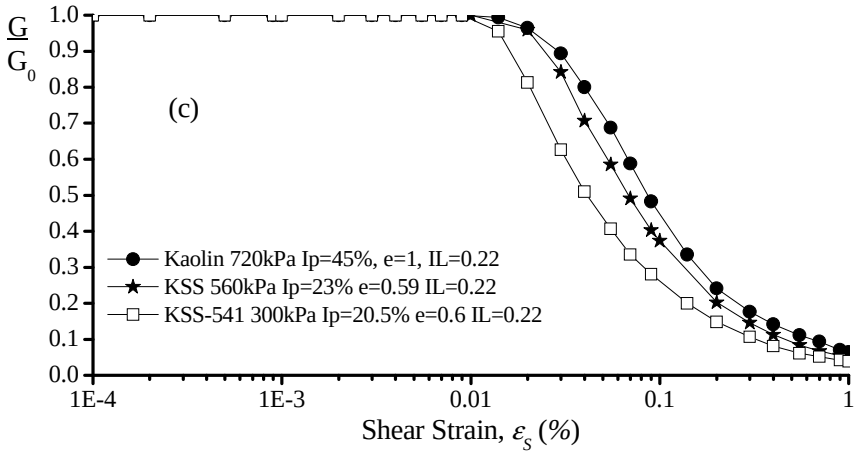

Figure 6-7 Normalised shear modulus degradation curves at (a) 1%/hr, (b) 300%/hr, (c) 180,000%/hr

6.3 Effect of strain rate on the initial elastic shear modulus

It was found that increased strain rate did not affect the value of initial elastic shear modulus G_{max} (very small strain shear modulus), measured using the local Hall Effect transducers, which relates closely to the value of initial elastic shear modulus derived from the axial bender elements, G_0, i.e. $G/G_0 = 1$. Evidence of this is presented in Figure 6-1, as well as other normalised shear modulus degradation curves throughout this chapter.

Other studies have shown that the initial elastic shear modulus (G_{max}) may increase with strain rate, often of the order of approximately 5-6% per logarithmic increase in strain rate (Leroueil *et al*., 1986, Vucetic *et al*., 2003). However Tatsuoka and Shibuya (1992) postulated that once a particular strain rate was exceeded there would be no further increase in initial shear modulus. The Simple Asymptotic Body (SAB) model from Di Benedetto and Tatsuoka (1997) predicts an increase in shear modulus with strain rate over a limited range of strain rate, and once this range of strain rates is exceeded the shear modulus would reduce in rate dependency to become rate independent (Figure 2-27). The SAB model was experimentally verified with the behaviour of Vallericca clay by d'Onofrio *et al*. (1999). Mukabi (1995) found that monotonic triaxial compression tests on Osaka Bay clay, in both drained and undrained conditions at strain rates from approximately 0.1%hr to 200%/hr, the initial elastic shear modulus was independent of rate. Thus finding the initial elastic shear modulus is strain rate independent is expected at high strain rates. This is consistent with Shibuya *et al*. (1996) and Santagata *et al*. (2007) whom conducted tests at maximum strain rates of 84%/hr and 4%/hr respectively, significantly less then many of those used in this study. Sorensen *et al*. (2010) found that the initial shear modulus is rate independent where creep induced change in void ratio is not significant. Thus the slowest strain rate tests of 1%/hr are sufficiently fast to avoid any visible effects of creep on the initial elastic shear modulus (G_{max}).

6.4 Effect of strain rate on the linear elastic threshold strain

The strain at which the linear elastic shear modulus degradation curve begins to degrade is known as the linear elastic threshold strain (Vucetic, 1994). It corresponds

to what is commonly known as the Y_1 surface in the framework of non linear soil behaviour proposed by Jardine (1992). The selection of the linear elastic threshold strain (ε_{EL}) is shown in Figure 6-8, where it is taken at a normalised shear modulus (G/G_0) of 0.99 as per Vucetic (1994). Figure 6-8 shows that with increasing strain rate the strain at which the normalised shear modulus begins to degrade will increase. In dynamic situations such as during an earthquake a higher linear elastic threshold would result in greater amplification of ground movements because the soil is not dissipating energy (Dobry and Vucetic, 1987). Each test on normally consolidated soil is included here to compare how soil index properties and current state effect the strain rate dependence of the linear elastic threshold strain.

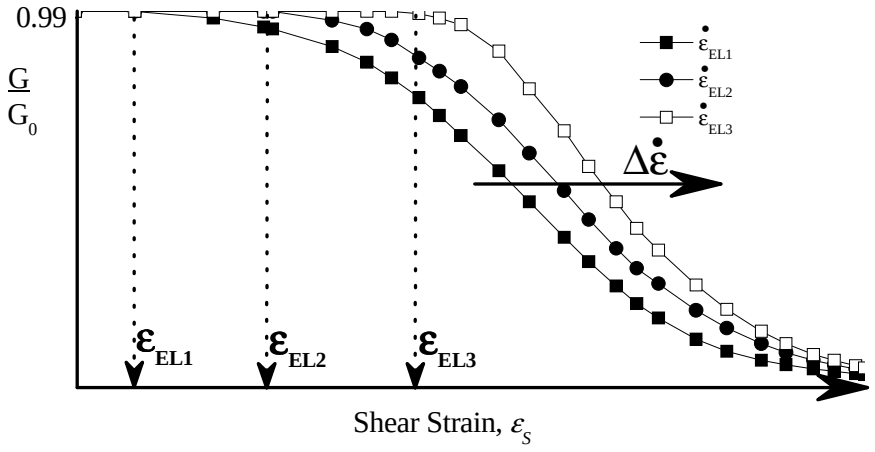

Figure 6-8 Depicting the selection of the linear elastic threshold strain (ε_{EL})

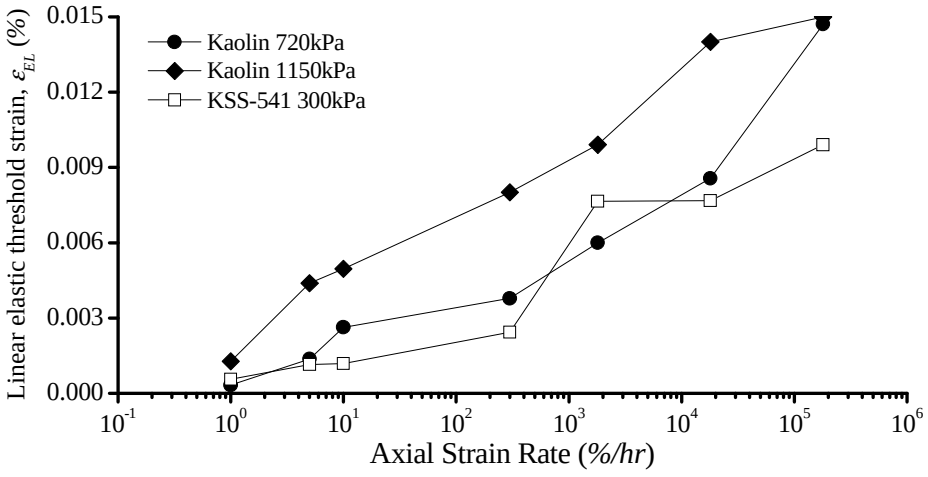

Figure 6-9 Linear elastic threshold strains at increasing axial strain rate

Figure 6-9 shows the effect of strain rate on the elastic threshold strain for Kaolin 720kPa and 1150kPa and KSS-541 300kPa. With increasing strain rate the linear elastic threshold strain increases for each soil. As shown in Figure 6-9, the increase in the linear elastic threshold strain is in the region of one order of magnitude at strain rates increasing between 1%/hr to 180,000%/hr.

The linear elastic threshold strains (for each soil) are compared to a proposed design chart from Vucetic (1994) in Figure 6-10. This is done to highlight the effect of strain rate against a linear elastic threshold that may be used for design in industry. The proposed design chart predicts a greater magnitude linear elastic threshold strain with plasticity index. Because of the limited scope of Figure 6-10 the variation of the linear elastic threshold is compared as a single line, defining the minimum and maximum linear elastic threshold strain for each soil at their particular plasticity indices. As shown previously in Figure 6-9, for each soil, the minimum linear elastic threshold strain is measured during 1%/hr tests, whilst the maximum is measured during 180,000%/hr tests.

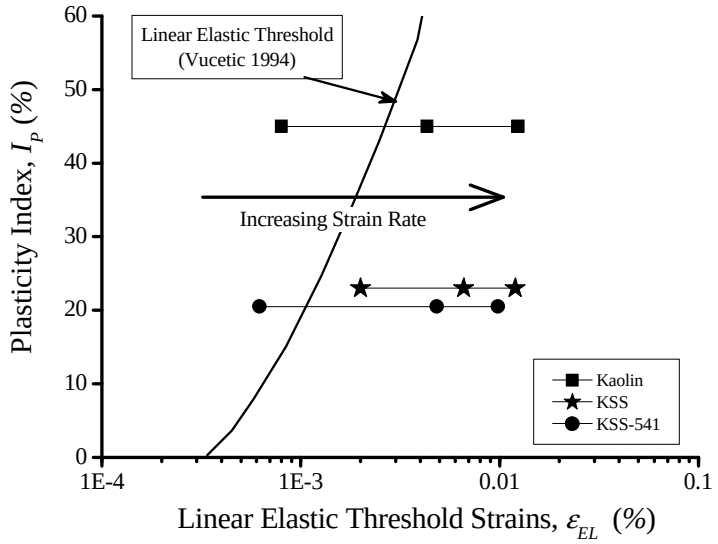

Figure 6-10 Comparison of linear elastic threshold strains measured at strain rates of 1%/hr , 300%/hr and 180,000%/hr with a proposed linear elastic strain threshold envelope based upon plasticity index by Vucetic (1994)

Figure 6-10 does not provide for demarcation of soils at different state (consolidated to different effective stresses). The points shown for Kaolin and KSS-541 are averaged from tests conducted at each initial effective stress, i.e. the maximum linear elastic threshold shown for Kaolin in Figure 6-10 is an average from the 180,000%/hr tests in Kaolin at 300, 720 and 1150kPa. The average 300%/hr linear elastic thresholds for each soil (of particular plasticity index) are also compared in Figure 6-10 for reference. The data points representing the average linear elastic threshold strain for 300%/hr tests lay between the minimum and maximum linear elastic threshold strains for each of the soils used in the current study. Unfortunately Vucetic (1994) did not provide the form of the relationship between the linear elastic threshold and plasticity index.

The effect of strain rate on the strain magnitude of the linear elastic threshold is highlighted when compared to the findings of Vucetic (1994). The design chart from Vucetic (1994) is an average based on a variety of laboratory tests, including cyclic triaxial and resonant column tests, possibly also conducted over a range of strain rates. The relationship between linear elastic threshold and plasticity index from Vucetic (1994) corresponds to the linear elastic threshold strains seen at the lower end of strain rates with the Kaolin and KSS-541 tests, yet is slightly lower than the minimum threshold strain seen at 1%/hr for KSS 560kPa. The linear elastic threshold was found to increase not only with plasticity but also with effective stress for a soil at a particular plasticity index. The relatively larger effective stress of KSS 560kPa, as well as the fact the other soils have been averaged at a range of effective stresses is the reason the linear elastic threshold strains for this soil are larger than those from Vucetic (1994). Therefore consideration of both strain rate and effective stress (in terms of liquidity index) is recommended before using information taken from Figure 6-10 on the linear elastic threshold strain.

To compare how the effect of strain rate on the linear elastic threshold strain varies with soil type and state, a model previously used to relate the linear elastic threshold strain to strain rate has been adopted. According to Shibuya *et al*. (1996) whom conducted tests at strain rates between 0.7 to 84%/hr and Santagata *et al*. (2007) whom conducted tests at strain rates from 0.05 to 4%/hr, the increase in elastic threshold increased with the square root of strain rate (Equation 6-6).

$$\varepsilon_{EL} = \varepsilon_{ELREF} \dot{\varepsilon}^{P} \quad (6\text{-}6)$$

The reference value of the linear elastic threshold strain (ε_{ELREF}) corresponds to the linear elastic threshold strain (ε_{EL}) at a reference strain rate. A reference strain rate of 60%/hr was used by Shibuya *et al*. (1996), whilst Santagata *et al*. (2007) used a 0.1%/hr strain rate test. The exponent *P*, which describes how the linear elastic threshold relates to strain rate was taken as 0.5 by both Shibuya *et al*. (1996) and Santagata *et al*. (2007). The form of Equation 6-6, using an exponent (*P*) of 0.5 as per both Shibuya *et al*. (1996) and Santagata *et al*. (2007), and the reference strain (ε_{ELREF}) for Kaolin consolidated to 720kPa is shown in Figure 6-11 for the strain rates used in the current study, with the reference linear elastic threshold strain taken as 1%/hr.

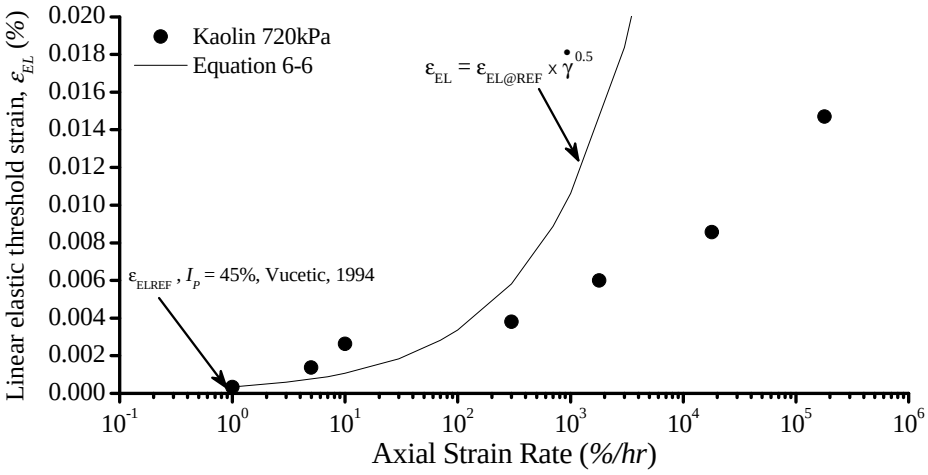

Figure 6-11 Comparison of the linear elastic threshold strain at increasing strain rate to previously assumed relationship (Equation 6-6) from Shibuya *et al.* (1996)

From Figure 6-11 above, taking the exponent *P* as 0.5 and values of reference elastic threshold strain from Vucetic (1994), imply a significantly higher threshold at high strain rates. The predicted threshold using Equation 6-6 for 180,000%/hr in Kaolin is 0.14%, which is inaccurate to results shown in Figure 6-11 by one order of magnitude. Also it is in excess of that from Figure 6-10 by two orders of magnitude. Thus the assumption that the relationship between strain rate and linear elastic threshold strain is related to the square root of the strain rate is unsuitable over a

larger range of strain rates and soils than from Shibuya *et al*. (1994) and Santagata *et al*. (2007).

The increase of the linear elastic threshold with strain rate was fitted using Equation 6-6 to find a suitable value of exponent *P* for each soil. Over the entire range of strain rates in this study (1%/hr to 180,000%/hr) the exponent *P* varies (depending on soil) between 0.12-0.26. Figure 6-12 presents Equation 6-6 compared to Kaolin consolidated to 720kPa, using the reference strain at taken at 1%/hr. The fitting of Equation 6-6 to Kaolin 720kPa shown in Figure 6-12 are from strain rates of, 1-10%/hr, 1-300%/hr, 300-180,000%/hr and 1-180,000%/hr.

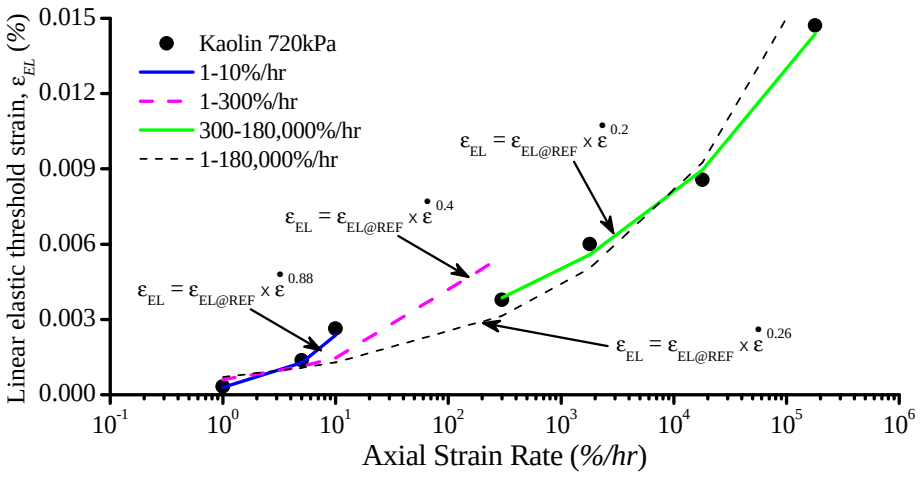

Figure 6-12 Fit of Equation 6-7 to Kaolin 720kPa, at various ranges of strain rate

At lower strain rates (1%/hr to 10%/hr) the increase varies with soil between values of exponent *P* (Equation 6-6) from 0.3 to 0.9. Therefore the values of exponent *P* of 0.5 as quoted by Shibuya *et al*. (1996) and Santagata *et al*. (2007) seem to be more relevant at lower strain rates. This also suggests that with increasing strain rate the increase of elastic threshold cannot be maintained to the same extent as seen at lower strain rates, and will possibly reach a limit to its dependence on strain rate, at strain rates in excess of those used in the current study.

It would be useful to predict the value of exponent *P* (Equation 6-6) that would be beneficial for a wide range of applications in geotechnical engineering. Because of the

large difference in the magnitude of exponent *P* (Equation 6-6) depending on the range of strain rates in question; it was considered over two different ranges of strain rates separately (1-10%/hr, and 10-180,000%/hr).

To make the predictions comparable to Shibuya *et al*. (1996) and Santagata *et al*. (2007) the values of *P* were compared at 1-10%/hr. Inclusion of 300%/hr data for consideration reduced the magnitude of the exponent *P* to the extent it was incompatible to Shibuya *et al*. (1996) and Santagata *et al*. (2007). Although the linear elastic threshold strain was found to increase with effective stress and plasticity index defining a relationship with a soil property such as liquidity index is not available due to the limited number of soils at these particular strain rates. The best relationship was found with plasticity index (Figure 6-13) however significant scatter is noted. The relationship with plasticity index in Equation 6-7 is consistent with Shibuya *et al*. (1996) and Santagata *et al*. (2007). The scatter between soil of particular plasticity index are also at odds with each other, whilst Kaolin displays decreasing strain rate effect with increasing effective stress, KSS-541 displays increasing strain rate effect with effective stress. This suggests some inherent variability between the results, and therefore plasticity index is best suited for approximation.

$$P = 0.1I_P(\%) + 0.31 \qquad (6\text{-}7)$$

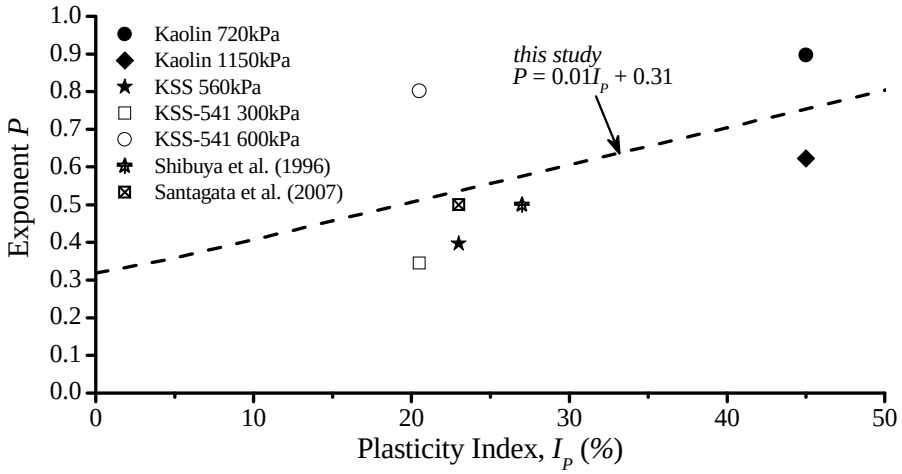

Figure 6-13 Relationship between strain rate exponent *P*, developed at strain rates from 1-10%/hr, and plasticity index

The remaining strain rates (300-180,000%/hr) were then considered separately. However there is little difference in the magnitude of the strain rate effect exponent when considering the range between 300%/hr to 180,000%/hr or for considering 10%/hr to 180,000%/hr (3% difference). The strain rate effect on the linear elastic threshold, (exponent *P*) from strain rates between 10%/hr to 180,000%/hr relates well to liquidity index (Figure 6-14). The suitability of liquidity index for describing the strain rate effect on the elastic threshold is interesting, and may suggest a link with undrained strain rate effects at large strains as described previously in Section 5.4.5.

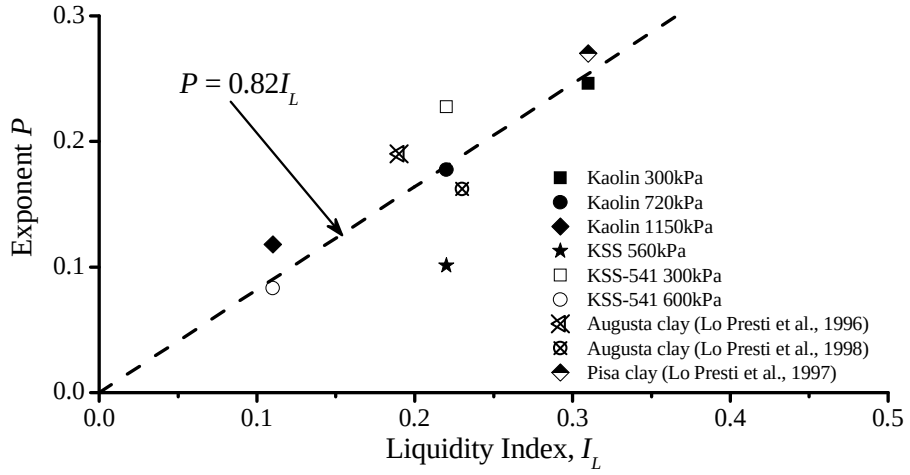

Figure 6-14 Relationship between strain rate exponent *P*, developed at strain rates from 10-180,000%/hr and liquidity index

Equation 6-8 presents the relationship between liquidity index and the strain rate effect on the linear elastic threshold at strain rates from 10%/hr to 180,000%/hr.

$$P = 0.82 I_L \qquad (6\text{-}8)$$

The proposed relationship in Equation 6-8 is also compared to data from other studies in Figure 6-14. Table 6-3 presents a summary of other studies included for comparison to Equation 6-8 in Figure 6-14.

Soil	Liquidity index, I_L	Type of test	Strain Rates (%/hr)	Reference
Augusta clay	0.19	RCT, CLTST	3-48,000	Lo Presti *et al*. (1996)
Augusta clay	0.23	MLTST-CLTST	6-135,000	Lo Presti *et al*. (1998)
Pisa clay	0.31	RCT, CLTST	2-1,500	Lo Presti *et al*. (1997)

Table 6-3 Summary of studies used to compare with predictions of strain rate effect on linear elastic threshold strain

There is limited data available in literature which describes the strain rate effect on the linear elastic threshold, particularly at high strain rates. However as shown in Table 6-3, data on two separate studies on different samples of Augusta clay (I_P = 29% (Lo Presti *et al*., 1996), and I_P = 38% (Lo Presti *et al*., 1998)) have included testing at maximum strain rates of similar magnitude to the current study. As shown in Figure 6-14, the relationship between the strain rate effect and liquidity index (Equation 6-8) describes the data from other studies well, confirming the validity of Equation 6-8. The range of liquidity indices used to determine Equation 6-8 is from 0.1 to 0.31. Therefore it is unclear if Equation 6-8 is applicable to soils at liquidity indices outside this range.

6.5 Effect of strain rate on the volumetric threshold strain

Vucetic (1994) termed the volumetric threshold strain as that which corresponds to the beginning of plastic and thus non recoverable deformation. It is also commonly known as the Y_2 surface in the framework describing the non linear behaviour of soils from Jardine (1992). The volumetric threshold strain is the point at which excess pore pressures begin to develop in undrained tests, and volumetric strains begin to develop in drained tests. In cyclic testing this is the strain at which the number of cycles begins to affect the stiffness of soils. Thus it is an important parameter in the degradation of stiffness with increased strain.

This section compares the effects of strain rate on the volumetric threshold strain to provide information on the proportion of elastic and plastic behaviour of soils, and how this may be affected by strain rate. Figure 6-15 presents a diagram of a stiffness degradation curve, and the corresponding volumetric threshold (ε_{SVT}) strain and how it

relates to the normalised shear modulus. The volumetric threshold strain was also discussed in Section 2.6.4.

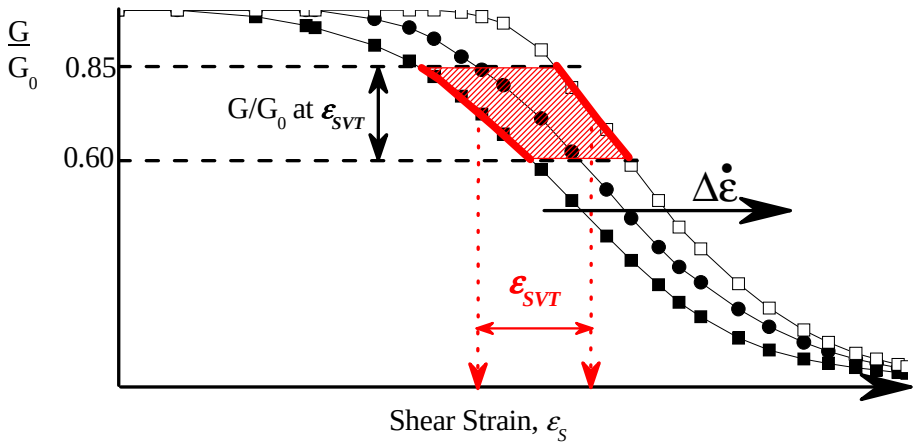

Figure 6-15 The typically assumed range of normalised shear modulus values corresponding to the volumetric threshold strain, overlain on strain rate dependent shear modulus degradation curves

There is little information on the relationship between the volumetric threshold strain and soil index properties. As highlighted in Figure 6-15 typically the volumetric threshold strain occurs at a normalised shear modulus (G/G_0) ranging from 0.6 to 0.85 (Vucetic, 1994, Ishihara, 1996). The range of strains which the volumetric threshold strain exists is typically between 0.01% - 0.1% (Vucetic, 1994). The normalised shear modulus at the volumetric threshold strain is often assumed at G/G_0 = 0.7 due to difficulties in obtaining information of this threshold strain, and the current lack of prediction methods (Santos and Correia, 2003).

Although previous studies on the strain rate effect on stiffness have measured excess pore pressures, and thus the volumetric threshold strain, these findings from previous studies have not been extended to develop a relationship between the volumetric threshold strain and strain rate. The capability to predict where this point would occur with increased strain rate would be beneficial to industry, and allow for more accurate predictions of a soil's response to strain rate and strain. For example the normalised shear modulus degradation curve has been shown in Section 6.2 to increase with strain rate (at a particular strain). If the volumetric threshold strain does not change with increased strain rate, the higher strain rate test would display less degradation of

stiffness before plastic deformations occur. Equally, it could also be that at higher strain rate the volumetric threshold strain increases at a higher proportion then the associated stiffness degradation curve. Therefore the higher strain rate test could thus display a greater amount of recoverable deformation. Thus determination of how the volumetric strain threshold relates to strain rate for different soils may provide some understanding on soil properties involved in the strain rate effect on stiffness and strength.

6.5.1 Use of excess pore pressure measurements to describe the volumetric threshold strain

The volumetric threshold strain is derived here as the strain at which excess pore pressures are first measured. Thus the measurement of the volumetric threshold strain is dependent on quality of excess pore pressure measurements. As highlighted in Section 4.4, the measurement of excess pore pressure is an obvious issue in high strain rate tests in soils with low coefficient of consolidation. Two issues in particular are a concern in high strain rate testing of soils, and are exacerbated at small strains; (1) the response time of the transducer and (2) the capture of accurate data. Both of these potential issues are discussed below.

For the excess pore pressure transducer used in this study (Section 3.4.6) the response time is 10-24ms for a 100kPa change in excess pore pressures (Balderas-Meca, 2004). The fastest strain rate tests would reach 1% strain by approximately 20ms, and thus at strains corresponding to the volumetric threshold strain as per Vucetic (1994) (≈ 0.01-0.1%) are close to the limit of the response time of these transducers. Thus the magnitude of excess pore pressures may be questionable, however because the volumetric threshold is taken as the point at which excess pore pressures are first initiated this measurement may be unaffected by the response time of the transducer. Deriving the strain at which excess pore pressures commence using small strain measurements was also dependent on the degree of conformity between local instrumentation and the pore pressure transducer. Comparing the value of normalised shear modulus at the volumetric threshold strain includes a third degree of conformity to which the normalised shear modulus was dependent (deviatoric stress).

Arguably the volumetric threshold strain may be more suitably defined using cyclic tests at strains close to that at which the volumetric strain is presumed to exist, or using drained stress path probes as per Jardine (1992) and Gasparre *et al*. (2007). Cyclic testing would also allow greater focus at the region where the volumetric threshold exists, increasing the number of data points in this area. Obviously this cannot be done during monotonic testing. The tests conducted here were generally set with a target large strain of either 15 or 20%. A maximum of 1000 points can be recorded during one monotonic ramp (1000 points are recorded for each test), and thus the number of points approximate to a particular strain is limited. To increase the number of data points available at small strains many tests were repeated, where they were sheared to typically 2-4%. In doing this a far higher number of points were recorded in the small strain domain. It is hoped this improved the measurement of soil behaviour including the accuracy of excess pore pressure measurements at small strains.

Because of the aforementioned issues with measurement of excess pore pressures at small strains, the relationship between the volumetric threshold strain and strain rate here are reported with a caveat that there may have been significant effects of compliance from the triaxial measurement system. Therefore the findings reported here should be used with caution.

6.5.2 Effect of strain rate on the volumetric threshold strain

Figure 6-16 presents the selection of the volumetric threshold strain from measurements of excess pore pressures. Note the test at 180,000%/hr displays negative excess pore pressure shortly after the selection of the volumetric threshold strain. Vucetic (1994) found the volumetric threshold strain to be unique for fine grained soil in both normally consolidated (positive excess pore pressures) and in heavily over consolidated (negative excess pore pressures) states. Because the volumetric threshold strain is unique it is thus unaffected by the development of negative excess pore pressure. To derive the volumetric threshold strain, the point at which a non-zero reading of excess pore pressure measurements is taken. As clearly shown in Figure 6-16 the volumetric threshold strain increases with strain rate.

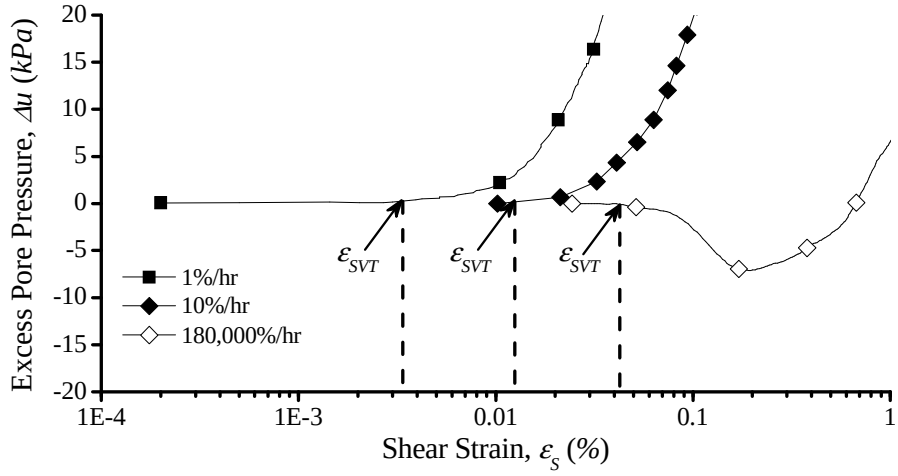

Figure 6-16 Depicting the selection of the volumetric threshold strain from excess pore pressures

Figure 6-17 presents the volumetric threshold strains measured during tests at strain rates from 1%/hr to 180,000%/hr in Kaolin 720kPa, KSS-541 600kPa, and KSS 560kPa. There is a relatively large increase in the magnitude of the volumetric threshold strain between tests at strain rates of 1%/hr and 5%/hr for KSS 560kPa and Kaolin 720kPa. These two soils display little variation of the volumetric threshold strain at strain rates between 5%/hr and 300%/hr. At strain rates in excess of 300%/hr the volumetric threshold strain increases with strain rate for all soils.

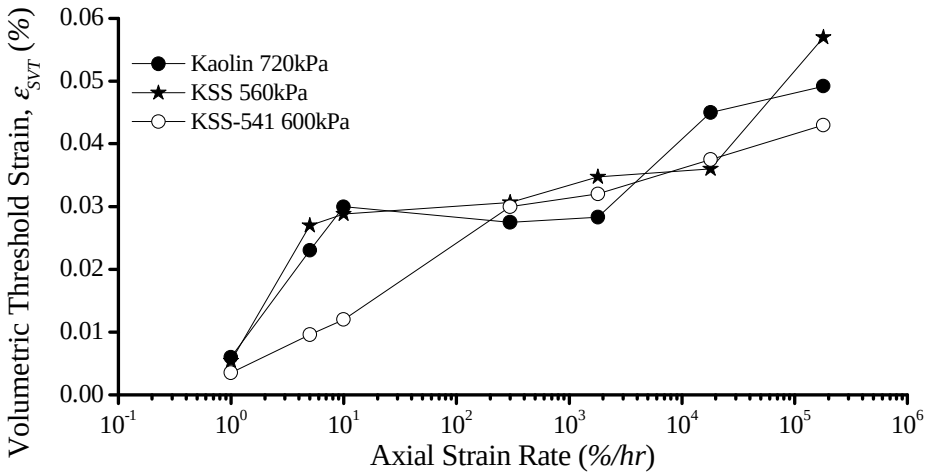

Figure 6-17 Variation of volumetric threshold strains with increasing axial strain rate

These observations on the volumetric threshold strain (ε_{SVT}) in Figure 6-17 reflect the trends noted between increasing strain rate on both volumetric strains (ε_v) and Poisson's ratio (υ) as previously discussed in Section 6.2.1. At these particular strains, the magnitude of volumetric strains (ε_v) and apparent Poisson's ratio (υ) indicated partially drained behaviour from samples tested at 1%/hr, undrained behaviour at strain rates from 5%/hr, and dilative behaviour at strain rates from 300%/hr (Section 6.2.1).

Figure 6-18 highlights the magnitude of the normalised shear modulus in relation to the volumetric threshold strains measured in Kaolin-720kPa. As was noted in Figure 6-17 for Kaolin at strain rates from 5%/hr to 300%/hr; there is little variation in the magnitude of the volumetric threshold strains. However at these strain rates (5%/hr to 300%/hr) there is considerable variation in the magnitude of the corresponding normalised shear modulus at the volumetric threshold strains (Figure 6-18). In contrast, Figure 6-18 shows at strain rates in excess of 300%/hr the variation in normalised shear modulus at the volumetric threshold strains became approximately constant. The magnitude of the normalised shear modulus corresponding at the volumetric threshold strains at strain rates between 300%/hr to 180,000%/hr, was found to be constant for all soils in this study.

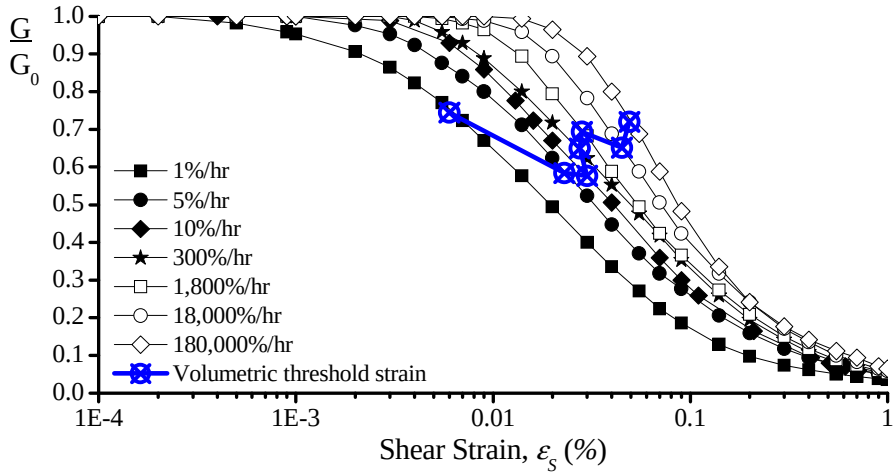

Figure 6-18 Normalised shear modulus degradation curves highlighting the volumetric threshold strain for Kaolin 720kPa

Therefore there appears to be a significant difference in how the normalised shear modulus at the volumetric threshold strain relates to strain rate, depending on the range of strain rates involved. It is considered the transition to approximately constant values of the normalised shear modulus at the volumetric threshold strain seen at strain rates in excess of 300%/hr correspond to fully undrained behaviour from the samples. To ensure results used for comparing the strain rate effects and soil properties are not obscured by consolidation effects the 1%/hr, 5%/hr and 10%/hr results are excluded from comparisons and the effect of strain rate on the volumetric threshold is considered only for 300%/hr to 180,000%/hr results.

Figure 6-19 compares the volumetric threshold strains from this study with those from a design chart (Vucetic, 1994). The volumetric threshold strains measured during 300%/hr and 180,000%/hr tests in the current study are presented in Figure 6-19. For soils tested at a range of initial effective stresses, the volumetric threshold strain at the particular strain rate for each effective stress is averaged, and presented in Figure 6-19, i.e. the lowest value for Kaolin in Figure 6-19 is the average of volumetric threshold strains measured during 300%/hr strain rate tests at 300kPa, 720kPa and 1150kPa.

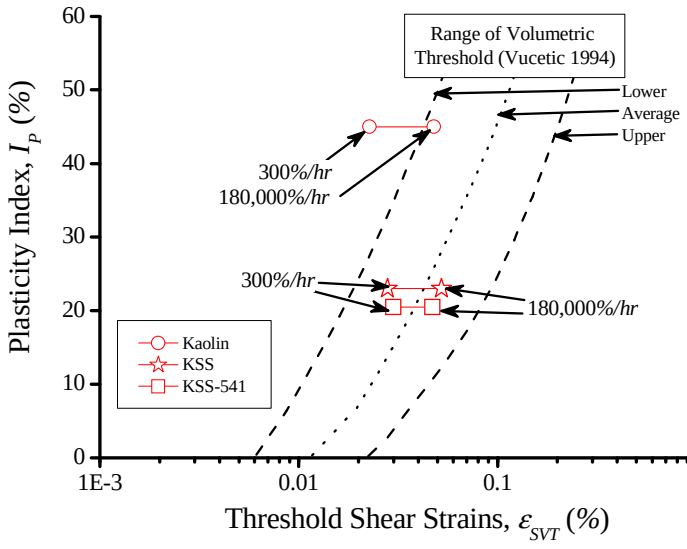

Figure 6-19 Comparison of average volumetric threshold strains of both 300%/hr & 180,000%/hr tests with envelope based on plasticity index from Vucetic (1994)

The average results for the KSS-541 and the KSS tests compare well with the range as defined by Vucetic (1994). The average volumetric threshold for the Kaolin tests is however slightly lower. The differences between the volumetric thresholds for these soils do not reflect the findings from Vucetic (1994) which predict the volumetric threshold strain to increase with plasticity index. Figure 6-19 suggests there may not be an issue with the response of pore pressure transducers because the results of higher strain rate tests are lower than those compiled from undrained tests by Vucetic (1994).

To compare the effect of strain rate on volumetric threshold strain for different soils, linear regression is performed on the volumetric threshold strain at strain rates between 300%/hr to 180,000%/hr. From this a coefficient λ_{VT} which describes the increase in volumetric threshold for a logarithmic increase in strain rate is defined. A logarithmic form was chosen in preference to an exponential form based on the superior agreement with the results from this study.

$$\frac{\varepsilon_{VT}}{\varepsilon_{VTREF}} = \lambda_{VT} \log\left(\frac{\dot{\varepsilon}}{\dot{\varepsilon}_{REF}}\right) \qquad (6\text{-}9)$$

The reference strain rate (ε_{SVTREF}) is taken as the volumetric threshold strain at 300%/hr. The coefficient from Equation 6-9 was found to relate best with plasticity index (Figure 6-20).

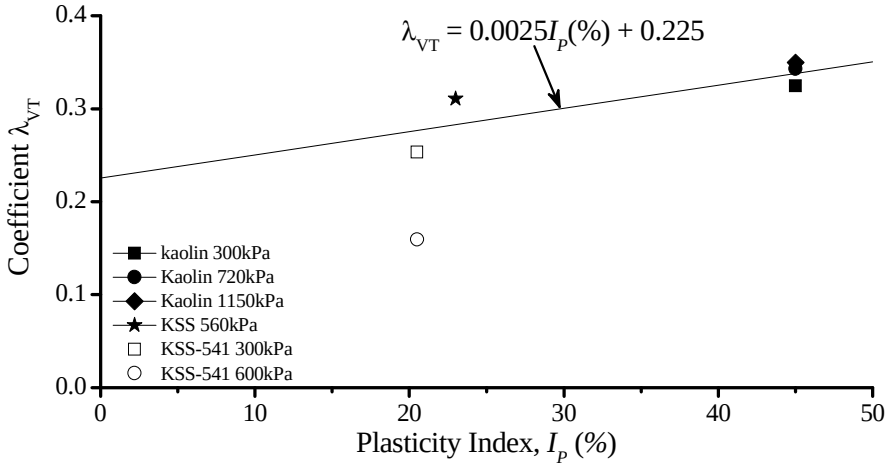

Figure 6-20 Relationship between λ_{VT} (Equation 6-9) and plasticity index

As shown in Figure 6-20 the coefficient describing the increase in volumetric threshold strain with strain rate (Equation 6-9) is very similar for the tests in Kaolin, each of which had been consolidated to a different effective stress. This suggests plasticity index may be a good indicator of the strain rate effect on the volumetric threshold, however significantly larger scatter is noted at lower plasticity index. The KSS-541 600kPa soil displays a significantly lower strain rate effect on the volumetric threshold strains, approximately 65% of that displayed by KSS-541 300kPa, and 50% of the Kaolin results. The large difference would suggest this result may be influenced by a larger than expected volumetric threshold strain at the 300%/hr test. However this and other observations made from Figure 6-20 can be more easily explained using Figure 6-21 which compares the normalised shear modulus at the volumetric threshold strain for each soil.

Because of the large difference in the coefficient describing the increase of the volumetric threshold strain with strain rate (λ_{VT}) in KSS-541 600kPa, Equation 6-10 which is a trend line of the other data (the KSS-541 600kPa result is excluded from development of Equation 6-10) in Figure 6-20 is preferred;

$$\lambda_{VT} = 0.0025 I_P(\%) + 0.225 \qquad (6\text{-}10)$$

As mentioned earlier the normalised shear modulus (G/G_0) was approximately constant at strain rates between 300%/hr to 180,000%/hr for each soil. Figure 6-21 presents the average value of normalised shear modulus (G/G_0) at the volumetric threshold strain (ε_{SVT}) from the tests between 300%/hr to 180,000%/hr for each particular soil. Figure 6-21 shows the average normalised shear modulus relates well to plasticity index. The relationship between plasticity index and the normalised shear modulus at the volumetric threshold strain is shown in Equation 6-11.

$$\left(G/G_0\right)_{\lambda VT} = 0.0063 I_P(\%) + 0.4237 \qquad (6\text{-}11)$$

The relationship between plasticity index and the normalised shear modulus may be reasonable because as discussed in Section 6.2.2, the magnitude of the shear modulus degradation curve is also controlled by plasticity index. Thus as the normalised shear

modulus at the volumetric threshold strain is controlled by plasticity index this would also control the volumetric threshold strain. The possibly erroneous volumetric threshold strain coefficient (λ_{VT}) from KSS-541 as mentioned previously maybe due to variability in some of the tests in this soil, in particular if the 300%/hr test is displaying a higher shear modulus curve as suspected, the volumetric threshold strain may be higher, thus reducing the coefficient describing the increase in volumetric threshold strain with strain rate.

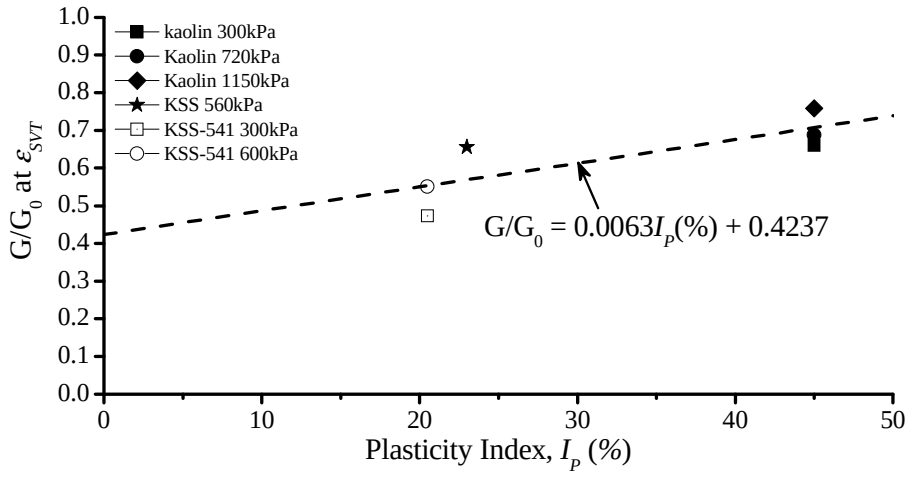

Figure 6-21 Relationship between averaged normalised shear modulus (G/G_0) at volumetric threshold strain (300%/hr-180,000%/hr) with plasticity index

Because the normalised shear modulus at the volumetric threshold strain does not vary significantly with increased strain rate (from 300%/hr to 180,000%/hr), the relationship shown in Figure 6-21 can be applied to static strain rate undrained testing. Unfortunately there is no relationship in the literature for comparison. The values of KSS-541 may seem slightly lower then expected based upon the typical range of normalised shear modulus values of 0.6 to 0.85 reported by Ishihara (1996). However the typical range from Ishihara (1996) may not be applicable to all soils. The values of normalised shear modulus (Figure 6-21) were also noted to vary with soil state, increasing with effective stress. With increasing effective stress, the normalised shear modulus of Kaolin varies by 6%. The magnitude of the normalised shear modulus (Figure 6-21) varies from Kaolin to KSS by 7%, and 27% from Kaolin to KSS-541. Therefore plasticity index appears to be more important than state to the magnitude of the normalised shear modulus at the volumetric threshold strain.

The magnitude of the normalised shear modulus measured at the volumetric threshold strain indicates the relative proportion of elastic and thus recoverable behaviour of soils. Figure 6-21 shows that soils of higher plasticity develop the volumetric threshold strain at comparatively higher normalised shear modulus, indicating that proportionally less stiffness degradation of these soils is recoverable. That increasing plastic behaviour is associated with soil of higher plasticity index seems intuitive. This suggests that clay fraction is controlling the behaviour of the soils at the volumetric threshold strains, and thus is controlling the effect of strain rate on stiffness at strains in excess of the volumetric threshold strain. To compare how the volumetric threshold strain may affect relate to the strain rate effect on stiffness it is compared with the strain rate coefficient in Section 6.6.

6.6 The strain rate coefficient, α(ε_S), on stiffness

Prior to this point in the chapter, focus has primarily been on the effect of strain rate on the linear elastic and volumetric threshold strains. This section describes the effect of strain rate on stiffness using the strain rate coefficient (Lo Presti *et al*., 1996, Tatsuoka *et al*., 1997, Vucetic *et al*., 2003) which is a direct measure of the strain rate effect on stiffness. The strain rate coefficient $\alpha(\varepsilon_S)$, compares the increase in stiffness due to increasing strain rate at equal magnitudes of strain. In this section the strain rate coefficient is compared at strains ranging from the linear elastic threshold to 1%. The strain rate coefficient thus ties together the effect of strain rate from the linear elastic threshold strain, to strains in excess of volumetric threshold strain.

Numerous studies have investigated the effect of strain rate on the shear modulus degradation curve using the strain rate coefficient (Lo Presti *et al*., 1996, Matesic and Vucetic, 2003, Vucetic and Tabata, 2003, Vucetic *et al*., 2003). The magnitude of the strain rate coefficient has been tentatively linked to index properties such as plasticity index and liquid limit by Vucetic and Tabata (2003), Vucetic *et al*. (2003). Lo Presti *et al*. (1997) compiled the strain rate coefficient from a variety of studies in fine grained soils, and suggested a possible link between the magnitudes of the strain rate effect on stiffness to plasticity index, however there was insufficient data to define a relationship.

To ensure the observations of this study are comparable to the previous investigations in the literature, the results from strain rate tests where the response of the samples was undrained (300%/hr to 180,000%/hr) were used to develop the strain rate coefficient. The results from this study are then compared to data from the literature to determine the effect of index properties on the strain rate effect on stiffness.

6.6.1 Determination of the strain rate coefficient, $\alpha(\varepsilon_S)$

To determine the strain rate coefficient $\alpha(\varepsilon_S)$, the difference in shear modulus with a logarithmic increase in strain rate was first determined (at an equal magnitude of strain) using Equation 6-12 from Vucetic *et al*. (2003). This process is illustrated in Figure 6-22.

$$m_G = \frac{\Delta G}{\Delta \log \dot{\varepsilon}} = \frac{(G)_{HIGH} - (G)_{LOW}}{\log\left(\dot{\varepsilon}_{HIGH} / \dot{\varepsilon}_{LOW}\right)} \qquad (6\text{-}12)$$

As shown in Figure 6-22 the parameter m_G represents the increase in shear modulus per logarithmic increase of strain rate. The values of shear modulus (Figure 6-22) are at equal magnitudes of strain.

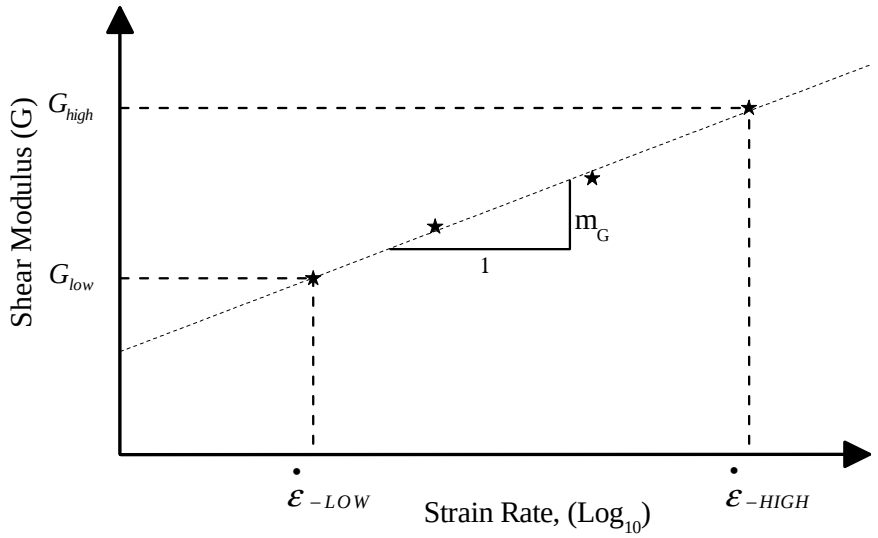

Figure 6-22 Development of m_G parameter (each point defined at identical magnitude of strain) from Equation 6-12

Matesic and Vucetic (2003) used Equation 6-12 to compare the effect of strain rate on shear modulus, however they found that normalising m_G by a reference value of shear modulus (G_{ref} or G_{low}) determined at a reference strain rate as per Yong and Japp (1967) and Isenhower and Stokoe (1981) gave a more consistent description of the effect of strain rate.

$$\alpha(\varepsilon_S) = \frac{m_G}{(G)_{LOW}} \qquad (6\text{-}13)$$

The reference shear modulus, G_{low} is the same as that in Figure 6-22. Equation 6-13 thus determines the fractional increase in stiffness per logarithmic increase in strain rate. The strain rate coefficient, $\alpha(\varepsilon_S)$ in Equation 6-13, is the same as that used by Lo Presti *et al*. (1996) amongst others as the strain rate coefficient.

Defining the strain rate coefficient in this way depends on the range of strain rates considered, for example if the linear elastic threshold strain is not exceeded at higher strain rates (assuming initial elastic shear modulus is rate independent) at this particular strain the value of m_G (Equation 6-12) will decrease.
The current study considers four strain rate tests to define the value of m_G, each at a constant strain rate of 300%/hr, 1,800%/hr, 18,000%/hr or 180,000%/hr. The reference strain rate, and hence the reference shear modulus is taken at 300%/hr in the current study.

6.6.2 Effect of strain and soil type on the strain rate coefficient

The strain rate coefficient; defined at discrete levels of strain is presented for Kaolin at 300, 720, and 1150kPa in Figure 6-23. Each point on Figure 6-23 represents four tests at strain rates from 300%/hr to 180,000%/hr. The strain rate coefficient is presented in the same manner in previous investigations (Lo Presti *et al*., 1996, Tatsuoka *et al*., 1997). For continuity the data from large strain measurements are shown in Figure 6-23 from 0.5% strain. The strain rate coefficient for large strain measurements was defined in the same way as that for small strain measurements.

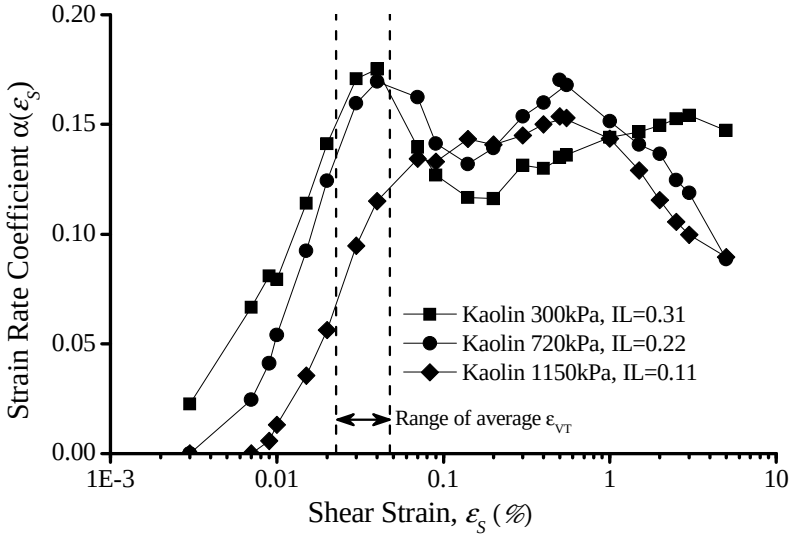

Figure 6-23 The range of the strain rate coefficient, with increasing level of strain in Kaolin

At lower levels of strain (0.002% to 0.03%), the strain rate coefficient clearly increases with increasing strain as shown in Figure 6-23. This is consistent with observations from Lo Presti *et al*. (1996) on the strain rate coefficient displayed by fine grained soils. The strain rate effects begin at comparatively higher levels of strain in the Kaolin consolidated to higher effective stress. This is expected because as discussed in Section 6.2.2 the magnitude of the linear elastic threshold strain increases (although the strain rate affect on magnitude of the linear elastic threshold strain decreases) with effective stress in a particular soil. At levels of strain less than the linear elastic threshold strain, the shear modulus was independent of strain rate (Section 6.3), and thus the magnitude of the strain rate coefficient tends to zero (Figure 6-23). From the level of strains at which the strain rate effects are first observed until the volumetric threshold strain (Figure 6-23) is intercepted each of the Kaolin soils display a similar increase in strain rate coefficient per increase in strain (approx 0.18 per logarithmic increase in strain). Until the volumetric threshold strain is intercepted, the magnitude of the strain rate coefficient (at an equal strain) increases with liquidity index.

When the volumetric threshold strain is intercepted (Figure 6-23) the strain rate effects begin to tend towards a similar magnitude (with increasing strain) for each of the Kaolin soils shown in Figure 6-23. For Kaolin consolidated to 300kPa and Kaolin

consolidated to 720kPa this involves a reduction in the strain rate coefficient. Thus the maximum strain rate effect in these particular soils is measured at strains close to the volumetric threshold. The maximum strain rate effect has also been measured at strains of this magnitude in KSS during Statnamic pile testing (Brown, 2008). The "peak" in the strain rate coefficient approximate to the volumetric threshold strains in Kaolin 300kPa and 720kPa may also reflect similar behaviour in KSS measured during high strain rate triaxial testing from Balderas-Meca (2004), although the strains in that study were measured using a global transducer.

Akai *et al*. (1975) amongst others report behaviour such as that displayed by Kaolin 1150kPa in Figure 6-23, where from a particular strain, the strain rate effect became constant without displaying a distinct "peak" strain rate coefficient. Therefore it appears a particular soil can display either type of behaviour, and apparently this depends on effective stress and subsequently moisture content and liquidity index.

The magnitude of the strain rate coefficient for results in Figure 6-23 appear to tend towards similar values at strains in excess of the volumetric threshold strain, and do not display any distinct trend with regards to the state of each soil. Therefore it appears the magnitude of the strain rate coefficient, although showing some scatter may be dependent on the plasticity index of the soil. However because this observation occurs at strains approximate to the range of the volumetric threshold strain this could also indicate that excess pore pressures are influencing the response of each soil. Unfortunately the magnitudes of excess pore pressures at these strains do not make it clear how effective stress changes may affect the strain rate coefficient. At strain rates in excess of 300%/hr the excess pore pressures are generally close to zero or slightly negative, therefore making comparisons between different soils difficult to interpret.

To verify the above observations for Kaolin the strain rate coefficient is compared for KSS-541 300kPa, and KSS-541 600kPa in Figure 6-24. For reference the Kaolin 720kPa result is also included in Figure 6-24.

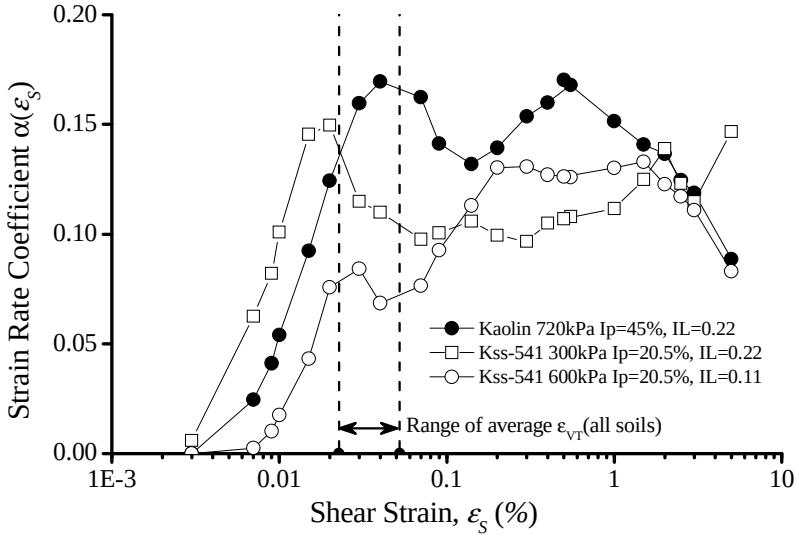

Figure 6-24Variation of strain rate coefficient with strain for KSS-541 and Kaolin 720kPa

The KSS-541 soils display a similar type of behaviour as seen in Kaolin described previously. At strains less then the volumetric threshold strain the soil consolidated to higher effective stress displays a lower strain rate coefficient, thus the strain rate coefficient reduces with reducing liquidity index at these strains. However once the volumetric threshold is exceeded the KSS-541 soils tend to similar values of strain rate coefficient. At these strains however both the KSS-541 soils display a lower strain rate coefficient then Kaolin, again suggesting a link between the magnitudes of the strain rate coefficient to plasticity index.

Thus according to trends in behaviour noted in Figures 6-23 and 6-24, the strain rate effect at medium strain (0.05%-0.5%) are dependent on different factors then both the small strain and large strain-undrained strain rate effect on strength as discussed in Section 5.4. As shown in Section 6-5 the soils of higher plasticity develop plastic strains after less degradation of the normalised shear modulus curve. This may reflect observations made here that once the volumetric threshold strain is exceeded and plastic deformations are beginning, soils of higher plasticity index display higher rate effects. In comparison to the strain rate effect at large strain in Section 5.4 it appears moisture content (or void ratio) is not as significant at these medium strains (0.05%-0.5%).

Based upon the greater strain rate coefficient measured in Kaolin; it appears at these strains the clay fraction is the dominant factor of the strain rate effect. This may reflect observations of soil behaviour noted by Sorensen *et al*. (2007) and Tatsuoka *et al*. (2008) (discussed in Section 2.4.2) in fine grained soils subjected to step-wise change in strain rate at different strains. Tatsuoka *et al*. (2008) explained that as strain increased, fine grained soils displayed a different response to a sudden change (increase or decrease) in strain rate. At lower strains the inter-particle bonds became stronger and stiffer with an increase in strain rate. At higher strains, as the soil approaches failure, the changes in soil fabric due to the development of irrecoverable plastic strains caused a different response to sudden increase in strain rate, with the soil displaying more temporary effects of strain rate.

This behaviour may be reflected in these constant strain rate tests by the reduction in strain rate coefficient of Kaolin as the samples approach failure, which based upon Figure 6-23 appears to be from approximately 0.5% strain. In contrast the KSS-541 soils display increasing strain rate effects as they approach larger strains to failure. This indicates that as plastic strains become more prominent within the soil, they affect the strain rate effect, with their effectiveness reflected apparently by the void ratio or moisture content of the soil, i.e. a soil of lower void ratio (for a particular clay fraction) displays a lower strain rate effect as plastic strains increase.

6.6.3 Comparison of the strain rate coefficient with previous research

To compare the findings from this study with those from the literature Figure 6-26 compares the strain rate coefficient (Equation 6-13) compiled from various studies by Tatsuoka *et al*. (1997). The strain rate coefficient from other studies shown in Figure 6-25 have been developed from various types of laboratory tests, including monotonic and cyclic triaxial, resonant column, and torsional shear testing. The range of maximum strain rates from other studies are from 30%/hr (Mukabi *et al*., 1991) to 48,000%/hr (Lo Presti *et al*., 1996). The reference strain rate, used to define the reference shear modulus from each study shown in Figure 6-25 is typically between 0.6%/hr to 2.4%/hr. The reference strain rate used in the current study is 300%/hr, which although is significantly larger than that used in previous investigations is the true minimum undrained strain rate for the soils in the current study. Figure 6-25

shows the strain rate coefficient from data of the current study lie within the range of strain rate coefficients measured in other studies.

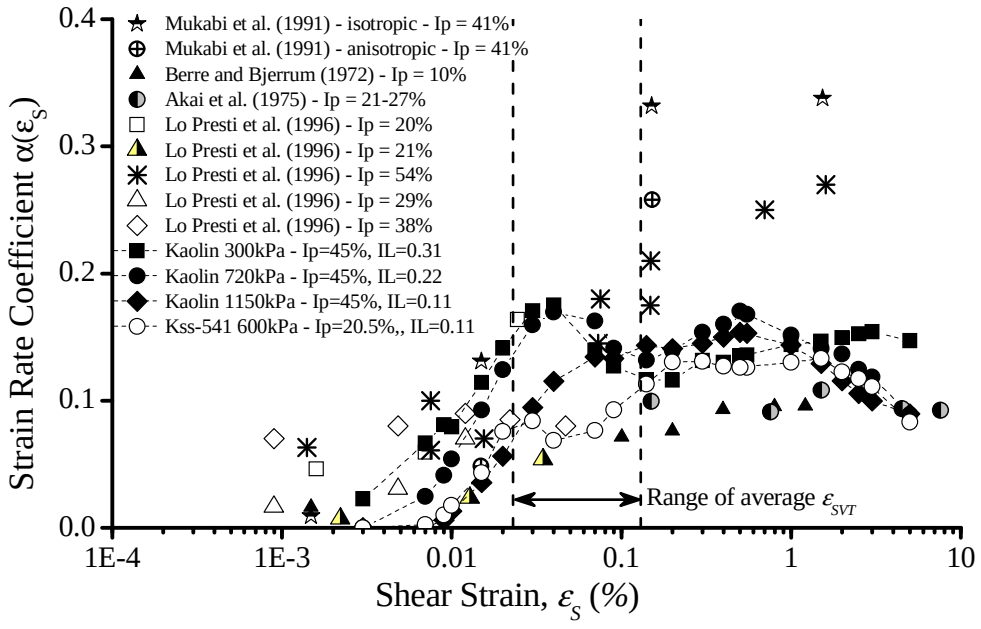

Figure 6-25 Comparison of the strain rate coefficient from various studies

As discussed previously, at lower strains, the strain rate coefficients of soils in the current study increase with strain. Within the range of strains 0.001% to 0.1%, the majority of other studies in Figure 6-25 also display an increasing strain rate coefficient. As the magnitude of strain reduces in Figure 6-25, a reduction in the strain rate coefficient to zero reflects strain rate independence of the initial elastic shear modulus (G_{max}). Thus the initial elastic shear modulus (G_{max}) for the majority of soils shown in Figure 6-25 appears to be independent of strain rate which is consistent with the findings of the current study.

Data from the current study indicate that for a particular soil the magnitude of the strain rate coefficient (at an equal strain) increased with liquidity index at strains less than the volumetric threshold strain. The data from other studies display similar magnitude strain rate coefficients to those of the current study (at strains <0.05%) however information on their liquidity indices are not available. However many of the data from other studies have similar magnitude of plasticity indices, yet display very

different magnitudes of strain rate coefficient, suggesting the state of the soils, and thus liquidity index may be important to the magnitude of the strain rate coefficient at these particular strains.

Previously it has been discussed that for soils tested in the current study the volumetric threshold strain appeared to have a significant impact on the relationship between increasing strain and the magnitude of the strain rate coefficient. At strains in excess of the volumetric threshold strain the magnitude of the strain rate coefficient tended to become approximately constant. Recognition of the volumetric threshold strains and how they relate to the strain rate coefficient was not given in previous studies. The volumetric threshold strains are not reported in previous studies however based on the plasticity indices of the soils shown in Figure 6-25 the average volumetric threshold strains can be determined from a design chart from Vucetic (1994) as discussed in Section 6.5.2. The average volumetric threshold strains (from Vucetic, 1994) shown in Figure 6-25 are for soils at plasticity indices of 10% and 54% which is the range of soils shown in Figure 6-25.

Figure 6-25 shows that at strains in excess of the volumetric threshold strain data from Berre and Bjerrum (1972), Akai *et al*. (1975) and isotropic tests from Mukabi *et al*. (1991) display approximately constant strain rate effects from the volumetric threshold strain. These studies thus appear to be consistent with observations from the soils tested in the current study. It is unclear if this observation is applicable to all soils, for example the soil at a plasticity index of 54% (Lo Presti *et al*., 1996) does not appear to display a constant strain rate coefficient at higher strain. Nonetheless consideration of the volumetric threshold strains in relation to the strain rate effect is recommended for future studies on the strain rate effects of fine grained soils at small strain.

The magnitude of strain rate effects for Kaolin in the current study also appeared to tend towards similar values at strains in excess of the volumetric threshold strain. The similar magnitude of the strain rate coefficient in Kaolin suggested that plasticity index may be more important to the strain rate effect rather then state. However from consideration of the variety of plasticity indices and their corresponding magnitude of strain rate coefficient shown in Figure 6-25 it appears that plasticity index may not

control the magnitude of the strain rate coefficient at medium strains. For example the strain rate coefficient measured by Mukabi *et al*. (1991) displays higher strain rate effects than other soils of higher plasticity index. It is possible this indicates that state may be more important to the strain rate coefficient (at medium strains) as then shown for soils in the current study. Future studies could incorporate soils of greater liquidity index than used in the current study (maximum I_L = 0.31) to determine if the effects of moisture content/void ratio influence the strain rate effect at medium strains.

6.7 Hyperbolic modelling of the strain rate effect

This section describes the modelling of the shear modulus degradation curve, and its dependence on strain rate using a simple hyperbolic model. Described previously in this chapter were the effects of strain rate on the linear elastic threshold strain, volumetric threshold strain and the strain rate coefficient. Uses of the linear elastic or volumetric threshold strain models as discussed in Section 6.4 and 6.5 are limited to that specific point (or strain) on a shear modulus degradation curve. The strain rate coefficient offers information on a wider range of strains; however its use in modelling is complicated due to the variance of the strain rate coefficient with strain. The convenience of a model which can describe the strain rate dependence of the shear modulus degradation curve through a single parameter would be simpler to use in industry. Developing a rate dependent parameter with such a model and relating it to a soil index property would be beneficial to industry.

Typical models used in dynamic soil analysis are mainly Ramberg-Osgood and Hardin-Drnevich based models (Benz, 2007) as well as the Jardine model (Jardine *et al*., 1986). A Hardin-Drnevich model, modified by Soga *et al*. (1995), is used to describe the strain rate dependence of different soils;

$$\frac{G}{G_0} = \frac{1}{(1+\zeta\varepsilon_S^{\beta})} \qquad (6\text{-}14)$$

Where ε_S is the shear strain, ζ and β are curve fit parameters. The ζ parameter controls the magnitude of the normalised shear modulus curve, with greater values of ζ representing more non linear shear modulus degradation curves. The β exponent

controls the shape of the normalised shear modulus curve. An increase in the β exponent (at particular ζ) reflects an increase of stiffness at lower strains.

The ζ and β parameters were obtained by linear regression of each strain rate test. An example of a curve fitting of Equation 6-14 is shown in Figure 6-26, where Equation 6-14 has been applied to the shear modulus degradation curve of Kaolin-720kPa at strain rate tests from 1%/hr to 180,000%/hr.

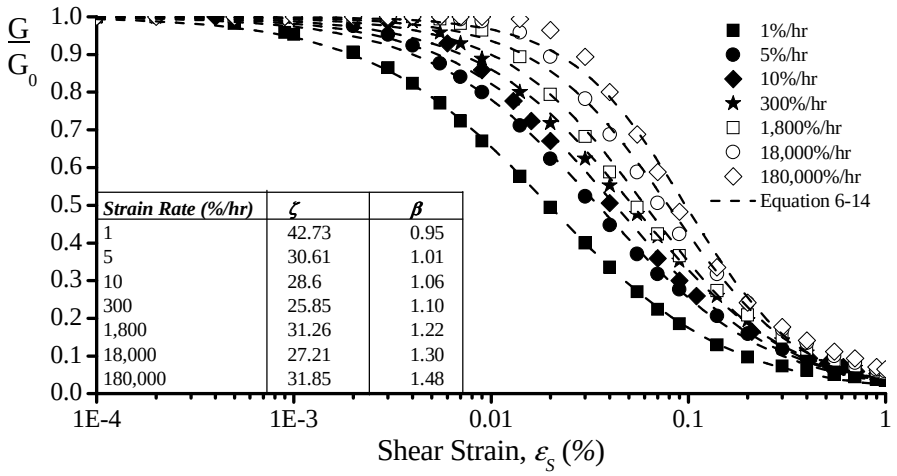

Strain Rate (%/hr)	*ζ*	*β*
1	42.73	0.95
5	30.61	1.01
10	28.6	1.06
300	25.85	1.10
1,800	31.26	1.22
18,000	27.21	1.30
180,000	31.85	1.48

Figure 6-26 Example of curve fit (Equation 6-14) at increased strain rates in Kaolin 720kPa

Equation 6-14 fits the results well (Figure 6-26). It is noted that close to the linear elastic threshold however, Equation 6-14 under predicts the normalised shear modulus, and subsequently the linear elastic threshold strain. For instances where this particular point is of significant importance, Equation 6-7 which describes the linear elastic threshold strain (Section 6.4) can also be used to better effect. At higher strains (~ >0.1%) Equation 6-14 tends to under predict the normalised shear modulus. Therefore there is a maximum strain for which Equation 6-14 can be considered adequate. From Figure 6-26 this appears to be 0.3%, however for other soils analysed in the current study, generally this limit is closer to 0.1% strain.

The magnitude of the ζ parameter is noted to vary little with strain rate (Figure 6-26), and is very close for soils of the same plasticity index. This parameter can thus be determined for a particular soil from standard strain rate testing. The value of ζ for the

soils tested in the current study range from approximately 30 in Kaolin, rising to 60 for KSS and 85 for KSS-541.

As shown in Figure 6-26 the β parameter increases with strain rate. The magnitude of the β parameter thus represents the strain rate effect on the stiffness degradation curve. Equation 6-15 was used to determine the normalised increase in the β parameter per logarithmic increase in strain rate;

$$\frac{\beta}{\beta_{REF}} = \chi \log\left(\frac{\dot{\varepsilon}}{\dot{\varepsilon}_{REF}}\right) \qquad (6\text{-}15)$$

The χ parameter thus describes the fractional increase in the exponent β per logarithmic increase in strain rate. For the data in the current study, the 300%/hr strain rate tests were chosen as the reference strain rate to avoid effects of partial consolidation in the subsequent strain rate parameter (χ). Figure 6-27 shows the strain rate parameter (χ) relates well to liquidity index.

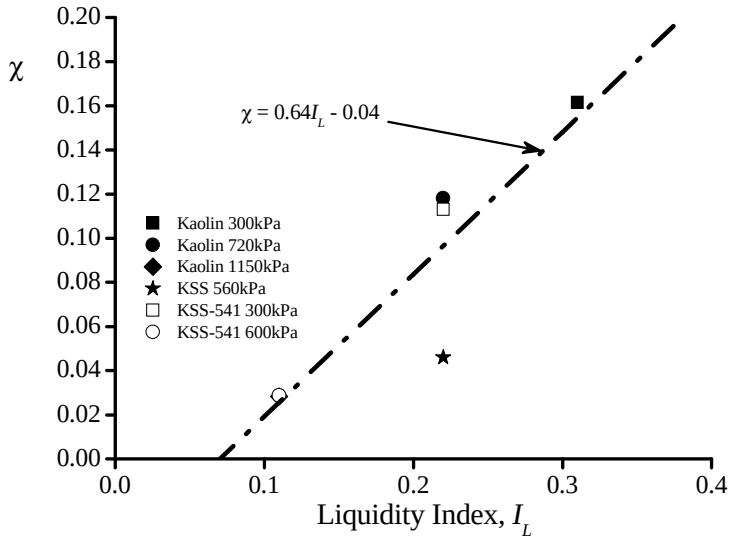

Figure 6-27 Relationship between the χ parameter (Equation 6-15) with liquidity index

Equation 6-16 presents the relationship between the strain rate parameter (χ) and liquidity index;

$$\chi = 0.64 I_L - 0.04 \quad (6\text{-}16)$$

The liquidity index was shown to be the controlling factor at strains less than the volumetric strain threshold in Section 6-4. The agreement between liquidity index and the strain rate parameter (χ) reflects this behaviour, measured at strains approximate to the linear elastic threshold. It was shown in Section 6-6 that plasticity index appears to control the strain rate effect at strains from the volumetric threshold strain. The relevance of Equation 6-14 extends to between 0.1-0.3% strains, which are slightly larger than the volumetric threshold strain (0.05%); however it is reasonable that liquidity index may be used to model strain rate effect to this level of strain.

Unfortunately the intercept in Equation 6-16 is negative, implying no rate effects at liquidity indices less then 0.07. Future studies may incorporate soils of such liquidity indices to determine how strain rate effects vary for soils in this state. It is unclear how the rate effects will change at low values of liquidity index, therefore it cannot be specified if the intercept in Equation 6-16 is valid.

6.7.1 Application of hyperbolic model to other studies

To establish if the relationship between strain rate and stiffness presented in Equation 6-16 from soils in this study are applicable to other soils, data published in literature are evaluated using Equation 6-14. Table 6-4 summarises previous investigations of strain rate effects on the shear modulus degradation curve which have been re-evaluated here using Equation 6-14. The studies summarised in Table 6-4 used undrained testing to study the effect of strain rate on stiffness. Table 6-4 highlights with the exception of data in Augusta clay, previous investigations utilised maximum strain rates typically two to three orders of magnitude less than those used in the current study.

Soil	Type of test	Strain Rate (%/hr)	Reference
NSF clay	Monotonic triaxial	0.6-84	Shibuya *et al*. (1996)
Augusta clay	RCT, CLTST	3-48,000	Lo Presti *et al*. (1996)
Augusta clay	MLTST-CLTST	6-135,000	Lo Presti *et al*. (1998)
Boston blue clay	Monotonic Triaxial	0.1-4	Santagata *et al*. (2007)

Table 6-4 Summary of studies re-evaluated using Equation 6-14 for comparison with predictions on the strain rate effect on shear modulus degradation curves

The corresponding index properties of soils collated from published studies are shown in Table 6-5.

Soil	Plasticity Index, I_P (%)	Void ratio, e	Liquid Limit, w_L	Liquidity index, I_L	Reference
NSF clay	27	1.16	56	0.51	Shibuya *et al*. (1996)
Augusta clay	29	0.684	49	0.19	Lo Presti *et al*. (1996)
Augusta clay	38	0.838	59	0.23	Lo Presti *et al*. (1998)
Boston blue clay	23	0.87	46	0.33	Santagata *et al*. (2007)

Table 6-5 Index properties of soils from studies summarised in Table 6-4

Equation 6-14 has been applied to the data from previous studies in the same way as to the data from this study as described above. Figure 6-28 presents an example of the fit of Equation 6-14 to the data from Augusta clay published by Lo Presti *et al*. (1996). Equation 6-14 describes the data at each strain rate in Figure 6-29 well. The ζ parameter was found to be similar for each strain rate test in a given soil. Subsequently the ζ parameter is assumed as constant for each soil, with the value of ζ determined using the least squares method in OriginPro7.5. The strain rate effect on the shear modulus degradation curve is reflected entirely through the exponent β which as shown in Figure 6-28 increases with strain rate.

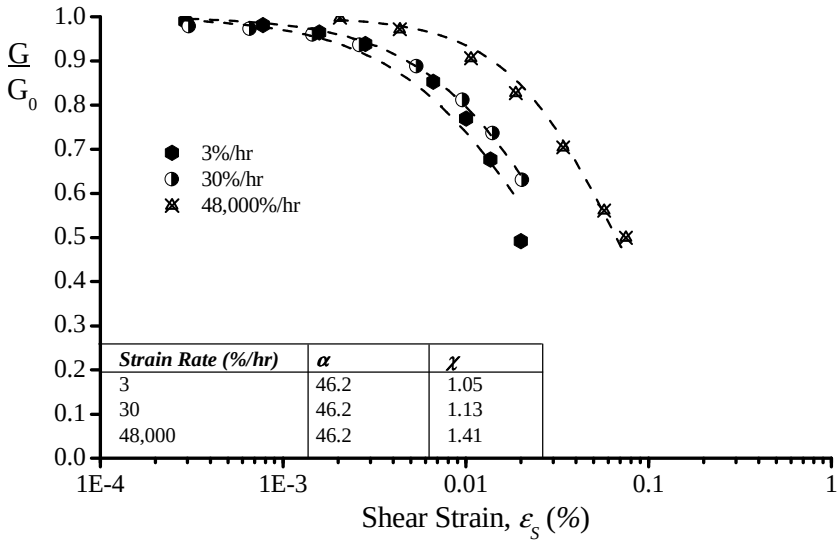

Strain Rate (%/hr)	*α*	*χ*
3	46.2	1.05
30	46.2	1.13
48,000	46.2	1.41

Figure 6-28 Fit of Equation 6-14 to Augusta clay (Lo Presti *et al*., 1996)

As was done with the data from the current study, Equation 6-15 was used to determine the strain rate parameter (χ) for each of the soils. The reference strain rate for each study is taken as the minimum strain rate test conducted in each study. Figure 6-29 presents the change strain rate parameter (χ) of both the data collated from literature and the data from the current study.

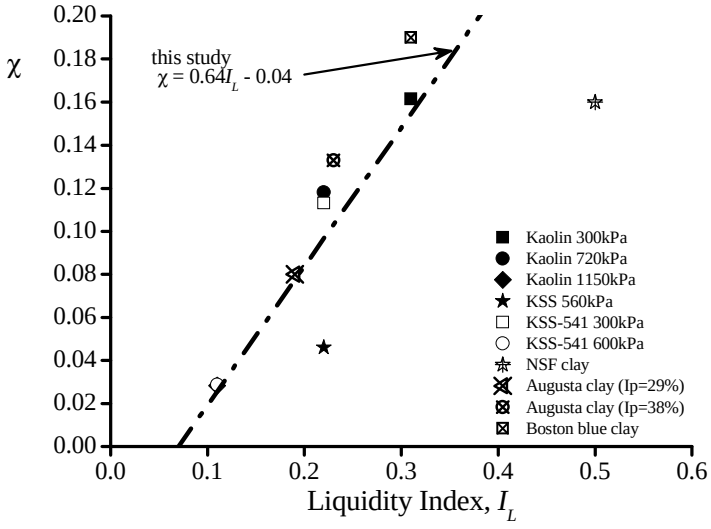

Figure 6-29 Comparison of strain rate effects on the normalised shear modulus degradation curves with increasing liquidity index

With the exception of NSF clay from Shibuya *et al*. (1996) the strain rate effects from other soils agree well with the relationship between the strain rate effect and liquidity index from the current study. This indicates liquidity index is a controlling factor of the strain rate effect at small strains (<0.1%) and that Equation 6-16 is applicable to a wider variety of soils than those tested in the current study. It is unclear as to what may cause the difference between Equation 6-16 and NSF clay. It is possible there is a limit to the strain rate effect of between 15 to 20%, per logarithmic increase in strain rate. Future testing of soils with a wider variety of liquidity index, particularly at values greater than 0.4, would clarify the relationship between strain rate effects and liquidity index (Equation 6-16).

6.8 Summary of the effect of strain rate on small strains

This chapter analysed and discussed the effect of strain rate ranging from 1%/hr to 180,000%/hr on the behaviour at small strains (<1%). The main focus of this chapter was the effect of strain rate on stiffness, and how the strain rate effects on stiffness are influenced by index properties of fine grained soils as well as their current state. The strain rate dependence of the linear elastic threshold strain, as well as the volumetric threshold strain was investigated. The effect index properties of fine grained soils have on these aspects of stiffness were compared at various strains through the strain rate coefficient. A hyperbolic model, used to describe the non linear behaviour of soils has been modified to make a single parameter rate dependent. This rate parameter has then been related to the index properties of the soils. Some findings of this chapter are outlined below;

1. At strain rates from 1%/hr to 180,000%/hr it was found that an increase in strain rate results in an increase in the stiffness degradation curve, i.e. an increase in strain rate resulted in the response of the soil becoming increasingly linear.

2. At high strain rates (>300%/hr) a Poisson's ratio in excess of 0.5 was measured, indicative of dilation or barrelling. Also at these strain rates the soils tended to display negative excess pore pressures at the start of shear which may support evidence of dilation during high strain rate testing.

3. The normalised shear modulus degradation curves from the soils in the current study were found to depend on the same factors as noted by Vucetic and Dobry (1991), principally plasticity index and, to a lesser extent, effective stress. Thus relating the effects on strain rate to soil index properties from these results should correspond to a wider variety of fine grained soils.

4. With increasing strain rate the initial elastic shear modulus (G_{max}) measured from local Hall Effect transducers was found to relate to the initial shear modulus as measured from bender element testing (G_0). Thus the initial shear modulus was found to be rate independent.

5. The linear elastic threshold strain was found to increase with strain rate. At lower strain rates (1-10%/hr) the increase in the linear elastic threshold strain was related to the square root of the strain rate, in agreement with Shibuya *et al*. (1996). However at higher strain rates (10-180,000%/hr) the strain rate effect on the linear elastic threshold reduced in magnitude. A relationship is proposed which related the strain rate effect on the linear elastic threshold to plasticity index at strain rates between 1-10%/hr; and to liquidity index for strain rates between 10-180,000%/hr. The relationship to liquidity index is assumed to reflect the influence of larger void spacing between the fine grained soils.

6. The volumetric threshold strain was also found to be rate dependent, however the value of the normalised shear modulus at the volumetric threshold strain was independent of strain rate from strain rates of 300%/hr to 180,000%/hr. The normalised shear modulus at the volumetric threshold strain was found to relate to plasticity index. This is assumed to reflect the increasing influence of clay fraction of the behaviour of these soils at these strains.

7. The strain rate coefficient was developed at strains ranging from the linear elastic threshold strain to 1%. It was found to increase with strain until the volumetric threshold strain is exceeded whereby it became constant until the strains approached larger strains closer to failure. Changes in the strain rate coefficient (with increasing magnitude of strain) reflect different properties

controlling the strain rate effect at different strains. At strains lower then the volumetric threshold strain the magnitude of the strain rate coefficient increased with liquidity index for a particular soil. At strains exceeding the volumetric threshold strain, the strain rate coefficient appeared to relate best with plasticity index for the soils used in the current study. However when compared with the strain rate coefficients (at strains in excess of the volumetric threshold strain) from literature it appears that the magnitude of the strain rate coefficient is more complex and is not dependent on the plasticity index. Some observations were made of how the magnitude of the strain rate coefficient changes with increasing strain for soils in the current study, as well as in the literature, which appear to correspond to the volumetric threshold strain. These observations suggest the volumetric threshold strain is an important parameter in the development of strain rate effects.

8. A hyperbolic model and its suitability for modelling the strain rate effects on stiffness have been assessed. A single parameter from this model was made rate dependent. This strain rate dependent parameter was related to the liquidity index and can be used to predict strain rate effects for tests at high strain rate.

7 Summary and Conclusions

7.1 Introduction

Fine grained soils display strain rate dependent behaviour which has implications for a wide range of geotechnical engineering events. The strength of fine grained soils is well known to be strain rate dependent. However current understanding of the factors which influence the effects of strain rate is limited. Accounting for strain rate effects in design involves costly and time consuming characterisation of strain rate effects using empirical studies or specialised testing. Such studies are limited in value to the broader understanding of strain rate effects in fine grained soils.

In order to improve the current understanding of the factors which influence the effect of strain rate on strength in fine grained soils, an investigation was undertaken in the University of Dundee using laboratory triaxial element testing over a wide range of strain rates in soils with various index properties. The conclusions drawn from this investigation are presented in this chapter along with recommendations for their use in geotechnical engineering. Recommendations for future research on strain rate effects are also presented.

7.2 The behaviour of fine grained soil in triaxial tests at a wide range of strain rate

The following is a summary of conclusions drawn for the shearing behaviour of normally consolidated, reconstituted, fine grained soils, tested at a wide range of constant strain rates (1%/hr to 180,000%/hr), in an electromechanical triaxial apparatus. The soils were testing after isotropic consolidation, and sheared monotonically in drained triaxial compression. Additionally some tests in over consolidated soils, which were also tested in effectively drained triaxial compression at strains rates of 300%/hr to 180,000%/hr are described. The conclusions presented here are from normally consolidated tests unless stated otherwise.

1. The deviatoric stress of normally consolidated fine grained soil was found to be heavily dependent on both the strain rate and the level of strain.

2. At low strains (<1%) a faster strain rate results in an increase in deviatoric stress.

3. At higher strains the samples display different behaviour depending on strain rate, ranging from strain hardening at the lower range of strain rates (1%/hr to 5%/hr), to clearly identifiable maximum/peak deviatoric stresses during the higher strain rate tests (300%/hr to 180,000%/hr).

4. At the lower range of strain rates (1-300%/hr), the comparative influence of strain hardening reduces at a higher strain rate, resulting in a decrease of the maximum strength. Increasing strain rate (in this range) corresponds to an increase in excess pore pressures (reducing effective stress) and reduction in volume change as with increased strain rate the response of the soil becomes undrained.

5. Although the triaxial tests were conducted in drained test conditions, the response of the soil is considered fully undrained at strain rates from 300%/hr as practically no volume change was recorded in tests at this strain rate. At strain rates in excess of 300%/hr; increasing strain rate results in an increase in deviatoric stress. This also corresponds to decreasing excess pore pressure and thus increasing effective stress.

6. Over consolidated soils (OCR 4 & 10), tested at strain rates at 300%/hr and 180,000%/hr also displayed an increase in deviatoric stress. At these strain rates, the over consolidated soils did not display volume change during shear.

7. The effective stress paths from slower strain rate tests (1-10%/hr) appear to tend towards critical state. At strain rates of 10%/hr and 300%/hr the effective stress paths tend towards critical state after the maximum deviatoric stress. At strain rates in excess of 300%/hr the stress paths of both normally and over consolidated soils initially follow the drained effective stress path, appearing as though drained stress paths (note no change in volume), expanding the state boundary surface further with increased strain rate.

8. For a particular soil type and state, where the response of the soil is undrained there does not appear to be an influence of strain rate on the magnitude of strain at maximum stress. The strain at failure decreases from partially drained tests. But when undrained there is no distinct trend meaning it is rate independent.

7.3 Effects which influence the magnitude of strain rate effects

The influence of the type of soil and effective stress on the magnitude of strain rate effects on strength was investigated. Some conclusions from these comparisons are presented below. All conclusions presented here are from tests on normally consolidated soils unless stated otherwise.

1. The magnitude of undrained strain rate effects were found to vary with the effective stress in a particular soil, reducing in soils consolidated to a higher effective stress.

2. The variation of the magnitude of undrained strain rate effects in soils of different plasticity indices indicate that plasticity index cannot be used alone as an indicator of the potential undrained strength strain rate effects.

3. By considering undrained strain rate effects in fine grained soils at an identical effective stress it was found that soils of greater plasticity index display greater strain rate effects.

4. The magnitude of the undrained strain rate effects on strength were found to be well accounted for by the liquidity index of each normally consolidated soil.

5. The magnitude of the undrained strain rate effect on strength was found not to be affected by the over consolidation ratio and can be predicted using the same relationship between liquidity index and undrained strain rate effects on strength as for normally consolidated soils. Note; these observations on over

consolidated soils may only be valid once a threshold strain rate has been exceeded.

6. The magnitude of the partially drained strain rate effect was found to be well accounted for by the coefficient of consolidation.

7.4 Incorporation of strain rate effects in design

The factors which influence the magnitude of undrained strain rate effects are summarised in regard to how they can be accounted for in design. Two aspects are assessed, the effect of strain rate on stiffness at small strains, and the effect of strain rate at large strains which represent the effect of strain rate on strength. These models are developed from tests on normally consolidated soils.

7.4.1 Small strains

Various aspects of the stiffness degradation curves of fine grained soils were assessed in terms of their dependence on strain rate including, the initial elastic shear modulus (G_{max}), the linear elastic threshold strain (ε_{EL}), and the volumetric threshold strain (ε_{SVT}). A hyperbolic model has also been assessed and made strain rate dependent which can also be used as it is simpler then using each aspect of deformation behaviour.

1. With increased strain rate the initial elastic stiffness (G_{max}) did not display any dependence on strain rate.

2. Both the linear elastic threshold strain and the volumetric threshold strain increased with strain rate.

3. A hyperbolic model was developed which can model the effect of strain rate on the stiffness degradation curves;

$$\frac{G}{G_0} = \frac{1}{(1+\varsigma\varepsilon_S^{\beta})} \qquad (6\text{-}14)$$

Where ε_S is the shear strain, ζ and β are curve fit parameters. The curve fit parameter ζ can be defined for a particular soil using standard strain rate testing. The effect of strain rate was modelled through the exponent β. The strain rate effect parameter (χ), which describes the fractional increase in the exponent β per logarithmic increase in strain rate (for strain rates between 300%/hr to 180,000%/hr) is defined per Equation 6-15;

$$\frac{\beta}{\beta_{REF}} = \chi \log\left(\frac{\dot{\varepsilon}}{\dot{\varepsilon}_{REF}}\right) \quad (6\text{-}15)$$

The magnitude of the strain rate effect parameter (χ) was found to relate to the liquidity index of the soils tested as part of the current study, and can be predicted for use in design using Equation 6-16;

$$\chi = 0.64 I_L - 0.04 \quad (6\text{-}16)$$

4. Through comparison with the effects of strain rate on the shear modulus degradation curves of several soils in the literature, it has been shown that the applicability of Equation 6-16 extends to a wider variety of soils than those tested as part of the current study. Note; the range of liquidity indices used to develop Equation 6-16 is from 0.11 to 0.31.

7.4.2 Large strains

The following points arose from development of the method to account for the large strain rate effect at large strains, representing the undrained strain rate effect on strength.

1. The liquidity index was found to control the magnitude of the undrained strain rate effect in Kaolin and KSS-541. However the liquidity index did not account for the magnitude of the undrained strain rate effect in KSS. The undrained strain rate effect in KSS was likely affected by it's significantly higher coefficient of consolidation.

2. Use of the normalised velocity, *V* was found to reduce scatter in the undrained strain rate effect between the different soils. This is despite no evidence of volume change measurements from the triaxial system during tests at these strain rates (300%/r to 180,000%/hr).

3. Equation 5-12, which modifies the normalised velocity, *V* (Finnie and Randolph, 1994) with the ratio between the clay fraction and moisture content, which reflect the influence of the liquidity index of each soil, reduced the scatter between the undrained strain rate effects of all soils used in the current study.

$$V_2 = \left(\frac{vd}{c_V}\right) / \left(\frac{CF}{w}\right) \qquad (5\text{-}12)$$

Where v is velocity, d is a characteristic length (often assumed as the drainage path length), c_v is the coefficient of consolidation, CF is the clay fraction, and w is the moisture content. The reduction of scatter with the use of the normalised velocity V_2 suggests this normalisation method is suitable for predictions of undrained strain rate effects on strength in fine grained soils, and thus could provide a practical benefit to industry.

7.5 Recommendations for future research

This section presents some recommendations for further research which have been highlighted throughout the course of this project. The main recommendations are focused on the development of greater understanding of the factors which influence the strain rate effects on fine grained soils. Some potential improvements to high strain rate testing with the triaxial apparatus are also highlighted.

7.5.1 Improvements to high strain rate triaxial testing systems

The literature review discussed some aspects of previous strain rate studies using the triaxial apparatus, highlighting the development of the triaxial systems and the benefits of improved technology and issues which have been encountered during high

strain rate testing. Balderas-Meca (2004) encountered significant difficulties due to the volume change within the triaxial cell due to the advancing loading ram. This issue has been addressed with the incorporation of a balancing system in the triaxial apparatus used in this research, which redistributed the cell fluid as the loading ram advanced into the cell. Issues with the potential difficulties of displacement control have also been addressed, with electromechanical triaxial systems able to provide better response at high strain rates than previous pneumatic systems. Some suggestions of areas for improvement of the triaxial systems are listed below.

1. One of the major shortcomings of high strain rate triaxial testing, and triaxial testing in general is the accurate measurement of excess pore pressures. In standard laboratory conditions (and strain rates) recommendations are available in many different standards on the maximum rate of strain which can be applied to a soil to maintain pore pressure equalisation. The issue of non uniform pore pressure development in fine grained soils is exacerbated during high strain rate tests. It is suggested that development of a pore pressure transducer which can be placed directly into the sample may provide more accurate representation of excess pore pressures. From the behaviour of samples analysed in this study, and the random proximity of the shear plane in relation to the mid height pore pressure transducer, it is suggested that multiple pore pressure transducers of this type could be necessary to capture the variation of excess pore pressures during high strain rate shear. Development of such a device would be beneficial to triaxial testing in general. The possibility of dilation during high strain rate testing has also been indicated by much of the soil behaviour as measured with local Hall effect devices, and excess pore pressure measurements. Improvements to the measurements of excess pore pressures would allow better quantification of such effects, and enable a greater understanding of the behaviour of both normally consolidated and over consolidated soils at high strain rates.

2. During testing with local Hall Effect transducers a large number of samples had to be discarded due to leaks in the membrane, most likely due to rupture in the liquid latex seals applied once the transducers are fixed in place. A more

suitable method of water-proofing this system would increase productivity in future testing.

7.5.2 Improvements to relationships with index properties

Throughout this research project relationships between index properties of fine grained soils have been presented and discussed. The limitations of these relationships in terms of their applicability to a wider range of index properties have also been highlighted. The following list summarises some of the areas where further research will offer potential for a greater understanding of the factors which affect strain rate effects in fine grained soils.

1. During this study comparisons were made between index properties and undrained strain rate effects. A wider variety of soils is required to construct a database to verify many of the observations in this study. In a more general sense a larger database of undrained strain rate tests is required.

2. Much of the relationships between index properties such as moisture content and liquidity index and the undrained strain rate effect infer significant undrained strain rate effects for soils at or close to the plastic limit. This study has found that undrained strain rate effects reduce with reducing moisture content, and in practical terms it may be expected that there would be no strain rate effects at or close to the plastic limit. Also a comparison between plasticity index and the undrained strain rate effect has shown that significant strain rate effects may be expected at low plasticity indices. Future testing could incorporate soils of lower plasticity index, both at the plastic limit and at higher liquidity index to verify some of the observations shown throughout this thesis.

3. Soils of significantly different activity and plasticity index may also affect strain rate effects in different ways that are unclear from this research, which is conducted in soils of similar activity. Much of this research has suggested clay fraction and its relationship with moisture content and void ratio affect the strain rate effects. Testing in soils of low clay fraction, for example less

then 35% which is mentioned as the limit below which the clay fraction will no longer dominate the mechanical behaviour of soil (Kumar and Muir-Wood, 1999) would provide some clarity on the effects of clay fraction.

4. An investigation into the effects of over consolidation on the strain rate effect with a larger range of OCR, and with a greater number of strain rate tests in over consolidated soils, as well as in different types of soils may also provide some answers on the factors that control strain rate. By varying the over consolidation ratio and by over consolidating in different ways (different pre-consolidation pressures) it may clarify how strain rate effects and the microstructure of soils interact. For example the over consolidated soil in this study share the same pre-consolidation pressure and display the same strain rate effect on maximum strength. It would be of interest to determine how the number of particle contacts, which varies with over consolidation would influence the strain rate at maximum strength for significantly higher OCR then used in this study.

References

Aas, G. (1965), 'A Study of the Effect of Vane Shape and Rate of Strain on Measured Values of In Situ Shear Strength of Clays.' *Proceedings of the 6th International Conference on Soil Mechanics Foundation Engineering*, Montreal, Volume I, pp. 141-145.

Adachi, T. & Okano, M. (1974), 'A constitutive equation for normally consolidated clay', *Soils and Foundations*, Volume 14, Number 4, pp. 53-73.

Adachi, T. & Oka, F. (1982), 'Constitutive equations for normally consolidated clay based on elasto-viscoplasticity', *Soils and Foundations*, Volume 22, Number 4, pp. 57-70.

Akai, K., Adachi, T., & Ando, N. (1975), 'Existence of a unique stress-strain-time relation of clays', *Soil and Foundations*, Volume 15, Number 1, March, pp. 1-16.

Al-Tabbaa, A. & Wood, D. M. (1987), 'Some measurements of the permeability of kaolin', *Géotechnique*, Volume 37, Number 4, pp. 499-514.

Alberro, J. & Santoyo, E. (1973), 'Long term behaviour of Mexico City clay', *Proceedings of the 8thInternational Conference on Soil Mechanics and Foundation Engineering*, Moscow, Volume 1, pp. 1-9.

Allam, M.M., & Sridharan, A. (1984), 'The shearing resistance of saturated clays', *Géotechnique*, Volume 34, Number 1, pp. 119-122.

Atkinson, J.H. (2000), 'Non-Linear soil stiffness in routine design', *Géotechnique*, Volume 50, Number 5, pp. 487-508.

Atkinson, J.H., Evans, J.S., & Ho, E.W.L. (1985), 'Non-uniformity of triaxial samples due to consolidation with radial drainage' *Géotechnique*, Volume 35, Number 3, pp. 353-356.

Balderas-Meca, J. (2004), 'Rate effects in rapid loading of clay soils', *PhD thesis*, University of Sheffield, UK.

Bemben, S. M. & Myers, H. J. (1974), 'The influence of rate of penetration on static cone resistance in Connecticut river valley varved clay', *Proceedings of the European symposium on penetration testing*, ESOPT, Stockholm, Volume 2, Number 2, pp. 33-34.

Benz, T. (2007), 'Small-strain stiffness and its numerical consequences', *Ph.D. Thesis*, University of Stuttgart

Berre, T. & Bjerrum, L. (1973), 'Shear strength of normally consolidated clays', *Proceedings of the 8th International Conference on soil mechanics and foundation engineering*, Volume 1, pp. 39-49.

Biscontin, G. & Pestana, J.M. (2001), 'Influence of Peripheral Velocity on Vane Shear Strength of an Artificial Clay', *Geotechnical Testing Journal*, Volume 24, Number 4, pp. 423-429.

Bjerrum, L. Simons, N. & Toblaa, I. (1958), 'The effect of time on the shear strength of a soft marine clay', *Proceedings of the Conference on earth pressure problems*, Volume 1, pp. 148-158.

Bjerrum, L. (1972), 'Embankments on soft ground', *Proceedings, ASCE, Speciality Conference on Performance of Earth-Supported Structures*, Lafayette, Indiana, Volume 2, pp. 1-54.

Bond, A.J. & Jardine, R.J. (1991), 'Effects of installing displacement piles in a high OCR clay', *Géotechnique*, Volume 41, Number 3, pp. 341-363.

Boukpeti, N., White, D.J., Randolph, M.F., Low, H.E. (2012) 'Strength of fine-grained soils at the solid–fluid transition' *Géotechnique*, Volume 62, Number 3, pp. 213-226.

Briaud, J.L., Garland, E. & Felio, G.Y. (1984), 'Rate of loading parameters for vertically loaded piles in clay', *Proceedings of the 16th Annual Offshore Technology Conference*, OCT, Houston, Texas, pp. 407-410.

Briaud, J.L. & Garland, E. (1985), 'Loading rate method for pile response in clay', *Journal of Geotechnical Engineering (ASCE)*, Volume 111, Number 3, pp. 319-335.

Brown, M. J. (2004), 'The rapid load testing of piles in fine grained soils', *PhD thesis*, University of Sheffield, UK.

Brown, M.J.**,** Anderson, W.F. & Hyde, A.F.L. (2004) 'Statnamic testing of model piles in a clay calibration chamber', *Journal of Physical Modelling in Geotechnics 4*, pp. 11-24.

Brown, M.J., Hyde, A.F.L. & Anderson, W.F. (2006), 'Analysis of a rapid load test on an instrumented bored pile in clay', *Géotechnique*, Volume 56, Number 9, pp. 627-638.

Brown, M.J. & Hyde, A.F.L. (2008a), 'Rate effects from pile shaft resistance measurements', *Canadian Geotechnical Journal*, Volume 45, Number 3, March, pp. 425-431.

Brown, M.J. & Hyde, A.F.L. (2008b), 'High penetration rate CPT to determine damping parameters for rapid load pile testing', *3rd International Conference on Geotechnical and Geophysical Site Characterisation Taipei*, Taiwan, April, pp. 657-663.

Brown, M.J. (2008) 'Recommendations for Statnamic use and interpretation of piles installed in clay'. In P. Holscher & F. van Tol (eds) *Proc. Int. Seminar on Rapid Load Testing on Piles, Netherlands,* 29-30th March, 2007. pp. 23-36.

Brown, M.J. & Powell, J.J.M. (2012) 'Comparison of rapid load pile testing of driven and CFA piles installed in high OCR clay'. *Soils & Foundations*, Volume 52, pp. 1033-1042.

Brown, M.J. & Powell, J.J.M. (2013) 'Comparison of rapid load test analysis techniques in clay soils'. ASCE *Journal of Geotechnical & Geoenvironmental Engineering*, Volume 139, pp. 152-161.

Burland, J.B. & Symes, M. (1982) 'A simple axial displacement gauge for use in the triaxial apparatus', *Géotechnique*, Volume 32, Number 1, pp. 62-65.

Carter, J.P. (1982), 'Predictions of the non-homogeneous behaviour of clay in the triaxial test', *Géotechnique*, Volume 32, pp. 55-58.

Casagrande, A. (1947). 'Classification and identification of soils', *Proc. ASCE*, 73(6) part 1, pp. 783-810.

Casagrande, A. & Shannon, W.L. (1948), 'Stress deformation and strength characteristics of soils under dynamic loads', *Proceedings of the Second International Conference on Soil Mechanics and Foundations Engineering*, Volume 5, pp. 29-34.

Casagrande, A. & Wilson, S.D. (1951), 'Effect of rate of loading on the strength of clays and shales at constant water content', *Géotechnique*, Volume 2, Number 3, June 1951. pp. 251-263.

Chow, S.H. & Airey, D.W. (2013), 'Soil strength characterisation using free falling penetrometers', *Géotechnique*, (in-print).

Chung, S.F., Randolph, M.F. & Schneider, J.A. (2006), 'Effect of penetration rate on penetrometer resistance in clay', *Journal of Geotechnical and GeoEnvironmental Engineering*, ASCE, Volume 132. Number 9, pp. 1188-1196.

Clayton, C.R.I. & Khratush, S.A. (1986), 'A new device for measuring local strains on triaxial specimens', *Géotechnique*, Volume 36, Number 4, pp. 593-597.

Crawford, C.B. (1959), 'The influence of rate of strain on effective stresses in a sensitive clay', *American Society Test. Mat. Special Tech Pub*. Number 254, pp. 36-61.

Danziger, F.A.B., & Lunne, T. (1997). 'Rate effect in cone penetration testing', *Géotechnique*, Volume 47, Number 5, pp. 901-914.

Darendeli, M.B. (2001) 'Development of a new family of normalised modulus reduction and material damping curves', *PhD thesis*, University of Texas at Austin, USA

Dayal, U. & Allen, J.H. (1975), 'The effect of penetration rate on the strength of remoulded clay and sand samples', *Canadian Geotechnical Journal*, Volume 12, Number 3, pp. 336-348.

d'Onofrio, A., Silvestri, F., Vinale, F., (1999) 'Strain rate dependent behaviour of a natural stiff clay', *Soils and Foundations*, Volume 39, Number 2, pp. 69-82.

Diaz-Rodriguez, J. A., Martinez-Vasquez, J. J., Carlos Santamarina, J. (2009). 'Strain rate effects in Mexico City Soil'. *Journal of Geotechnical and Geoenvironmental Engineering*, Volume 135, Number 2, pp. 300-305.

Di Benedetto, H., & Tatsuoka, F. (1997) 'Small strain behaviour of geomaterials; Modelling of strain rate effects', *Soils and Foundations*, Volume 37, Number 2, pp. 127-138.

Dobry, R. & Vucetic, M. (1987) 'Dynamic properties and seismic response of soft clay deposits', *Proceedings of the International Symposium on Geotechnical Eng. Of Soft Soils*, Mexico City, Volume 2, pp. 51-87.

Duncan, J.M. & Dunlop, P. (1986) 'The significance of cap and base restraint', ASCE, JSMFD, Volume 94, Number SM1, pp. 271-290.

Finnie, I.M.S. & Randolph, M.F. (1994), 'Punch-through and liquefaction induced failure of shallow foundations on calcareous sediments', *Proceedings of the 7th International Conference on Behaviour of Offshore Structures*, BOSS '94, Boston, pp. 217-230.

Gasparre, A. (2005), 'Advanced laboratory characterisation of London Clay', *PhD thesis*, Imperial College, London, UK.

Gasparre, A., Nishimura, S., Coop, M. R. & Jardine, R. J. (2007). 'The influence of structure on the behaviour of London Clay'. *Géotechnique*, Volume 57, Number 1, pp. 19–31.

Germaine, J.T. & Ladd, C.C. (1988), 'Triaxial testing of saturated cohesive soils. Advanced Triaxial Testing of Soil and Rock', *ASTM Special Technical Publication Number977*, ASTM Philadelphia, Pa., pp. 421-459.

Ghezzehei, T.A. & Or, D. (2001), 'Rheological Properties of Wet Soils and Clays under Steady and Oscillatory Stresses', *Soil Sci. Am. J.*, Volume 65, pp. 624-637.

Gibson, G.C. & Coyle, H.M. (1968), 'Soil damping constants related to common soil properties in sands and clays (Bearing Capacity for Axially Loaded Piles)', *Texas A&M University, Texas, USA, Texas Transportation Institute*, Research Report 125-1, Study 2-5-67-125.

Graham, J., Crooks, J.H.A. & Bell, A.L. (1983), 'Time effects on the stress-strain behaviour of natural soft clays', *Géotechnique*, Volume 33, Number 3, pp. 327-340.

Guven, N. (1992). 'Rheological aspects of aqueous smectite suspensions. Clay-Water Interface and its Rheological Implications', *Boulder, CO: The Clay Minerals Society, CMS Workshop Lectures*, Volume 4, pp. 82-125.

Hardin, B. O. & Drnevich, V.P. (1972). 'Shear Modulus and Damping in Soils: Measurement and Parameter Effects,' *Journal of Soil Mechanics and Foundation Engineering Div.*, ASCE, Volume 98, Number SM6, June, pp. 603-624.

House, A. R., Oliveira, J. R. M. S. & Randolph, M. F. (2001), 'Evaluating the coefficient of consolidation using penetration Tests', *International Journal of Physical Modelling in Geotechnics*, Volume 1, Number 3, pp. 17-25.

Hyde, A.F.L., Robinson, S.A. & Anderson W.F. (2000), 'Rate effects in clay soils and their relevance to Statnamic pile testing, *Proceedings of the 2nd International Statnamic Seminar*, Tokyo, pp. 303-309.

Head, K.H. (1986), 'Manual of soil laboratory testing', Volume 2 and 3, *Pentech Press*, London, UK.

Hight, D.W. (1983), 'Laboratory investigations of sea bed clays', *PhD thesis*, Imperial College, London, UK.

Hight, D.W., Jardine, R.J., Gens, A., (1987) 'The behaviour of soft clays', *Chapter 2, Special Publication, "Embankments on Soft Clays"*, Bulletin of the Public Works research centre. Greece, pp. 33-158.

Heuckel, T.A., (1992) 'Water-mineral interaction in hygromechanics of clays exposed to environmental loads: a mixture-theory approach', *Canadian Geotechnical Journal*, Volume 29, Number 6, pp. 1071-1086.

Ishihara, K. (1996), 'Soil Behaviour in Earthquake Geotechnics', *Oxford University Press*, Oxford.

Israelachvili, J.N., Adams, G.E., (1978) 'Measurement of forces between two mica surfaces in aqueous electrolyte solution', Journal of Chemical Society, Faraday Transactions. I, 74: pp. 975-1001.

Jaeger, R.A., DeJong, J.T., Boulanger, R.W., Low, H.E & Randolph, M.F. (2010), 'Variable penetration rate CPT in an intermediate soil', *Proceedings of the International Symposium on cone Penetration Testing*, Huntington Beach, CA, USA.

Jardine, R. J., Symes, M. J. R. P. & Burland, J. B. (1984). 'The measurement of soil stiffness in the triaxial apparatus'. *Géotechnique* Volume 34, Number 3, pp. 232-340.

Jardine, R.J., Potts, D.M., Fourie, A.B., Burland, J.B., (1986) 'Studies of the influence of non-linear stress-strain characteristics in soil-structure interaction', *Géotechnique*, Volume 36, Number 3, pp. 337-396.

Jardine, R.J., (1992) 'Some observations on the kinematic nature of soil stiffness', *Soils and Foundations*, Volume 32, Number 2, pp. 111-124.

Karmakar, S., & Kushwaha, R.L. (2007), 'Development and laboratory evaluation of a rheometer for soil visco-plastic parameters', *Journal of Terramechanics*, Volume 44, Issue 2, pp. 197-204.

Kim, K., Prezzi, M., & Salgado, R. (2006). 'Interpretation of cone penetration tests in cohesive soils'. *FHWA/IN/JTRP-2006/22, SPR-2632*, Joint Transportation Research Program, Purdue University, USA.

Kim, K., Prezzi, M., Salgado, R., & Lee, W. (2008). 'Effect of Penetration Rate on Cone Penetration Resistance in Saturated Clayey Soils', *Journal Geotechnical Geoenvironmental Engineering*, ASCE, Volume 134, Number 8, pp. 1142- 1153.

Kokusho, T. (1980). 'Cyclic Triaxial Test of Dynamic Soil Properties for Wide Strain Range', *Soils and Foundations*, Volume 20, Number 2, pp. 45-60.

Kokusho, T., Yoshida, Y. & Esashi, Y., (1982) 'Dynamic soil properties of soft clay for wide strain range', *Soils and Foundations*, Volume 22, Number 4, pp. 1–18.

Krieg, S., (2000). 'Viskoses Bodenverhalten von Mudde, Seeton und Klei', Vero¨.entlichungen des Ins. fu¨r Boden.- Felsmechanik der Uni. Fridericiana in Karlsruhe, Nr. 150.

Kulhawy, F.H. & Mayne, P.W. (1990), 'Manual on estimating soil properties for foundation design', *Electric Power Research Institute*, Report EL-6800, Palo Alto.

Kumar, G.V., Muir Wood, D., (1999) 'Fall cone and compression tests on clay-gravel mixtures' *Géotechnique*, Volume 49, Number 6, pp. 727-739.

Kutter, B.L., Sathialingam, N., (1992) 'Elastic-viscoplastic modelling of the rate-dependent behaviour of clays', *Géotechnique*, Volume 42, Number 3, pp. 427-441.

Ladd, C.C., & Foot, R., (1974) 'New design procedure for stability of soft clays', *Journal of Geotechnical Engineering* (ASCE), Volume 100, Number 7, pp. 763-786.

Ladd, C.C., Foot, R., Ishihara, K., Schlosser, F., Poulos, H.G. (1977), 'Stress-deformation and strength characteristics', *Proceedings of the 9th International Conference on Soil Mechanics and Foundation Engineering*, Tokyo, Volume 2, pp. 421-494.

Lefebvre, G. & LeBoeuf, D. (1987), 'Rate effects and cyclic loading of sensitive Clays', *Journal of Geotechnical Engineering* (ASCE), Volume 113, Number 5, pp. 476-489.

Lehane, B.M., O'Loughlin, C.D., Gaudin, C. & Randolph, M.F. (2009). 'Rate effects on penetrometer resistance in kaolin', *Géotechnique*, Volume 59, Number 1, pp. 41-52.

Leinenkugel, H.J. (1976) 'Deformations und festigkeitsverhalten bindiger erdstoffe', Institute for Soil Mechanics and Foundation Mechanics, University of Karlsruhe, Germany, Volume 66. (in German)

Lemos, L.J.L. (1986), 'Rate effects on residual strength', *PhD thesis*, Imperial College of Science and Technology, University of London. U.K.

Lemos, L.J.L. (1991), 'Shear strength of shear surfaces under fast loading', *European Conference on Soil Mechanics*, Florence, Volume 1, pp. 137-141.

Lemos, L.J.L. & Vaughan, P.R. (2000), 'Clay-interface shear resistance', *Géotechnique*, Volume 50, Number 1, pp. 55-64.

Leroueil, S., Kabbaj, M., Tavenas, F. & Bouchard, R. (1985), 'Stress-strain-strain rate relation for the compressibility of sensitive natural clays', *Géotechnique*, Volume 35, Number 2, pp. 159-180.

Leroueil, S., Marquez, M.E.S. (1996), 'Importance of strain rate and temperature effects in geotechnical engineering', *Session on measuring and modelling time dependent soil behaviour*, ASCE Convention, Washington, Geotechnical Special Publications 61: 1-60.358.

Liyanapathirana, D.S., Carter, J.P. & Airey, D.W. (2005), 'Numerical modelling of non-homogeneous behaviour of structured soils during triaxial tests', *International Journal of Geomechanics*, ASCE. Volume 5, Number 1, pp. 10-23.

Lo Presti, D.C.F., Jamiolkowski, M., Pallara, O. & Cavallaro, A. (1996): 'Rate and creep effect on the stiffness of soils', *ASCE Convention, Geotechnical Special Publication*, Washington, Number 61, pp. 166-180.

Lo Presti, D.C.F., Jamiolkowski, M., Pallara, O. & Cavallaro, A., Pedroni, S. (1997), 'Shear modulus and damping of soils', *Géotechnique,* Volume 47, Number 3, pp. 603-617.

Lo Presti, D.C.F., Pallara, O., Cavallaro, A., Maugeri, M., (1998) 'Non linear stress-strain relations of soils for cyclic loading', *11th European Conf. on Earthquake Engineering,*

Low, P.F. (1976), 'Viscosity of interlayer water in montmorillonite', *Soil Science Society of America Journal*, Volume 40, Number 4, pp. 500-505.

Lunne, T., Robertson, P.K. & Powell, J.J.M (1997), 'Cone penetration testing in geotechnical practice', *Blackie Academic and Professional*, 1st Edition, London, UK.

Lupini, J.F., Skinner, A.E., & Vaughan, P.R. (1981), 'The drained residual strength of cohesive soils', *Géotechnique,* Volume 31, Number 2, pp. 181-213.

Mahajan, S. P. & Budhu, M. (2009). 'Shear viscosity of clays using the fall cone test', *Géotechnique*, Volume 59, Number 6, pp. 539-543.

Massarsch, K. R. (2004), 'Deformation properties of fine-grained soils from seismic tests', *Keynote lecture, International Conference on Site Characterization*, ISC'2, 19-22 September. Porto, pp. 1-14.

Matešic, L. & Vucetic, M. (2003). 'Strain-rate effect on soil secant shear modulus at small cyclic strains'. *J. Geotechnical Geoenvironmental Engineering, ASCE* 129. Number 6, pp. 536-549.

Mesri, G. & Castro, A. (1987). 'Cα/Cc concept and K0 during secondary compression'. *J. Geotechnical Engineering, ASCE,* 113, Number 3, pp. 230-247.

Mitchell, J.K. & Soga, K. (2005) 'Fundamentals of Soil Behaviour', 3rd Edition, John Wiley and Sons.

Muir Wood, D. (1990), 'Soil behaviour and critical state soil mechanics', *Cambridge University Press,* UK.

Mukabi, J. N., Tatsuoka, F. & Hirose, K. (1991). 'Effect of strain rate on small strain stiffness of Kaolin In: CU Triaxial Compression', *Proc. 26th Japan National Conf. on SMFE,* Nagano, pp. 659-662.

Mukabi, J. (1995), 'Deformation characteristics at small strains of clays in triaxial tests', *Doctor of Engineering thesis,* University of Tokyo, Japan.

Mukabi, J. N. & Tatsuoka, F. (1999a). 'Effects of stress path and ageing in reconsolidation on deformation characteristic of stiff clays'. *Proc. 2nd Int. Symp. Pre-failure Deformation Characteristics of Geomaterials,* IS Torino 1, pp. 131-140.

Mukabi, J. N. & Tatsuoka, F. (1999b) 'Influence of reconsolidation stress history and strain rate on the behaviour of kaolin over a wide range of strain', *Geotechnics for Developing Africa*, Wardle, Blight & Fourie (eds)

Olson, R.E. & Parola, J.F. (1967), 'Dynamic shearing properties of compacted clay', *Proceedings of the International Symposium on Wave Propagation and Dynamic Properties of Earth Materials,* University of New Mexico, 23-25 August, University of New Mexico Press, Albuquerque, New Mexico, pp. 173-182.

Olson, R.E., & Campbell, L.M. (1964) Discussion of 'Importance of free ends in Triaxial testing', Rowe, P.W., & Barden, L.M., *ASCE, JSMFD*, Volume 90, Number SM6, pp. 167-173.

O' Reilly, M.P., Brown, S.F. & Overy, R.F. (1989). 'Viscous effects observed in tests on an anisotropically normally consolidated silty clay', *Géotechnique,* Volume 39, Number 1, pp. 153-158.

Oka, F., Kodaka, T., Kimoto, S., Ishigaki, S. & Tsuji, C. (2003), 'Step-changed strain rate effect on the stress–strain relations of clay and a constitutive modelling' *Soils and Foundations,* Volume 43, Number 4, pp. 189-202.

Powell, J.J.M. & Brown, M.J. (2006), 'Statnamic pile testing for foundation re-use', *International Conference on the Re-use of Foundations for Urban Sites*, UK, 19-20th Oct, pp. 223-236.

Powrie, W. (2004) 'Soil mechanics, Concepts and applications', 2nd Edition, Spon Press.

Quinn, T.A.C. & Brown, M.J. (2011) 'Effect of strain rate on isotropically consolidated kaolin over a wide range of strain rates in the triaxial apparatus'. *5th Int. Symp on Deformation Characteristics of Geomaterials*, Seoul, 31st Aug-3 Sept, 2011. pp. 607-613.

Quinn, T.A.C., Robinson, S**.,** Brown, M.J. (2012) 'High strain rate characterisation of kaolin and its application to rapid load pile testing'. *9th Int. Conf. on Testing & Design Methods for Deep Foundations*, (IS Kanazawa 2012), Kanazawa, Japan, 18-20th Sept., 2012. pp. 311-319.

Randolph, M.F. & Deeks, A.J. (1992),'Dynamic and static soil models for axial response', *In F.B.J. Barends (ed), International Conference on the Application of Stress Wave Theory to Piles*, 4th, The Hague, The Netherlands, 21-24 September. Rotterdam, A.A. pp.3-14

Randolph, M.F. & Hope, S. (2004), 'Effect of cone velocity on cone resistance and excess pore pressures', *Proceedings of the International Symposium on Engineering Practice and Performance of Soft Deposits*, pp. 147-152.

Rattley, M. J., Richards, D. J. & Lehane, B. M. (2008), 'The uplift response of transmission tower foundations', *J. Geotech. Geoenviron. Engng* ASCE, Volume 134, Number 4, pp. 531–540.

Rattley, M.J., Hill, A.J., Thomas, S. & Sampurno, B. (2011), 'Strain rate dependent simple shear behaviour of deepwater sediments in offshore Angola', *Proceedings of the 2nd International Symposium on Frontiers in Offshore Geotecnhics*, Perth, Australia, 2010 pp. 377-382.

Rees, S. (2013) 'What is triaxial testing; Part 2 of 3'. *Geotechnical-white-papers*, www.gdsinstruments.com

Resendiz, D. (1965), 'Considerations on the solid-liquid interaction in clay-water system', *Proceedings of the 6th International Conference on Soil Mechanics and Foundation Engineering*, Montreal. Volume1. pp. 97.

Richardson, A. M. & Whitman, R. V. (1963). 'Effect of strain rate upon undrained shear resistance of a saturated remoulded fat clay'. *Géotechnique* 13, Number 4, pp. 310–324.

Richardson, A. M., (1963). 'Effect of strain-rate on shear resistance of a saturated fat clay', *Sc.D.thesis. M.I. T.*, Cambridge, *Mass.*

Rodriguez, J., Alvarez, C., Velandia, E. (2008). 'Load rate effects on high strain tests in high plasticity soils. *8th Int. Conf. on the Application of Stress Wave Theory to piles*. Lisbon. pp. 131-134.

Roscoe, K.H., Schofield, A.N. & Wroth, C.P. (1958), 'On the yielding of soils', *Géotechnique*, Volume 8, Number 1, pp 22-53.

Rossato, G., Ninis, L. & Jardine, R.J. (1992), 'Properties of some kaolin based model clay soils', *ASTM Geotechnical Testing Journal*, Volume 15, Number 2, June. pp. 166-179.

Roy, M., Tremblay, M., Tavenas, F. & La Rochelle, P. (1982), 'Development of pore pressures in quasi-static penetration tests in sensitive clay, *Canadian Geotechnical Journal*. Volume 19, Number 2, pp. 124- 138.

Roy, M. & LeBlanc A. (1988), 'The In-Situ Measurement of the Undrained Shear Strength of Clays Using the Field Vane', *Vane Shear Strength Testing in Soils: Field and Laboratory Studies*, ASTM STP 1014, pp. 117-128.

Rowe, P.W. & Barden, L. (1964) 'Importance of free ends in triaxial testing', ASCE, JSMFD, Volume 90, Number SM1, pp. 1-27.

Salgado, R., Prezzi, M., Kim, K., & Lee, W., (2013), 'Penetration rate effects on cone resistance measured in a calibration chamber, Geotechnical and Geophysical Site Characterization 4', *Proceedings of the 4th International Conference on Site Characterization 4,* ISC-4, Volume 2, pp. 1025-1030.

Santagata, M., Germaine, J.T., Ladd, C.C. (2007), 'Small-Strain nonlinearity of normally consolidated clay', Journal *of Geotechnical and Geoenvironmental Engineering*, Volume 133, Number 1, pp. 72-82.

Santagata, M. (2008), 'Effects of stress history on the stiffness of a soft clay', *Proceedings of the 4th International Symposium on Deformational Characteristics of Geomaterials*, IS Atlanta '08, Atlanta, pp. 95-123.

Santos, J.A. & Gomes Correia, A. (2000), 'Shear modulus of soils under cyclic loading at small to medium strain level', *12th World Conference on Earthquake Engineering*, paper ID 0530, Auckland, New Zealand.

Santos, J.A., Gomes Correia, A., Modaressi, A., Lopez-Caballero, F., Carrilho Gomes, R. (2003) 'Validation of an elastoplastic model to predict secant shear modulus of natural soils by experimental results', *3rd International Symposium on Deformation Characteristics of Geomaterials*, Lyon, September 22-24th.

Sathialingam, N. & Kutter, B. L. (1989). 'The effects of high strain rate and high frequency loading on soil behaviour in centrifuge model tests'. *Report submitted to Naval Civil Engineering Laboratory*, Port Hueneme, California.

Sathialingam, N. (1991) 'Elastic - viscoplastic modelling of rate dependent behaviour of clays', *PhD thesis*, University of California Davis, USA.

Schofield, A.N. & Wroth, C.P. (1968), 'Critical State Soil Mechanics', *McGraw-Hill*, London, UK.

Seed, H. B., Woodward, R. J. & Lundgren, R. (1964), 'Fundamental aspects of the Atterberg limits', *Journal of Soil Mechanic Foundations*. Div., ASCE 90, Number SM6, pp. 75-105.

Sheahan, T.C., Ladd, C.C. & Germaine, J.T. (1996). Rate dependant undrained shear behaviour of saturated clay', *Journal of Geotechnical Engineering*, ASCE, Volume 122, Number 2, pp. 99-108.

Sheeran, D. & Krizek, R.J. (1971). 'Preparation of homogeneous soil samples by slurry consolidation'. *Journal of Materials*, Volume 6, Number 2. pp. 356-373.

Sheng, D., Westerberg, B., Mattson, H., Axelsson, (1997) 'Effects of end restraint and strain rate in triaxial tests', *Computers and Geotechnics*, Volume 21, Number 3, pp. 163-182.

Shibuya, S., Mitachi, T., Hosomi, A. & Hwang, S.C. (1996), 'Strain rate effects on stress-strain behaviour of clay as observed in monotonic and cyclic triaxial tests. *Proceedings of sessions sponsored by the ASCE Geotechnical Engineering Division in conjunction with the ASCE Convention in Washington*, D.C., pp. 214-227.

Silva, M. F., White, D. J. & Bolton, M. D. (2006), 'An analytical study of the effect of penetration rate on piezocone tests in clay', *International Journal for Numerical Analytical Methods in Geomechanics*, Volume 30, Number 6, pp. 501-527.

Skempton, A.W. (1985), 'Residual Strength of clays in landslides, folded strata and the laboratory', *Géotechnique*, Volume 35, Number 1, pp. 3-18.

Soga, K., Nakagawa, K. & Mitchell, J.K. (1995), 'Measurement of stiffness degradation characteristics of clays using a torsional shear device', *1st International Conference on Earthquake Geotechnical Engineering*, Tokyo.

Soga, K. & Mitchell, J.K. (1996), 'Rate dependant deformation of structured natural clays,' *Proc of the ASCE National Convention - Measuring and Modelling Time*

Dependant Soil Behaviour, ASCE. Geotechnical Special Publication 61, Washington DC, 10-14 November, New York, pp. 243-257.

Sorensen, K.K., (2006) 'Influence of viscosity and ageing on the behaviour of clays', *PhD thesis*, University College London

Sorensen, K.K, Baudet, B. & Tatsuoka, F. (2007). 'Coupling of ageing and viscous effects in an artificially structured clay'. *Proceedings of the geotechnical symposium on soil stress–strain behaviour: measurement, modelling and analysis*, Rome.

Sorensen, K.K, Baudet, B. & Simpson, B. (2010). 'Influence of strain rate and acceleration on the bheaviour of reconstituted clays at small strains', *Géotechnique*, Volume 60, Number 10, pp. 751-763.

Tatsuoka, F., & Shibuya, S. (1992) 'Deformation characteristics of soils and soft rocks from field and laboratory tests', Keynote Lecture, *Proc. 9th Asian reg. Conf. on SMFE*, Bangkok, 1991, 2, pp. 101-170.

Tatsuoka, F., Jardine, R.J., Lo Presti, D., Di Benedetto, H. & Kodaka, T., (1997), 'Characterising the pre-failure deformation properties of geomaterials', *Proceedings of the International Conference on Soil Mechanics and Foundations*, Theme Lecture Session 1, XIV ICSMFE, Hamburg, Balkema, Volume 4, pp. 2129-2164.

Tatsuoka, F., Ishihara, M., Di Benedetto, H. & Kuwano, R. (2002). 'Time- dependent shear deformation characteristics of geomaterials and their simulation'. *Soils and Foundations*. 42, Number 2, pp. 103–129.

Tatsuoka, F., Di Benedetto, H., Enomoto, T., Kawabe, S., Kongkitul., (2008) 'Various viscosity types of geomaterials in shear and their mathematical expression', *Soils and Foundations*, Volume 48, Number 1, pp. 41-60.

Terzaghi, K., Peck, R.B., Mesri, G. (1996) 'Soil Mechanics in Engineering Practice', 3rd Edition, John Wiley and Sons.

Tika, T. M. (1989), 'The effect of fast shearing on the residual strength of soils', *PhD Thesis*, Imperial College of Science and Technology, University of London, U.K.

Tika, T.E., Vaughan, P.R. & Lemos, L.J.L. (1996), 'Fast shearing of pre-existing shear zones in soil', *Géotechnique*, Volume 46, Number 2, pp. 197-233.

Triantafyllidis, T. (2001). 'On application of the Hiley formula in driving long piles', *Géotechnique*, Volume 51, Number 10, pp. 891-895.

Vaid, Y.P. & Campanella, R.G. (1977), 'Time-dependant behaviour of undisturbed clay', *Journal of Geotechnical Engineering Division, ASCE,* Volume 103, Number 7, pp. 693-709.

Vardenega, P.J., & Bolton, M.D. (2011) 'Practical methods to estimate the non-linear shear stiffness of fine grained soils', *International Symposium on Deformation Characteristics of Geomaterials,* September 2011, Seoul, Korea

Viggiani, G. & Atkinson, J. H. (1995a). 'Interpretation of bender element tests', *Géotechnique* Volume 45, Number 1, pp. 149-154.

Viggiani, G. & Atkinson, J. H. (1995b). 'Stiffness of fine-grained soil at very small strains', *Géotechnique* Volume 45, Number 2, pp. 249-265.

Vucetic, M. & Dobry, R. (1991). 'Effect of soil plasticity on cyclic response. *Journal of Geotechnical Engineering (ASCE)*',Volume 117, Number 1, pp. 89-117.

Vucetic, M. (1994), 'Cyclic threshold shear strains in soils'. *Journal of Geotechnical Engineering, ASCE, Volume 120, Number 12, pp. 2208-2228.*

Vucetic, M. & Tabata, K., (2003). 'Influence of soil type on the effect of strain rate on small-strain cyclic shear modulus' *Soils and Foundations.* Volume 43, Number 5, pp. 161-173.

Vucetic, M., Tabata, K., Matesic, L. (2003). 'Effect of average straining rate on shear modulus at small cyclic strains'. *Proc. 3rd Int. Symp. Deformation Characteristics of Geomaterials, IS Lyon*.

Whitman, R.V, (1957), 'The behaviour of soils under transient loadings', *Proceedings of the International Conference on Soil Mechanics and Foundation Engineering,* Volume 4, pp. 207-210.

Wroth, C.P. (1975), 'In-Situ measurement of initial stresses and deformation characteristics', *Proceedings, ASCE Speciality Conference on In-Situ Measurement of Soil Properties*, Volume 2, Raleigh, pp. 180-230.

Wroth, C.P., & Houlsby, G.T. (1985) 'Soil mechanics-property characterisation, and analysis procedures', *Proc. 11th Conf. Soil Mech., San Francisco,* 1, pp. 1-55.

Yong, R.N. & Japp, R.D. (1969), 'Stress-strain behaviour of clays in dynamic compression. Vibration Effects of Earth-quakes on Soils and Foundation', *ASTM STP 450, American Society for Testing Materials*, pp. 233-262.

Yusoff, N.A., Hird, C.C., & Hyde, A.F.L. (2008), 'A Rowe cell vane shear apparatus to determine rate effects for fine grained soils', *In 2nd International Workshop, International Press-in Association*, New Orleans, USA, December, pp. 1-7.

Zhu, J.G. & Yin, J.H. (2000), 'Strain rate dependent stress strain behaviour of overconsolidated Hong Kong marine clay', *Canadian Geotechnical Journal*, Volume 37, Number 6, pp. 1272-1282.